Fall 12-17-2021

Analysis of Spore Shape Determination in Streptomyces

Ning Sun
Duquesne University

ANALYSIS OF SPORE SHAPE DETERMINATION IN *STREPTOMYCES*

A Dissertation

Submitted to the Bayer School of Natural and Environmental Sciences

Duquesne University

In partial fulfillment of the requirements for

the degree of Doctor of Philosophy

By

Ning Sun

December 2021

ANALYSIS OF SPORE SHAPE DETERMINATION IN *STREPTOMYCES*

By

Ning Sun

Approved November 5, 2021

Joseph R. McCormick, Ph.D. Professor of Biological Sciences (Committee Chair)	Jana Patton-Vogt, Ph.D. Professor of Biological Sciences (Committee Member)
John F. Stolz, Ph.D. Professor of Biological Sciences (Committee Member)	Mihaela Rita Mihailescu, Ph.D. Professor of Chemistry & Biochemistry (Committee Member)
Ellen S. Gawalt, Ph.D. Dean, Bayer School of Natural and Environmental Sciences Professor of Chemistry and Biochemistry	Jana Patton-Vogt, Ph.D. Professor and Chair of Biological Sciences

ABSTRACT

ANALYSIS OF SPORE SHAPE DETERMINATION IN *STREPTOMYCES*

By

Ning Sun

December 2021

Dissertation supervised by Joseph R. McCormick, Ph.D.

Streptomycetes are Gram-positive, soil-dwelling bacteria that possess a complex life cycle with the alternation of vegetative mycelium, aerial mycelium, and spores. *Streptomyces. coelicolor* spore maturation is a complex process that involves spore shape metamorphosis from cylindrical pre-spores into ellipsoid spores, but the details of this process have remained enigmatic. Previously, our lab identified a novel gene *ssdA* that might play a role in spore shape determination using a transposon-based insertion mutagenesis in *S. coelicolor*. In this study, I isolated a *S. coelicolor ssdA*-null mutant that showed increased colony hydrophobicity and misshapen spores in sizes and shapes, confirming the phenotype of the *ssdA* insertion mutant. In order to further investigate the function of *ssdA*, I switched the model species to *S. venezuelae* due to its advantages. Here, I demonstrate that a *S. venezuelae ssdA* mutant showed delayed morphological differentiation on both solid and liquid media, arising in part from germination

and growth defects of the mutant. The *ssdA* mutant also generated heterogeneously-sized spores, possibly due to sporulation and cell-cell separation defects. Deletion of *ssdA* also resulted in spore sensitivity to heat, osmotic stress, and cell-wall targeting antibiotics. The spore sacculus was isolated and a preliminary HPLC-MS result demonstrated the accumulation of peptidoglycan muropeptides in the *ssdA* mutant. SsdA-EGFP localizes in vegetative hyphae, sporulation septa, and the periphery of spores, consistent with its roles in cell wall development. A bacterial two-hybrid assay shows that the central cytoplasmic region of SsdA interacts with a dynamin-like, sporulation-specific protein DynB, explaining the septal localization of SsdA-EGFP. Of interest, *ssdA* also affects *Streptomyces*'s exploration, a novel growth mode. *whiD* is a regulatory gene in *Streptomyces* that potentially controls *ssdA* expression. Here I show that the *S. venezuelae whiD* mutant has a white colony and produces heterogeneously sized spores, indicating a sporulation defect. Also the *whiD* mutant is drastically sensitive to heat and slightly sensitive to salt, different from the sensitivity profile for the *ssdA* mutant. Further elucidation the regulatory mechanism of WhiD will provide more insights into the sporulation and spore maturation in this filamentous bacterium.

ACKNOWLEDGEMENT

Frist and foremost, I would like to express my sincere gratitude to my advisor, Dr. Joseph McCormick. Joe had been helping me starting from my PhD program application while I was still in China and all the way to the completion of my PhD. He is an excellent mentor who helps me to shape my research perspectives, teaches me how to think about scientific questions as well as how to solve the problems. As an international student, I have to overcome many challenges, especially my English writing and speaking. Joe definitely devotes a lot of his time to the edits and proofreading for my research writing. I have learned a tremendous amount while working in his lab and none of this work would have been possible without his guidance. His mentorship has left a positive and powerful mark on my research and will continue to influence me in my future career .

Next, I would like to express my sincere thanks to my committee members including Dr. Jana Patton-Vogt, Dr. John Stolz and Dr. Mihaela Rita Mihailescu. All of them have been extremely supportive throughout my entire PhD study. Each of them has provided thoughtful and constructive advice to my work and stimulated meaningful discussions for my research. I also appreciate their enthusiasm on providing a recommendation letter and helping my future career. I want to give special thanks to Dr. John Stolz for teaching and assistance with the TEM microscopy.

I also would like to sincerely thank my amazing collaborators Dr. Evi Stegmann and her student Irina Voitsekhovskaia at University of Tübingen (Germany). Irina has diligently devoted her time to performing the HPLC-MS experiments and elucidating the structures for the muropeptides. Dr. Stegmann has provided valuable feedback on the result interpretation and discussions. I am also grateful for my another collaborator Dr. Klas Flärdh at Lund University

(Sweden), who has sent many bacterial strains to the McCormick lab and generously observed the protein localization for me using fluorescence microscopy. In addition, Dr. Susan Schlimpert at John Innes Centre (U.K.) also kindly sent us some bacterial strains. I was able to observe the localization of my protein by engineering the vector she sent to me. The bacterial two-hybrid vectors directly facilitated me to discover an interacting partner of SsdA.

It is such a pleasure and honor to work in the McCormick lab with many supportive people, both past and present. Dr. Jennifer Bennet conducted an excellent transposon-based screening and discovered the novel gene that directly leads to my PhD project. Dr. Metis Hasipek taught me the basic operations of *Streptomyces* and bacterial two-hybrid assay when I joined the lab. Dr. Stuart Cantlay provided me lots of knowledge about *S. venezuelae* and hands-on experiences on microscopy. Drs Sumedha Sethi and Joseph Sallmen have been my compatriots for the majority of my time in the lab, and they had helped me through all of the challenges that I have to face, including coursework, proposal defense, experimental difficulties, etc. Joe continued to help me and sent the bacterial strains from U.K. after he left the lab. Jeevitha Jeevan has become one of my close friend. She helped manage the lab and also offered me personal help during my life hardship, which I am extremely grateful. Catherine Bruno and Lili Macharashvili are incredibly supportive while I work on my thesis writing. Catherine has been working diligently with our lab aids and ensured me an ample supply for solutions and media as well as maintained a clean and neat lab environment.

In addition to the research part, I would like to thank Drs. Kasey Christopher, Jason Heming, Elisabeth Chalovich and Mrs. Lalitha Rajakumar for being incredible mentors in teaching. They are all extremely helpful for enhancing my teaching strategy and building confidence when teaching in front of students. Special thanks to Kasey, who is the first teaching

faculty I assisted with after I joined the program. She is an extremely diligent professor and her dedication to teaching has absolutely influenced and will continue influence me in the future.

As a student in the Biology Department, I must thank Ms. Pam Ferchak and Terri Widernholfer in the Biology office as well as Heather Costello in the Dean's office for providing me numerous administrative supports over the past years. Ms. Kim Nath and Elizabeth Cochran have to be acknowledged for efficient management of the departmental equipment. I also would like to thank the Department of Biological Sciences at Duquesne University as a whole to provide me graduate teaching assistantships. My research would not have been possible without these supports.

Then I would like to thank my cohorts Narthana Jeganathar Kanmanii, Kenzie Pereira, Michael Wells, Wes Bowman, and Al Al Muatasim Al Zadjali. It has been a great pleasure studying with such a friendly and fun group. I want to extend my special thanks to Narthana and Kenzie, who threw a wonderful baby shower for me and help me went through the hardest time of my life after my daughter was born.

Last but not the least, I must thank my wonderful family. I would like first to thank my parents, Qichang Sun and Yuzhi Gao. I would never have this accomplishment without your unconditional love and support. Thank you Daddy and Mommy. I would also like to thank my brother, Kun Sun, who helps me take care of all of the family responsibilities in China. My parents-in-law came to U.S. twice to help take a very good care of my daughter, which I cannot thank them enough. My husband, Zhihao, gives me lots of help and support both in life and in research. Graduate school would have been increasingly difficult without his support. Last, I want to thank my daughter Riley Sun for being in my life and bringing me endless happiness!

ATTRIBUTIONS

Dr. Jennifer Bennett performed the Tn5-based insertion mutagenesis in *S. coelicolor* and identified *ssdA* as a spore shape determination gene during her PhD study in Dr. McCormick's lab.

Garrett Kandel, an undergraduate student from Otterbein University, constructed pGK1 (cosmid 3B6 $ssdA_{sco}$::*aac(3)IV*) using a recombineering method.

Irina Voitsekhovskaia, a PhD student from Dr. Evi Stegmann's lab at University of Tübingen (Germany) isolated the spore sacculus and performed HPLC-MS analysis.

Dr. Klas Flärdh at Lund University (Sweden) performed and confirmed fluorescent protein fusion localization.

Streptomyces. venezuelae 5' triphosphate end-capture RNA-seq was conducted and deposited onto StrepDB by Dr. Mark Buttner's lab at John Innes Centre.

TABLE OF CONTENTS

LIST OF TABLES

LIST OF FIGURES

LIST OF ABBREVIATIONS

B. subtilis	*Bacillus subtilis*
C. crescentus	*Caulobacter crescentus*
c-di-GMP	3', 5'-cyclic diguanosine monophosphate
Cryo-ET	Cryogenic-electron tomography
E. coli	*Escherichia coli*
EGFP	Enhanced green fluorescent protein
GFP	Green fluorescent protein
GlcNAc	N-acetylglucosamine
GTase	Glycosyltransferase
Hi-C	High-throughput chromosome conformation capture
HPLC-MS	High performance liquid chromatography–mass spectrometry
IF	Intermediate filament
MurNAc	N-acetylmuramic acid
NO	Nucleoid occlusion
PBP	Penicillin-binding protein
aPBP	Class A Penicillin-binding protein
bPBP	Class B Penicillin-binding protein
PG	Peptidoglycan
RPF	Resuscitation-promoting factor
S. coelicolor	*Streptomyces. coelicolor*
S. venezuelae	*Streptomyces venezuelae*

SEDS	Shape, elongation, division and sporulation
SSSC	*Streptomyces* spore wall synthesizing complex
TEM	Transmission electron microscopy
TIPOC	Tip-organizing center
TM	Transmembrane
TMA	Trimethylamine
TPase	Transpeptidase
TSS	Transcription start site
VOC	Volatile organic compound
WT	Wild type

CHAPTER 1: LITERATURE REVIEW

Bacteria exist in a wide variety of shapes and sizes. In addition to the well-known rods and spheres, more irregular shapes also exist, such as stars, helices, with appendages, and branched filaments (Kysela et al., 2016). The characteristic shape of a given bacterial species is faithfully maintained from generation to generation, although it might be periodically modified in response to developmental cues or to adapt to environmental changes. It is believed that specific morphologies are the joint consequences of fitness and selective pressures (Caccamo and Brun, 2018). Great progress has been being made over the past decades in understanding how bacterial shape is determined. Peptidoglycan (PG) plays a crucial role in shape determination in bacteria, but it cannot explain the exceptions that some cell-wall deficient bacteria are also able to adopt different shapes (Allan et al., 2009). It is widely accepted that the generation of bacterial shape depends on a complex interplay between the PG biosynthetic machinery and its regulatory elements (cytoskeletal proteins) (Young, 2010). In the next two sections, I will discuss PG and cytoskeletal proteins, and how they dictate bacterial shape.

PEPTIDOGLYCAN IS A MAJOR DETERMINANT OF BACTERIAL CELL SHAPE

Diversity of peptidoglycan

Peptidoglycan (PG), also known as murein, is a major component of the bacterial cell wall, a structure that resides outside of the cytoplasmic membrane in most bacteria. PG is formed as a polymeric macromolecular meshwork that confers a structural support for the cell so that it can withstand turgor pressure to maintain a specific shape and size. The basic structure of PG consists of linear glycan strands of alternating β-1,4-linked N-acetylmuramic acid (MurNAc) and N-acetylglucosamine (GlcNAc) sugars, which are cross-linked via peptide bonds between short oligopeptides covalently attached to the MurNAc (Vollmer et al., 2008a). In Gram-negative

bacteria like *Escherichia coli* (*E. coli*), the most common pentapeptide stem is L-Ala-D-Glu-mDAP-D-Ala-D-Ala (mDAP: meso-diaminopimelic acid).While the basic PG precursor unit is remarkably conserved (GlcNAc-MurNAc), the amino acid composition of the stem peptide, type and extent of the peptide cross-links, and glycan chain length can vary between species, through the life cycle, or in response to environmental stresses (Kuhn, 2019; Schleifer and Kandler, 1972). The glycan strands can also be modified by N-deacetylation and O-acetylation on either or both sugar subunits (Vollmer et al., 2008a). See review by Vollmer et al., 2008 for an extensive summary on PG structure and architecture. A host of PG-related enzymes, such as PG synthases, flippases, and hydrolases, work together and contribute to the diversity of PG structure. Enzymatic dysfunction would affect the chemical composition of the PG, and thus possibly impact cell viability.

Biosynthesis of the PG precursor

The PG biosynthesis starts in the cytoplasm, where the precursor uridine-diphosphate GlcNAc (UDP-GlcNAc) is first produced (Barreteau et al., 2008). UDP-MurNAc is then synthesized from UDP-GlcNAc by enzymes MurA and MurB. The pentapeptide moiety is added to the UDP-MurNAc by amino acid ligases MurC-F in a series of stepwise, ATP-dependent reactions. The UDP-MurNAc-pentapeptide intermediate is then transferred onto the lipid carrier of undecaprenyl phosphate by the integral membrane protein MraY, resulting in the formation of uridine monophosphate (UMP) and the undecaprenyl-pyrophosphate MurNAc-pentapeptide, also known as Lipid I (Unsleber et al., 2019). Subsequent addition of GlcNAc from UDP-GlcNAc to Lipid I by MurG results in formation of Lipid II (the undecaprenyl-pyrophosphate MurNAc-GlcNAc pentapeptide).

To synthesize the PG, Lipid II needs to translocate from the inner to the outer leaflet of the cytoplasmic membrane, and this process is mediated by lipid flippase(s). The players that fulfill this function are still controversial. One candidate is MurJ, an integral membrane protein that belongs to the multidrug/oligosaccharidyl-lipid/polysaccharide (MOP) exporter superfamily (Meeske et al., 2015; Sham et al., 2014). *murJ* is an essential gene in *E. coli* and depletion of the gene product results in cell shape defects and lysis (Ruiz, 2008). In *Bacillus subtilis* (*B. subtilis*), *murJ* is dispensable, but it forms a synthetic lethal pair with a gene encoding an alternative flippase Amj (alternate to MurJ) (Meeske et al., 2015). *amj* is up-regulated in the absence of MurJ, suggesting that it serves as a defense mechanism against naturally occurring MurJ antagonists (Meeske et al., 2015). In addition, FtsW is another protein that has the flippase activity. It binds Lipid II *in vitro*, and is able to flip fluorescently labelled Lipid II in liposomes and *E. coli* cytoplasmic membrane vesicles (Mohammadi et al., 2014; Mohammadi et al., 2011). FtsW is a widely conserved integral membrane protein belonging to the SEDS (shape, elongation, division and sporulation) family, and is involved in cell wall synthesis and cell division.

Polymerization of PG

After being flipped to the external side of the cytoplasmic membrane, the cargo Lipid II is incorporated into the nascent PG chain by enzymes known as glycosyltransferase (GTase) and transpeptidase (TPase), which catalyze the linear polymerization of glycan chains and stem peptide crosslinking, respectively. The undecaprenyl pyrophosphate is released after polymerization and is flipped back to the inner leaflet, which will undergo dephosphorylation to recycle the lipid carrier for accepting new precursors (Manat et al., 2014). There are different types of TPase depending on the donor muropeptide (Kuhn, 2019). A universal class of TPase is DD-TPase, which catalyzes the crosslink between the D-Ala at position 4 of a donor

pentapeptide and the mDAP at position 3 of the acceptor stem peptide (4-3 crosslink), either directly or through intermediate peptides. The DD-TPases belongs to class B penicillin-binding protein (bPBPs), which are monofunctional TPases with a non-catalytic "pedestal" domain at the N-terminus to keep the TPase domain away from the membrane and to interact with other proteins (Egan et al., 2020). PBPs were named due to the fact they are the targets of β-lactam antibiotics, such as penicillin, which covalently bind to the catalytic site as a suicide substrate and inactivate their crosslinking activities. *E. coli* has two DD-TPases or bPBPs, PBP2 and PBP3, which are involved in cell elongation and cell division, respectively (Table 1.1). Deletion of either gene will lead to eventually lyse of the cells (Kuhn, 2019). In addition to these monofunctional bPBPs, bacterial cells also contain ubiquitously bifunctional, Class A PBPs (aPBPs) with both GTase and TPase activities. PBP1A and PBP1B are the most important aPBPs and both contain a non-catalytic domain that regulates the GT51-type GTase and Ser-type TPase activity (Typas et al., 2010). Either PBP1A or PBP1B is dispensable for cell viability in many organisms (Hoskins et al., 1999; Paik et al., 1999; Yousif et al., 1985). Although both proteins are semi redundant, PBP1A is preferentially involved in the synthesis of PG during cell elongation while PBP1B mainly functions during division (Denome et al., 1999; Kuhn, 2019). Recent research also demonstrated that PBP1A and PBP1B are more important for growth at alkaline and acidic pH values, respectively, to ensure the bacteria can grow in a wide range of environmental conditions (Mueller et al., 2019). PBP1A also forms a cooperative interaction with PBP2. *In vitro*, binding of PBP2 enhances PBP1A GTase activity, and this interaction also boosts PBP2 TPase activity, increasing the attachment of newly synthesized PG material to sacculus (Banzhaf et al., 2012). In view of its essential role in PG biosynthesis, aPBPs are attractive targets for development of antibacterial drugs to combat antibiotic-resistant bacteria.

An extensive summary on PBP structure and function can be found in a review (Sauvage et al., 2008).

For decades it was thought that aPBPs were the only proteins that have a PG polymerase activity. Recently, it was shown that cell wall synthesis is actually mediated by two different polymerase systems (Meeske et al., 2016). In addition to the well-known aPBPs, the SEDS proteins comprise a second class of bacterial cell wall polymerase, which works in concert with their cognate bPBP to constitute a PG synthase machine. SEDS-bPBP systems are in fact more broadly conserved than aPBPs, although both systems are commonly present in bacteria and functional in parallel (Meeske et al., 2016). RodA was the first identified SEDS protein harboring a novel GTase activity in both *B. subtilis* and *E. coli*, and possibly other bacteria (Cho et al., 2016; Meeske et al., 2016). The RodA PG polymerase repeatedly works with PBP2 for PG transglycosylation and transpeptidation during cell elongation (Cho et al., 2016; Meeske et al., 2016; Sjodt et al., 2020). A recent study showed that PBP2 and RodA form a complex dependent on interaction between their transmembrane and periplasmic domains, rather than their catalytic domains (Liu et al., 2020). In parallel, SEDS-family protein FtsW and its cognate PBP3 provide PG polymerase and crosslinking activity within the divisome, the protein complex involved in cell division (Taguchi et al., 2019). A crystal structure of the RodA-PBP2 complex from *Thermus thermophilus* reveals two main interaction interfaces between the proteins with a 1:1 stoichiometric relationship (Sjodt et al., 2020). Intriguingly, in the complex, RodA shows an approximately 10 Å shift in transmembrane helix 7, resulting in exposure of a large membrane-accessible cavity, possibly for Lipid II accommodation. PBP2 allosterically activates RodA GTase activity through its N-terminal pedestal domain (Sjodt et al., 2020). Negative-stain electron microscopy revealed that the PBP2 in the complex adopts a broad range of

conformations from an extended to a compact conformation, possibly either to facilitate PG polymerization or to favor peptide crosslinking during cell wall synthesis (Sjodt et al., 2020).

PG hydrolysis and remodeling

PG hydrolases play major roles in PG remodeling, maturation and turnover during growth, cell division, cell shape maintenance, bacterial interactions, etc. Each organism encodes many hydrolases that seem to be redundant. Typically each hydrolase has a substrate and PG-linkage specificity, and they only function under certain circumstances (Kuhn, 2019). According to its cleavage site, PG hydrolases can be classified into 5 groups: (1) amidases that cleave the amide bond between MurNAc and L-Ala, the first amino acid of stem peptide; (2) endopeptidases that cleave amide bonds between amino acids within pentapeptide and peptide cross-links; (3) carboxypeptidases that remove the C-terminal amino acid of the peptide stem; (4) N-acetylmuramidases (lysozymes and lytic transglycosylases) that cleave the glycosidic bond between MurNAc and GlcNAc; and (5) N-acetylglucosaminidases that cleave glycosidic bond between the GlcNAc and MurNAc (Vollmer et al., 2008b) (Fig. 1.1). Next, I will describe a few situations in which hydrolases play a role during morphogenesis.

E. coli contains 3 amidases or N-acetylmuramyl-L-Ala amidases, AmiA, AmiB and AmiC, which play roles in septal PG cleavage and drive cell separation during cytokinesis. Double and triple amidase mutants form long chains of cells, and rings of thickened murein appear at division sites in isolated sacculi (Heidrich et al., 2001; Uehara et al., 2010). The amidases are activated by two different pathways: AmiA and AmiB are activated at the cytokinetic ring by outer membrane protein EnvC (Peters et al., 2013; Uehara et al., 2010), while AmiC is activated by the outer-membrane-anchored lipoprotein NlpD (Uehara et al., 2010). Both activator proteins contain a LytM domain (M23 peptidase), although they are not hydrolases

themselves. The EnvC-mediated activation of amidases requires the recruitment of EnvC by FtsEX to the septum by a direct interaction between EnvC and FtsX (Yang et al., 2011). In *B. subtilis*, FtsEX is reported to activate endopeptidases CwlO or LytE during cell elongation (Pichoff et al., 2019). In addition to control of periplasmic hydrolase activity, FtsEX is also a member of the divisome and coordinates PG synthesis of the septum with PG hydrolysis (Pichoff et al., 2019). Similarly, NlpD is reported to couple peptidoglycan hydrolysis and outer-membrane invagination during cell division of *E. coli* (Tsang et al., 2017). PBP5 is the main DD-carboxypeptidases in *E. coli* for shape maintenance. The morphology of PBP5-deficient cell is slightly altered; with deletion of additional DD-carboxypeptidases, the cells become branch, kink and bend (Nelson and Young, 2000).

THE CYTOSKELETON IS A REGULATOR OF BACTERIAL CELL SHAPE

PG must be expanded and remodeled in order for the cell to grow, divide, or change its morphology. PG remodeling requires hydrolysis of the pre-existing PG material and synthesis of new cell wall, which involves the coordinated action of a large number of PG-related enzymes. PG enzymes must be spatially regulated so that the sacculus integrity is not compromised. It is now well known that most bacteria and archaea, like eukaryotes, contain a cytoskeleton. The bacterial cytoskeleton contains proteins that are homologous in structure to eukaryotic tubulin, actin, and analogous to intermediate filaments. Studies in recent years have demonstrated that cytoskeletal proteins play a central role in regulating PG synthesis and hydrolysis in time and place. In the next sections, I will describe the cytoskeletal players together with their associated proteins and their connection with bacterial shape via regulating PG synthesis.

Tubulin-like cytoskeleton

Central Bacterial division protein FtsZ

The tubulin-like protein FtsZ is central to cell division and its polymerized protofilaments form the FtsZ ring, also called the Z ring, at future division sites (Anderson et al., 2004). FtsZ is highly conserved in almost all bacteria and archaea (andMargolin, 2000; 2005). In eukaryotes, nearly all chloroplasts and many mitochondria, which are believed to derive from cyanobacteria and α-proteobacteria, respectively, use FtsZ to divide as well (Margolin, 2000). The crystal structure of FtsZ from the thermophilic bacterium *Thermotoga maritima* revealed that the resemblance of FtsZ to eukaryotic tubulin is due to a conserved tertiary structure rather than the primary sequence throughout the proteins (Löwe, 1998; Lowe and Amos, 1998). FtsZ has four conserved domains based on structural and phylogenetic analysis: a highly conserved N-terminal globular core that contains a GTPase domain, a short, C-terminal conserved (CTC) domain which is called CTT (C-terminal tail) in some literature articles, a flexible and unstructured C-terminal linker (CTL) that connects the GTPase domain to the CTC, and an extreme C-terminal variable (CTV) domain that is highly variable in both length and amino acid composition (Buske and Levin, 2013; Mahone and Goley, 2020; Vaughan et al., 2004). Crystal structures revealed that the N-terminal GTPase domain and CTC fold independently and form two globular structures (Adams and Errington, 2009; Oliva et al., 2004).

FtsZ polymerizes into protofilaments by association of one FtsZ monomer with another in a head-to-tail fashion. The N-terminal GTPase domain is required for FtsZ polymerization, and the key FtsZ residues at the dimer interface are located in this domain (Koppelman et al., 2004; Lu et al., 2001; Redick et al., 2005). The FtsZ polymer is dynamic and its assembly/disassembly occurs in a GTP-dependent manner (Bramhill and Thompson, 1994; Erickson et al., 1996; Mukherjee and Lutkenhaus, 1994). *In vitro*, the single-stranded FtsZ protofilaments have the ability to further assemble into bundles, sheets, tubules, and mini-rings,

depending on the experimental conditions used (Bramhill and Thompson, 1994; Mukherjee and Lutkenhaus, 1994). The assembly of FtsZ monomer into protofilaments is cooperative and occurs at a critical concentration of around 1 μM (Mukherjee and Lutkenhaus, 1998; Romberg et al., 2001). However, when the concentration increases to around 3 μM, an additional assembly event occurs, which might represent protofilaments being held together into high-order structures through extensive lateral interactions (Adams and Errington, 2009; Chen and Erickson, 2005). The CTC is important for interactions between FtsZ and some modulatory proteins. In *E. coli* FtsA and ZipA, two essential proteins of the Z-ring structure and function, are membrane tethers of FtsZ by interacting with the CTC domain (Haney et al., 2001; Ma and Margolin, 1999; Mosyak et al., 2000). In *Caulobacter crescentus* (*C. crescentus*), deletion of the CTC results in disruption of the FtsZ-FtsA interaction (Din et al., 1998). EzrA, an inhibitor of FtsZ assembly in *B. subtilis*, disrupts assembly of FtsZ, but does not appear to interact with a truncated protein missing the CTT region (Huber et al., 2008).

It has been reported that the CTV domain in *B. subtilis* is both necessary and sufficient to induce lateral interactions *in vitro* (Buske and Levin, 2012). Specifically, replacing the 6-resiude CTV of *B. subtilis* with the 4-residue CTV of *E. coli* completely abolished *B. subtilis* FtsZ protofilaments lateral interactions while the *E. coli* FtsZ chimeric protein constructed from swapping the CTV with *B. subtilis* CTV formed higher-order structures. Furthermore, site-directed mutagenesis of the CTV region suggested that charged amino acids of the CTV played an important role in lateral interactions. In addition, the CTL domain has also been implicated in a role of regulating lateral interactions. Deletion of the CTL domain in FtsZ of *C. crescentus* resulted in a hyper-stable filament superstructure *in vitro* (Sundararajan and Goley, 2017).

Bacterial division site selection

Regulation of the Z-ring positioning and, thus, the initiation of cell division in the right time and place plays an important role in accurately determining cell length. There are two partially redundant, negative regulatory mechanisms for spatial control of cell division: the Min system and nucleoid occlusion (NO) system (Adams and Errington, 2009; Rothfield et al., 2005).

The min system involves a cell division inhibitor that has a higher concentration at cell poles and lower concentration at midcell, which leaves the midcell as the only site for Z-ring assembly (Margolin, 2000; Rothfield et al., 2005). It consists of three proteins in *E. coli*: MinC, D, and E. MinC is an inhibitor of cell division by directly interacting with FtsZ CTT to prevent formation of a stable Z ring at the sites close to cell poles (de Boer et al., 1989; Hu et al., 1999). MinC oscillates rapidly in a pole-to-pole manner under of control of MinD and MinE (Hu and Lutkenhaus, 1999, 2001; Raskin and de Boer, 1999). MinD activates MinC activity by interacting with MinC, while MinE is a topological specificity factor and forms a MinE ring at or near the midcell to restrict active MinC to the vicinity of the cell poles (de Boer et al., 1989; Hu and Lutkenhaus, 1999; Rothfield et al., 2005). MinD is a weak ATPase whose hydrolytic activity is stimulated by MinE in the presence of phospholipid vesicles, indicating that MinD has to be bound to a membrane surface for ATP hydrolysis (Hu and Lutkenhaus, 2001). MinD can bind to both MinE and MinC, and recruits them to the membrane, although MinE is the preferred binding partner (Hu et al., 2003; Lackner et al., 2003). When the cell grows long enough, FtsZ assembles into a ring-like structure at the midcell when the concentration of MinC drops below a critical level (Lutkenhaus, 2007; Rothfield et al., 2005). Thus, cells can actually control their lengths by altering the ratio of MinC to MinDE to create the MinC-free zone in which division can take place (Young, 2010).

The NO system prevents Z-ring assembly in the vicinity of the nucleoid before replication or chromosome segregation is complete to ensure cell division occurs at the mid-cell (Rothfield et al., 2005; Woldringh et al., 1990). It is mediated by FtsZ inhibitor proteins SlmA in *E. coli* and Noc in *B. subtilis* (Bernhardt and De Boer, 2005; Wu and Errington, 2004). Mutation in either of the encoding genes results in a synthetic lethal phenotype with a *min* mutation (Wu and Errington, 2004). Although possessing similar modes of action, SlmA and Noc have no homology in sequence. SlmA is a putative DNA-binding protein belonging to TetR family and is bound to specific DNA sites that are evenly distributed on the chromosome but not the Ter region (Cho et al., 2011). SlmA dimer-of-dimers spreads along the DNA and forms a highly-order nucleoprotein complex to prevent Z-ring formation in the vicinity of the DNA complex (Cho et al., 2011; Tonthat et al., 2013). Noc, a member of the ParB-family, is also a sequence-specific DNA-binding protein that has 74 binding sites on the chromosome except for the Ter region in *B. subtilis* (Wu et al., 2009). This study also showed that inserting an array of new Noc-binding sites near the replication terminus of the chromosome delays division and results in elongated cells, which serves as an example of how nucleoid occlusion can regulate cell length.

The divisome assembly, activation, and control of PG synthesis during cell division

FtsZ is the first localized component of the division machinery that forms the Z ring at the inner membrane of the midcell envelope, marking the site for future cell division (Bi and Lutkenhaus, 1991). The Z-ring assembly occurs in a rapid and dynamic process with turnover of FtsZ monomer in the ring occurring with a half time of 8-9 s (Anderson et al., 2004), and during which spiral-like structures of FtsZ have been observed, suggesting that during Z-ring formation, the spiral intermediates may be produced and the Z ring forms by the collapse of a helical intermediate (Ben-Yehuda and Losick, 2002; Michie et al., 2006; Thanedar and Margolin, 2004).

Once assembled, the Z ring functions as a scaffold to recruit other cell division proteins, known as divisome, to the midcell (Goehring and Beckwith, 2005; Vicente and Rico, 2006).

The divisome assembly in *E. coli* and *B. subtilis* occurs in a two-step mechanism (Aarsman et al., 2005; Gamba et al., 2009). The early step involves the essential protein FtsZ, FtsZ tether proteins FtsA and ZipA (EzrA in *B. subtilis*), FtsZ ring stabilization protein ZapA, and FtsEX, which localize at midcell in contract with the inner face of the cytoplasmic membrane. The late step consists of the assembly of the remaining divisome proteins including FtsK, FtsQLB subcomplex, FtsW-FtsI (PBP3) subcomplex, and FtsN, which have the main domain located outside of the cytoplasmic membrane. In addition, other proteins such as the PG synthase PBP1B, PG hydrolases, and outer membrane proteins LpoB, CpoB, and TolA also associate with the divisome (Gray et al., 2015). A detailed list of divisome components of *E. coli* and *B. subtilis* are summarized in Table 1.1 and Table 1.2, respectively. A time delay between the assembly of the early proteins and late proteins has been observed (Aarsman et al., 2005; Gamba et al., 2009). In *E. coli*, the localization studies suggested that the divisome assembly occurs in a roughly linear pathway, while in *B. subtilis* the late divisome proteins assemble interdependently. However, a more recent work in *E. coli* provided a revised model that the production of the division apparatus occurs by the sequential assembly of at least three subcomplexes (Goehring et al., 2006). Following the completion of divisome assembly, the Z ring constricts ahead of the leading edge of the newly synthesized division septum, which results in cell division. The division modes are different between organisms: in *E. coli* septal PG synthesis is accompanied by the constriction of the outer membrane; whereas in *B. subtilis* a complete cross wall is usually formed before daughter cells subsequently separate (Adams and

Errington, 2009). The distinction is probably due to the difference of cell envelope structures between Gram-positive and Gram-negative bacteria.

During cell division, new PG of the septum must be synthesized and/or existing PG must be remodeled to create cell poles for both daughter cells. Multiple divisome proteins have been reported to stimulate septal PG synthesis, directly or indirectly. ABC-transporter like protein complex FtsEX, which interacts with FtsA, is required for septal PG synthesis and hydrolysis (Du et al., 2016, 2020). PBP3(FtsI)-FtsW subcomplex works in concert with PBP1B to contribute to septal PG synthesis (Bertsche et al., 2006; Taguchi et al., 2019). In *E. coli*, PBP1B requires FtsW and PBP3 for septal localization and the three proteins were found to form a ternary septal synthase complex (Leclercq et al., 2017). FtsQ-FtsL-FtsB complex seems to function as a key checkpoint for septal PG synthesis (Boes et al., 2019; Egan et al., 2020). In the divisome, FtsQLB inhibits PBP1B and PBP3 activity until enough FtsN accumulates at mid-cell (Ursinus et al., 2004; Yahashiri et al., 2015). When above a crucial threshold, FtsN triggers septation by relieving the inhibition of PBP1B and PBP3 exerted by FtsQLB (Liu et al., 2015). The C-terminal SPOR domain of FtsN may contribute to its midcell localization via specific recognition of septal PG. In addition to guiding septal PG synthesis, FtsZ has been reported to be involved in preseptal elongation, a transition event that is independent on PBP3 (FtsI) and happens after cell elongation ends and before cell division commences (Potluri et al., 2012). Immediately prior to any visible membrane invagination, new PG is incorporated into a ring-like structure around midcell, a process that requires the presence of FtsZ and ZipA, but does not require the participation of downstream members of the divisome, or the MreB-directed cell wall elongation complex (Varma et al., 2007). Enzymes for Lipid II synthesis and PG synthesis are

recruited to the Z ring to carry out lateral cell wall elongation (Aaron et al., 2007; Varma et al., 2007).

Actin-like cytoskeleton

Bacterial cell elongation central protein MreB

The actin-like cytoskeletal protein MreB is widespread in bacteria (Carballido-López, 2006). It is essential for determination and maintenance of cell shape in most rod-shaped or curved bacteria, although there are some exceptions with some *Actinobacteria* or *Rhizobiales* lacking MreB (Shi et al., 2018). *E. coli* MreB forms membrane-bound, anti-parallel double protofilaments that are essential for rod-shape determination (van den Ent et al., 2014). Like eukaryotic actin proteins, they locate just beneath the cell surface and undergo reversible polymerization, which is regulated by binding and hydrolysis of ATP.

MreB was first identified by mutations altering cell shape in *E. coli* (Wachi et al., 1987). It appears to be essential in most bacteria that contain MreB with an exception of *Streptomyces* (Carballido-López, 2006). Although there is only one MreB homolog in *E. coli*, many bacteria, particularly Gram-positives, have multiple MreB homologs. *B. subtilis* has three paralogues, MreB, Mbl, and MreBH, and they appear to have partially redundant functions (Kawai et al., 2009). Depletion of MreB or inhibition of its filament formation (for example, with A22, i.e. S-(3,4-dichlorobenzyl) isothiourea) results in elongation cessation, diameter (width) enlarging, and growth with a spherical morphology in both *E. coli* and *B. subtilis* (Jones et al., 2001; Kruse et al., 2005). In contrast, *B. subtilis mbl* mutants are highly twisted and bent at irregular angles, and some cells are affected in width with bulging and lysis (Jones et al., 2001). *B. subtilis mreBH* mutants have narrow and longer cells, especially under low Mg^{2+} conditions (Carballido-López et al., 2006; Kawai et al., 2009).

The exact localization pattern of MreB in bacterial cells has been a highly debated subject (Errington, 2015). Early studies of MreB localization using fluorescent protein fusion revealed long helical filaments that encircle the cytoplasm (Divakaruni et al., 2007; Figge et al., 2004; Jones et al., 2001; White et al., 2010). However, more recent data using higher-resolution imaging techniques indicated that MreB forms discrete short membrane-bound patches or filaments and the long helical localization pattern was an artifact generated by the fluorescent protein tag in the MreB-GFP fusion (Billaudeau et al., 2019; Swulius and Jensen, 2012). Multiple studies have shown that these filaments rotate independently around the cell circumference (Errington, 2015; Garner et al., 2011; van Teeffelen et al., 2011). A22 treatment in *E. coli* decreases the number of moving MreB puncta but does not affect velocity, indicating that MreB motion is not caused by MreB treadmilling (Shi et al., 2018; van Teeffelen et al., 2011). Instead, MreB dynamics are closely dependent on cell-wall assembly, which was supported by the fact that MreB rotation is inhibited by some antibiotics that disrupt cell-wall crosslinking (Dominguez-Escobar et al., 2011; Garner et al., 2011; van Teeffelen et al., 2011). This suggests that the cell-wall synthesis machinery either forms a novel type of extracellular motor that guides the motion of cytoplasmic MreB, or is indirectly required for activity of an unidentified motor (van Teeffelen et al., 2011).

Controlling PG synthesis during cell elongation

In rod-shaped bacteria, the elongasome (also called the Rod complex) is a multi-protein complex organized by MreB, and is used to facilitate insertion into the lateral cell wall during cell elongation. Different from general actin proteins, *E. coli* MreB can bind directly to the cytoplasmic face of the inner membrane through an N-terminal amphipathic helix (Salje et al., 2011). To exert its role in the regulation of cell wall growth, which occurs in the periplasm,

MreB also interacts with the conserved inner-membrane proteins MreC, MreD and RodZ (Alyahya et al., 2009; Bendezu et al., 2009; Kruse et al., 2005; Typas et al., 2011). Genes encoding MreC and MreD are located immediately downstream of *mreB* and are also essential proteins that have similar depletion phenotypes as *mreB* (Kruse et al., 2005). In addition to interact with MreB, MreC also interacts with MreD and several PBPs, including PBP2. MreC has been suggested to function in activating cylindrical peptidoglycan synthesis during elongation and is thought to induce conformational changes in PBP2 that plays a central role in both stimulating GTase activity of RodA and modulating MreB filament formation to orient new synthesis (Egan et al., 2020; Rohs et al., 2018). A crystal structure of PBP2 from *Helicobacter pylori* reveals a "closed" conformation at the N-terminal region in an unbound state. Upon binding with MreC, PBP2 "opens up" and reveals a hydrophobic zipper as the interaction interface, which is essential for maintaining cell shape and growth (Contreras-Martel et al., 2017). *In vivo* fluorescence resonance energy transfer (FRET) data suggest that MreC and MreD affect the conformation of the RodA–PBP2 complex differently, allowing switching PBP2 activity between "on" and "off" states and thus contributing to the regulation of cell wall synthesis during elongation (Liu et al., 2020). The confirmational changes of PBP2-RodA induced by MreC possibly corresponds to the one in PBP2 as observed in the MreC-PBP2 crystal structure (Liu et al., 2020).

RodZ is a bitopic integral membrane protein that is required for rod shape maintenance. *E. coli* RodZ has an N-terminal helix-turn-helix motif at the cytoplasmic domain that is required for binding MreB while its periplasmic domain interacts with several cell wall-synthesis enzymes (Morgenstein et al., 2015; Van Den Ent et al., 2010). Deletion of *rodZ* leads to misassembly of MreB and a round cell phenotype that can be rescued by an overdose of FtsZ (thus its name)

(Bendezu et al., 2009). Moreover, deletion of *rodZ* abolishes the rotation of MreB around the cell circumference (Morgenstein et al., 2015). RodZ mediates MreB motion by coupling MreB to periplasmic PBP2 (TPase) and/or RodA (GTase), which form a stable subcomplex during cylindrical PG synthesis. Intriguingly, MreB rotation is not necessary for rod shape determination but may promote the robustness of the cell wall (Morgenstein et al., 2015)
In addition, RodZ can modulate the curvature localization of MreB to regulate cell shape (Bratton et al., 2018; Colavin et al., 2018). In *E. coli* and *B. subtilis*, MreB polymers are preferentially localized to areas of the cell with specific curved geometries except for the area of cell poles. In the absence of RodZ, MreB loses its curvature preference and cells lose rod shape (Bratton et al., 2018; Colavin et al., 2018). Induction of RodZ expression increases the curvature sensitivity of MreB and decreases cell width in a concentration-dependent manner.

Intermediate filament-like cytoskeleton

Bacterial intermediate filaments (IFs) have been identified and are also involved in bacterial shape determination and maintenance. IF-like proteins are widespread in bacteria and share a similar domain arrangement, composed of a central rod domain with alternating coiled-coil segments and short linkers and flanked by head and tail domains (Bagchi et al., 2008). They can spontaneously assemble into filaments or sheets without nucleotide binding and hydrolysis (Lin and Thanbichler, 2013).

Crescentin (CreS) was the first identified IF-like protein in prokaryotes, and it plays a role in generating curvature in *C. crescentus* (Ausmees et al., 2003). CreS forms a filamentous structure that is anchored at the curvature of the inner membrane parallel to the long cell axis in an MreB-dependent manner (Charbon et al., 2009; Woldemeskel and Goley, 2017). It is believed that physical force applied to the underlying cell envelope by CreS reduces the rate of new PG

incorporation, while the opposite side of the cell wall will grow with a comparatively faster rate, resulting in a curved sacculus (Cabeen et al., 2009). Deletion of the crescentin-encoding gene *creS* results in straight rod-shaped cells in *C. crescentus* (Ursell et al., 2014); the loss of curvature is a slow, growth-dependent process that allows a cell to remodel its PG in the absence of crescentin for a straight-cell morphology (Cabeen et al., 2009).

Another IF-like protein is FilP in *S. coelicolor*, a filamentous multicellular bacterium with polar growth at hyphal tips. Deletion of *filP* leads to defects in growth and morphology with reduced rigidity and elasticity of the hyphae (Bagchi et al., 2008). Cell wall structure is not substantially affected after deletion of *filP* (Fuchino et al., 2013). FilP can assemble readily and spontaneously into a regularly cross-linked network structure *in vitro*, consisting primarily of hexagonal elements, and the *in vivo* localization is consistent with a network structure of FilP, indicating that FilP is likely to provide a direct mechanical support to the cell tips (Fuchino et al., 2013). Further study revealed that Na^+ and K^+ cations play important roles in induction of the hexagon meshwork (Javadi et al., 2019). Under different buffer conditions, FilP forms compact striated protofilaments, filament bundles, hexagon network, or their mixtures (Bagchi et al., 2008; Fuchino et al., 2013; Javadi et al., 2019). Since FilP cytoskeleton forms polar gradients in hyphae undergoing active growth, it provides an example where polar growth is coupled to the formation of an IF cytoskeleton in bacteria. Details about the connection between DivIVA, FilP, and Scy (an additional IF protein) in hyphal tip extension of *Streptomyces* are discussed in a later section.

Bactofilin is another class of cytoskeletal element that are widely conserved among bacteria. In *C. crescentus*, the bactofilins BacA and BacB form a sheet-like polymer that lines the inner membrane of the stalked cell pole and recruits the bifunctional PBP called PBPC to the base of the stalk during the transition from swarmer to stalked cell (Kuhn et al., 2010), thus

complementing the function of the actin- or tubulin-like cytoskeleton in the regulation of PG biogenesis. The extent to which these cytoskeletal elements are scaffolds for coordinating peptidoglycan synthesis and hydrolysis remains to be addressed.

STREPTOMYCES IS A MODEL ORGANISM TO STUDY BACTERIAL CELL MORPHOLOGY

Streptomyces, members of the phylum Actinobacteria with high G+C content, are among the most morphologically complex bacteria (Chater and Losick, 1997; Chater and Chandra, 2006). These Gram-positive, largely soil-dwelling bacteria are nature's most powerful chemists and produce a diversity of secondary metabolites, including antibiotics, immune-suppressors, and other biologically active compounds (Hopwood, 2007). *Streptomyces* also exhibits a complex life cycle with the alternation between unicellular spores and multicellular mycelia. The inter-conversion between these two distinct forms makes it an attractive model for the study of prokaryotic development.

Streptomyces life cycle

The *Streptomyces* life cycle starts with the germination of dormant uninucleoid spores when they encounter suitable conditions. Spore germination involves swelling of the spore, polarization of growth and formation of one or two germ tubes. The germ tubes grow by tip extension and occasionally branches, forming a vegetative mycelium (Flärdh and Buttner, 2009; Flärdh et al., 2012). During the growth of vegetative hyphae, chromosomal DNA is replicated, but cell division occurs only occasionally to from vegetative cross-walls, dividing the vegetative hypha into elongated compartments that contain multigenomic DNA without obvious segregation or condensation (Bush et al., 2015). In response to nutrient depletion and other signals such as extracellular signalling cascades, stress response, and metabolism, the aerial

hyphae grow into the air by breaking colony surface tension and escaping the aqueous environment to form an aerial mycelium (McCormick and Flärdh, 2012). The growth of aerial hyphae is also accompanied by extensive replication of chromosomes. After aerial hyphae stop extending, these sporogenic hyphae synchronously form septa that divide the syncytial compartments into long strings of prespores with each containing a single chromosome. The prespore compartments then undergo change their shapes, thicken their cell walls and eventually produce a polyketide pigment as prespores develop into a chain of mature spores. The unicellular spores are then dispersed and help bacteria survive harsh conditions. Upon encountering new favorable conditions, the spores can initiate germination to start a new life cycle. In addition to this classically-defined life cycle, a subset *Streptomyces* species can exhibit a different mode of development termed "exploration" (Fig. 1.3) (Jones and Elliot, 2017; Jones et al., 2017). Explorer cells are a type of non-branching vegetative hyphae that can rapidly transverse solid surfaces. Exploration is triggered by fungal interactions, low glucose or abundant amino acids, and requires the production of volatile organic compound (VOC) trimethylamine (TMA), which alkalinizes the medium and further induces exploratory growth in other physically separated growing cells (Jones et al., 2019). The study of the biological roles of VOCs are starting to emerge, and recently it was shown that reduced iron availability in the environment surrounding exploratory cells affected interspecies interactions, indicating an important role for VOC in modulating microbial behaviors and their communities (Jones et al., 2019).

Streptomyces **developmental genes and regulation**

A programmed regulatory pathway controls *Streptomyces* morphological differentiation. Two classes of genes are involved to regulate the process: *bld* (bald) and *whi* (white). The *bld* genes are required for the formation of a fluffy aerial mycelium, and therefore mutants for these

loci fail to form an aerial mycelium and give rise to a "bald" and lustrous colony surface (Champness, 1988; Merrick, 1976). The *bld* genes are divided into two classes (Bush et al., 2019). The typical and well-known class is defined as positive regulators, and mutants for these genes are unable to initiate development and thus are trapped into the vegetative mycelium stage. The second group is defined as negative regulators. It is a smaller but rising class, including members BldD, BldC, and BldO. Deletion of these genes results in colonies entering development prematurely, bypassing the aerial hyphae stage and promoting sporulation in the vegetative mycelium (Flärdh and McCormick, 2017). The *whi* genes are necessary for the formation of mature spores, mutations at these loci result in colonies that can make aerial filaments but fail to produce the spores with polyketide spore pigment, resulting in a characteristic "white" or light-grey colony surface compared with the darker color in wild type (Chater, 1972; Hopwood et al., 1970; Ryding et al., 1999).

Over the past decades, some progress has been made in the dissection of how these Bld and Whi proteins regulate the cell biological processes underlying the morphological and physiological differentiation, particularly in *S. coelicolor*, *S. griseus*, and *S. venezuelae* (Bush et al., 2015). BldD is a master regulator that sits at the top of the developmental regulatory network. It represses transcription of various genes involved in development and, thus, controls the onset of differentiation and the transition between developmental stages in *Streptomyces* (Bush et al., 2015). Using ChIP-chip analysis, over 150 BldD-binding targets have been identified in *S. coelicolor*, including approximately 42 additional genes that encode regulatory proteins, including BldA, WhiB, BldM, BldC and at least two developmentally important sigma factors: σ^{WhiG} and σ^{BldN} (den Hengst et al., 2010; Tschowri et al., 2014) . The activity of BldD is regulated by the second messenger 3', 5'-cyclic diguanosine monophosphate (c-di-GMP), which

mediates the dimerization of BldD by forming a novel c-di-GMP tetramer at the BldD dimer interface (Tschowri et al., 2014). Intracellular c-di-GMP is synthesized by diguanylate cyclases containing a conserved GGDEF domain and degraded by phosphodiesterases containing an EAL domain (Hull et al., 2012). In *S. coelicolor*, it has been reported that CdgB functions as a diguanylate cyclase, and there are another 7 proteins containing the GGDEF motif in genome (Tran et al., 2011). Of note, some proteins contain both GGDEF and EAL domains, such as RmdA and RmdB (Gallagher et al., 2020; Hull et al., 2012). So far only the phosphodiesterase activity of RmdA and RmdB were reported. Genetic analysis showed that both CdgB and RmdAB are involved in *Streptomyces* development. Recently, a novel protein, RsiG, a cognate anti-sigma of factor of σ^{WhiG}, was identified and reported to be regulated by c-di-GMP in *S. venezuelae* (Gallagher et al., 2020). σ^{WhiG}, one of the direct targets repressed by BldD, is known to play a role in the transition from aerial hyphae into spores and spore maturation, and its activity is controlled by RsiG in a c-di-GMP-dependent manner (Gallagher et al., 2020; McCormick and Flärdh, 2012). Specifically, when the intracellular concentration of c-di-GMP is high, RsiG is "armed" with a c-di-GMP dimer, and sequesters σ^{WhiG}, preventing its interaction with core RNA polymerase and thus blocking morphological differentiation. When the c-di-GMP level is reduced, σ^{WhiG}-RsiG heterodimer disassociates, allowing σ^{WhiG}-guided transcription (Gallagher et al., 2020). Collectively, the intracellular concentration of c-di-GMP serves as the major checkpoint in *Streptomyces* development, the onset and later stages of morphological differentiation controlled by BldD and σ^{WhiG}-RsiG, respectively. How the intracellular c-di-GMP is changed to regulate BldD and σ^{WhiG}-RsiG activity needs further investigation.

Another important regulator of development is the WhiAB heterodimer. WhiA is a transcriptional regulator belonging to a eukaryotic-like homing endonuclease family that contains the fold but not the catalytic side chains (Kaiser et al., 2009; Knizewski and Ginalski, 2007). WhiB is the founding member of Wbl (WhiB-like) family, the proteins of which are Actinomycete-specific and carry a [4Fe-4S] iron-sulfur cluster (den Hengst and Buttner, 2008; Soliveri et al., 2000). ChIP-seq analysis in combination with microarray transcriptional profiling, revealed that WhiA functions almost equally as either an activator or repressor of the expression of around 240 genes in *S. venezuelae* (Bush et al., 2013). A genome-wide ChIP-seq study on WhiB revealed a strikingly identical WhiB regulon to that of WhiA, and each being dependent on the presence of the other for *in vivo* DNA binding, suggesting that WhiA and WhiB function cooperatively as a heterodimer to regulate expression of a common set of WhiAB targets (Bush et al., 2016). Several genes encoding key proteins involved in cell division and chromosome segregation, such as *ftsZ*, *ftsW*, and *ftsK*, are directly activated by WhiAB (Bush et al., 2013; Bush et al., 2016). Sporulation-specific sigma factor σ^{WhiG} and the diguanylate cyclase CdgB are also WhiAB targets. One example of the genes that are repressed by WhiAB is *filP*, encoding a key IF protein of the polarisome that directs apical growth. This might explain the orderly cessation of aerial apical growth prior to sporulation-specific cell division.

Recently, a novel gene *bldO*, activated by WhiAB, was identified and characterized (Bush et al., 2017). Strikingly, ChIP-seq analysis revealed a single target of BldO for repression in the entire genome, *whiB*. Either deletion of *bldO* or overexpression of *whiB* causes precocious hyper-sporulation (Bush et al., 2017). Thus, in addition to the global regulator BldD, BldO is the second identified repressor that participates in multi-layer control for *whiB* through the single BldO-WhiB link (Flärdh and McCormick, 2017). The signal that BldO responds to is still

unknown, and it is speculated that a ligand may interact with its C-terminal domain to control its activity.

BldC is another developmental transcription factor either as a repressor or an activator of transcription (Bush et al., 2019). Deletion of *bldC* in *S. venezuelae* resulted in a bald phenotype due to bypassing the formation of the aerial mycelium. BldC is a small protein with a winged Helix-Turn-Helix motif related to the DNA-binding domains of MerR-family (Hunt et al., 2005). However, unlike classical members of the MerR family, BldC binds to DNA at a variable number of direct repeats, thus allowing a cooperative, head-to-tail oligomerization on target DNA (Schumacher et al., 2018). For example, BldC forms a head-to-tail oligomerization of two BldC monomers on the two directs repeats of *whiI* promoter; whereas it forms a head-to-tail oligomerization of four BldC monomers on the four direct repeats of *smeA* promoter.

Germination and hyphal growth

Streptomyces spores, or exospores, remain physiologically inert and dormant in the environment until they encounter favorable conditions. Although the signals that trigger spore germination for *B. subtilis* have been extensively studied, very little information has been discovered for *Streptomyces*. An early study showed that divalent cations, such as Ca^{2+} and Mg^{2+}, stimulate *Streptomyces* spore germination (Eaton and Ensign, 1980; Hirsch and Ensign, 1976), although the underlying mechanism remains unclear. In order to resuscitate dormant spores, *Streptomyces* requires the action of resuscitation-promoting factors (Rpfs), a type of cell wall hydrolase or cell wall-lytic enzyme that cleave and remodel the spore peptidoglycan during germination (Sexton et al., 2015). The *S. coelicolor* genome encodes 5 potential Rpfs, and one of the proteins, RpfA, is required for spore germination and is controlled by three nucleotide second messengers at multiple levels (St-Onge et al., 2015). The first level is at transcription

initiation by the cyclic AMP receptor protein (CRP); the second level is transcriptional attenuation mediated by a riboswitch in response to cyclic di-AMP; and the third one is at posttranslational proteolysis as a part of the stringent response to the levels of ppGpp (St-Onge et al., 2015). After receiving and responding to the signals, the spore initiates germination by swelling. Subsequently, polar growth initiates to produce one or two germ tubes. Extensive protein synthesis occurs at this stage to prepare for vegetative growth (Strakova et al., 2013). The determination of a polarized growth site also requires the activity of cell wall-lytic enzymes to hydrolyze the old spore PG and remodel the cell wall for new vegetative hyphae polar growth (Sexton et al., 2020). Germ tubes grow by tip extension and branching to produce a network in the vegetative mycelium. Using cryogenic-electron tomography (cryo-ET), Sexton and Tocheva (2020) found that the PG thickness of the germinating spore and germ tube are comparable to those seen in mature spores and vegetative hyphae, respectively. Furthermore, it seems that the inner layer of the spore wall is continuous with the new vegetative germ tube cell wall, and the outer layer of the spore wall and spore coat are peeled away from where the germ tube has emerged, suggesting that the inner and outer layers of spore wall have different structures and functions during germination and vegetative growth (Beskrovnaya et al., 2021; Sexton and Tocheva, 2020).

Different from eukaryotes, the prokaryotic homolog of the cytoskeletal actin and tubulin proteins in *Streptomyces* are not involved in polar growth, as strains lacking either *ftsZ* or *mreB* are still viable and grow by tip extension (Mazza et al., 2006; McCormick et al., 1994). Instead, the apical growth of *Streptomyces* is directed by the polarisome (also called the tip-organizing center (TIPOC)) that consists of three scaffolding proteins: DivIVA, Scy, and FilP (Bush et al., 2015; Caccamo and Brun, 2018; Flärdh et al., 2012; Holmes et al., 2013). The three coil-coiled

proteins are able to interact with each other, contributing to a stabilized polarisome. DivIVA was the first identified component of the *S. coelicolor* polarisome. It is essential for viability and localizes at the tips of hyphae and potential sites for branching along the hyphae (Flärdh, 2003; Hempel et al., 2008). DivIVA is directly involved in hyphal tip extension and branching site establishment, suggesting a role in directing cell wall synthesis and thus cell shape determination. Scy (*Streptomyces* cytoskeletal element), is an IF protein that colocalizes with DivIVA and has been suggested to function as a scaffold to stabilize the polarisome by interacting with DivIVA (Holmes et al., 2013). In *S. coelicolor*, Scy also interacts with, and recruits, ParA to the tips of aerial hyphae and regulates ParA polymerization along the hyphae, suggesting a potential role of coordination of hyphal growth and chromosome segregation into prespore compartments (Ditkowski et al., 2013). FilP, encoded by the gene downstream of *scy*, is an IF-like protein that forms a interconnected network *in vitro*. In *S. coelicolor*, immunofluorescence microscopy revealed that FilP accumulates in polar gradients that localizes immediately behind DivIVA in hyphae undergoing active tip extension (Fuchino et al., 2013). Live cell imaging in *S. venezeulae* further demonstrates that this apical gradient localization pattern is growth-dependent and immediately dissipates upon growth arrest (Fröjd and Flärdh, 2019). *filP* or *scy* was dispensable for viability, but the mutation in either of them caused irregular hyphal morphology and defective polar growth (Bagchi et al., 2008). DivIVA is required to recruit FilP to the apical gradient, and deletion of *filP* affects the amount and distribution of DivIVA foci at the tips, which might explain the defective morphology of *filP* mutant. How DivIVA coordinates the cell wall machinery and contributes to the cell morphology is largely unknown. It has reported that DivIVA interacts with a cellulose synthase-like protein (ClsA) at the hyphal tip to coordinate intracellular and extracellular activities (Xu et al., 2008). ClsA is a membrane protein responsible

for synthesizing β-glycan-containing polysaccharides, and was reported to be involved in *Streptomyces* hyphal growth and morphological differentiation (Xu et al., 2008). GlxA is another protein localized at hyphal tips and is required for glycan deposition. *glxA* sits immediately downstream of *clsA*, and encodes a radical copper oxidase, suggesting that it may oxidize the glycan as it is secreted (Chaplin et al., 2015; Liman et al., 2013).

Cell division

Filamentous *Streptomyces* possess two distinct types of cell division during the life cycle that lead to formation of vegetative cross-walls and sporulation septa. The two modes of cell division are different in various aspects. Vegetative-type cell division only occurs occasionally in the branching mycelium, which divide the vegetative hyphae into long compartments containing mutigenomic DNA. However, sporulation-specific cell division occurs in sporogenic aerial hyphae during reproductive growth, where dozens of evenly-distributed sporulation septa are formed simultaneously along the hyphae. The outcome of this development-associated division leads to formation of prespore compartments, with only one copy of the chromosome in each. Moreover, cross-wall formation does not require constriction of cell membrane and thus there is no cell-cell separation, whereas during the formation of sporulation septa, cell-cell separation subsequently occurs to form individual spores. Although differences exist, both forms of cell division are directed by cell division protein FtsZ (Bush et al., 2015). Proteins involved in sporulation-specific cell division is summarized in Table 1.3.

In rod-shaped bacteria, like *E. coli* and *B. subtilis*, conditional mutations of *ftsZ* results in a filamentous morphology at restrictive temperatures and eventually loose viability. In contrast, *Streptomyces ftsZ* null mutant is viable, although it is blocked septum formation, indicating that cell division is dispensable for *Streptomyces* vegetative growth but required for sporulation

(Cantlay et al., 2021; McCormick, 2009; McCormick et al., 1994). Obvious homologs of proteins for negative control systems that spatially regulate septum formation, such as Min system and NO system, are missing in streptomycetes. Therefore, it was reasonable to speculate that *Streptomyces* may use a positive control mechanism for cell division site determination. In other words, some proteins arrive earlier to recruit FtsZ at the future division sites. The first protein that is known to fulfill this function is SsgA (sporulation of *Streptomyces* griseus), which was initially identified as suppressing a hyper-sporulating mutant of *S. griseus* (Kawamoto and Ensign, 1995). SsgA is the founding member of the family of SsgA-like proteins (SALPs), which are exclusively present in sporulating Actinomycetes and include SsgA-G paralogs in *Streptomyces* (Noens et al., 2005; Traag and van Wezel, 2008). It was reported that each player of the SALPs has an a specific role during sporulation and spore maturation in *S. coelicolor* with SsgA and SsgB being required for sporulation-specific cell division (Keijser et al., 2003; Noens et al., 2005). Interestingly, transcription of *ssgA* in *S. coelicolor* does not depend on the *whi* sporulation genes, but instead depends on the IclR-family regulator SsgR encoded by the gene immediately upstream *ssgA* (Traag et al., 2004). In contrast, the transcription of *ssgA* in *S. griseus* is strongly affected by *adpA*, not by the SsgR homologue, indicating a different regulatory mechanism of *ssgA* in two phylogenetically different *Streptomyces* species (Yamazaki et al., 2003). Furthermore, both *ssgA* and *ssgB* are directly repressed by master regulator BldD, and transcription initiation of *ssgB* is mediated by BldD-repressed SigH, a sigma factor involved in regulation of stress responses, forming a two-layer control of *ssgB* by BldD (den Hengst et al., 2010; Kelemen et al., 2001; Kormanec and Sevcikova, 2002).

SsgA has a highly dynamic localization pattern during development and it is believed to localize to the sites where cell wall is being actively remodeled, such as at hyphal tips, branch

sites, and future division sites (Jakimowicz and van Wezel, 2012; Noens et al., 2007). In sporogenic cells, SsgA forms foci at sites of future cell division and is thought to recruit SsgB (Noens et al., 2007). SsgB then recruits FtsZ, which forms Z ring in an evenly spaced ladder-like pattern along the sporogenic hyphae (Willemse et al., 2011). SsgB stimulates GTP-induced FtsZ polymerization *in vitro* (Willemse et al., 2011). Crystal structure of SsgB from *Thermobifida fusca* revealed similarity to a class of single-stranded DNA/RNA-binding proteins, but the electro-negative surface indicates that SALPs are not likely to bind nucleic acid. The conserved hydrophobic site of SsgB might be the potential site for protein–protein interaction (Xu et al., 2009). The detailed mechanism regarding how SsgA and SsgB control the Z-ring assembly is still unknown and required further study.

In addition to the SALPs, another Actinomycete-specific integral membrane protein, CrgA, is reported to influence Z-ring formation (Del Sol et al., 2006; Del Sol et al., 2003). Overexpression of CrgA inhibits the formation of productive Z ring, thus resulting in proteolytic turnover of FtsZ.

To ensure septum formation and cell-cell separation, the early stages of divisome assembly requires FtsZ to be tethered and stabilized onto the cytoplasmic membrane, but FtsZ does not directly interact with the membrane. Intriguingly, *Streptomyces* lacks FtsA, ZipA and Zap proteins which traditionally anchor Z ring to the membrane and enhance Z-ring stability in other bacteria. In *B. subtilis*, it has reported that SepF is required for proper sporulation septation, and it functions as a Z-ring membrane anchor and stabilizes FtsZ protofilaments *in vitro* (Duman et al., 2013; Hamoen et al., 2006; Singh et al., 2008). Most *Streptomyces* contains three SepF homologs SepF1, SepF2, and SepF3. Schlimpert et. al., (2017) found that SepF and SepF2 are part of the divisome by directly or indirectly interacting with FtsZ. Kotun in our lab found that

Δ*sepF* mutant is almost as defective as Δ*ftsZ* mutant in *S. coelicolor* and SepF interacts with FtsZ (Kotun, 2013).

DynA and DynB are two dynamin-like, sporulation-specific proteins that localize at the septum as a ladder and stabilize the Z ring in *S. venezuelae* (Schlimpert et al., 2017). Bacterial Two-hybrid assays revealed that neither DynA nor DynB directly interacts with FtsZ but exerts its function via physical interaction with SsgB and SepF2 (Schlimpert et al., 2017). It is not known if DynAB are involved in remodeling cell membrane and catalyzing membrane fusion. PG synthesis and membrane invagination are required to drive cell division.

SepH, an Actinobacteria-specific protein, is also integral for stabilizing the Z ring at sporulation septa (Ramos-León et al., 2021). SepH directly interacts with FtsZ via a conserved helix-turn-helix motif and regulates the dynamics of the Z-ring formation in both filamentous *Streptomyces* and rod-shaped mycobacterium species. However, it is unclear how SepH is initially localized and whether it interacts with other proteins for positioning of the Z ring. In addition, SepH is also important for cell division during vegetative growth, and deletion of *sepH* results in fewer cross-wall formation.

SepX is a newly identified actinobacteria-signature membrane protein that is crucial for both types of cell division (Bush et al., 2021). SepX stabilizes the sporulation-specific Z ring via interaction with DynB. Strikingly, deletion of *sepX* almost abolishes cross-wall formation, and thus affects the fitness of colonies and coordinated progression through the life cycle.

Chromosome segregation and condensation

Different from the canonical circular chromosome in most bacteria, *Streptomyces* possesses a linear chromosome. The genome size is almost the largest for the bacteria domain. Its sporogenic hyphae are multigenomic compartments that contain 50 or more copies of the

linear chromosome. The DNA copies initially exist as an uncondensed form, which then undergo extensive segregation and condensation into unigenomic spores (Flärdh and Buttner, 2009). Chromosome segregation in *Streptomyces* predominantly involves the *parABS* system, similar to many other bacterial chromosome and plasmid partitioning systems. ParA ATPase assembles into helical filaments along the length of the sporogenic cell of aerial hyphae, and DNA-binding protein ParB specifically binds to the centromere-like sequences *parS* sites forming a nucleoprotein complex (Jakimowicz et al., 2002; Jakimowicz et al., 2007). *S. coelicolor* contains more than 20 copies of *parS* in the chromosome around the origin of replication (*oriC*) site, more than any other bacterial chromosome characterized so far, indicating a complexity of the segregation mechanism (Jakimowicz et al., 2002). ATP hydrolysis of ParA drives ParB foci to evenly distribute between the Z ring along the hyphae, with each potential prespore compartment containing a ParB focus and presumably one copy of chromosome (Donczew et al., 2016; Jakimowicz et al., 2005; Jakimowicz et al., 2007). Recently, it has been reported that ParB in *B. subtilis* and *Myxococcus xanthus* is indeed a conserved CTPase, whose hydrolytic activity is modulated by *parS* DNA recognition (Osorio-Valeriano et al., 2019; Soh et al., 2019). Although variable in amino acid sequence, ParB protein architecture is highly conserved in bacteria, indicating that CTP-binding might be a conserved feature in all members of ParB family. In addition, deletion of *parA* results in both chromosome segregation and sporulation septation defects, suggesting an interaction between chromosome segregation and future division site selection (Jakimowicz et al., 2007). Further study using time-lapse microscopy in *S. venezuelae* revealed that FtsZ ring assembly is affected by ParA and ParB , reinforcing this hypothesis (Donczew et al., 2016). They also found that both ParA and ParB affect the hyphal extension rate and sporogenic hyphae growth stops at the time of ParA accumulation and Z-ring formation,

indicating the existence of a potential checkpoint between the cessation of extension and sporulation that involves the ParA and ParB proteins (Donczew et al., 2016). After ParB foci are evenly distributed, ParA filaments disappear. ParJ, an actinobacteria signature protein, is reported to interact directly with ParA *in vitro* to regulate ParA depolymerization (Ditkowski et al., 2010). In addition, it is also noteworthy to mention that ParAB are also involved in the anchorage of a chromosome to new hyphae during branching and subsequent hyphal extension (Kois-Ostrowska et al., 2016). During vegetative growth, ParA localizes at the hyphal tips and interacts with Scy, a component of the apical protein complex (polarisome) (Ditkowski et al., 2013; Kois-Ostrowska et al., 2016). In the multigenomic hyphae, ParA tightly anchors a single leading copy chromosome at the hyphal tip while whereas ParB binds at *oriC* regions of every copy of chromosome (Kois-Ostrowska et al., 2016). During spore germination and branching, ParA captures one of the daughter chromosomal copies to the new hyphal tip and coordinates with other members of polarisome for apical tip extension (Kois-Ostrowska et al., 2016). Therefore, besides chromosome segregation, ParAB have a novel role in hyphal tip establishment and extension.

In addition to the *par* system, a FtsK (SpoIIIE) homolog, also plays a role in chromosome segregation in *Streptomyces*. FtsK functions as a translocase to pump DNA through septa before its closing. *S. coelicolor* FtsK localizes at the sporulation septa, but it is not required for sporulation septation or Z-ring assembly (Ausmees et al., 2007; Dedrick et al., 2009; Wang et al., 2007). Furthermore, deletion of *ftsK* causes irregular DNA content in the spores (Ausmees et al., 2007). Strikingly, *ftsK*-null mutant can result in large deletions near the termini of the linear chromosome, which could account for the this probably the abnormal colony appearance after restreaking (Ausmees et al., 2007; Wang et al., 2007).

In addition, *Streptomyces* chromosome segregation also involves SMC (structural maintenance of chromosome) and ScpAB (segregation and condensation proteins) that work in concert as a protein complex (Kois et al., 2009). Deletion of *smc* affects the formation of ParB complexes and causes a slight defect in chromosome partitioning that led to 7-8% anucleate spores, whereas *scpAB*-null mutant showed bilobed nucleoids in certain spore compartments, suggesting that they participate in the chromosome compaction (Dedrick et al., 2009; Kois et al., 2009).

The *smeA-sffA* is a conserved, developmentally-regulated operon encoding two proteins: SmeA (a small putative membrane protein) and SffA (a SpoIIIE/FtsK-family protein) that contains an N-terminal transmembrane segment and a C-terminal FtsK ATPase-like domain (Ausmees et al., 2007). Developmentally-controlled transcription of *smeA-sffA* occurs after Z-ring formation in an early *whi* gene-dependent manner. Interestingly, this transcription does not depend on a regular septation or presence of a functional FtsZ (Ausmees et al., 2007). SffA-EGFP is first found as a weak signal along the cell periphery in some early non-constricted sporogenic hyphae, but then relocalizes and accumulates as a strong fluorescent foci at sporulation septa, where it colocalizes with FtsK. However, there is no obvious functional redundancy detected between *ftsK* and *sffA*. In the absence of *smeA*, SffA remains localized over the cell periphery even after sporulation, indicating that SmeA helps direct SffA to the sporulation septa. Although a *smeA-sffA* null mutant has a very slight defect in sporulation septation, chromosome segregation, and spore maturation, the exact function remains unclear (Ausmees et al., 2007).

Spore maturation

S. coelicolor spore maturation involves the production of a thick spore (exospore) cell wall and spore shape metamorphosis from cylindrical prespores to ellipsoidal spores. The spore shape transformation in *S. venezuelae* is not as dramatic as in *S. coelicolor*, as judged from the scanning electron microscopy and transmission electron microscopy images, where it was shown that *S. venezuelae* mature spores are more cylindrical, with subtle rounding up (Bush et al., 2013; Bush et al., 2015). Cell-cell separation in *S. venezuelae* occurs via a rapid mechanical process, called "V snapping" (Zhou et al., 2016). Immature spores remain associated with each other in the spore chain as they undergo maturation, likely held in place by the rodlet ultrastructure that forms a sheath on the surface of aerial hyphae. The mature spores enable them to be dispersed and survive in a dormant state, and to are able to withstand adverse conditions. Compared to endospores produced by *Bacillus* and other genera of the Firmicutes (low GC gram-positives), *Streptomyces* spores are less resistant to a variety of stresses, such as heat and desiccation, and this might be caused by a residual low level metabolic activity in *Streptomyces* exospores (Beskrovnaya et al., 2021).

In addition, distinct changes occur for cell wall structure and composition from exponentially growing vegetative hyphae to the aerial hyphae that undergo sporulation. A high-resolution analysis of the PG composition of *S. coelicolor* using HPLC-MS/MS revealed that the PG in the spore wall features an increase in 3-3 crosslinks and a decrease in 3-4 crosslinks (van der Aart et al., 2018). Deacetylation of MurNAc to MurN was also notably prominent in spores (van der Aart et al., 2018). Major PG hydrolysis takes place during the course of development, producing over 80 different muropeptides.

Spore wall assembly

The formation of a thick cell wall in *Streptomyces* is directed by MreB, an actin-like protein that is involved in lateral cell wall elongation in rod-shaped bacteria. *mreB* is located within the *mre* gene cluster that includes *mreB*, *mreC*, *mreD*, *pbp2*, and *sfr* (*rodA*). *Streptomyces* also contains a *mreB*-like gene *mbl* at a different location of the chromosome (Sigle et al., 2015; Vollmer et al., 2019). MreB does not appear to play an important role during vegetative growth, but is involved in differentiation and spore formation. Deletion of *mreB* in *S. coelicolor* results in swollen spores and increased sensitivity to moderate heat and detergent, indicating the spore wall is compromised (Mazza et al., 2006). The subcellular localization of MreB–EGFP further corroborates its role in spore wall assembly. The fluorescent signal is first detected at septa of sporogenic hyphae as a ladder, then at the poles in each prespore compartment. Subsequently the signal spreads out to form a ring-like structure adjacent to membrane of maturing spores before disappearing in the fully mature spores (Mazza et al., 2006). MreB has been confirmed as a membrane-associated protein, but how it is tethered to membrane needs further investigation. Similar to a *mreB* mutant, all individual mutants in the *mre* gene cluster and a *mreB mbl* double mutant also exhibited swollen spores and sensitivity to different stresses (Heichlinger et al., 2011; Kleinschnitz et al., 2011a; Mazza et al., 2006). Mbl-mCherry colocalizes with MreB-EGFP at sporulation septa and in maturing spores. Mbl requires MreB for proper localization, while MreB localizes independent of Mbl (Heichlinger et al., 2011).

MreBCD, Mbl, PBP2 and Sfr (RodA-like protein) constitute core components of the *Streptomyces* spore wall synthesizing complex (SSSC), analogous to the elongasome in rod-shaped bacteria (Heichlinger et al., 2011; Kleinschnitz et al., 2011a). In addition, *S. coelicolor* homologs of RodZ and FtsI, as well as two additional penicillin-binding proteins: SCO3901 and SCO3580 are also part of the complex. Extensive protein interactions among the complex were

detected using a bacterial two-hybrid assay (Kleinschnitz et al., 2011a). Of which, MreC and RodZ demonstrated the most interacting partners, indicating a central role of the two proteins in the complex (Kleinschnitz et al., 2011a; Sigle et al., 2015). Very importantly, the interactions found in the *S. coelicolor* SSSC resembles those reported for rod-shaped bacteria (Kleinschnitz et al., 2011a). Further interaction partners and possible additional members of the SSSC complex were identified by a BACTH screening of *S. coelicolor* genomic library using MreB, MreC, MreD, PBP2, Sfr, or RodZ as a bait. The interacting partners were grouped into several classes: ABC-transporters, cell morphogenic proteins, cell wall synthesis proteins, and uncategorized others (Kleinschnitz et al., 2011b; Vollmer et al., 2019). A complete list of the SSSC components is listed in Vollmer et al. (2019). Examples of SSSC members include SCO2578 (known as PdtA) and SCO2584, homologes of TagF and TagV involved in wall teichoic acid synthesis. These acids synthesis is required for normal spore envelope assembly (Kleinschnitz et al., 2011b; Sigle et al., 2016).

PkaI, encoded by *sco4778* in *S. coelicolor*, is an eukaryotic type serine/threonine protein kinase (eSTPK). Interestingly, PkaI was the most frequently captured prey proteins when screening with MreC, MreD, PBP2, Sfr, or RodZ (Kleinschnitz et al., 2011a; Sigle et al., 2015; Vollmer et al., 2019). Moreover, PkaI also interacts with another three PBP proteins FtsI, SCO3901 and SCO3580 (Kleinschnitz et al., 2011a). There are another 4 genes flanking *pkaI* in the cluster: *sco4775* (*pkaH*), *sco4776*, *sco4777* (*pkaD*), and *sco4770* (*pkaJ*). The extensive interactions between PkaI and SSSC proteins strongly suggests that the activity of SSSC is controlled by protein phosphorylation. An *in vitro* study has demonstrated that PkaI is able to phosphorylate MreC and PBP2 and PkaH phosphorylates MreC (Ladwig et al., 2015; Vollmer et al., 2019). Deletion of *pkaI* or the five-gene cluster resulted in abnormal sporulation and aberrant

spores with a defective spore envelope (Ladwig et al., 2015). Expressing a second copy of any one of the five eSTPK genes under the control of its native promoter caused a similar phenotype. These results indicate that balanced phosphorylation level is crucial for sporulation and cell wall integrity. In addition to genomic library screening using bacterial two-hybrid vectors, transposon mutagenesis was also employed to identify additional genes involved in morphological differentiation (Vollmer et al., 2019). Identified targets include proteins involved in transcriptional regulation, nucleotide synthesis, polysaccharide biosynthesis and some other proteins with known or unknown functions, some of which were investigated in the previous two-hybrid screenings. With the identification of the massive SSSC complex, future work will focus on the elucidation of how the individual SSSC members contribute to sporulation and synthesis of spore envelope. One protein (SsdA) not identified as part of the SSSC complex is the subject of this dissertation (Chapter 2).

DNA compaction and preservation of the genome

To maintain genetic integrity, the spore chromosome needs to be compacted to prevent damage (McCormick and Flärdh, 2012). In *Streptomyces* spores, several developmentally-controlled nucleoid-associated proteins have been reported to compact and protect nucleoid structure. One example is the HU-like protein HupS, which carries an N-terminal domain that is similar to that of HU proteins and a C-terminal extension with an unusual alanine- and lysine-rich motif of eukaryotic linker H1-histone (Salerno et al., 2009; Yokoyama et al., 2001). In *S. coelicolor*, *hupS* is upregulated in sporogenic aerial hyphae in a *whiA*, *whiG*, and *whiI*-dependent manner (Salerno et al., 2009). In spores, HupS is associated with the nucleoid, contributing to spore nucleoid compaction, and also affects spore maturation, as evidenced by defective heat resistance and spore pigmentation in the mutant. In addition to HupS, HupA is another HU-like

protein in *Streptomyces*, but it is specifically expressed in vegetative hyphae, indicating HupA and HupS have specialized roles in nucleoid architecture during different developmental stages (Salerno et al., 2009).

Another type of protein that is specifically associated with the spore nucleoid are Dps proteins, including DpsA, DpsB, and DpsC in *S. coelicolor* (Facey et al., 2009). Dps protein belong to the ferritin family and can oxidize iron and form ferric oxide, which may protect DNA from oxidative damage (Szafran et al., 2020). In unicellular bacteria, the Dps proteins have been reported to fulfill this function (Chen and Helmann, 1995), however, there is no obvious upregulation of expression for *S. coelicolor* Dps during oxidative challenge. Deletion of any gene encoding the three proteins resulted in irregular chromosome condensation and sporulation septation. *dpsA* and *dpsC* are also developmentally regulated, and are specifically expressed in sporogenic compartments of aerial hyphae dependent on the presence of WhiG. Moreover, the *dps* genes are also induced in vegetative hyphae in a stress-dependent manner, suggesting an additional role of *dps* in chromosome organization of vegetative hypahe in response to stress.

Finally, a novel nucleoid-associated and actinobacterial-specific protein, sIHF, was characterized in *S. coelicolor* (Swiercz et al., 2013). sIHF associates with nucleoids, affecting chromosome segregation and condensation during sporulation. *In vitro* studies showed that the DNA-binding capability of sIHF is DNA length-dependent rather than DNA sequence-dependent, without any obvious structural preferences (Swiercz et al., 2013). The crystal structure revealed that sIHF is composed of two domains: a long N-terminal helix and a C-terminal helix-two turns-helix domain with two distinct DNA interaction sites, indicating a potential role in bridging DNA molecules. All these nucleoid-associated proteins are likely to work in concert to condense the chromosome and protect it from damage during sporulation, spore maturation and dormancy.

The *Streptomyces* chromosome structure during development has been investigated in recent years. Studies showed that *oriC* regions of the chromosome are positioned centrally in pre-spore compartments of sporogenic hyphae (Donczew et al., 2016; Szafran et al., 2021). Recent application of the chromosome conformation capture method (Hi-C) demonstrated dramatic rearrangement of *S. venezuelae* chromosome organization, from an open to a closed conformation, during sporogenic development (Szafran et al., 2021). Specifically, at entry to sporulation, two arms of the linear chromosome are spatially separated. However, during sporogenic cell division, arms are closely aligned within the central core region, leading to a closed confirmation. The confirmational change is mediated by the segregation protein ParB binding on *oriC* region, condensin SMC binding preferentially on the central core region, and compaction protein HupS binding predominately at chromosomal terminal regions.

Assembly and synthesis of the spore coat and pigment deposition

Streptomyces aerial mycelium contains a hydrophobic sheath consisting of chaplins (Chps) and rodlins (Rdls), which allows the aerial hyphae to break the surface tension of the aqueous environment (Flärdh and Buttner, 2009). In addition, several other cell surface proteins were identified in *S. coelicolor* and termed spore-associated proteins (Sap), including SapA, SapB, and SapC, E, and D. SapA and SapB are chromosomally-encoded and were first identified though a non-lethal detergent wash on the mature spores of *S. coelicolor* with a molecular weight of 13 and 3 kilodaltons, respectively (Guijarro et al., 1988). Their production commences during formation of the aerial mycelium, and the function of SapB has been studied. SapB is a lantibiotic-like peptide derived from processing RamS, which is a product of a developmentally-regulated gene in the four-gene operon. RamS is proteolytically cleaved and further modified after translation (Kodani et al., 2004). SapB plays a similar role with chaplin proteins that act as

a surfactant for aerial hyphae formation. It is essential for aerial hyphae formation on a rich medium or medium with high osmolarity (Capstick et al., 2007; de Jong et al., 2012). Exogenous application of SapB is capable of suppressing chaplin-deficient strain loss of aerial hyphae production (Capstick et al., 2007). Different from SapAB, SapCED are expressed from the *sapCED* operon that is under control of SapRS and located within the terminal inverted repeats of the linear plasmid, SCP1(Bentley et al., 2004; Sallmen II, 2019). They were identified from *S. coelicolor* stain HU3, which has the plasmid SCP1 incorporated into the chromosome and overexpresses SapC-E due to a spontaneous mutation *sapRS* (Bentley et al., 2004). No function has been assigned for SapA and SapCED. Further study will be needed to elucidate the roles of these coat proteins in *Streptomyces* development. Our lab has identified the composition of additional spore-associated coat proteins using mass spectrometry in *S. coelicolor* and *S. venezuelae* (Joe W. Sallmen Dissertation, 2019), and their functions need to be further studied.

Streptomyces spore maturation culminates in the deposition of a grey polyketide pigment on the spore surface, but the exact function of the spore pigment has yet to be determined. It has been postulated that the pigment functions as a barrier to protect spores against UV damage in the environment because deletion of the genes responsible for spore pigment synthesis in *S. griseus* resulted in a slight increase in sensitivity to UV radiation (Beskrovnaya et al., 2021; Funa et al., 2005). *Streptomyces* spore pigment is synthesized by enzymes encoded in the complex *whiE* gene cluster consisting of a potential seven-gene operon (ORFI to -VII) and one divergently transcribed gene, ORFVIII (Davis and Chater, 1990). Genes in this locus encode proteins that constitute a Type II polyketide synthase pathway, responsible for the biosynthesis of a cyclized or aromatic polyketides (Davis and Chater, 1990). ORFVIII encodes a putative flavin adenine dinucleotide-dependent hydroxylase that is involved in introduction of a hydroxyl

group to the cyclized polyketide at the late biosynthetic pathway (Davis and Chater, 1990). Deletion of this gene in *S. coelicolor* resulted in spore color change from the usually grey to greenish (Kelemen et al., 1998; Yu and Hopwood, 1995). In *Streptomyces halstedii*, disruption of ORFVIII homolog also resulted in spore pigment color change, in this case from green to lilac (Blanco et al., 1993). It is well-known that *S. venezuelae* NRRL B-65442, the working model extensively used in *Streptomyces* community, produces spores with a green pigment, but the reason was unknown. Recently, whole genome sequence comparison revealed that NRRL B-65442 acquired a single nucleotide mutation in ORFVIII (*vnz_33525*) of *whiE* gene cluster, resulting in an amino acid substitution from tryptophan to arginine and thus inactivation of a spore polyketide hydroxylase activity (Gomez-Escribano et al., 2021). It is still not clear why mutation in ORFVIII, i.e. missing the oxidative modification, results in a color change.

Although efforts have been made, our understanding of spore maturation process for *Streptomyces* is still limited. Using a random genome-wide transposon-insertion mutagenesis, Bennett identified a novel gene that may play a role in spore maturation for *S. coelicolor* (Bennett, 2006). The insertion mutant exhibited a hydrophobic aerial mycelium and produced spores of heterogeneous sizes, shapes, and spore wall thickness. The gene was named *ssdA* as a spore shape determination gene due to its striking spore shape defect in the insertion mutant. In my study, I first isolated an *ssdA* null mutant in *S. coelicolor* and verified its phenotype is similar with the insertion mutant. Then I characterized the gene *ssdA* in a different *Streptomyces* species *S. venezuelae*. In addition, I initiated the characterization of *whiD*, a transcriptional regulator that potentially regulates late steps of spore maturation process.

Table 1.1 Divisome proteins important for maintenance of cell length in *E. coli*

Protein	Function	Essential	Loss-of-function Phenotype	Reference
FtsZ	Cytoskeletal protein, recruit other components of divisome	Yes	Filamentous cell	(Hirota et al., 1968; Lutkenhaus et al., 1980)
FtsA	Tether FtsZ to membrane	Yes	Filamentous cell with shallow constrictions	(Martin et al., 2004; Pichoff and Lutkenhaus, 2005)
ZipA	Tether FtsZ to membrane	Yes	Filamentous cell with no constriction	(Hale and de Boer, 1997; Pichoff and Lutkenhaus, 2002)
ZapA	Stabilize the Z ring by inhibition of FtsZ GTPase activity	No	No obvious cell division and septation defect	(Johnson et al., 2004; Small et al., 2007)
ZapB	Stabilize divisome by interaction with FtsZ	No	Elongated cell	(Ebersbach et al., 2008)
ZapC	Stabilize the Z ring by inhibition of FtsZ GTPase activity	No	Slightly elongated cell	(Durand-Heredia et al., 2011; Hale et al., 2011)

Protein	Function	Essential	Loss-of-function Phenotype	Reference
ZapD	Stabilize the Z ring by reduction of FtsZ GTPase activity	No	No obvious cell division defect, but significantly elongated cell when coupled with *zapA* and/or *zapC* mutant	(Durand-Heredia et al., 2012)
FtsEX	ATP-binding subunit (FtsE) and transmembrane subunit (FtsX) of ABC transporter family; stabilize the Z ring; potentially involved in salt transport	No	Salt-dependent. No salt: filamentous cell. Salt over 0.5%: viable although mild filamentation.	(De Leeuw et al., 1999; Schmidt et al., 2004)
FtsK	N-terminus stabilize the Z ring; C-terminus is a DNA translocase coupling chromosome segregation with cell division	Yes	Filamentous cell with no constriction; DNA segregation defect	(Aussel et al., 2002; Wang and Lutkenhaus, 1998; Yu et al., 1998)

Protein	Function	Essential	Loss-of-function Phenotype	Reference
FtsQ	Stabilize the Z ring	Yes	Filamentous cell	(Carson et al., 1991; Chen et al., 1999)
FtsL	Stabilize the Z ring	Yes	Filamentous cell	(Ghigo and Beckwith, 2000)
FtsB (DivIC)	Stabilize the Z ring	Yes	Filamentous cell	(Buddelmeijer et al., 2002; Gonzalez and Beckwith, 2009)
FtsW	Probable PG glycosyltransferase; Stabilize the Z ring	Yes	Filamentous cell	(Boyle et al., 1997; Pastoret et al., 2004)
FtsI (PBP3)	PG transpeptidase in septum; activate constriction of the Z ring	Yes	Filamentous cell with shallow constriction	(Ishino and Matsuhashi, 1981; Pogliano et al., 1997; Spratt, 1975)
FtsN	Activate constriction of the Z ring	Yes	Filamentous cell	(Dai et al., 1993; Liu et al., 2015)

Table 1.2 Divisome proteins important for maintenance of cell length in *B. subtilis*

Protein	Function	Essential	Loss-of-function Phenotype	Reference
FtsZ	Cytoskeletal protein, recruits other components of divisome	Yes	Filamentous cells (vegetative stage); no septum (sporulation stage)	(Beall and Lutkenhaus, 1991)
FtsA	Tethers FtsZ to membrane;	No[1]	Filamentous cells during vegetative growth; sporulation defect	(Beall and Lutkenhaus, 1992; Feucht et al., 2001; Gholamhoseinian et al., 1992)
SepF	Tether FtsZ to membrane; Stabilize the Z ring; Septum formation	No	Reduced cell division frequency; thick and morphologically abnormal septa	(Gündoğdu et al., 2011; Hamoen et al., 2006)

Protein	Function	Essential	Loss-of-function Phenotype	Reference
ZapA	Stabilizes the Z ring by inhibition of FtsZ GTPase activity and formation a higher-order assemblies of FtsZ protofilaments	No	No obvious cell division and septation defect; severe division block in combination with ezrA or divIVA mutation, or in cells with lower levels of FtsZ	(Gueiros-Filho and Losick, 2002)
EzrA	Modulates frequency and position of the Z ring; negative regulator (promotes disassembly of FtsZ)	No	Increased frequency of Z rings, and thus minicells	(Haeusser et al., 2004; Levin et al., 1999; Singh et al., 2007)

Protein	Function	Essential	Loss-of-function Phenotype	Reference
FtsEX	ATP-binding subunit of ABC transporter family; initiation of sporulation and placement of asymmetrical septa; cell elongation; activate CwlO	No	Supposedly asymmetric septum forms at medial instead at polar; both cells and spores with reduced length	(Garti-Levi et al., 2008; Meisner et al., 2013)
SpoIIIE (FtsK)	Chromosome segregation during sporulation; correct localization of the σ^F activity; membrane fusion after prespore engulfment	Yes for sporulation; No for vegetative division	DNA segregation defect in endospore; membrane fusion defect	(Sharp and Pogliano, 1999, 2003; Wu and Errington, 1994, 1997)
DivIB (FtsQ)	Stabilizes the division complex; vegetative division at high temperature; sporulation at all temperatures and	Yes at high temperature ; no at low up to 37°C	Filamentous cells; delayed and less efficient sporulation septa formation; thick PG in the	(Harry et al., 1993; Real et al., 2005; Rowland et al., 1997; Thompson et al., 2006)

Protein	Function	Essential	Loss-of-function Phenotype	Reference
	engulfment process; chromosome segregation;		complete septa; inability of engulfment	
FtsL[2]	Assembly of divisome, particularly DivIB and DivIC;	Yes	Filamentous cells (vegetative stage); no septum (sporulation stage)	(Daniel et al., 1998)
DivIC (FtsB)	Vegetative division and sporulation; Specific role unknown; Interacts with FtsL and DivIC.	Yes	Filamentous cells (vegetative stage); no septum (sporulation stage)	(Henriques et al., 1992; Katis et al., 1997)
SpoVE[3] (FtsW)	Probable PG glycosyltransferase	Yes for sporulation; No for vegetative division	Normal vegetative growth; sporulation defect	(Henriques et al., 1992)
YlaO[4] (FtsW)	Probable PG glycosyltransferase	Yes	Filamentous cells	(Gamba et al., 2016; Henriques et al., 1998)

Protein	Function	Essential	Loss-of-function Phenotype	Reference
PBP 2B (FtsI)	PG transpeptidase in septum;	Yes	Filamentous cells with shallow constrictions in most cells	(Daniel et al., 2000)
DivIVA	Controls site specificity of MinCD with MinJ	Yes	Filamentous cells without constrictions and some minicells; abnormal sporulation	(Cha and Stewart, 1997; Edwards and Errington, 1997)
GpsB or YpsB	Paralog of DivIVA; interact with and shuttle of PBP1 between division and elongation	No	Normal morphology; synthetic lethal with ftsA and synthetic sick in division and elongation with ezrA	(Claessen et al., 2008; Tavares et al., 2008)

1. *ftsA* was able to be deleted although the previous attempt was not successful (Margolin, 2000).
2. *B. subtilis* FtsL shares little sequence homology with *E. coli* FtsL (Henriques et al., 1992).
3. SpoVE was referred as an *E. coli* homolog of FtsW because its encoding gene *spoVE* is located at a conserved position between *murD* and *murG,* where *ftsW* is located in *E. coli* (Errington et al., 2003).

4. YlaO was referred as an *E. coli* homolog of FtsW because it shares both sequence and function similarity with *E. coli* FtsW (Beall and Lutkenhaus, 1991; Gamba et al., 2016).

Table 1.3 Divisome proteins in *Streptomyces*

Protein	Function	Essential (?)	Loss-of-function Phenotype	Reference
FtsZ	Cytoskeletal protein, recruit other components of divisome	No	No vegetative division and sporulation division; filamentous cell	(Cantlay et al., 2021; McCormick et al., 1994)
SsgA	Recruit SsgB to membrane	No	No sporulation division; filamentous cell	(Yamazaki et al., 2003)
SsgB	Recruit FtsZ to membrane	No	No sporulation division; filamentous cell	(Keijser et al., 2003; Willemse et al., 2011)
SepF	Stabilize the divisome and sporulation septation	No	No vegetative division and sporulation division; filamentous cell	(Kotun, 2013); Sen et. al., unpublished
FtsEX	Stabilize the divisome	No	Mild effect on sporulation	(Kotun, 2013)
FtsK	Chromosome segregation during sporulation	No	Mild effect on sporulation	(Ausmees et al., 2007; Dedrick et al., 2009; Wang et

Protein	Function	Essential (?)	Loss-of-function Phenotype	Reference
				al., 2007)
FtsQ (DivIB)	Stabilize the divisome	No	Vegetative division defect; Sporulation septation defect	(McCormick and Losick, 1996)
FtsL-DivIC	Stabilize the divisome	No	Vegetative division defect; medium-dependent sporulation	(Bennett et al., 2007; Cantlay et al., 2021)
FtsW-FtsI	Stabilize the divisome	No	Vegetative division defect; medium-dependent sporulation	(Bennett et al., 2009; Cantlay et al., 2021; Mistry et al., 2008)
DynAB	Stabilize the Z ring during sporulation-specific cell division	No	Sporulation septation defect	(Schlimpert et al., 2017)
SepH	Stabilize the Z ring during vegetative division and sporulation division	No	Cross-wall formation defect; sporulation septation defect	(Ramos-León et al., 2021)

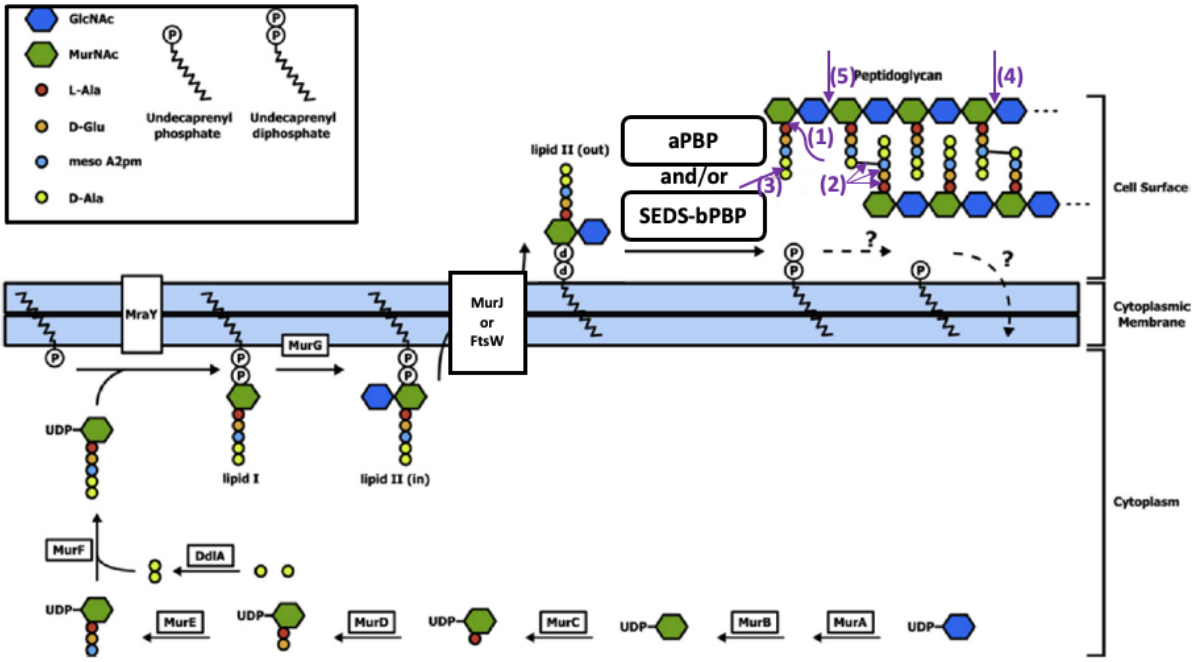

Figure 1.1 Peptidoglycan composition and its synthesis. A key for the of peptidoglycan (PG) precursors is illustrated in the box. PG precursors are synthesized by a series of reactions in the cytoplasm. Lipid I and Lipid II are linked to the cytoplasmic membrane by lipid carrier undecaprenyl diphosphate. Lipid II is flipped across the inner leaflet to the out leaflet of cytoplasmic membrane by flippase MurJ or FtsW. PG polymerization involves two different PBP enzymes: aPBP (containing both glycosyltransferase (GTase) activity and transpeptidase (TPase) activity) and SEDS-bPBP (forming a GTase-TPase complex). Lipid carrier undecaprenyl diphosphate is dephosphorated and flipped back to inner leaflet of the cytoplasmic membrane by a unknown mechanism. Abbreviations: GlcNAc (N-acetylglucosamine), MurNAc (N-acetylmuramic acid), L-Ala (L-alanine) in red, D-Glu (D-glumatic acid), mDAP (meso-diaminopimelic acid), and D-Ala (D-alanine) in purple. (1) to (5) represent cleavage sites of diverse PG hydrolases: (1) amidases, (2) endopeptidases, (3) carboxypeptidases, (4) muramidases, and (5) glucosaminidases. Adapted from Unsleber et al. (2019).

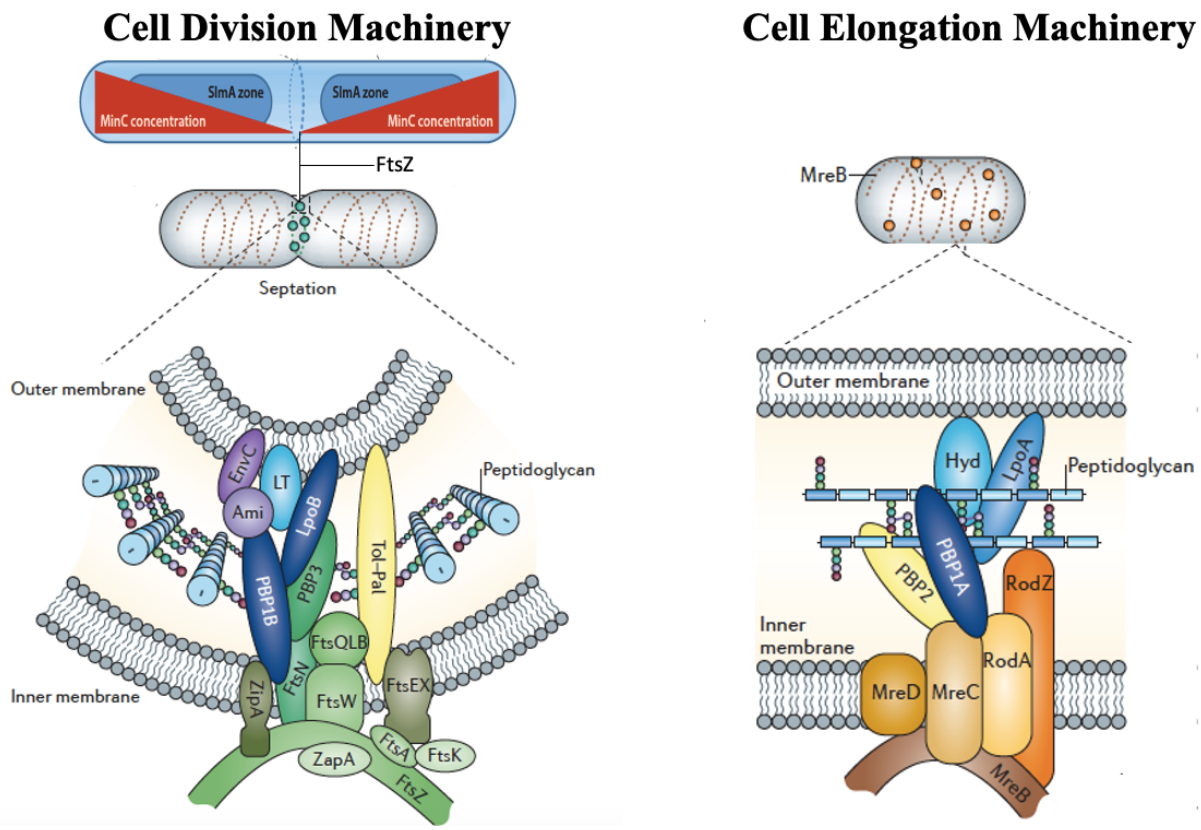

Figure 1.2 Cell division and cell elongation machineries in *E. coli.* The divisome (on the lower left) functions at the cell center and is anchored by cytoskeletal protein FtsZ. The elongasome or the Rod complex (on the lower right) works along the lateral side wall of the cylindrical cell and is anchored by cytoskeletal protein MreB. The cell division complex consists of FtsZ, other inner membrane-associated cell division proteins, the PG synthases PBP1B and PBP3, lytic transglycosylase (LT), and amidase enzymes (Ami) with their activators (EnvC), as well as the Tol–Pal complex for constriction of the outer membrane. The top figure on the left demonstrates two negative regulatory systems of FtsZ in an elongating *E. coli* cell prior to septation. When the cell grows to a sufficient length, the concentration of MinC (in a gradient represented by the red triangle) drops below a critical level at midcell to allow assembly of the FtsZ ring. SlmA binds to the bacterial chromosome and inhibits FtsZ assembly in an area around the nucleoid (central dark blue zone). The two FtsZ inhibitors ensure the Z ring only assembles at the midcell. The elongation complex consists of MreB, MreCD, RodZ, RodA, the PG synthase PBP1A and PBP2, and some hydrolases (Hyd). Activity of the PBPs is regulated in part by outer membrane-anchored lipoproteins such as LpoA and LpoB. Figures are adapted from Typas et al. (2011); Young (2010).

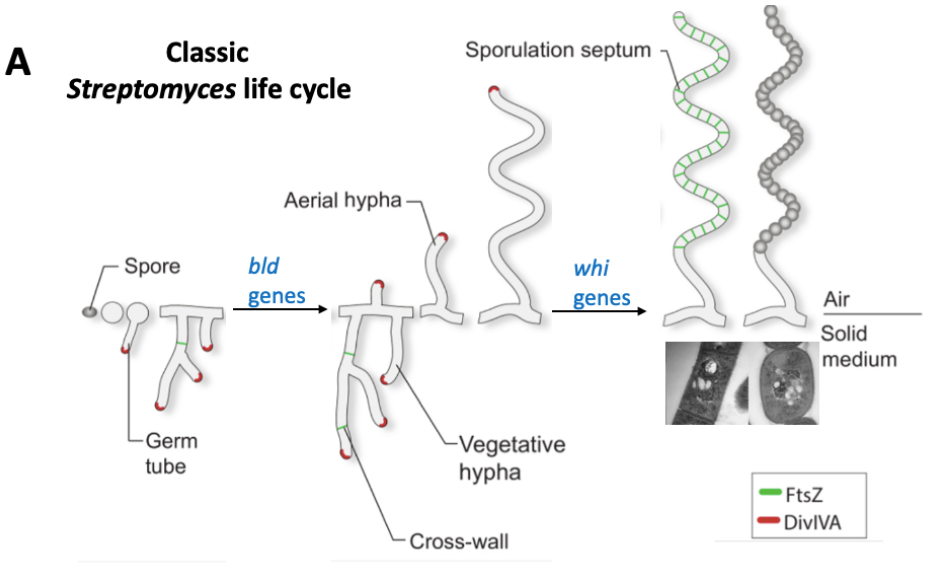
A
Classic
Streptomyces life cycle
Sporulation septum
Aerial hypha
Spore
bld
genes
whi
genes
Air
Solid
medium
Germ
tube
Vegetative
hypha
Cross-wall
FtsZ
DivIVA

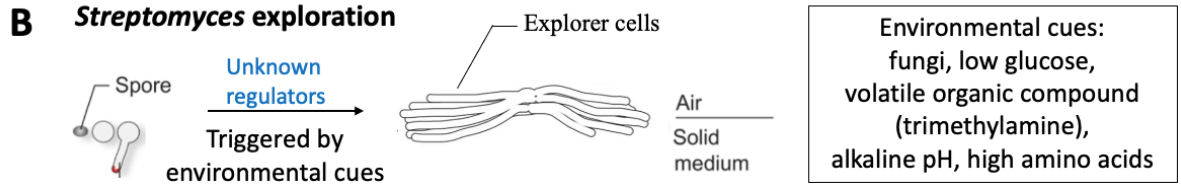
B
Streptomyces exploration
Explorer cells
Spore
Unknown
regulators
Triggered by
environmental cues
Air
Solid
medium
Environmental cues:
fungi, low glucose,
volatile organic compound
(trimethylamine),
alkaline pH, high amino acids

Figure 1.3 The classic *Streptomyces* life cycle and *Streptomyces* exploration. (A) The classic *Streptomyces* life cycle starts with spore germination and the formation of a germ tube. Germ tubes grow by tip extension and branching to form a dense network of vegetative hyphae. Polar growth and branch initiation of the vegetative hyphae is directed by a landmark protein DivIVA (red). In response to nutrient depletion and other unknown signals, aerial hyphae break the surface tension and grow into the air. Finally, aerial hyphae differentiate into long chains with cylindrical prespore compartments, which undergo cell wall thickening and spore shape metamorphosis into matured ellipsoidal spores. Formation of cross-walls and sporulation septa are both dependent on FtsZ (green). The transition from vegetative hyphae to aerial hypha requires the *bld* genes, and the transition from aerial hyphae to spore chains requires the *whi* genes. Figure A is adapted from Schlimpert et al. (2016). Transmission electron microscopy (TEM) images are from Bennett (2006). (B) *Streptomyces* can deviate from the classic life cycle, and initiate exploratory growth, which does not require Bld or Whi developmental regulators. Explorer cells grow as nonbranching vegetative hyphae, and are capable of rapidly traversing surfaces and was first identified by coculture with yeast. Some of the cues that stimulate exploration have been identified. Once yeast has consumed the local glucose supply from the medium, *Streptomyces* begin to produce the volatile trimethylamine (TMA). TMA release leads to a localized increase in pH and promotes the initiation of exploration in the TMA producer and nearby exploration-competent cells. Figure B is adapted from Jones et al. (2019).

REFERENCES

Aaron, M., Charbon, G., Lam, H., Schwarz, H., Vollmer, W., and Jacobs‐Wagner, C. (2007). The tubulin homologue FtsZ contributes to cell elongation by guiding cell wall precursor synthesis in *Caulobacter crescentus*. Mol Microbiol *64*, 938-952.

Aarsman, M.E., Piette, A., Fraipont, C., Vinkenvleugel, T.M., Nguyen‐Distèche, M., and den Blaauwen, T. (2005). Maturation of the *Escherichia coli* divisome occurs in two steps. Mol Microbiol *55*, 1631-1645.

Adams, D.W., and Errington, J. (2009). Bacterial cell division: assembly, maintenance and disassembly of the Z ring. Nat Rev Microbiol *7*, 642-653.

Allan, E., Hoischen, C., and Gumpert, J. (2009). Bacterial L‐forms. Adv Appl Microbiol *68*, 1-39.

Alyahya, S.A., Alexander, R., Costa, T., Henriques, A.O., Emonet, T., and Jacobs-Wagner, C. (2009). RodZ, a component of the bacterial core morphogenic apparatus. Proc Natl Acad Sci USA *106*, 1239-1244.

Anderson, D.E., Gueiros-Filho, F.J., and Erickson, H.P. (2004). Assembly dynamics of FtsZ rings in *Bacillus subtilis* and *Escherichia coli* and effects of FtsZ-regulating proteins. J Bacteriol 1*86,* 5775-5781.

Ausmees, N., Kuhn, J.R., and Jacobs-Wagner, C. (2003). The bacterial cytoskeleton: an intermediate filament-like function in cell shape. Cell 1*15,* 705-713.

Ausmees, N., Wahlstedt, H., Bagchi, S., Elliot, M.A., Buttner, M.J., and Flärdh, K. (2007). SmeA, a small membrane protein with multiple functions in St*reptomyces* sporulation including targeting of a SpoIIIE/FtsK‐like protein to cell division septa. Mol Microbiol 6*5,* 1458-1473.

Aussel, L., Barre, F.-X., Aroyo, M., Stasiak, A., Stasiak, A.Z., and Sherratt, D. (2002). FtsK is a DNA motor protein that activates chromosome dimer resolution by switching the catalytic state of the XerC and XerD recombinases. Cell 1*08,* 195-205.

Bagchi, S., Tomenius, H., Belova, L.M., and Ausmees, N. (2008). Intermediate filament-like proteins in bacteria and a cytoskeletal function in *Streptomyces.* Mol Microbiol 7*0,* 1037-1050.

Banzhaf, M., van den Berg van Saparoea, B., Terrak, M., Fraipont, C., Egan, A., Philippe, J., Zapun, A., Breukink, E., Nguyen-Disteche, M., den Blaauwen, T., *et al.* (2012). Cooperativity of peptidoglycan synthases active in bacterial cell elongation. Mol Microbiol 8*5,* 179-194.

Barreteau, H., Kovač, A., Boniface, A., Sova, M., Gobec, S., and Blanot, D. (2008). Cytoplasmic steps of peptidoglycan biosynthesis. FEMS Microbiol Rev 3*2,* 168-207.

Beall, B., and Lutkenhaus, J. (1991). FtsZ in *Bacillus subtilis* is required for vegetative septation and for asymmetric septation during sporulation. Genes Dev 5*,* 447-455.

Beall, B., and Lutkenhaus, J. (1992). Impaired cell division and sporulation of a *Bacillus subtilis* strain with the *ftsA* gene deleted. J Bacteriol 1*74,* 2398-2403.

Ben-Yehuda, S., and Losick, R. (2002). Asymmetric cell division in *B. subtilis* involves a spiral-like intermediate of the cytokinetic protein FtsZ. Cell 1*09,* 257-266.

Bendezu, F.O., Hale, C.A., Bernhardt, T.G., and de Boer, P.A. (2009). RodZ (YfgA) is required for proper assembly of the MreB actin cytoskeleton and cell shape in *E. coli.* EMBO J 2*8,* 193-204.

Bennett, J. (2006). Molecular genetic analysis of division and development in *Streptomyces coelicolor.* (Ph. D. dissertation. Duquesne University, Pittsburgh, PA).

Bennett, J.A., Aimino, R.M., and McCormick, J.R. (2007). *Streptomyces coelicolor g*enes *ftsL* and *divIC* play a role in cell division but are dispensable for colony formation. J Bacteriol 1*89,* 8982-8992.

Bennett, J.A., Yarnall, J., Cadwallader, A.B., Kuennen, R., Bidey, P., Stadelmaier, B., and McCormick, J.R. (2009). Medium-dependent phenotypes of *Streptomyces coelicolor w*ith mutations in *ftsI* or *ftsW*. J Bacteriol 1*91,* 661-664.

Bentley, S., Brown, S., Murphy, L., Harris, D., Quail, M., Parkhill, J., Barrell, B., McCormick, J., Santamaria, R., and Losick, R. (2004). SCP1, a 356 023 bp linear plasmid adapted to the ecology and developmental biology of its host, *Streptomyces coelicolor* A3 (2). Mol Microbiol 51*, 1*615-1628.

Bernhardt, T.G., and De Boer, P.A. (2005). SlmA, a nucleoid-associated, FtsZ binding protein required for blocking septal ring assembly over chromosomes in *E. coli.* Mol Cell 18*, 5*55-564.

Bertsche, U., Kast, T., Wolf, B., Fraipont, C., Aarsman, M.E., Kannenberg, K., von Rechenberg, M., Nguyen-Disteche, M., den Blaauwen, T., Holtje, J.V., e*t al. (2*006). Interaction between two murein (peptidoglycan) synthases, PBP3 and PBP1B, in *Escherichia coli.* Mol Microbiol 61*, 6*75-690.

Beskrovnaya, P., Sexton, D.L., Golmohammadzadeh, M., Hashimi, A., and Tocheva, E.I. (2021). Structural, Metabolic and Evolutionary Comparison of Bacterial Endospore and Exospore Formation. Front Microbiol 12*, 6*30573.

Bi, E., and Lutkenhaus, J. (1991). FtsZ ring structure associated with division in *Escherichia coli. N*ature 35*4, 1*61-164.

Billaudeau, C., Yao, Z., Cornilleau, C., Carballido-Lopez, R., and Chastanet, A. (2019). MreB Forms Subdiffraction Nanofilaments during Active Growth in *Bacillus subtilis.* mBio 10.

Boes, A., Olatunji, S., Breukink, E., and Terrak, M. (2019). Regulation of the Peptidoglycan Polymerase Activity of PBP1b by Antagonist Actions of the Core Divisome Proteins FtsBLQ and FtsN. mBio 10.

Boyle, D.S., Khattar, M.M., Addinall, S.G., Lutkenhaus, J., and Donachie, W.D. (1997). *ftsW is* an essential cell‐division gene in *Escherichia coli.* Mol Microbiol 24*, 1*263-1273.

Bramhill, D., and Thompson, C.M. (1994). GTP-dependent polymerization of *Escherichia coli* FtsZ protein to form tubules. Proc Natl Acad Sci USA 91*, 5*813-5817.

Bratton, B.P., Shaevitz, J.W., Gitai, Z., and Morgenstein, R.M. (2018). MreB polymers and curvature localization are enhanced by RodZ and predict *E. coli's* cylindrical uniformity. Nat Commun 9, *2*797.

Buddelmeijer, N., Judson, N., Boyd, D., Mekalanos, J.J., and Beckwith, J. (2002). YgbQ, a cell division protein in *Escherichia coli an*d *Vibrio cholerae,* localizes in codependent fashion with FtsL to the division site. Proc Natl Acad Sci USA 99*, 6*316-6321.

Bush, M.J., Bibb, M.J., Chandra, G., Findlay, K.C., and Buttner, M.J. (2013). Genes required for aerial growth, cell division, and chromosome segregation are targets of WhiA before sporulation in *Streptomyces venezuelae.* mBio 4, *e*00684-00613.

Bush, M.J., Chandra, G., Al-Bassam, M.M., Findlay, K.C., and Buttner, M.J. (2019). BldC Delays Entry into Development To Produce a Sustained Period of Vegetative Growth in *Streptomyces venezuelae.* mBio 10.

*B*ush, M.J., Chandra, G., Bibb, M.J., Findlay, K.C., and Buttner, M.J. (2016). Genome-wide chromatin immunoprecipitation sequencing analysis shows that WhiB is a transcription factor that cocontrols its regulon with WhiA To initiate developmental cell division in *Streptomyces.* mBio 7, *e*00523-00516.

Bush, M.J., Chandra, G., Findlay, K.C., and Buttner, M.J. (2017). Multi-layered inhibition of *Streptomyces* development: BldO is a dedicated repressor of *whiB*. Mol Microbiol 10*4, 7*00-711.

Bush, M.J., Gallagher, K.A., Chandra, G., Findlay, K.C., and Schlimpert, S. (2021). Multicellular growth and sporulation in filamentous actinobacteria require the conserved cell division protein SepX. bioRxiv.

Bush, M.J., Tschowri, N., Schlimpert, S., Flardh, K., and Buttner, M.J. (2015). c-di-GMP signalling and the regulation of developmental transitions in streptomycetes. Nat Rev Microbiol 13*, 7*49-760.

Buske, P., and Levin, P.A. (2013). A flexible C-terminal linker is required for proper FtsZ assembly in vitro and cytokinetic ring formation in vivo. Mol Microbiol 89*, 2*49-263.

Buske, P.J., and Levin, P.A. (2012). Extreme C terminus of bacterial cytoskeletal protein FtsZ plays fundamental role in assembly independent of modulatory proteins. J Biol Chem 28*7, 1*0945-10957.

Cabeen, M.T., Charbon, G., Vollmer, W., Born, P., Ausmees, N., Weibel, D.B., and Jacobs-Wagner, C. (2009). Bacterial cell curvature through mechanical control of cell growth. EMBO J 28*, 1*208-1219.

Caccamo, P.D., and Brun, Y.V. (2018). The Molecular Basis of Noncanonical Bacterial Morphology. Trends Microbiol 26*, 1*91-208.

Cantlay, S., Sen, B.C., Flärdh, K., and McCormick, J.R. (2021). Influence of core divisome proteins on cell division in *Streptomyces venezuelae* ATCC 10712. Microbiology 16*7, 0*01015.

Capstick, D.S., Willey, J.M., Buttner, M.J., and Elliot, M.A. (2007). SapB and the chaplins: connections between morphogenetic proteins in *Streptomyces coelicolor.* Mol Microbiol 64*, 6*02-613.

Carballido-López, R. (2006). The bacterial actin-like cytoskeleton. Microbiol Mol Biol Rev 70*, 8*88-909.

Carballido-López, R., Formstone, A., Li, Y., Ehrlich, S.D., Noirot, P., and Errington, J. (2006). Actin homolog MreBH governs cell morphogenesis by localization of the cell wall hydrolase LytE. Dev Cell 11*, 3*99-409.

Carson, M.J., Barondess, J., and Beckwith, J. (1991). The FtsQ protein of *Escherichia coli:* membrane topology, abundance, and cell division phenotypes due to overproduction and insertion mutations. J Bacteriol 17*3, 2*187-2195.

Cha, J.H., and Stewart, G.C. (1997). The *divIVA* minicell locus of Bac*illus subtilis.* J Bacteriol 17*9, 1*671-1683.

Champness, W.C. (1988). New loci required for *Streptomyces coelicolor mo*rphological and physiological differentiation. J Bacteriol 17*0, 1*168-1174.

Chaplin, Amanda K., Petrus, Marloes L.C., Mangiameli, G., Hough, Michael A., Svistunenko, Dimitri A., Nicholls, P., Claessen, D., Vijgenboom, E., and Worrall, Jonathan A.R. (2015). GlxA is a new structural member of the radical copper oxidase family and is required for glycan deposition at hyphal tips and morphogenesis of *Streptomyces lividans.* Biochem J 46*9, 4*33-444.

Charbon, G., Cabeen, M.T., and Jacobs-Wagner, C. (2009). Bacterial intermediate filaments: *in vivo* assembly, organization, and dynamics of crescentin. Genes Dev 23*, 1*131-1144.

Chater, K. (1972). A morphological and genetic mapping study of white colony mutants of *Streptomyces coelicolor.* Microbiology 72*, 9*-28.

Chater, K., and Losick, R. (1997). Mycelial life style of *Streptomyces coelicolor* A3 (2) and its relatives (New York: Oxford University Press).

Chater, K.F., and Chandra, G. (2006). The evolution of development in *Streptomyces* analysed by genome comparisons. FEMS Microbiol Rev 30*, 6*51-672.

Chen, J.C., Weiss, D.S., Ghigo, J.-M., and Beckwith, J. (1999). Septal localization of FtsQ, an essential cell division protein in *Escherichia coli.* J Bacteriol 18*1, 5*21-530.

Chen, L., and Helmann, J.D. (1995). Bacillus subtilis MrgA is a Dps (PexB) homologue: evidence for metalloregulation of an oxidative‐stress gene. Mol Microbiol 18*, 2*95-300.

Chen, Y., and Erickson, H.P. (2005). Rapid in vitro assembly dynamics and subunit turnover of FtsZ demonstrated by fluorescence resonance energy transfer. J Biol Chem 28*0, 2*2549-22554.

Cho, H., McManus, H.R., Dove, S.L., and Bernhardt, T.G. (2011). Nucleoid occlusion factor SlmA is a DNA-activated FtsZ polymerization antagonist. Proc Natl Acad Sci USA 108, *377*3-3778.

Cho, H., Wivagg, C.N., Kapoor, M., Barry, Z., Rohs, P.D., Suh, H., Marto, J.A., Garner, E.C., and Bernhardt, T.G. (2016). Bacterial cell wall biogenesis is mediated by SEDS and PBP polymerase families functioning semi-autonomously. Nat Microbiol 1, 1-*8*.

Claessen, D., Emmins, R., Hamoen, L.W., Daniel, R.A., Errington, J., and Edwards, D.H. (2008). Control of the cell elongation–division cycle by shuttling of PBP1 protein in *Bacillus subtilis.* Mol Microbiol 68, *102*9-1046.

Colavin, A., Shi, H., and Huang, K.C. (2018). RodZ modulates geometric localization of the bacterial actin MreB to regulate cell shape. Nat Commun 9, 1*28*0.

Contreras-Martel, C., Martins, A., Ecobichon, C., Trindade, D.M., Mattei, P.J., Hicham, S., Hardouin, P., Ghachi, M.E., Boneca, I.G., and Dessen, A. (2017). Molecular architecture of the PBP2-MreC core bacterial cell wall synthesis complex. Nat Commun 8, 7*76*.

Dai, K., Xu, Y., and Lutkenhaus, J. (1993). Cloning and characterization of *ftsN*, an essential cell division gene in *Escherichia coli* isolated as a multicopy suppressor of *ftsA12 (T*s). J Bacteriol 175, *379*0-3797.

Daniel, R., Harry, E., Katis, V., Wake, R., and Errington, J. (1998). Characterization of the essential cell division gene ftsL *(yll*D) of *Bacillus subtilis* and its role in the assembly of the division apparatus. Mol Microbiol 29, *593*-604.

Daniel, R.A., Harry, E.J., and Errington, J. (2000). Role of penicillin‐binding protein PBP 2B in assembly and functioning of the division machinery of *Bacillus subtilis. Mol* Microbiol 35, *299*-311.

Davis, N., and Chater, K. (1990). Spore colour in *Streptomyces coelicolor A3 (2*) involves the developmentally regulated synthesis of a compound biosynthetically related to polyketide antibiotics. Mol Microbiol 4, 1*679*-1691.

de Boer, P.A., Crossley, R.E., and Rothfield, L.I. (1989). A division inhibitor and a topological specificity factor coded for by the minicell locus determine proper placement of the division septum in *E. coli.* Cell 56, *641*-649.

de Jong, W., Vijgenboom, E., Dijkhuizen, L., Wösten, H.A., and Claessen, D. (2012). SapB and the rodlins are required for development of *Streptomyces coelicolor* in high osmolarity media. FEMS Microbiol Lett 329, *154*-159.

De Leeuw, E., Graham, B., Phillips, G.J., Ten Hagen‐Jongman, C.M., Oudega, B., and Luirink, J. (1999). Molecular characterization of *Escherichia coli* FtsE and FtsX. Mol Microbiol 31, *983*-993.

Dedrick, R.M., Wildschutte, H., and McCormick, J.R. (2009). Genetic interactions of *smc*, *ftsK*, and *parB* genes in *Streptomyces coelicolor and t*heir developmental genome segregation phenotypes. J Bacteriol 191, *320*-332.

Del Sol, R., Mullins, J.G., Grantcharova, N., Flardh, K., and Dyson, P. (2006). Influence of CrgA on assembly of the cell division protein FtsZ during development of *Streptomyces coelicolor.* J Bacteriol 188, *154*0-1550.

Del Sol, R., Pitman, A., Herron, P., and Dyson, P. (2003). The product of a developmental gene, *crgA*, that coordinates reproductive growth in *Streptomyces* belongs to a novel family of small actinomycete-specific proteins. J Bacteriol 185, *667*8-6685.

den Hengst, C.D., and Buttner, M.J. (2008). Redox control in actinobacteria. Biochim Biophys Acta 1780*, 120*1-1216.

den Hengst, C.D., Tran, N.T., Bibb, M.J., Chandra, G., Leskiw, B.K., and Buttner, M.J. (2010). Genes essential for morphological development and antibiotic production in *Streptomyces coelicolor* are targets of BldD during vegetative growth. Mol Microbiol 78, *361*-379.

Denome, S.A., Elf, P.K., Henderson, T.A., Nelson, D.E., and Young, K.D. (1999). *Escherichia coli* mutants lacking all possible combinations of eight penicillin binding proteins: viability, characteristics, and implications for peptidoglycan synthesis. J Bacteriol 181, *398*1-3993.

Din, N., Quardokus, E.M., Sackett, M.J., and Brun, Y.V. (1998). Dominant C‐terminal deletions of FtsZ that affect its ability to localize in *Caulobacter* and its interaction with FtsA. Mol Microbiol 27, *105*1-1063.

Ditkowski, B., Holmes, N., Rydzak, J., Donczew, M., Bezulska, M., Ginda, K., Kedzierski, P., Zakrzewska-Czerwinska, J., Kelemen, G.H., and Jakimowicz, D. (2013). Dynamic interplay of ParA with the polarity protein, Scy, coordinates the growth with chromosome segregation in *Streptomyces coelicolor.* Open Biol 3, 1*30*006.

Ditkowski, B., Troc, P., Ginda, K., Donczew, M., Chater, K.F., Zakrzewska-Czerwinska, J., and Jakimowicz, D. (2010). The actinobacterial signature protein ParJ (SCO1662) regulates ParA polymerization and affects chromosome segregation and cell division during Strep*tomyces* sporulation. Mol Microbiol 78, *140*3-1415.

Divakaruni, A.V., Baida, C., White, C.L., and Gober, J.W. (2007). The cell shape proteins MreB and MreC control cell morphogenesis by positioning cell wall synthetic complexes. Mol Microbiol 66, *174*-188.

Dominguez-Escobar, J., Chastanet, A., Crevenna, A.H., Fromion, V., Wedlich-Soldner, R., and Carballido-Lopez, R. (2011). Processive movement of MreB-associated cell wall biosynthetic complexes in bacteria. Science 333, *225*-228.

Donczew, M., Mackiewicz, P., Wróbel, A., Flärdh, K., Zakrzewska-Czerwińska, J., and Jakimowicz, D. (2016). ParA and ParB coordinate chromosome segregation with cell elongation and division during *Streptomyces* sporulation. Open Biol 6, 1*50*263.

Du, S., Pichoff, S., and Lutkenhaus, J. (2016). FtsEX acts on FtsA to regulate divisome assembly and activity. Proc Natl Acad Sci USA 113, *E505*2-5061.

Du, S., Pichoff, S., and Lutkenhaus, J. (2020). Roles of ATP Hydrolysis by FtsEX and Interaction with FtsA in Regulation of Septal Peptidoglycan Synthesis and Hydrolysis. mBio 11.

*Dum*an, R., Ishikawa, S., Celik, I., Strahl, H., Ogasawara, N., Troc, P., Löwe, J., and Hamoen, L.W. (2013). Structural and genetic analyses reveal the protein SepF as a new membrane anchor for the Z ring. Proc Natl Acad Sci USA 110, *E46*01-E4610.

Durand-Heredia, J., Rivkin, E., Fan, G., Morales, J., and Janakiraman, A. (2012). Identification of ZapD as a cell division factor that promotes the assembly of FtsZ in *Escherichia coli.* J Bacteriol 194, *318*9-3198.

Durand-Heredia, J.M., Helen, H.Y., De Carlo, S., Lesser, C.F., and Janakiraman, A. (2011). Identification and characterization of ZapC, a stabilizer of the FtsZ ring in *Escherichia coli.* J Bacteriol 193, *140*5-1413.

Eaton, D., and Ensign, J.C. (1980). *Streptomyces viridochromogenes* spore germination initiated by calcium ions. J Bacteriol 143, *377*-382.

Ebersbach, G., Galli, E., Møller‐Jensen, J., Löwe, J., and Gerdes, K. (2008). Novel coiled‐coil cell division factor ZapB stimulates Z ring assembly and cell division. Mol Microbiol 68, *720*-735.

Edwards, D.H., and Errington, J. (1997). The *Bacillus subtilis* DivIVA protein targets to the division septum and controls the site specificity of cell division. Mol Microbiol 24, *905*-915.

Egan, A.J.F., Errington, J., and Vollmer, W. (2020). Regulation of peptidoglycan synthesis and remodelling. Nat Rev Microbiol 18, *446*-460.

Erickson, H.P., Taylor, D.W., Taylor, K.A., and Bramhill, D. (1996). Bacterial cell division protein FtsZ assembles into protofilament sheets and minirings, structural homologs of tubulin polymers. Proc Natl Acad Sci USA 93, *519*-523.

Errington, J. (2015). Bacterial morphogenesis and the enigmatic MreB helix. Nat Rev Microbiol 13, *241*-248.

Errington, J., Daniel, R.A., and Scheffers, D.-J. (2003). Cytokinesis in bacteria. Microbiol. Mol. Biol. Rev. 67, *52*-65.

Facey, P., Hitchings, M., Saavedra‐Garcia, P., Fernandez‐Martinez, L., Dyson, P., and Del Sol, R. (2009). *Streptomyces coelicolor* Dps‐*l*ike proteins: differential dual roles in response to stress during vegetative growth and in nucleoid condensation during reproductive cell division. Mol Microbiol 73, *118*6-1202.

Feucht, A., Lucet, I., Yudkin, M.D., and Errington, J. (2001). Cytological and biochemical characterization of the FtsA cell division protein of *Bacillus subtilis.* Mol Microbiol 40, *115*-125.

Figge, R.M., Divakaruni, A.V., and Gober, J.W. (2004). MreB, the cell shape-determining bacterial actin homologue, co-ordinates cell wall morphogenesis in *Caulobacter crescentus. Mol* Microbiol 51, *132*1-1332.

Flärdh, K. (2003). Essential role of DivIVA in polar growth and morphogenesis in *Streptomyces coelicolor A3(2)*. Mol Microbiol 49, *152*3-1536.

Flärdh, K., and Buttner, M.J. (2009). *Streptomyces* morphogenetics: dissecting differentiation in a filamentous bacterium. Nat Rev Microbiol 7, 3*6*-49.

Flärdh, K., and McCormick, J.R. (2017). The *Streptomyces* O-B *o*ne connection: a force within layered repression of a key developmental decision. Mol Microbiol 104, *695*-699.

Flärdh, K., Richards, D.M., Hempel, A.M., Howard, M., and Buttner, M.J. (2012). Regulation of apical growth and hyphal branching in *Streptomyces.* Curr Opin Microbiol 15, *737*-743.

Fröjd, M.J., and Flärdh, K. (2019). Apical assemblies of intermediate filament-like protein FilP are highly dynamic and affect polar growth determinant DivIVA in *Streptomyces venezuelae.* Mol Microbiol 112, *47*-61.

Fuchino, K., Bagchi, S., Cantlay, S., Sandblad, L., Wu, D., Bergman, J., Kamali-Moghaddam, M., Flardh, K., and Ausmees, N. (2013). Dynamic gradients of an intermediate filament-like cytoskeleton are recruited by a polarity landmark during apical growth. Proc Natl Acad Sci USA 110, *E18*89-1897.

Funa, N., Funabashi, M., Ohnishi, Y., and Horinouchi, S. (2005). Biosynthesis of hexahydroxyperylenequinone melanin via oxidative aryl coupling by cytochrome P-450 in *Streptomyces griseus.* J Bacteriol 187, *814*9-8155.

Gallagher, K.A., Schumacher, M.A., Bush, M.J., Bibb, M.J., Chandra, G., Holmes, N.A., Zeng, W., Henderson, M., Zhang, H., Findlay, K.C., et *al. (202*0). c-di-GMP Arms an Anti-sigma to Control Progression of Multicellular Differentiation in *Streptomyces.* Mol Cell 77, *586*-599 e586.

Gamba, P., Hamoen, L.W., and Daniel, R.A. (2016). Cooperative recruitment of FtsW to the division site of *Bacillus subtilis.* Front Microbiol 7, 1*80*8.

Gamba, P., Veening, J.-W., Saunders, N.J., Hamoen, L.W., and Daniel, R.A. (2009). Two-step assembly dynamics of the *Bacillus subtilis* divisome. J Bacteriol 191, *418*6-4194.

Garner, E.C., Bernard, R., Wang, W., Zhuang, X., Rudner, D.Z., and Mitchison, T. (2011). Coupled, circumferential motions of the cell wall synthesis machinery and MreB filaments in *B. subtilis. Sci*ence 333, *222*-225.

Garti‐Levi, S., Hazan, R., Kain, J., Fujita, M., and Ben‐Yehuda, S. (2008). The FtsEX ABC transporter directs cellular differentiation in *Bacillus subtilis.* Mol Microbiol 69, *101*8-1028.

Ghigo, J.-M., and Beckwith, J. (2000). Cell division in *Escherichia coli:* role of FtsL domains in septal localization, function, and oligomerization. J Bacteriol 182, *116*-129.

Gholamhoseinian, A., Shen, Z., Wu, J.-J., and Piggot, P. (1992). Regulation of transcription of the cell division gene *ftsA* during sporulation of Bacil*lus subtilis.* J Bacteriol 174, *464*7-4656.

Goehring, N.W., and Beckwith, J. (2005). Diverse paths to midcell: assembly of the bacterial cell division machinery. Curr Biol 15, *R51*4-R526.

Goehring, N.W., Gonzalez, M.D., and Beckwith, J. (2006). Premature targeting of cell division proteins to midcell reveals hierarchies of protein interactions involved in divisome assembly. Mol Microbiol 61, *33*-45.

Gomez-Escribano, J.P., Holmes, N.A., Schlimpert, S., Bibb, M.J., Chandra, G., Wilkinson, B., Buttner, M.J., and Bibb, M.J. (2021). *Streptomyces venezuelae NRRL* B-65442: genome sequence of a model strain used to study morphological differentiation in filamentous actinobacteria. J Ind Microbiol and Biotechnol.

Gonzalez, M.D., and Beckwith, J. (2009). Divisome under construction: distinct domains of the small membrane protein FtsB are necessary for interaction with multiple cell division proteins. J Bacteriol 191, *281*5-2825.

Gray, A.N., Egan, A.J., Van't Veer, I.L., Verheul, J., Colavin, A., Koumoutsi, A., Biboy, J., Altelaar, A.M., Damen, M.J., and Huang, K.C. (2015). Coordination of peptidoglycan synthesis and outer membrane constriction during *Escherichia coli cell* division. elife 4, e*07*118.

Gueiros-Filho, F.J., and Losick, R. (2002). A widely conserved bacterial cell division protein that promotes assembly of the tubulin-like protein FtsZ. Genes Dev 16, *254*4-2556.

Guijarro, J., Santamaría, R., Schauer, A., and Losick, R. (1988). Promoter determining the timing and spatial localization of transcription of a cloned *Streptomyces coelicolor gene* encoding a spore-associated polypeptide. J Bacteriol 170, *189*5-1901.

Gündoğdu, M.E., Kawai, Y., Pavlendova, N., Ogasawara, N., Errington, J., Scheffers, D.J., and Hamoen, L.W. (2011). Large ring polymers align FtsZ polymers for normal septum formation. EMBO J 30, *617*-626.

Haeusser, D.P., Schwartz, R.L., Smith, A.M., Oates, M.E., and Levin, P.A. (2004). EzrA prevents aberrant cell division by modulating assembly of the cytoskeletal protein FtsZ. Mol Microbiol 52, 8*01*-814.

Hale, C.A., and de Boer, P.A. (1997). Direct binding of FtsZ to ZipA, an essential component of the septal ring structure that mediates cell division in *E. coli.* Cell 88, 1*75*-185.

Hale, C.A., Shiomi, D., Liu, B., Bernhardt, T.G., Margolin, W., Niki, H., and de Boer, P.A. (2011). Identification of *Escherichia coli* ZapC (YcbW) as a component of the division apparatus that binds and bundles FtsZ polymers. J Bacteriol 193, *1393*-1404.

Hamoen, L.W., Meile, J.C., De Jong, W., Noirot, P., and Errington, J. (2006). SepF, a novel FtsZ - interacting protein required for a late step in cell division. Mol Microbiol 59, 9*89*-999.

Haney, S.A., Glasfeld, E., Hale, C., Keeney, D., He, Z., and de Boer, P. (2001). Genetic analysis of the *Escherichia coli* FtsZ.ZipA interaction in the yeast two-hybrid system. Characterization of FtsZ residues essential for the interactions with ZipA and with FtsA. J Biol Chem 276, *1198*0-11987.

Harry, E.J., Stewart, B.J., and Wake, R.G. (1993). Characterization of mutations in divIB of Bacill*us subtilis and c*ellular localization of the DivIB protein. Mol Microbiol 7, 61*1*-621.

Heichlinger, A., Ammelburg, M., Kleinschnitz, E.M., Latus, A., Maldener, I., Flardh, K., Wohlleben, W., and Muth, G. (2011). The MreB-like protein Mbl of *Strep*t*omyces coelicolor* A3(2) depends on MreB for proper localization and contributes to spore wall synthesis. J Bacteriol 193, *1533*-1542.

Heidrich, C., Templin, M.F., Ursinus, A., Merdanovic, M., Berger, J., Schwarz, H., de Pedro, M.A., and Holtje, J.V. (2001). Involvement of N-acetylmuramyl-L-alanine amidases in cell separation and antibiotic-induced autolysis of *Escherichia coli.* Mol Microbiol 41, 1*67*-178.

Hempel, A.M., Wang, S.B., Letek, M., Gil, J.A., and Flardh, K. (2008). Assemblies of DivIVA mark sites for hyphal branching and can establish new zones of cell wall growth in *Strept*o*myces coelicolor.* J Bacteriol 190, *7579*-7583.

Henriques, A., De Lencastre, H., and Piggot, P. (1992). A *Bacillus subtilis* morphogene cluster that includes *spoVE* is homologous to the *mra* region of *Escherichia coli.* Biochimie 74, 7*35*-748.

Henriques, A.O., Glaser, P., Piggot, P.J., and Moran Jr, C.P. (1998). Control of cell shape and elongation by the *rodA* gene in *Bacillus subtilis.* Mol Microbiol 28, 2*35*-247.

Hirota, Y., Ryter, A., and Jacob, F. (1968). Thermosensitive mutants of *E. coli* affected in the processes of DNA synthesis and cellular division. In Cold Spring Harbor symposia on quantitative biology (Cold Spring Harbor Laboratory Press), pp. 677-693.

Hirsch, C.F., and Ensign, J.C. (1976). Nutritionally defined conditions for germination of *Streptomyces viridochromogenes* spores. J Bacteriol 126, *13-2*3.

Holmes, N.A., Walshaw, J., Leggett, R.M., Thibessard, A., Dalton, K.A., Gillespie, M.D., Hemmings, A.M., Gust, B., and Kelemen, G.H. (2013). Coiled-coil protein Scy is a key component of a multiprotein assembly controlling polarized growth in *Streptomyces.* Proc Natl Acad Sci USA 110, *E397*-406.

Hopwood, D.A. (2007). *Streptomyces* in nature and medicine: the antibiotic makers (New York: Oxford University Press).

Hopwood, D.A., Wildermuth, H., and Palmer, H.M. (1970). Mutants of *Streptomyces coelicolor* defective in sporulation. J Gen Microbiol 61, 3*97*-408.

Hoskins, J., Matsushima, P., Mullen, D.L., Tang, J., Zhao, G., Meier, T.I., Nicas, T.I., and Jaskunas, S.R. (1999). Gene disruption studies of penicillin-binding proteins 1a, 1b, and 2a in *Streptococcus pneumoniae.* J Bacteriol 181, *6552*-6555.

Hu, Z., and Lutkenhaus, J. (1999). Topological regulation of cell division in *Escherichia coli* involves rapid pole to pole oscillation of the division inhibitor MinC under the control of MinD and MinE. Mol Microbiol 34, 8*2-9*0.

Hu, Z., and Lutkenhaus, J. (2001). Topological regulation of cell division in *E. coli:* spatiotemporal oscillation of MinD requires stimulation of its ATPase by MinE and phospholipid. Mol Cell 7, 13*37*-1343.

Hu, Z., Mukherjee, A., Pichoff, S., and Lutkenhaus, J. (1999). The MinC component of the division site selection system in Escher*ichia coli intera*cts with FtsZ to prevent polymerization. Proc Natl Acad Sci USA 96, 1*481*9-14824.

Hu, Z., Saez, C., and Lutkenhaus, J. (2003). Recruitment of MinC, an inhibitor of Z-ring formation, to the membrane in *Escherichia coli:* role of MinD and MinE. J Bacteriol 185, *196*-203.

Huber, T., Menon, S., and Sakmar, T.P. (2008). Structural basis for ligand binding and specificity in adrenergic receptors: implications for GPCR-targeted drug discovery. Biochem 47, 1*101*3-11023.

Hull, T.D., Ryu, M.H., Sullivan, M.J., Johnson, R.C., Klena, N.T., Geiger, R.M., Gomelsky, M., and Bennett, J.A. (2012). Cyclic Di-GMP phosphodiesterases RmdA and RmdB are involved in regulating colony morphology and development in *Streptomyces coelicolor. J Ba*cteriol 194, *4642*-4651.

Hunt, A.C., Servín-González, L., Kelemen, G.H., and Buttner, M.J. (2005). The *bldC* developmental locus of *Streptomyces coelicolor* encodes a member of a family of small DNA-binding proteins related to the DNA-binding domains of the MerR family. Journal bacteriol 187, *716*-728.

Ishino, F., and Matsuhashi, M. (1981). Peptidoglycan synthetic enzyme activities of highly purified penicillin-binding protein 3 in *Escherichia coli:* a septum-forming reaction sequence. Biochem Biophys Res Commun 101, *905*-911.

Jakimowicz, D., Chater, K., and Zakrzewska‐Czerwi´nska, J. (2002). The ParB protein of *Streptomyces coelicolor* A3 (2) recognizes a cluster of *parS* sequences within the origin‐proximal region of the linear chromosome. Mol Microbiol 45, 1*365*-1377.

Jakimowicz, D., Gust, B., Zakrzewska-Czerwinska, J., and Chater, K.F. (2005). Developmental-stage-specific assembly of ParB complexes in *Streptomyces coelicolor* hyphae. J Bacteriol 187, *3572*-3580.

Jakimowicz, D., and van Wezel, G.P. (2012). Cell division and DNA segregation in *Streptomyces*: how to build a septum in the middle of nowhere? Mol Microbiol 85, 3*93*-404.

Jakimowicz, D., Zydek, P., Kois, A., Zakrzewska-Czerwinska, J., and Chater, K.F. (2007). Alignment of multiple chromosomes along helical ParA scaffolding in sporulating *Streptomyces* hyphae. Mol Microbiol 65, 6*25*-641.

Javadi, A., Soderholm, N., Olofsson, A., Flardh, K., and Sandblad, L. (2019). Assembly mechanisms of the bacterial cytoskeletal protein FilP. Life Sci Alliance 2.

Jo*hn*son, J.E., Lackner, L.L., Hale, C.A., and De Boer, P.A. (2004). ZipA is required for targeting of DMinC/DicB, but not DMinC/MinD, complexes to septal ring assemblies in *Escherichia coli.* J Bacteriol 186, 2*418-2*429.

Jones, L.J., Carballido-López, R., and Errington, J. (2001). Control of cell shape in bacteria: helical, actin-like filaments in *Bacillus subtilis. Cell 1*04, 91*3-92*2.

Jones, S.E., and Elliot, M.A. (2017). *Streptomyces* Exploration: Competition, Volatile Communication and New Bacterial Behaviours. Trends Microbiol 25, 522-*53*1.

Jones, S.E., Ho, L., Rees, C.A., Hill, J.E., Nodwell, J.R., and Elliot, M.A. (2017). *Streptomyces* exploration is triggered by fungal interactions and volatile signals. Elife 6.

Jone*s,* S.E., Pham, C.A., Zambri, M.P., McKillip, J., Carlson, E.E., and Elliot, M.A. (2019). *Streptomyces* volatile compounds influence exploration and microbial community dynamics by altering iron availability. MBio 10, e00*171*-00119.

Kaiser, B.K., Clifton, M.C., Shen, B.W., and Stoddard, B.L. (2009). The structure of a bacterial DUF199/WhiA protein: domestication of an invasive endonuclease. Structure 17, 136*8-1*376.

Katis, V., Harry, E., and Wake, R. (1997). The *Bacillus subtilis* division protein DivIC is a highly abundant membrane‐bound protein that localizes to the division site. Mol Microbiol 26, 104*7-1*055.

Kawai, Y., Asai, K., and Errington, J. (2009). Partial functional redundancy of MreB isoforms, MreB, Mbl and MreBH, in cell morphogenesis of *Bacillus subtilis.* Mol Microbiol 73, 719-*73*1.

Kawamoto, S., and Ensign, J.C. (1995). Cloning and characterization of a gene involved in regulation of sporulation and cell division of *Streptomyces griseus.* Actinomycetologica 9, 136-*15*1.

Keijser, B.J., Noens, E.E., Kraal, B., Koerten, H.K., and van Wezel, G.P. (2003). The *Streptomyces coelicolor ssgB* gene is required for early stages of sporulation. FEMS Microbiol Lett 225, 59-*67.*

Kelemen, G.H., Brian, P., Flärdh, K., Chamberlin, L., Chater, K.F., and Buttner, M.J. (1998). Developmental regulation of transcription of *whiE*, a locus specifying the polyketide spore pigment in *Streptomyces coelicolor* A3 (2). J Bacteriol 180, 25*15-25*21.

Kelemen, G.H., Viollier, P.H., Tenor, J., Marri, L., Buttner, M.J., and Thompson, C.J. (2001). A connection between stress and development in the multicellular prokaryote *Streptomyces coelicolor* A3(2). Mol Microbiol 40, 804-*81*4.

Kleinschnitz, E.M., Heichlinger, A., Schirner, K., Winkler, J., Latus, A., Maldener, I., Wohlleben, W., and Muth, G. (2011a). Proteins encoded by the mre gene cluster in *Streptomyces coelicolor* A3(2) *c*ooperate in spore wall synthesis. Mol Microbiol 79, 136*7-1*379.

Kleinschnitz, E.M., Latus, A., Sigle, S., Maldener, I., Wohlleben, W., and Muth, G. (2011b). Genetic analysis of SCO2997, encoding a TagF homologue, indicates a role for wall teichoic acids in sporulation of *Streptomyces coelicolor* A3(2*).* J Bacteriol 193, 60*80-6*085.

Knizewski, L., and Ginalski, K. (2007). Bacterial DUF199/COG1481 proteins including sporulation regulator WhiA are distant homologs of LAGLIDADG homing endonucleases that retained only DNA binding. Cell Cycle 6, 1666-*1*670.

Kodani, S., Hudson, M.E., Durrant, M.C., Buttner, M.J., Nodwell, J.R., and Willey, J.M. (2004). The SapB morphogen is a lantibiotic-like peptide derived from the product of the developmental gene *ramS* in *Streptomyces coelicolor.* Proc Natl Acad Sci USA 101, 11*448*-11453.

Kois, A., Swiatek, M., Jakimowicz, D., and Zakrzewska-Czerwinska, J. (2009). SMC protein-dependent chromosome condensation during aerial hyphal development in *Streptomyces.* J Bacteriol 191, 31*0-319*.

Kois-Ostrowska, A., Strzałka, A., Lipietta, N., Tilley, E., Zakrzewska-Czerwińska, J., Herron, P., and Jakimowicz, D. (2016). Unique function of the bacterial chromosome segregation machinery in apically growing *Streptomyces*-targeting the chromosome to new hyphal tubes and its anchorage at the tips. PLoS Genet 12, e10*064*88.

Koppelman, C.M., Aarsman, M.E., Postmus, J., Pas, E., Muijsers, A.O., Scheffers, D.J., Nanninga, N., and den Blaauwen, T. (2004). R174 of *Escherichia coli* FtsZ is involved in membrane interaction and protofilament bundling, and is essential for cell division. Mol Microbiol 51, 645-*65*7.

Kormanec, J., and Sevcikova, B. (2002). The stress-response sigma factor sigma(H) controls the expression of *ssgB*, a homologue of the sporulation-specific cell division gene *ssgA*, in *Streptomyces coelicolor* A3(2)*.* Mol Genet Genomics 267, 53*6-54*3.

Kotun, A.M. (2013). Genetic and biochemical analyses of *Streptomyces coelicolor* FtsZ*, S*epF, and other possible FtsZ-interacting proteins. (Duquesne University).

Kruse, T., Bork-Jensen, J., and Gerdes, K. (2005). The morphogenetic MreBCD proteins of *Escherichia coli* form *an* essential membrane-bound complex. Mol Microbiol 55, 78-*89.*

Kuhn, A. (2019). Bacterial cell walls and membranes (Springer).

Kuhn, J., Briegel, A., Morschel, E., Kahnt, J., Leser, K., Wick, S., Jensen, G.J., and Thanbichler, M. (2010). Bactofilins, a ubiquitous class of cytoskeletal proteins mediating polar localization of a cell wall synthase in *Caulobacter crescentus. EMBO J* 29, 327-*33*9.

Kysela, D.T., Randich, A.M., Caccamo, P.D., and Brun, Y.V. (2016). Diversity Takes Shape: Understanding the Mechanistic and Adaptive Basis of Bacterial Morphology. PLoS Biol 14, e10*025*65.

Lackner, L.L., Raskin, D.M., and De Boer, P.A. (2003). ATP-dependent interactions between *Escherichia coli* Min *prot*eins and the phospholipid membrane *in vitro.* J Bacteriol 185, 73*5-749*.

Ladwig, N., Franz-Wachtel, M., Hezel, F., Soufi, B., Macek, B., Wohlleben, W., and Muth, G. (2015). Control of Morphological Differentiation of *Streptomyces coelicolor* A3(2) by Phosphorylation of MreC and PBP2. PLoS One 10, e01*254*25.

Leclercq, S., Derouaux, A., Olatunji, S., Fraipont, C., Egan, A.J., Vollmer, W., Breukink, E., and Terrak, M. (2017). Interplay between penicillin-binding proteins and SEDS proteins promotes bacterial cell wall synthesis. Sci Rep 7, 1-13.

Levin, P.A., Kurtser, I.G., and Grossman, A.D. (1999). Identification and characterization of a negative regulator of FtsZ ring formation in *Bacillus subtilis.* Proc Natl Acad Sci USA 96, 964*2-9*647.

Liman, R., Facey, P.D., van Keulen, G., Dyson, P.J., and Del Sol, R. (2013). A laterally acquired galactose oxidase-like gene is required for aerial development during osmotic stress in *Streptomyces coelicolor. PLoS O*ne 8, e541*12*.

Lin, L., and Thanbichler, M. (2013). Nucleotide‐independent cytoskeletal scaffolds in bacteria. Cytoskeleton 70, 409-*42*3.

Liu, B., Persons, L., Lee, L., and de Boer, P.A. (2015). Roles for both FtsA and the FtsBLQ subcomplex in FtsN‐stimulated cell constriction in *Escherichia coli.* Mol *Microbiol* 95, 945-*97*0.

Liu, X., Biboy, J., Consoli, E., Vollmer, W., and den Blaauwen, T. (2020). MreC and MreD balance the interaction between the elongasome proteins PBP2 and RodA. PLoS Genet 16, e10*09276*.

Löwe, J. (1998). Crystal Structure Determination of FtsZ from *Methanococcus jannaschii.* J Struct Biol 124, 235-243.

Lowe, J., and Amos, L.A. (1998). Crystal structure of the bacterial cell-division protein FtsZ. Nature 391, 203-206.

Lu, C., Stricker, J., and Erickson, H.P. (2001). Site-specific mutations of FtsZ--effects on GTPase and *in vitro* assembly. BMC Microbiol 1, 7.

L*ut*kenhaus, J. (2007). Assembly dynamics of the bacterial MinCDE system and spatial regulation of the Z ring. Annu Rev. Biochem 76, 539-562.

Lutkenhaus, J., Wolf-Watz, H., and Donachie, W. (1980). Organization of genes in the *ftsA-envA* region of the *Escherichia coli* genetic map and identification of a new *fts* locus (*ftsZ*). J Bacteriol 142, 615-620.

Ma, X., and Margolin, W. (1999). Genetic and functional analyses of the conserved C-terminal core domain of *Escherichia coli* FtsZ. J Bacteriol 181, 7531-7544.

Mahone, C.R., and Goley, E.D. (2020). Bacterial cell division at a glance. J Cell Sci 133.

Ma*nat,* G., Roure, S., Auger, R., Bouhss, A., Barreteau, H., Mengin-Lecreulx, D., and Touzé, T. (2014). Deciphering the metabolism of undecaprenyl-phosphate: the bacterial cell-wall unit carrier at the membrane frontier. Microbial Drug Resistance 20, 199-214.

Margolin, W. (2000). Themes and variations in prokaryotic cell division. FEMS Microbiol Rev 24, 531-548.

Margolin, W. (2005). FtsZ and the division of prokaryotic cells and organelles. Nat Rev Mol Cell Biol 6, 862-871.

Martin, M.E., Trimble, M.J., and Brun, Y.V. (2004). Cell cycle‐dependent abundance, stability and localization of FtsA and FtsQ in *Caulobacter crescentus.* Mol Microbiol 54, 60-74.

Mazza, P., Noens, E.E., Schirner, K., Grantcharova, N., Mommaas, A.M., Koerten, H.K., Muth, G., Flardh, K., van Wezel, G.P., and Wohlleben, W. (2006). MreB of *Streptomyces coelicolor* is not essential for vegetative growth but is required for the integrity of aerial hyphae and spores. Mol Microbiol 60, 838-852.

McCormick, J.R. (2009). Cell division is dispensable but not irrelevant in *Streptomyces.* Curr Opin Microbiol 12, 689-698.

McCormick, J.R., and Flärdh, K. (2012). Signals and regulators that govern *Streptomyces* development. FEMS Microbiol Rev 36, 206-231.

McCormick, J.R., and Losick, R. (1996). Cell division gene *ftsQ* is required for efficient sporulation but not growth and viability in *Streptomyces coelicolor A3(2).* J Bacteriol 178, 5295-5301.

McCormick, J.R., Su, E.P., Driks, A., and Losick, R. (1994). Growth and viability of *Streptomyces coelicolor* mutant for the cell division gene *ftsZ*. Mol Microbiol 14, 243-254.

Meeske, A.J., Riley, E.P., Robins, W.P., Uehara, T., Mekalanos, J.J., Kahne, D., Walker, S., Kruse, A.C., Bernhardt, T.G., and Rudner, D.Z. (2016). SEDS proteins are a widespread family of bacterial cell wall polymerases. Nature 537, 634-638.

Meeske, A.J., Sham, L.-T., Kimsey, H., Koo, B.-M., Gross, C.A., Bernhardt, T.G., and Rudner, D.Z. (2015). MurJ and a novel lipid II flippase are required for cell wall biogenesis in *Bacillus subtilis.* Proc *N*atl Acad Sci USA 112, 6437-6442.

Meisner, J., Montero Llopis, P., Sham, L.T., Garner, E., Bernhardt, T.G., and Rudner, D.Z. (2013). FtsEX is required for CwlO peptidoglycan hydrolase activity during cell wall elongation in *Bacillus subtilis.* Mol Microbiol 89, 1069-1083.

Merrick, M. (1976). A morphological and genetic mapping study of bald colony mutants of *Streptomyces coelicolor.* Microbiology 96, 299-315.

Michie, K.A., Monahan, L.G., Beech, P.L., and Harry, E.J. (2006). Trapping of a spiral-like intermediate of the bacterial cytokinetic protein FtsZ. J Bacteriol 188, 1680-1690.

Mistry, B.V., Del Sol, R., Wright, C., Findlay, K., and Dyson, P. (2008). FtsW is a dispensable cell division protein required for Z-ring stabilization during sporulation septation in *Streptomyces coelicolor.* J Bacteriol 190, 5555-5566.

Mohammadi, T., Sijbrandi, R., Lutters, M., Verheul, J., Martin, N.I., den Blaauwen, T., de Kruijff, B., and Breukink, E. (2014). Specificity of the transport of lipid II by FtsW in *Escherichia coli.* J Biol Chem 289, 14707-14718.

Mohammadi, T., van Dam, V., Sijbrandi, R., Vernet, T., Zapun, A., Bouhss, A., Diepeveen-de Bruin, M., Nguyen-Disteche, M., de Kruijff, B., and Breukink, E. (2011). Identification of FtsW as a transporter of lipid-linked cell wall precursors across the membrane. EMBO J 30, 142*5-1*432.

Morgenstein, R.M., Bratton, B.P., Nguyen, J.P., Ouzounov, N., Shaevitz, J.W., and Gitai, Z. (2015). RodZ links MreB to cell wall synthesis to mediate MreB rotation and robust morphogenesis. Proc Natl Acad Sci USA 112, 12*510*-12515.

Mosyak, L., Zhang, Y., Glasfeld, E., Haney, S., Stahl, M., Seehra, J., and Somers, W.S. (2000). The bacterial cell-division protein ZipA and its interaction with an FtsZ fragment revealed by X-ray crystallography. EMBO J 19, 317*9-3*191.

Mueller, E.A., Egan, A.J., Breukink, E., Vollmer, W., and Levin, P.A. (2019). Plasticity of *Escherichia coli* cell wall metabolism promotes fitness and antibiotic resistance across environmental conditions. Elife 8.

Mukh*er*jee, A., and Lutkenhaus, J. (1994). Guanine nucleotide-dependent assembly of FtsZ into filaments. J Bacteriol 176, 27*54-2*758.

Mukherjee, A., and Lutkenhaus, J. (1998). Dynamic assembly of FtsZ regulated by GTP hydrolysis. EMBO J 17, 462-*469*.

Nelson, D.E., and Young, K.D. (2000). Penicillin binding protein 5 affects cell diameter, contour, and morphology of *Escherichia coli.* J Bacteriol 182, 17*14-1*721.

Noens, E.E., Mersinias, V., Traag, B.A., Smith, C.P., Koerten, H.K., and van Wezel, G.P. (2005). SsgA-like proteins determine the fate of peptidoglycan during sporulation of *Streptomyces coelicolor. Mol Mi*crobiol 58, 929-*94*4.

Noens, E.E., Mersinias, V., Willemse, J., Traag, B.A., Laing, E., Chater, K.F., Smith, C.P., Koerten, H.K., and van Wezel, G.P. (2007). Loss of the controlled localization of growth stage-specific cell-wall synthesis pleiotropically affects developmental gene expression in an *ssgA* mutant of *Streptomyces coelicolor.* Mol Microbiol 64, 124*4-1*259.

Oliva, M.A., Cordell, S.C., and Löwe, J. (2004). Structural insights into FtsZ protofilament formation. Nat Struct Mol Biol 11, 124*3-1*250.

Osorio-Valeriano, M., Altegoer, F., Steinchen, W., Urban, S., Liu, Y., Bange, G., and Thanbichler, M. (2019). ParB-type DNA segregation proteins are CTP-dependent molecular switches. Cell 179, 1512-1524. e1515.

Paik, J., Kern, I., Lurz, R., and Hakenbeck, R. (1999). Mutational analysis of the *Streptococcus pneumoniae* bimodular class A penicillin-binding proteins. J Bacteriol 181, 3852-3856.

Pastoret, S., Fraipont, C., Den Blaauwen, T., Wolf, B., Aarsman, M.E., Piette, A., Thomas, A., Brasseur, R., and Nguyen-Distèche, M. (2004). Functional analysis of the cell division protein FtsW of *Escherichia coli.* J Bacteriol 186, 8370-8379.

Peters, N.T., Morlot, C., Yang, D.C., Uehara, T., Vernet, T., and Bernhardt, T.G. (2013). Structure-function analysis of the LytM domain of EnvC, an activator of cell wall remodelling at the *Escherichia coli* division site. Mol Microbiol 89, 690-701.

Pichoff, S., Du, S., and Lutkenhaus, J. (2019). Roles of FtsEX in cell division. Res Microbiol 170, 374-380.

Pichoff, S., and Lutkenhaus, J. (2002). Unique and overlapping roles for ZipA and FtsA in septal ring assembly in *Escherichia coli.* EMBO J 21, 685-693.

Pichoff, S., and Lutkenhaus, J. (2005). Tethering the Z ring to the membrane through a conserved membrane targeting sequence in FtsA. Mol Microbiol 55, 1722-1734.

Pogliano, J., Pogliano, K., Weiss, D.S., Losick, R., and Beckwith, J. (1997). Inactivation of FtsI inhibits constriction of the FtsZ cytokinetic ring and delays the assembly of FtsZ rings at potential division sites. Proc Natl Acad Sci USA 94, 559-564.

Potluri, L.P., Kannan, S., and Young, K.D. (2012). ZipA is required for FtsZ-dependent preseptal peptidoglycan synthesis prior to invagination during cell division. J Bacteriol 194, 5334-5342.

Ramos-León, F., Bush, M.J., Sallmen, J.W., Chandra, G., Richardson, J., Findlay, K.C., McCormick, J.R., and Schlimpert, S. (2021). A conserved cell division protein directly regulates FtsZ dynamics in filamentous and unicellular actinobacteria. Elife 10, e63387.

Raskin, D.M., and de Boer, P.A. (1999). MinDE-dependent pole-to-pole oscillation of division inhibitor MinC in *Escherichia coli.* J Bacteriol 181, 6419-6424.

Real, G., Autret, S., Harry, E.J., Errington, J., and Henriques, A.O. (2005). Cell division protein DivIB influences the Spo0J/Soj system of chromosome segregation in *Bacillus subtilis.* Mol Microbiol 55, 349-*367*.

Redick, S.D., Stricker, J., Briscoe, G., and Erickson, H.P. (2005). Mutants of FtsZ targeting the protofilament interface: effects on cell division and GTPase activity. J Bacteriol 187, 2*727-27*36.

Rohs, P.D.A., Buss, J., Sim, S.I., Squyres, G.R., Srisuknimit, V., Smith, M., Cho, H., Sjodt, M., Kruse, A.C., Garner, E.C., et al. *(*2018*).* A central role for PBP2 in the activation of peptidoglycan polymerization by the bacterial cell elongation machinery. PLoS Genet 14, e10*077*26.

Romberg, L., Simon, M., and Erickson, H.P. (2001). Polymerization of FtsZ, a bacterial homolog of tubulin, is assembly cooperative J Biol Chem 276, 11*743*-11753.

Rothfield, L., Taghbalout, A., and Shih, Y.-L. (2005). Spatial control of bacterial division-site placement. Nat Rev Microbiol 3, 959-*96*8.

Rowland, S., Katis, V., Partridge, S., and Wake, R. (1997). DivIB, FtsZ and cell division in *Bacillus subtilis*. Mol Microbiol 23, 295-*30*2.

Ruiz, N. (2008). Bioinformatics identification of MurJ (MviN) as the peptidoglycan lipid II flippase in *Escherichia coli.* Proc Natl Acad Sci USA 105, 15*553*-15557.

Ryding, N.J., Bibb, M.J., Molle, V., Findlay, K.C., Chater, K.F., and Buttner, M.J. (1999). New sporulation loci in *Streptomyces coelicolor A3(2).* J Bacteriol 181, 5*419-5*425.

Salerno, P., Larsson, J., Bucca, G., Laing, E., Smith, C.P., and Flärdh, K. (2009). One of the two genes encoding nucleoid-associated HU proteins in *Streptomyces coelicolor* is developmentally regulated and specifically involved in spore maturation. J Bacteriol 191, 64*89-6*500.

Salje, J., van den Ent, F., de Boer, P., and Lowe, J. (2011). Direct membrane binding by bacterial actin MreB. Mol Cell 43, 478-*48*7.

Sallmen II, J.W. (2019). Genetic and Biochemical Analysis of a Conserved, Multi-Gene System Regulating Spore-Associated Proteins in *Streptomyces coelicolor. (*Duquesne University).

Sauvage, E., Kerff, F., Terrak, M., Ayala, J.A., and Charlier, P. (2008). The penicillin-binding proteins: structure and role in peptidoglycan biosynthesis. FEMS Microbiol Rev 32, 234-258.

Schleifer, K.H., and Kandler, O. (1972). Peptidoglycan types of bacterial cell walls and their taxonomic implications. Bacteriological Rev 36, 407-477.

Schlimpert, S., Flardh, K., and Buttner, M. (2016). Fluorescence time-lapse imaging of the complete *S.* venez*uelae* life cycle using a microfluidic device. J Vis Exp 108, 53*863.*

Schlimpert, S., Wasserstrom, S., Chandra, G., Bibb, M.J., Findlay, K.C., Flardh, K., and Buttner, M.J. (2017). Two dynamin-like proteins stabilize FtsZ rings during *Streptomyces* sporulation. Proc Natl Acad Sci USA 114, E6*176*-E6183.

Schmidt, K.L., Peterson, N.D., Kustusch, R.J., Wissel, M.C., Graham, B., Phillips, G.J., and Weiss, D.S. (2004). A predicted ABC transporter, FtsEX, is needed for cell division in *Escherichia coli.* J Bacteriol 186, 78*5-79*3.

Schumacher, M.A., den Hengst, C.D., Bush, M.J., Le, T.B.K., Tran, N.T., Chandra, G., Zeng, W., Travis, B., Brennan, R.G., and Buttner, M.J. (2018). The MerR-like protein BldC binds DNA direct repeats as cooperative multimers to regulate *Streptomyces* development. Nat Commun 9, 1139.

Sexton, D.L., Herlihey, F.A., Brott, A.S., Crisante, D.A., Shepherdson, E., Clarke, A.J., and Elliot, M.A. (2020). Roles of LysM and LytM domains in resuscitation-promoting factor (Rpf) activity and Rpf-mediated peptidoglycan cleavage and dormant spore reactivation: Peptidoglycan cleavage and cellular resuscitation by Rpfs. J Biol Chem 295, 91*71-9*182.

Sexton, D.L., St-Onge, R.J., Haiser, H.J., Yousef, M.R., Brady, L., Gao, C., Leonard, J., and Elliot, M.A. (2015). Resuscitation-promoting factors are cell wall-lytic enzymes with important roles in the germination and growth of *Streptomyces coelicolor. J Bact*eriol 197, 84*8-86*0.

Sexton, D.L., and Tocheva, E.I. (2020). Ultrastructure of Exospore Formation in *Streptomyces* Revealed by Cryo-Electron Tomography. Front Microbiol 11, 581*135*.

Sham, L.-T., Butler, E.K., Lebar, M.D., Kahne, D., Bernhardt, T.G., and Ruiz, N. (2014). MurJ is the flippase of lipid-linked precursors for peptidoglycan biogenesis. Science 345, 22*0-22*2.

Sharp, M.D., and Pogliano, K. (1999). An *in vivo* membrane fusion assay implicates SpoIIIE in the final stages of engulfment during *Bacillus subtilis* sporulation. Proc Natl Acad Sci USA 96, 145*53*-14558.

Sharp, M.D., and Pogliano, K. (2003). The membrane domain of SpoIIIE is required for membrane fusion during *Bacillus subtilis* sporulation. J Bacteriol 185, 2*005-2*008.

Shi, H., Bratton, B.P., Gitai, Z., and Huang, K.C. (2018). How to Build a Bacterial Cell: MreB as the Foreman of *E. coli* Construction. Cell 172, 12*94-1*305.

Sigle, S., Ladwig, N., Wohlleben, W., and Muth, G. (2015). Synthesis of the spore envelope in the developmental life cycle of *Streptomyces coelicolor.* Int. J. of Med. Microbiol. 305, 18*3-18*9.

Sigle, S., Steblau, N., Wohlleben, W., and Muth, G. (2016). Polydiglycosylphosphate transferase PdtA (SCO2578) of *Streptomyces coelicolor* A3(2) is crucial for proper sporulation and apical tip extension under stress conditions. Appl Environ Microbiol 82, 566*1-5*672.

Singh, J.K., Makde, R.D., Kumar, V., and Panda, D. (2007). A membrane protein, EzrA, regulates assembly dynamics of FtsZ by interacting with the C-terminal tail of FtsZ. Biochem 46, 110*13*-11022.

Singh, J.K., Makde, R.D., Kumar, V., and Panda, D. (2008). SepF increases the assembly and bundling of FtsZ polymers and stabilizes FtsZ protofilaments by binding along its length. J Biol Chem 283, 31*116*-31124.

Sjodt, M., Rohs, P.D., Gilman, M.S., Erlandson, S.C., Zheng, S., Green, A.G., Brock, K.P., Taguchi, A., Kahne, D., and Walker, S. (2020). Structural coordination of polymerization and crosslinking by a SEDS–bPBP peptidoglycan synthase complex. Nat Microbiol 5, 813-*82*0.

Small, E., Marrington, R., Rodger, A., Scott, D.J., Sloan, K., Roper, D., Dafforn, T.R., and Addinall, S.G. (2007). FtsZ polymer-bundling by the *Escherichia coli* ZapA orthologue, YgfE, involves a conformational change in bound GTP. J Mol Biol 369, 21*0-22*1.

Soh, Y.-M., Davidson, I.F., Zamuner, S., Basquin, J., Bock, F.P., Taschner, M., Veening, J.-W., De Los Rios, P., Peters, J.-M., and Gruber, S. (2019). Self-organization of *parS* centromeres by the ParB CTP hydrolase. Science 366, 11*29-1*133.

Soliveri, J.A., Gomez, J., Bishai, W.R., and Chater, K.F. (2000). Multiple paralogous genes related to the *Streptomyces coelicolor* developmental regulatory gene *whiB* are present in *Streptomyces* and other actinomycetes. Microbiology (Reading) 146 (P*t 2), 333-34*3.

Spratt, B.G. (1975). Distinct penicillin binding proteins involved in the division, elongation, and shape of *Escherichia coli* K12. Proc Natl Acad Sci USA 72, 299*9-3*003.

St-Onge, R.J., Haiser, H.J., Yousef, M.R., Sherwood, E., Tschowri, N., Al-Bassam, M., and Elliot, M.A. (2015). Nucleotide second messenger-mediated regulation of a muralytic enzyme in *Streptomyces.* Mol Microbiol 96, 779-*79*5.

Strakova, E., Bobek, J., Zikova, A., Rehulka, P., Benada, O., Rehulkova, H., Kofronova, O., and Vohradsky, J. (2013). Systems insight into the spore germination of *Streptomyces coelicolor.* J Proteome Res 12, 525-*53*6.

Sundararajan, K., and Goley, E.D. (2017). The intrinsically disordered C-terminal linker of FtsZ regulates protofilament dynamics and superstructure in vitro. J Biol Chem 292, 20*509*-20527.

Swiercz, J.P., Nanji, T., Gloyd, M., Guarne, A., and Elliot, M.A. (2013). A novel nucleoid-associated protein specific to the actinobacteria. Nucleic Acids Res 41, 417*1-4*184.

Swulius, M.T., and Jensen, G.J. (2012). The helical MreB cytoskeleton in *Escherichia coli* MC1000/pLE7 is an artifact of the N-Terminal yellow fluorescent protein tag. J Bacteriol 194, 63*82-6*386.

Szafran, M.J., Jakimowicz, D., and Elliot, M.A. (2020). Compaction and control—the role of chromosome-organizing proteins in *Streptomyces.* FEMS Microbiol Rev 44, 725-*73*9.

Szafran, M.J., Malecki, T., Strzalka, A., Pawlikiewicz, K., Dulawa, J., Zarek, A., Kois-Ostrowska, A., Findlay, K.C., Le, T.B.K., and Jakimowicz, D. (2021). Spatial rearrangement of the *Streptomyces venezue*lae linear chromosome during sporogenic development. Nat Commun 12, 522*2.*

Taguchi, A., Welsh, M.A., Marmont, L.S., Lee, W., Sjodt, M., Kruse, A.C., Kahne, D., Bernhardt, T.G., and Walker, S. (2019). FtsW is a peptidoglycan polymerase that is functional only in complex with its cognate penicillin-binding protein. Nat Microbiol 4, 587-*59*4.

Tavares, J.R., de Souza, R.F., Meira, G.L.S., and Gueiros-Filho, F.J. (2008). Cytological characterization of YpsB, a novel component of the idivisome. J Bacteriol 190, 70*96-7*107.

Thanedar, S., and Margolin, W. (2004). FtsZ exhibits rapid movement and oscillation waves in helix-like patterns in *Escherichia coli.* Curr Biol 14, 1167-1173.

Thompson, L., Beech, P., Real, G., Henriques, A., and Harry, E. (2006). Requirement for the cell division protein DivIB in polar cell division and engulfment during sporulation in *Bacillus subtilis.* J Bacteriol 188, 7677-7685.

Tonthat, N.K., Milam, S.L., Chinnam, N., Whitfill, T., Margolin, W., and Schumacher, M.A. (2013). SlmA forms a higher-order structure on DNA that inhibits cytokinetic Z-ring formation over the nucleoid. Proc Natl Acad Sci USA 110, 10586-10591.

Traag, B.A., Kelemen, G.H., and Van Wezel, G.P. (2004). Transcription of the sporulation gene ssgA is activated by the IclR-type regulator SsgR in a *whi*-independent manner in *Streptomyces coelicolor* A3(2). Mol Microbiol 53, 985-1000.

Traag, B.A., and van Wezel, G.P. (2008). The SsgA-like proteins in actinomycetes: small proteins up to a big task. Antonie Van Leeuwenhoek 94, 85-97.

Tran, N.T., Den Hengst, C.D., Gomez-Escribano, J.P., and Buttner, M.J. (2011). Identification and characterization of CdgB, a diguanylate cyclase involved in developmental processes in *Streptomyces coelicolor.* J Bacteriol 193, 3100-3108.

Tsang, M.J., Yakhnina, A.A., and Bernhardt, T.G. (2017). NlpD links cell wall remodeling and outer membrane invagination during cytokinesis in *Escherichia coli. PLoS G*enet 13, e1006888.

Tschowri, N., Schumacher, M.A., Schlimpert, S., Chinnam, N.B., Findlay, K.C., Brennan, R.G., and Buttner, M.J. (2014). Tetrameric c-di-GMP mediates effective transcription factor dimerization to control *Streptomyces* development. Cell 158, 1136-1147.

Typas, A., Banzhaf, M., Gross, C.A., and Vollmer, W. (2011). From the regulation of peptidoglycan synthesis to bacterial growth and morphology. Nat Rev Microbiol 10, 123-136.

Typas, A., Banzhaf, M., van Saparoea, B.v.d.B., Verheul, J., Biboy, J., Nichols, R.J., Zietek, M., Beilharz, K., Kannenberg, K., and von Rechenberg, M. (2010). Regulation of peptidoglycan synthesis by outer-membrane proteins. Cell 143, 1097-1109.

Uehara, T., Parzych, K.R., Dinh, T., and Bernhardt, T.G. (2010). Daughter cell separation is controlled by cytokinetic ring‐activated cell wall hydrolysis. EMBO J 29, 1412-1422.

Unsleber, S., Wohlleben, W., and Stegmann, E. (2019). Diversity of peptidoglycan structure-Modifications and their physiological role in resistance in antibiotic producers. Int J Med Microbiol 309, 15*1332*.

Ursell, T.S., Nguyen, J., Monds, R.D., Colavin, A., Billings, G., Ouzounov, N., Gitai, Z., Shaevitz, J.W., and Huang, K.C. (2014). Rod-like bacterial shape is maintained by feedback between cell curvature and cytoskeletal localization. Proc Natl Acad Sci USA 111, E1*025*-1034.

Ursinus, A., van den Ent, F., Brechtel, S., de Pedro, M., Holtje, J.V., Lowe, J., and Vollmer, W. (2004). Murein (peptidoglycan) binding property of the essential cell division protein FtsN from *Escherichia coli.* J Bacteriol 186, 67*28-6*737.

van den Ent, F., Izore, T., Bharat, T.A., Johnson, C.M., and Lowe, J. (2014). Bacterial actin MreB forms antiparallel double filaments. Elife 3, e026*34*.

Van Den Ent, F., Johnson, C.M., Persons, L., De Boer, P., and Löwe, J. (2010). Bacterial actin MreB assembles in complex with cell shape protein RodZ. EMBO J 29, 108*1-1*090.

van der Aart, L.T., Spijksma, G.K., Harms, A., Vollmer, W., Hankemeier, T., and van Wezel, G.P. (2018). High-resolution analysis of the peptidoglycan composition in *Streptomyces coelicolor.* J Bacteriol 200, e0*0290*-00218.

van Teeffelen, S., Wang, S., Furchtgott, L., Huang, K.C., Wingreen, N.S., Shaevitz, J.W., and Gitai, Z. (2011). The bacterial actin MreB rotates, and rotation depends on cell-wall assembly. Proc Natl Acad Sci USA 108, 15*822*-15827.

Varma, A., de Pedro, M.A., and Young, K.D. (2007). FtsZ directs a second mode of peptidoglycan synthesis in *Escherichia coli.* J Bacteriol 189, 56*92-5*704.

Vaughan, S., Wickstead, B., Gull, K., and Addinall, S.G. (2004). Molecular evolution of FtsZ protein sequences encoded within the genomes of archaea, bacteria, and eukaryota. J Mol Evol 58, 19-*29.*

Vicente, M., and Rico, A.I. (2006). The order of the ring: assembly of *Escherichia coli* cell division components. Mol Microbiol 61, 5-8.

*V*ollmer, B., Steblau, N., Ladwig, N., Mayer, C., Macek, B., Mitousis, L., Sigle, S., Walter, A., Wohlleben, W., and Muth, G. (2019). Role of the Streptomyces spore wall synthesizing complex SSSC in differentiation of *Streptomyces coelicolor* A3(2). Int J Med Microbiol 309, 15*1327*.

Vollmer, W., Blanot, D., and de Pedro, M.A. (2008a). Peptidoglycan structure and architecture. FEMS Microbiol Rev 32, 149-167.

Vollmer, W., Joris, B., Charlier, P., and Foster, S. (2008b). Bacterial peptidoglycan (murein) hydrolases. FEMS Microbiol Rev 32, 259-286.

Wachi, M., Doi, M., Tamaki, S., Park, W., Nakajima-Iijima, S., and Matsuhashi, M. (1987). Mutant isolation and molecular cloning of mre genes, which determine cell shape, sensitivity to mecillinam, and amount of penicillin-binding proteins in *Escherichia coli.* J Bacteriol 169, 4935-4940.

Wang, L., and Lutkenhaus, J. (1998). FtsK is an essential cell division protein that is localized to the septum and induced as part of the SOS response. Mol Microbiol 29, 731-740.

Wang, L., Yu, Y., He, X., Zhou, X., Deng, Z., Chater, K.F., and Tao, M. (2007). Role of an FtsK-like protein in genetic stability in *Streptomyces coelicolor* A3(2). J Bacteriol 189, 2310-2318.

White, C.L., Kitich, A., and Gober, J.W. (2010). Positioning cell wall synthetic complexes by the bacterial morphogenetic proteins MreB and MreD. Mol Microbiol 76, 616-633.

Willemse, J., Borst, J.W., de Waal, E., Bisseling, T., and van Wezel, G.P. (2011). Positive control of cell division: FtsZ is recruited by SsgB during sporulation of *Streptomyces.* Genes Dev 25, 89-99.

Woldemeskel, S.A., and Goley, E.D. (2017). Shapeshifting to Survive: Shape Determination and Regulation in *Caulobacter crescentus.* Trends Microbiol 25, 673-687.

Woldringh, C., Mulder, E., Valkenburg, J., Wientjes, F., Zaritsky, A., and Nanninga, N. (1990). Role of the nucleoid in the toporegulation of division. Res Microbiol 141, 39-49.

Wu, L.J., and Errington, J. (1994). *Bacillus subtilis* SpoIIIE protein required for DNA segregation during asymmetric cell division. Science 264, 572-575.

Wu, L.J., and Errington, J. (1997). Septal localization of the SpoIIIE chromosome partitioning protein in *Bacillus subtilis.* EMBO J 16, 2161-2169.

Wu, L.J., and Errington, J. (2004). Coordination of cell division and chromosome segregation by a nucleoid occlusion protein in *Bacillus subtilis.* Cell *1*17, 91*5-92*5.

Wu, L.J., Ishikawa, S., Kawai, Y., Oshima, T., Ogasawara, N., and Errington, J. (2009). Noc protein binds to specific DNA sequences to coordinate cell division with chromosome segregation. EMBO J 28, 194*0-1*952.

Xu, H., Chater, K.F., Deng, Z., and Tao, M. (2008). A cellulose synthase-like protein involved in hyphal tip growth and morphological differentiation in *Streptomyces. J Bact*eriol 190, 49*71-4*978.

Xu, Q., Traag, B.A., Willemse, J., McMullan, D., Miller, M.D., Elsliger, M.A., Abdubek, P., Astakhova, T., Axelrod, H.L., Bakolitsa, C., et al. *(*2009*).* Structural and functional characterizations of SsgB, a conserved activator of developmental cell division in morphologically complex actinomycetes. J Biol Chem 284, 25*268*-25279.

Yahashiri, A., Jorgenson, M.A., and Weiss, D.S. (2015). Bacterial SPOR domains are recruited to septal peptidoglycan by binding to glycan strands that lack stem peptides. Proc Natl Acad Sci USA 112, 11*347*-11352.

Yamazaki, H., Ohnishi, Y., and Horinouchi, S. (2003). Transcriptional switch on of *ssgA* by A-factor, which is essential for spore septum formation in *Streptomyces griseus. J Bact*eriol 185, 12*73-1*283.

Yang, D.C., Peters, N.T., Parzych, K.R., Uehara, T., Markovski, M., and Bernhardt, T.G. (2011). An ATP-binding cassette transporter-like complex governs cell-wall hydrolysis at the bacterial cytokinetic ring. Proc Natl Acad Sci USA 108, E1*052*-1060.

Yokoyama, E., Doi, K., Kimura, M., and Ogata, S. (2001). Disruption of the hup gene encoding a histone-like protein HSl and detection of HSl2 of *Streptomyces lividans.* Res Microbiol 152, 71*7-72*3.

Young, K.D. (2010). Bacterial shape: two-dimensional questions and possibilities. Annu Rev Microbiol 64, 223-*24*0.

Yousif, S.Y., Broome-Smith, J.K., and Spratt, B.G. (1985). Lysis of *Escherichia coli* by beta-lactam antibiotics: deletion analysis of the role of penicillin-binding proteins 1A and 1B. J Gen Microbiol 131, 28*39-2*845.

Yu, T.-W., and Hopwood, D.A. (1995). Ectopic expression of the *Streptomyces coelicolor whiE* genes for polyketide spore pigment synthesis and their interaction with the act genes for actinorhodin biosynthesis. Microbiology 141, 2779-2791.

Yu, X.-C., Weihe, E.K., and Margolin, W. (1998). Role of the C terminus of FtsK in *Escherichia coli* chromosome segregation. J Bacteriol 180, 6424-6428.

Zhou, X., Halladin, D.K., and Theriot, J.A. (2016). Fast mechanically driven daughter cell separation is widespread in actinobacteria. MBio 7, e00952-00916.

CHAPTER 2: CHARACTERIZATION OF A NOVEL GENE *SSDA* FOR SPORE SHAPE DETERMINATION IN *STREPTOMYCES*

INTRODUCTION

Bacterial cell shape is an inherited characteristic that is maintained or remolded to allow for proper growth, division, and survival during unfavorable conditions. Peptidoglycan (PG), a major component of cell wall, is both necessary and sufficient for cell shape maintenance in almost all bacteria (Woldemeskel and Goley, 2017). Therefore, its synthesis and hydrolysis has to be precisely controlled in time and place. Cytoskeletal proteins have been shown to play a crucial role in spatial regulation of PG synthesis and, thus, contribute to bacterial morphological diversity (Caccamo and Brun, 2018; Woldemeskel and Goley, 2017). In rod-shaped bacteria, such as *E. coli* and *B. subtilis*, the tubulin-homolog FtsZ is a central protein that directs the cell wall synthesis and/or remodeling of new septa during cell division, while the actin-like cytoskeletal protein MreB directs the new peptidoglycan insertion through the lateral wall during cell elongation (Egan et al., 2020; Young, 2010).

Unlike the conventional rod-shaped bacteria, which divide by binary division and grow by lateral cell wall extension, the Gram-positive soil-living bacterium *Streptomycetes* has a complex life cycle with the alternation between unicellular spores and multicellular mycelial life style (Flärdh and Buttner, 2009). Under favorable conditions, *Streptomyces* starts its life cycle with the germination of dormant uninucleoid spores to form one or two germ tubes. Hyphae of *Streptomyces* exhibit polar growth by tip extension and branch initiation to form a vegetative meshwork (Flärdh and Buttner, 2009; Flärdh et al., 2012). In response to nutrient depletion, the aerial hyphae grow into the air to form an aerial mycelium (McCormick and Flärdh, 2012), although some species, such as *S. venezuelae* and *S. griseus*, can also differentiate in liquid

culture (Schlimpert et al., 2016). The aerial hyphae then continue to differentiate into long strings of prespores, and eventually into the mature spore chains. Sporulation-specific cell division requires the conserved cytoskeletal protein FtsZ, which localizes in the form of ladders at regular intervals, called Z rings, along the sporogenic hyphae (McCormick, 2009). The Z rings provide a scaffold to recruit other cell division proteins and coordinate peptidoglycan synthesis at the nascent division septum. These rings are stabilized by two dynamin-like proteins DynA and DynB (Schlimpert et al., 2017) and an Actinobacteria-signature protein SepH (Ramos-León et al., 2021).

In rod-shaped bacteria, the Mre proteins are key components of the elongation complex (elongasome or the Rod complex) for lateral wall synthesis (Young, 2010). *Streptomyces* contains a complete *mre* gene cluster encoding MreB, MreC, MreD, PBP2, and Sfr (RodA) and a *mreB*-like gene *mbl* at a different location of the chromosome, however, they are not required for vegetative growth (Sigle et al., 2015; Vollmer et al., 2019). By contrast, they are reported to be involved in sporulation in *S. coelicolor*, most likely by directing PG synthesis at the lateral spore walls instead of the hyphal tips. All individual mutants in the *mre* gene cluster and an *mreB mbl* double mutant are viable (Heichlinger et al., 2011; Kleinschnitz et al., 2011; Mazza et al., 2006). However, all these mutants produce large swollen spores that frequently germinated prematurely, indicating the spore wall was compromised. Moreover, spores for all the mutants had lost their characteristic resistance to adverse conditions and were susceptible to moderate heat, high salt, and cell wall damage agents lysozyme or vancomycin (Kleinschnitz et al., 2011; Mazza et al., 2006), further confirming the integrity of the spore envelope is impaired. Fluorescent fusion proteins of MreB and Mbl of *S. coelicolor* localize to sites of spore wall synthesis during the conversion of aerial hyphae into spore chains (Heichlinger et al., 2011). These data suggested

that the Mre proteins, which direct PG incorporation at the lateral wall during elongation growth of rod-shaped bacteria, have a different role in *Streptomyces* and are involved in the synthesis of the thickened spore envelope. The Mre protein complex that is involved in this process is referred to as the *Streptomyces* spore wall synthesizing complex (SSSC), and more protein members in this complex have been identified by protein-protein interaction analyses and transposon mutagenesis (Kleinschnitz et al., 2011; Vollmer et al., 2019). However, the mechanism by which the SSSC contributes to the thickened spore envelope is unknown.

Streptomyces growth is polarized with apical tip extension. The apical growth is directed by the polarisome (also called the tip-organizing center (TIPOC)) consisting of three scaffold proteins DivIVA, Scy, and FilP (Bush et al., 2015; Caccamo and Brun, 2018; Holmes et al., 2013). DivIVA, the first identified component in *S. coelicolor* polarisome, is essential for viability (Flärdh, 2003; Hempel et al., 2008). It localizes at hyphal tips and future branching sites for apical growth and branching site establishment, suggesting a role in directing cell wall synthesis and thus cell shape determination. Scy (*Streptomyces* cytoskeletal element) is an intermediate filament (IF)-like protein and interacts with DivIVA to stabilize the polarisome (Holmes et al., 2013). In *S. coelicolor*, Scy also interacts with and recruits chromosome segregation protein ParA to the hyphal tips and regulates ParA polymerization along the hyphae, suggesting a potential role in coordinating hyphal growth and chromosome segregation (Ditkowski et al., 2013). FilP is another IF-like protein that forms an interconnected network *in vitro*. Immunofluorescence microscopy in *S. coelicolor* showed that FilP localizes immediately behind DivIVA and distributes in polar gradients (Fuchino et al., 2013). Live cell imaging in *S. venezeulae* further demonstrated that this apical gradient localization pattern is growth-dependent and disassembles upon growth arrest (Fröjd and Flärdh, 2019). DivIVA is required to recruit FilP

to create the apical gradient, and deletion of *filP* affects the amount and distribution of DivIVA foci at the tips. Furthermore, mutation in either *filP* or *scy* causes an irregular hyphal morphology and defective polar growth (Bagchi et al., 2008; Fuchino et al., 2013).

To identify additional targets involved in the morphological differentiation of *Streptomyces*, transposon mutagenesis was used in our laboratory to screen for new genes in *S. coelicolor* and identified a strain with an insertion mutation in a gene that was named *ssdA* that showed increased colony hydrophobicity, thickened cell wall, and heterogeneous spore sizes and shapes, indicating a potential role for the gene product at the late stage of life cycle (Bennett, 2006). In this chapter, I will describe the characterization of *ssdA*. Due to the great advantages of *S. venezuelae* as a new model organism, such as rapid growth and synchronous sporulation in submerged culture, most of this work was carried out in *S. venezuelae*. The places where the *S. coelicolor* was used to supplement the analysis will be denoted or explained in this section.

MATERIALS AND METHODS

Bacterial strains, media, and growth conditions

E. coli strains used in this study are listed in Table 2.1. The *E. coli* strains TG1, JM109, and TOP10 were used for basic cloning and maintenance of plasmid, and were grown at 37°C in/on LB (Lennox) medium, which contains 0.5 % NaCl and 0.1% glucose (Sambrook et al., 1989). LB was supplemented with antibiotics, when appropriate, at the following final concentrations: ampicillin (100 μg/ml), carbenicillin (100 μg/ml), kanamycin (50 μg/ml), apramycin (50 μg/ml), chloramphenicol (25 μg/ml), or hygromycin (50 μg/ml). When hygromycin was used, LB medium without salt (NaCl) was used as the growth medium. *E. coli* strains BW25113/pIJ790 and BT340 were grown at 30°C to ensure propagation of the temperature sensitive plasmids, and BT340 was grown at 42°C to induce the expression of FLP recombinase. When growing *E. coli* strains for competent cell production, SOB medium (Stuttard, 1982) was used as the growth medium.

Streptomyces strains used in this study are listed in Table 2.2. *S. venezuelae* strains were grown at 30°C using MYM (maltose-yeast extract-malt extract) (Kieser et al., 2000) liquid and solid media made with 50% deionized water and 50% tap water and supplemented with R2 trace element solution at 1:500 (Kieser et al., 2000). When appropriate, the final concentrations of the following antibiotics were added: apramycin (50 μg/ml), nalidixic acid (20 μg/ml), or hygromycin (50 μg/ml). *S. coelicolor* strains were grown on SFM (soy flour mannitol) (Kieser et al., 2000) at 30°C and were supplemented with the final concentrations of the following antibiotics when appropriate: apramycin (50 μg/ml), nalidixic acid (20 μg/ml), kanamycin (50 μg/ml), or hygromycin (50 μg/ml).

Plasmids and general DNA techniques

Plasmids and cosmids used in this study are listed in Table 2.3. Primers used in this study are listed in Table 2.4. Plasmid DNA was extracted using the ZR Plasmid Miniprep Kit (Zymo, D4016). Following alkaline lysis, Cosmid DNA was extracted by phenol/chloroform and ethanol precipitation (Sambrook et. al, 1989). A salting out procedure was used to isolate genomic DNA from *Streptomyces* (Kieser et al., 2000). Extracted DNA samples were resuspended in sterile Tris-EDTA or nanopure water supplemented with RNaseA. DNA restriction enzymes (New England Biolabs), *Taq* and Phusion Polymerase (New England Biolabs) were used following the manufacturers' instructions.

Isolation of a *ssdA*-null mutant for *S. venezuelae* and *S. coelicolor*

A *ssdA*-null for *S. venezuelae* was isolated using a recombineering (recombination-mediated genetic engineering) method to replace the entire *ssdA* gene (*vnz23885*) with an apramycin resistant gene *aac*(*3)IV* (Gust et al., 2003a; Gust et al., 2003b). Specifically, oligonucleotides 45 and 46 were used to amplify and add *ssdA* homology to the *aac(3)IV* cassette isolated from *Eco*RI/*Hin*dIII-digested plasmid pIJ773. The generated PCR product was electroporated into the *E. coli* strain BW25112/pIJ790 containing cosmid Sv-6-E-07 to create cosmid pNS22. pNS22 was then introduced into the chromosome of *S. venezuelae* strain NRRL B-65442 via homologous recombination after conjugation. The candidates that were apramycin-resistant and kanamycin-sensitive were selected and verified by PCR using primers 47 and 48. One successfully verified strain was named NS6 (Δ*ssdA*::*acc(3)IV*).

In addition, an unmarked in-frame deletion of *ssdA* was also constructed *in vivo* by removing the antibiotic-resistance cassette from pNS22 via site-specific recombinase (Gust et al., 2004). Specifically, cosmid pNS22 was transformed into the *E. coli* strain BT340 selecting at

30°C. Transformants were streaked and incubated at 42°C to induce expression of FLP recombinase and the excision of the *aac(3)IV* cassette to create cosmid pNS23 that contains an 81-bp *frt* scar in place of *ssdA*. In order to reintroduce an *oriT* for conjugation, the restriction fragment liberated from *Eco*RI/*Hin*dIII-digested pIJ799 was used to change *bla* (ampicillin resistance gene) in the cosmid backbone of pNS23 into *oriT-aac(3)IV* by recombineering, creating pNS24. pNS24 was conjugated into *S. venezuelae,* the cosmid was integrated by single homologous recombination and apramycin-resistant colonies that contain the Δ*ssdA*::*frt* by gene conversion were selected and restreaked on antibiotic-free medium. Apramycin-sensitive candidates were identified and loss of *ssdA* was verified by PCR and sequencing. The candidates that contain the unmarked Δ*ssdA*::*frt* allele were selected and one stain was named NS7 (Δ*ssdA*::*frt*).

The isolation of a *ssdA*-null mutant in *S. coelicolor* was conducted following a similar way as described above for *S. venezuelae*. Briefly, the apramycin-resistance gene *aac*(*3)IV* was used to replace the entire *ssdA* gene in cosmid 3B6 to generate pGK. pGK1 was then introduced into the chromosome of *S. coelicolor* strain MT1110 via homologous recombination after conjugation. The candidates that were apramycin-resistant and kanamycin-sensitive were selected and one represented strain was named NS30 (Δ$ssdA_{sco}$::*acc(3)IV*).

Construction of a SsdA-EGFP expression strain

A cosmid containing a *ssdA-egfp* strain was constructed by using *E. coli* recombineering. Specifically, oligonucleotides 57 and 58 were used to amplify and add *ssdA* homology to the *egfp-aac(3)IV-oriT* cassette of cosmid H24 ParB (Jakimowicz et al., 2005). The PCR product was electroporated into the *E. coli* strain BW25113/pIJ790 containing cosmid Sv-6-E-07 to recombine with the 3' end of *ssdA* and create cosmid pNS25. Cosmid pNS25 was introduced into

the chromosome of *S. venezuelae* strain via homologous recombination after conjugation. Marker replacement candidates that were apramycin-resistance and kanamycin sensitive were selected and verified by both PCR and sequencing methods using primers 59 and JS3 to verify the junction between *ssdA* and *egfp*. One correct candidate expressing a *ssdA-egfp* fusion as the only allele of *ssdA* was named NS18 [WT *ssdA-egfp-aac(3)IV*]. A linker peptide with the sequence LPGPE was present between SsdA and EGFP (Jakimowicz et al., 2005).

To ensure the *ssdA-egfp* fusion was functional, a plasmid containing *ssdA-egfp* expressed from its own promoter was constructed to complement Δ*ssdA*::*frt* mutant NS14. First, pNS25 was digested by *Nde*I to remove the *aac(3)IV-oriT* sequence in the cosmid. The remaining sequence in pNS25 was self-ligated to create pNS27. Oligonucleotides 47 and 48 were used to amplify *ssdA-egfp* together with its promoter region using pNS27 as a template. The PCR product was ligated into pCR4-TOPO (Invitrogen) to create pNS36. pNS36 was digested by *Eco*RV and *Spe*I and the resulting fragment was inserted into *Eco*RV/*Spe*I-digested pMS82 to generate pNS46. pNS46 was introduced into the chromosome of Δ*ssdA*::*frt* mutant strain NS7 of *S. venezuelae* by integration at the ΦBT1 attachment site to produce NS24 (Δ*ssdA*::*frt* $attB_{\Phi BT1}$::P_{ssdA}-*ssdA-egfp*).

A construct containing *ssdA-egfp* expressed from a constitutive *ermE** promoter was also created. First, oligonucleotides 104 and 108 were used to amplify *ssdA-egfp* fusion fragment using pNS25 as a template. The generated PCR product was ligated into pCR4-TOPO (Invitrogen) to create pNS87. pNS87 was digested with *Nde*I and *Hin*dIII, and the resulting fragment was inserted into *Nde*I/*Hin*dIII-digested pIJ10257 to generate pNS88. pNS88 was introduced into the chromosome of wild type strain and Δ*ssdA*::*frt* mutant NS7 of *S. venezuelae* by integration at the ΦBT1 attachment site to produce NS44 and NS45, respectively.

Construction of genetic complementation strains for *ssdA*-null mutants for *S. venezuelae* and *S. coelicolor*

Genetic complementation strains were constructed by integrating a vector *in trans* at the ΦBT1 attachment site that contains the *ssdA* coding region and its promoter region. Specifically, oligonucleotides 47 and 48 were used to amplify *ssdA* together with its promoter region using Phusion high fidelity polymerase (NEB). The PCR product was inserted into pCR2.1-TOPO (Invitrogen) to create pNS33. pNS33 was sequenced for junctions using primers M13 Forward and M13 Reverse. pNS33 was digested by *Eco*RV and *Spe*I, and the generated restriction fragment was inserted into the *Eco*RV/*Spe*I-digested pMS82 to create pNS40. pNS40 was introduced into the chromosome of *ssdA* mutant strains NS6 and NS7 of *S. venezuelae* by integration at the ΦBT1 attachment site to produce NS12 (*ΔssdA*::*aac(3)IV attB*$_{\Phi BT1}$::P_{ssdA}-*ssdA*) and NS14 (*ΔssdA*::*frt attB*$_{\Phi BT1}$::P_{ssdA}-*ssdA*), respectively.

The complementation vector containing *ssdA* in *S. coelicolor* was constructed in a similar way as for in *S. venezuelae*. Briefly, primers 78 and 79 were used to amplify the entire *ssdA* coding region and its promoter region for *S. coelicolor* using cosmid 3B6 as a template. The PCR product was ligated into pMS82 to create pNS73. pNS73 was introduced into the chromosome of Δ*ssdA*$_{sco}$::*aac(3)IV* mutant strain NS30 of *S. coelicolor* by site-specific integration at the ΦBT1 attachment site to produce NS37 (Δ*ssdA*$_{sco}$::*aac(3)IV attB*$_{\Phi BT1}$::P_{ssdA}-*ssdA*$_{sco}$).

Growth curve determination

The same amount of spores for each tested strains were inoculated in 5 ml of MYM liquid and grown at 30°C for the indicated time points. Cultures were taken at the indicated times and OD_{600} was measured using a 96-well plate reader (SpectraMax i3).

Spore germination experiments

Approximate 10^6 spores for each tested strains were inoculated in 5 ml of MYM liquid and grown at 30°C for the indicated time points. Cultures were taken and germinating spores were examined using a phase-contrast microscope described below. Germ tube length was measured manually using the measurement feature of ImageJ software.

Light microscopy

For phase-contrast microscopy, all samples were analyzed using a Nikon phase-contrast microscope (Eclipse E400) with 100x Oil objective (NA=1.25), and images were captured using a MicroPublisher 5.0 digital camera (QImaging) and the associated QCapture software. Micrographs were processed using ImageJ software (Stecher et al., 2020). For imaging aerial hyphae, coverslips were placed on the surface of colonies grown on MYM agar at 30°C for 4 days. The coverslip impressions were lifted and mounted in 20% glycerol. For imaging individually dispersed spores, a small aliquot of diluted spore suspension was mounted on a slide coated with a thin layer of an agarose pad (1.5% agarose in PBS).

For fluorescence microscopy, all samples were analyzed using a Nikon upright epifluorescence microscope (Eclipse Ni-U) with a Nikon Plan Apo λ 100x Oil objective (NA=1.4) and images were captured using a Nikon DS-Qi2 monochrome camera. For fusion protein localization observations, cells growing in liquid MYM medium were directly mounted on a thin 1.5% agarose pad in PBS. For staining cell wall and nucleoids, cells grown in liquid MYM medium or a coverslip impression from cells grown on solid MYM medium were fixed with ice-cold methanol, washed twice with PBS, and mounted in 20 μg/ml of propidium iodide (Molecular Probes) and 10 μg/ml of fluorescein conjugated wheat germ agglutinin (FITC-WGA, Molecular Probes) in PBS. Fixed and stained samples were spotted onto 1.5% agarose pads in

PBS. In the case where membrane staining dye FM 4-64 (Molecular Probes) was used, the methanol fixation step was omitted. In the case of using vancomycin to label cell wall, fluorescently labelled vancomycin (BODIPY™ FL Conjugate) and unlabeled vancomycin were mixed in a 1:1 ratio. Vancomycin mixtures were added to the liquid MYM culture to the concentration of 1 μg/ml, incubated for 5 mins at 30°C, and imaged immediately.

Transmission electron microscopy

A mycelial lawn that was grown for 4 days at 30°C on MYM agar was scraped and transferred into 2-ml screw tube. Cells were fixed with 2.5% glutaraldehyde in 0.05 M cacodylate (pH7.2) at 4°C overnight, which was followed by washing with 0.05 M cacodylate at room temperature for 5-10 min three times. Then 2% osmium tetroxide in 0.05 M cacodylate was added for post-fixation for 1 hour at room temperature, and washed with 0.5 M sodium acetate (pH 7.2) three times each for 10 min. The generated samples were dehydrated by successive transfer in increasing concentration of ethanol (50% -100%). The dehydrated samples were washed with 100% of propylene oxide three times for 20 min, and followed by washing with propylene oxide: Spurr's (1:1) for 30 mins and then washing with Spurr's overnight. The samples were polymerized overnight in a 60°C oven. Thin sections were cut with a glass knife, mounted and stained sequentially with 2% uranyl acetate and 1% lead citrate. Thin sections were analyzed using a JEM-1210 (JEOL) operating at 60 KeV and images were captured using Orca-HR CCD camera (Hamamatsu).

Spore size measurement

Spores were harvested from a cell lawn growing 4-5 days on MYM agar. The spore suspension was passed through a sterile cotton ball in a sterile syringe to remove mycelia and other debris. The spore suspension was imaged by phase-contrast microscopy as described above.

Spore lengths were determined using the measurement tool of the Nikon NIS-Elements software BR (Version 5.02.00) either automatically or manually.

Spore stress assays

For a heat stress assay, fresh spores were harvested after growth for 4-5 days on MYM agar. The generated spore suspension was passed through a sterile cotton to remove mycelia and other debris. 100 µl of 10^{-10} dilution of spores in nano-pure water were treated at 55°C for designated times and plated on LB plates. After incubation at 30°C at least for 1 day, the CFU (colony-forming unit) were counted and spore viability was calculated.

For antibiotic stress assays, spore suspensions of WT and Δ*ssdA* mutant strains containing approximate 10^{12} viable spores were plated on the LB agar. Sterile filter discs (110 mm) were placed on the surface of the inoculated agar, and 10 µl of antibiotic stock containing the designated amounts of antibiotic were added on the surface of discs. Sizes of inhibition zones were measured after incubation at 30°C for 1 day. The amount of antibiotics used are as follows: ampicillin 100 µg, carbenicillin 200 µg, chloramphenicol 200 µg, kanamycin 5 µg, and vancomycin 0.5 µg. In the case of penicillin, commercially available diffusion discs containing 10 µg of penicillin from BD company were placed directly on the LB agar plate.

For a salt stress assay, 10-fold serial dilutions of spores were spotted on LB agar plates containing different concentrations of NaCl. Photographs were taken after 2 days of incubation at 30°C. For a lysozyme stress assay, 10-fold serial dilutions of spores were spotted on the LB agar plates containing different concentrations of lysozyme added from a stock just before pouring plates. Plates were used the same day. Photographs were taken after 3 days of incubation at 30°C.

Phylogenetic analysis

The amino acid sequence of SsdA of *S. venezuelae* were extracted from StrepDB (http://strepdb.streptomyces.org.uk) and used to search against KEGG genes of prokaryotes (https://www.genome.jp/tools/fasta/). Alignment of SsdA was generated using embedded Clustal W in MEGA. The phylogenetic tree was generated using the maximum-likelihood method and the best fit model predicted by MEGA version X (Kumar et al., 2018; Stecher et al., 2020). Tree reliability was estimated by bootstrapping with 100 replicates.

β-lactamase assay

Primers used for construction of plasmids used in this assay are listed on Table 2.4. The first and first two transmembrane (TM) segments of *ssdA* were amplified adding flanking *Stu*I/*Bam*HI restriction sites. The PCR products were digested with *Stu*I/*Bam*HI and ligated into *Stu*I/*Bam*HI-digested pGWS793 (Zhang et al., 2016) to create pNS69 and pNS70. Plasmids were sequenced to verify the reading frame. β-lactamase assays were conducted following a previous protocol (Zhang et al., 2016). Briefly, plasmids expressing different BlaM-fusion proteins were transformed into *E. coli* JM109 cells. Transformants were grown in liquid LB medium until OD_{600} was between 0.4 to 0.6. Cells were washed twice with LB to remove accumulated β-lactamases and resuspended in 1 ml LB supplemented with 10% glycerol. 0.5 µl cell suspension was spotted onto LB agar with different concentrations of carbenicillin, and plates were incubated at 37°C overnight for observation.

Bacterial two-hybrid assay

Primers used for construction of plasmids used in this assay are listed on Table 2.4. The large central cytoplasmic domain of *ssdA* and its variants were amplified adding flanking *Kpn*I/*Xba*I restriction sites. The PCR products were cloned into pCR2.1-TOPO or pCR4-TOPO

and were sequenced to ensure the integrity and fidelity of the inserts. Each verified plasmid was digested with *Kpn*I/*Xba*I and ligated into *Kpn*I/*Xba*I-digested bacterial-two hybrid vectors pUT18, pUT18C, pKT25, and pKNT25. Restriction enzyme digestion and sequence analysis were used to verify the insert orientation and reading frame of each two-hybrid construct. Plasmid pairs were co-transformed into the *E. coli* strain BTH101 by electroporation or chemical transformation. The visualization of possible protein-protein interaction was performed following the manufacturer's manual (Euromedex) with the following modifications. Cotransformants were plated on LB agar containing ampicillin (100 μg/ml) and kanamycin (50 μg/ml), and incubated overnight at 37°C. Individual colonies from these plates were picked and patched on MacConkey agar containing 1% maltose, 0.5 mM IPTG, ampicillin (100 μg/ml), and kanamycin (50 μg/ml) and incubated overnight at 30°C before visual observations.

Spore sacculus isolation, PG separation and enzyme digestion, and HPLC-MS analysis

S. venezuelae spores were harvested after growth on MYM agar plate for 5 days at 30°C. *S. coelicolor* spores were harvested after growth on SFM plate for 7 days at 30°C. Spore suspensions were filtered through the cotton to remove the mycelial debris. To isolate the spore sacculus, spores were resuspended in 0.25% SDS in 0.1 M Tris-HCL (pH 6.8) and boiled at 100°C for 1 h. After centrifugation, pellets were washed 5 times with deionized H_2O and resuspended in 1 mL of deionized H_2O. Resuspended pellets were sonicated for 30 mins. 500 μl of DNase and RNase mix (15 μg/ml DNase and 60 μg/ml RNase in 0.1 M Tris-HCl, pH 6.8) was added and samples were incubated for 60 mins at 37°C with shaking. Then samples were treated with 500 μl of trypsin solution (50 μg/ml trypsin in deionized H_2O) and incubated at 37°C for additional 60 mins with shaking. The generated suspensions were boiled for 3 mins at 100°C for enzyme inactivation followed by centrifugation for 5 mins at 14,000 rpm at room temperature.

Pellets were washed with 1 ml of deionized H_2O. The pellets were resuspended in 500 µl of 1 M HCl and incubated for 4 h at 37°C with shaking to release wall teichoic acids. The suspensions were centrifugated 5 mins at 14,000 rpm and washed with diH_2O until the pH was approximately at 5–6. The final pellets were resuspended in 100–250 µl of digestion buffer (12.5 mM sodium dihydrogen-phosphate, pH 5.5) and 1/10 volume of a mutanolysin solution (5,000 U/ml of mutanolysin in deionized H_2O) was added. Samples were incubated overnight at 37°C with shaking, centrifugated and saved for HPLC-MS analysis.

For HPLC-MS analyses, the generated muropeptide samples were analyzed with an Agilent HPLC-ESI-MS system (LC/MSD Ultra Trap System XCT 6330, Waldbronn, Germany), using a linear gradient of eluent A = 0.1% formic acid in water and eluent B = 0.06% formic acid in methanol (time in min: t0 = t5 = 5% B, t155 = t180 = 30% B, 0.5 ml min−1, 52°C) on a Reprosil Gold 300 C18 column (250 × 4.6 mm ID, 5 µm, Dr.Maisch, Ammerbuch). The injection volume was 100 µl. Detection of m/z values was conducted with Agilent Data Analysis for 6300 Series Ion Trap LC/MS 6.1 (version 3.4) software (Bruker-Daltonik).

***S. venezuelae* exploration growth test**

The exploration growth test was conducted following a previous study with minor revisions (Jones et al., 2017). *S. venezuelae* strains were grown in liquid MYM medium for 15 hours, and the OD_{600} was measured. 3 µL of *S. venezuelae* cultures were spotted onto the yeast extract (YP) solid medium or YP supplemented with 2% glycerol solid medium. The volume of bacteria needed for Δ*ssdA* mutant was adjusted to reflect the same OD_{600} with wildtype. In the case that *S. venezuelae* coluture with yeast, *Saccharomyces. cerevisiae* strain BY4741 (*MATa his3*Δ1 *leu2*Δ0 *ura3*Δ0 *met15*Δ0) (Baker Brachmann et al., 1998) was grown in liquid yeast extract peptone dextrose/glucose (YPD) medium overnight. 3 µL of *S. venezuelae* cultures were

spotted adjacent to 3 μL *S. cerevisiae* on the surface of YPD agar medium. All plates were incubated at 30°C for up to 14 days before analysis.

RESULTS

Identification and verification of a transposon-based insertion mutant for *S. coelicolor*

Previously, our lab created a Tn5-based transposon system for random insertional mutagenesis in *S. coelicolor* (Bennett, 2006). Using this system, Bennett identified an insertion mutant that displayed a reduced level of grey pigment in the aerial mycelium and a high frequency of misshapen spores in sizes and shapes (Bennett, 2006). In addition, TEM microscopy revealed that the cell wall of some spores appeared thinker for the insertion mutant than wild type. The insertion site was located in *sco5181*, which was named *ssdA* for spore shape determination due to the dramatic spore shape defect for the insertion mutant.

To confirm the phenotype of the initial insertion mutant, a Δ$ssdA_{sco}$ null mutant (NS30, Δ$ssdA_{sco}$::*aac(3)IV*) was isolated for *S. coelicolor* by replacing the entire coding region of $ssdA_{sco}$ with an apramycin-resistance cassette using a recombineering method. Phenotypes were first examined on a solid medium, and the results showed that a Δ$ssdA_{sco}$ null mutant had a whitish aerial mycelium compared to wild type and accumulated droplets of water on the spore surface, which were similar to the initial insertion mutant (Fig. 2.1A-C). Phase-contrast microscopy analysis revealed the presence a large number of heterogeneously shaped and/or sized spores for the majority of spore chains for the Δ$ssdA_{sco}$ null mutant (Fig 2.1D). The abnormal spores were present in different morphologies, including very round, swollen, mini-sized, and elongated spores. The observed phenotypes of the null-mutant are consistent with what were reported for the insertion mutant in Bennett's dissertation (Bennett, 2006). To further confirm that the observed phenotypes resulted from the absence of $ssdA_{sco}$, a genetic complementation strain (Δ$ssdA_{sco}$/$ssdA_{sco}^{+}$) was constructed by integration of pNS73, which contains $ssdA_{sco}$ as the only complete gene and its promoter region, at the $attB_{\Phi BT1}$ locus of the Δ$ssdA_{sco}$ null mutant

chromosome. The developmental phenotypes of the genetically complemented strain were restored to the wide type (Fig 2.1B and D), indicating the observed defects were caused by introduced *ssdA*$_{sco}$ mutant, not by mutation(s) unlinked to the introduced deletion. Meanwhile, another genetic complementation strain (Δ*ssdA*$_{sco}$/*ssdA*$_{sve}^{+}$) was constructed in a similar way as Δ*ssdA*$_{sco}$/*ssdA*$_{sco}^{+}$. Plasmid pNS41, containing *S. venezuelae ssdA* and its associated promoter region (Fig. 2.2A), was integrated into the at the *attB*$_{\Phi BT1}$ locus of the Δ*ssdA*$_{sco}$ null mutant chromosome. The results showed that *S. venezuelae ssdA* was also able to restore the defective phenotypes to the wild-type level (Fig. 2.1B and D), indicating a functional conservation for *ssdA* between *S. coelicolor* and *S. venezuelae*. Considering the great advantages of *S. venezuelae* in rapid growth and ability of sporulation in liquid culture, I switched my work from *S. coelicolor* to *S. venezuelae* to characterize the function of *ssdA*.

SsdA is widespread in Actinomycetes

SsdA is a putative integral membrane protein of 883 amino acids and it is encoded by *vnz23885* in *S. venezuelae* (Gomez-Escribano et al., 2021). *ssdA* is associated with two downstream genes, *slpE* (*vnz23875*) and a *slpE*-like gene (*vnz2380*), forming a potential three-gene operon, which is supported by a study for whole-genome transcription start sites in both *S. coelicolor* (Jeong et al., 2016) and *S. venezuelae* (http://streptomyces.org.uk/vnz_tss.html on the StrepDB) (Fig. 2.2A). This genomic organization is also conserved in other *Streptomyces* species, but not in other actinomycetes. *slpE* encodes a mycelium-associated lipoprotein and shows significant amino acid similarity to SlpD proteinase and Tap (tripeptidyl aminopeptidase). SlpD was shown to be essential for viability and SlpE was required for growth on minimal medium in *S. coelicolor* (Binnie et al., 1995). The C-terminus of SsdA is similar to a conserved lysophosphatidylglycerol (LPG) synthase transmembrane (TM) domain (Fig. 2.3A), which might

function as a membrane tether rather than an enzyme due to the lack of the catalytic domain of the LPG synthase.

Phylogenetic analysis revealed that SsdA homologues exist extensively in actinomycetes (Fig. 2.2B), with an exception that it is missing in *Corynebacterium*. The sequence conservation of SsdA in sporulating actinomycetes, particularly in *Streptomycetes*, is higher than other rod-shaped actinomycetes, including *Bifidobacterium*, *Nocardia*, *Rhodococcus*, and *Mycobacterium*, indicating a potential role of SsdA in mycelial and branching life style. Of the sporulating actinomycetes, *Kitasatospora setae* and *Catenulispora acidiphila* were found to have two full-length SsdA homologs in the genome. Some *Streptomyces* species contain the second gene that is similar with only the LPG synthase TM domain. Of interest, SsdA homolog is also found in *Mesorhizobium* sp. B2-3-3, a type of alpha proteobacteria, with 80.34% identity (99% coverage and E value=0). *Mesorhizobium* is a genus living in the soil, which may have acquired the gene from *Streptomyces* through horizontal gene transfer.

SsdA is a predicted integral membrane protein

SsdA is predicted to have 4 transmembrane segments in the N-terminal domain and 8 transmembrane segments in the C-terminal domain. In between the two transmembrane domains is a large soluble domain predicted by web-based serve TMHMM version 2.0 (Krogh et al., 2001) (Fig. 2.3A).

β-lactamase, encoded by *blaM*, is a useful marker to study membrane protein orientation in bacteria (Broome-Smith et al., 1990). To provide support for the membrane topology model of SsdA (Fig. 2.3A), I created two constructs of gene fusions with BlaM fused at the C-terminal end of each of the first 2 predicted TM segments and conducted a β-lactamase assay in *E. coli*. β-lactamase is a periplasmic enzyme that can degrade antibiotics by hydrolysis of the β-lactam ring,

such as carbenicillin and ampicillin. If the TM segment orients BlaM toward the outside of cell, it will convey antibiotic resistance and grow on the medium containing the antibiotic (Broome-Smith et al., 1990; Zhang et al., 2016). Here two BlaM-fusion proteins were expressed, one with the N-terminal 77 amino acids containing the first predicted TM segment of SsdA fused to BlaM and the other one with the N-terminal 161 amino acids containing the first two predicted TM segments of SsdA. Plasmid-containing *E. coli* cultures were spotted on LB medium containing different concentrations of carbenicillin. As shown in Fig. 2.3B, a strain that has the first predicted TM segment fused to BlaM grew while the one that has fusion of the first two predicted TM segments did not grow on the LB plates with carbenicillin, suggesting that the N-terminus of SsdA locates in the cytoplasm. If the predicted third and fourth TM segments are correct, the large central domain from amino acid 226 to 581of SsdA localizes in the cytoplasm.

Deletion of *ssdA* results in delayed morphological differentiation on solid MYM medium

In order to investigate the role of SsdA in *S. venezuelae* development, a *ssdA* null mutant was generated by replacing the entire coding region of *ssdA* with an apramycin-resistance cassette using a PCR-targeting recombineering method (NS6, Δ*ssdA*::*aac(3)IV*). In addition, an unmarked in-frame mutant NS7 was also isolated by removing the resistance cassette (NS7, Δ*ssdA*::*frt*). I concluded that *ssdA* is non-essential for viability. Both the marked and unmarked *ssdA* deletion strains displayed similar phenotypes on MYM solid medium (data not shown), suggesting that a Δ*ssdA*::*aac(3)IV* mutation did not have a polar effect on the downstream genes. The unmarked in-frame *ssdA* mutant NS7 was used for all future studies, and will be referenced as Δ*ssdA*.

The Δ*ssdA* mutant showed delayed morphological differentiation on solid medium (e.g., 24 hours), and formed a less pigmented aerial mycelium (spore pigment) than wild type even

after prolonged incubation for 7 days, suggesting a sporulation defect (Fig. 2.4A and 2.4B). To confirm the phenotype that was observed was due to the absence of *ssdA*, a genetic complementation strain (NS14, Δ*ssdA*/*ssdA*$^{+}$) was constructed by integration of pNS41 at the ΦBT1 *attB* locus of the Δ*ssdA* mutant chromosome (Fig. 2.2A). The developmental phenotype of the genetically complemented strain was restored to the wide-type level, indicating the observed phenotypes were caused by introduced *ssdA* mutant. The results suggest that deletion of *ssdA* resulted in defective sporulation on solid medium.

In addition, variants of truncational SsdA were created to genetically complement the Δ*ssdA* mutant using a similar way with NS14 construction. Results showed that only full-length of *ssdA* restored normal morphological differentiation on solid medium, indicating that all three domains of SsdA are important for proper function of SsdA (Fig. 2.5).

Deletion of *ssdA* resulted in delayed growth in liquid MYM medium

S. venezuelae differentiates in liquid culture, thus growth and development were also observed in MYM liquid medium (Fig. 2.6A). Initially, at early time points, especially for the first 12 hours, the WT strain grew faster than the Δ*ssdA* mutant. However, the optical density of Δ*ssdA* mutant was comparable to the WT level after 22 hours. Growth of WT produced considerable spores by 24 hours in MYM liquid, as demonstrated by a dark green cell pellet after centrifugation of the culture (Fig. 2.6B). The green pigment accumulated with spores was not formed in Δ*ssdA* mutant even after prolonged incubation (40 hours). The complemented strain grew as well as WT, and spore pigment was restored to WT level as well (data not shown). The results indicate that deletion of *ssdA* resulted in growth and sporulation defects in liquid culture as well.

The Δ*ssdA* mutant showed delayed growth (increasing in optical density) at very early time points, thus the rate of spore germination was tested by inoculation of fresh spores into liquid medium. As shown in Fig. 2.7A, after 2.5 hours, the majority of spores of WT germinated and already made identifiable germ tubes. At the same incubation time, a significant fraction of spores of Δ*ssdA* had not germinated, and those Δ*ssdA* spores that were already geminated had shorter germ tubes than those of WT. Moreover, swollen spores during early germination for the Δ*ssdA* were more irregular in size and shape when compared to those of the WT (Fig. 2.7A and data not shown), which might be caused by the heterogeneously sized and shaped spores used for inoculation. The growth difference between the strains became more obvious after 4 hours of incubation. By the 5.5-hour time point, hyphae of the WT strain started to branch, however, the Δ*ssdA* mutant still showed shorter, unbranched germ tubes. Germ tube length measurements indicated that WT strain extended the germ tube from 2.5 hours to 4 hours at an average rate of approximately 0.11 ± 0.05 μm/min and from 4 hours to 5.5 hours at an average rate of 0.28 ± 0.10 μm/min, while the Δ*ssdA* mutant had a much lower average extension rate at around 0.05 ± 0.04 μm/min from 2.5 hours to 4 hours and 0.11 ± 0.08 μm/min from 4 hours to 5.5 hours (Fig. 2.7B and C). The WT extension rate is similar to previously reported hyphal extension rate for *S. coelicolor* grown on solid medium (Allan and Prosser, 1983). The data indicate that the Δ*ssdA* mutant has a germination and growth defect. The defects were complemented by addition of WT *ssdA in trans* (data not shown). At later times, I did not observe an overt variation in branching frequency between WT and the *ssdA* mutant. Collectively, I speculated that a combination of delayed and defective germination and slower hypha extension account for the observed growth defect (Fig. 2.6A and 2.7).

Deletion of *ssdA* has no overt effect on DivIVA-mCherry localization

DivIVA is an essential landmark protein that localizes at the tip of hyphal filaments, and is part of the machinery (polarisome) required for cell extension in Streptomyces (Flärdh, 2003). To investigate the relationship between SsdA and DivIVA, a plasmid carrying DivIVA-mCherry was introduced into the WT and Δ*ssdA* mutant strains. One extra copy expressing DivIVA did not suppress the growth and differentiation delay for the Δ*ssdA* mutant (data not shown). Due to the germination and growth delay of the Δ*ssdA* mutant, DivIVA-mCherry localization was observed after 6.5 hours of growth in the WT background and 8 hours of growth in the Δ*ssdA* background. At those time points, both WT and Δ*ssdA* had developed into a similar stage where they had already branched extensively. The results showed that although the localization of DivIVA was not disrupted in the absence of *ssdA*, the intensity of the fluorescence foci was overall lower for the Δ*ssdA* mutant than that of WT (Fig. 2.8A and B), suggesting that SsdA affects the amount of DivIVA at the hyphal tips. However, an independent examination of DivIVA-mCherry localization in the exponentially growing hyphae by Dr. Klas Flärdh at Lund University did not support the reduced fluorescence intensity in the Δ*ssdA* mutant (Fig. 2.8C). The reason that caused the discrepancy is not known yet. Further confirmation of the result is needed.

Deletion of *ssdA* results in spore size heterogeneity

In order to study the function of *ssdA* during *S. venezuelae* spore formation, spore morphology following growth and development on MYM solid medium was examined. Coverslip impression slides of spores produced on solid medium were observed under phase-contrast microscopy. Overall, the length of mature spores of the Δ*ssdA* mutant was more heterogeneous than the WT parent (Fig. 2.9A and B). Statistical analysis of the spore length

revealed subtle, but significant differences in spores between WT and the Δ*ssdA* mutant. The mean length was 1.20 ± 0.32 μm for wild type, 1.47 ± 0.81 μm for the Δ*ssdA* mutant, and 1.28 ± 0.33 μm for the *ssdA*/*ssdA*$^{+}$. The irregular spore shapes caused by deletion of *ssdA* was not as dramatic as in *S. coelicolor*, which is why the gene was named (Fig 2.1D). This might be explained by the fact that *S. venezuelae* mature spores are more rectangular, while *S. coelicolor* spores are more ellipsoid (Bush et al., 2015; Flärdh and Buttner, 2009).

To further investigate the sporulation phenotype, aerial hyphae were observed by staining the cell wall with WGA, cell membrane with FM4-64, and nucleoids with DAPI. WT stains produced evenly-sized ellipsoid spores as demonstrated by FM4-64 staining (Fig. 2.9C). In the Δ*ssdA* mutant, some spore chains were indistinguishable from the WT. In other cases, there are frequent spore chains failing to complete cell wall maturation (Fig. 2.9C), resulting in more box-shaped spores. In addition, the septal staining by FM4-64 was more uneven in the Δ*ssdA* mutant with the membrane dye concentrating in some septa, while even staining was observed in the WT. TEM microscopy showed that in addition to the irregular sizes, some spore chains of the Δ*ssdA* mutant barely rounded up and lead to the cell-cell separation defect (Fig. 2.9D). This also explains the frequent persistence of box-shaped spores in mature spore chains. Collectively, deletion of *ssdA* resulted in heterogeneous spore sizes and shapes due to sporulation defects.

The effect of deleting *ssdA* on sporulation in liquid was more dramatic. At 24 hours, the WT already produced significant amounts of spores, while the Δ*ssdA* mutant was still in the mycelium stage (data not shown). When observed at 40 hours (Fig. 2.19B and C), the Δ*ssdA* mutant was still in a very heterogeneous state with mixtures of spores and mycelia. When considering only spores or spore chains, the developing mutant hyphae were significantly longer than those of WT with an average length of 5.9 ± 3.95 μm compared to that of the wild type

being on average 2.64 ± 1.26 μm in length, indicating that the mutant is defective in completing cell separation for spores.

Deletion of *ssdA* results in disruption of FtsZ-ypet localization at sporulation septa

FtsZ, the bacterial tubulin homologue, is a critical protein involved in cell division by forming cytokinetic Z rings at each sporulation septum, marking the sites for future sporulation septation (Grantcharova et al., 2005; Schwedock et al., 1997). To investigate if the observed sporulation defect in *ssdA*-deficient strain is due to disrupted FtsZ localization, an integration plasmid pKF351 carrying FtsZ-Ypet (Schlimpert et al., 2017) was introduced into WT and Δ*ssdA* mutant strains. FtsZ-Ypet formed the ladders along the sporogenic hyphae under both conditions (Fig. 2.10A). The distance between two adjacent Z rings was measured and results revealed a significantly increased average spacing in the *ΔssdA* mutant when compared to the WT, with 1.21 ± 0.29 μm in WT and 1.39 ±0.58 μm in *ΔssdA* mutant (Fig. 2.10B). In the absence of *ssdA*, the average size of mature spores (1.47 ± 0.81 μm, Fig. 2.9B) is slightly larger than the average distance of Z rings, which might be caused by cell-cell separation defect in the mutant. The results suggest that the heterogeneous spore sizes are partly due to uneven placement of the Z rings.

SsdA-EGFP localizes in vegetative hyphae, at sporulation septa, and periphery of mature spores

To investigate the subcellular localization of SsdA to better appreciate where and when it functions, *egfp* was fused to the 3'end of *ssdA* by recombineering and the fusion gene was integrated at the native locus as the only copy. To ensure the fusion protein was functional, the *ssdA-egfp* fusion gene together with the promoter region was amplified and inserted into pMS82, which was used to complement the Δ*ssdA* mutant to create strain NS24 (Δ*ssdA*::*frt*

attB$_{\Phi BT1}$::P_{ssdA}-*ssdA*). Results showed that the fusion protein was functional, as demonstrated by the restoration of the normal morphological differentiation on solid MYM medium and normal growth on high-salt medium (Fig. 2.11). However, due to the weak signal of SsdA-EGFP and strong autofluorescence in *S. venezuelae*, it was difficult to distinguish if the fluorescence signal was caused by the fusion protein or autofluorescence. This also indicated that SsdA accumulates at a low level. Therefore, I also expressed the *ssdA-egfp* fusion gene under the control of the strong, constitutive *ermE** promoter, which was integrated into the chromosome ΦBT1 attachment site for both WT and Δ*ssdA.* In both strains, the same localization pattern was observed. Specifically, SsdA-EGFP localized in the vegetative hyphae as widely-spaced ladders and bright spots, possibly representing sites of cross wall and potentially future branching points (Fig. 2.12A). Localization was also present at sporulation septa, forming a ladder-like localization pattern along the sporogenic hyphae (Fig. 2.12B). At a late stage, SsdA-EGFP could be observed at the periphery of mature and released spores (Fi. 2.13C). The localization patter is consistent with the idea that SsdA might be involved in vegetative growth, sporulation and spore wall maturation.

Deletion of *ssdA* results in an altered peptidoglycan layer

Streptomyces spores have a thickened cell wall, enabling the resistant cells to survive detrimental conditions, such as moderate heat, high salt, and cell wall damaging agents (Sigle et al., 2015). Encoding crucial members of the *Streptomyces* spore wall synthesizing complex (SSSC), *mreB* mutant and, *mreB*-like gene, *mbl* mutant had been reported to be sensitive to treatments with heat, detergent, high salt, lysozyme and vancomycin in *S. coelicolor* (Heichlinger et al., 2011; Mazza et al., 2006; Sigle et al., 2015). To investigate whether Δ*ssdA* mutant spores have impaired spore envelope integrity, the sensitivity of Δ*ssdA* mutant to various

types of stresses were tested. As shown in Fig. 2.14A, after 20 mins of incubation at 55°C, 32.2% of the WT spores survived while 22.2% of the Δ*ssdA* mutant had survived. After extended incubation (40 min), the survival rate dropped to 6% for WT and 2% for Δ*ssdA* mutant. The spore viability was restored after reintroduction of *ssdA* into the mutant, with the survival rate of 33.8% and 4.6% after 20 min and 40 min treatment, respectively. Overall, deletion of *ssdA* resulted in a mild but significant sensitivity to heat stress at 55°C.

The susceptibility of Δ*ssdA* mutant to osmotic stress was tested by supplementing LB medium with different concentrations of NaCl. As shown in Fig. 2.14B, the growth of WT was not affected under all of the tested conditions. However, the Δ*ssdA* mutant started to show sensitivity at 1% of NaCl and was unable to grow on medium with 3% NaCl. The resistance of Δ*ssdA* mutant to salt stress was able to be restored by introduction of *ssdA*, expressed from its promoter, *in trans* into the chromosome (Fig. 2.11B). These results suggested that deletion of *ssdA* results in an impaired spore envelope.

PG is a macromolecular meshwork that consists of alternating residues of β-(1,4) linked GlcNAc and MurNAs glycan strands crosslinked by short peptide stems attached to MurNAc (Vollmer et al., 2008a). To further investigate whether the deletion mutant of *ssdA* has altered cell wall properties, I tested the sensitivity to a range of cell-wall targeting antibiotics. To do this, wild type and Δ*ssdA* mutant spores were plated and filter discs containing antibiotics were applied. I first tested β-lactam antibiotics that inhibit the PG synthesis of bacterial cell walls by binding to the transpeptidase (Sarkar et al., 2017). As shown in Fig. 2.15A, the Δ*ssdA* mutant produced significantly larger inhibition zones than that of WT for ampicillin, carbenicillin, and penicillin (Fig. 2.9A), indicating that the Δ*ssdA* mutant was more susceptible to the β-lactam antibiotics. Next I tested another antibiotic vancomycin, which belongs to glycopeptide

antibiotics and targets to terminal D-Ala-D-Ala precursor of PG and prevents PG crosslinking and, thus, cell wall synthesis (Munita and Arias, 2016). Consistently, deletion of *ssdA* also resulted in a significantly larger inhibition zone, indicating increased sensitivity to vancomycin (Fig. 2.15A and C). As a control, I also tested another two antibiotics, which function intracellularly by targeting the ribosome and inhibiting protein synthesis, kanamycin and chloramphenicol. The results showed that the sensitivity of Δ*ssdA* mutant to kanamycin and chloramphenicol was not affected (Fig. 2.15B and 2.9C). These results indicate that absence of *ssdA* specifically affects the PG peptide stem crosslinking and thus PG synthesis.

Lysozyme is a hydrolase that catalyzes the hydrolysis of the glycosidic bond between MurNAc and GlcNAc residues in PG (Vollmer et al., 2008b), thus the sensitivity of the Δ*ssdA* mutant to lysozyme was measured as an alternative target of cell wall integrity. Unexpectedly, *S. venezuelae* is extraordinarily resistant to lysozyme even at the concentration of 1 mg/ml (Fig. 2.16), rendering the sensitivity test to lysozyme inconclusive. Considering the functional conservation of SsdA in *Streptomyces* species (Fig 2.1 and Fig. 2.19), lysozyme sensitivity was tested for the *S. coelicolor* mutant. Serial dilutions of spores were spotted on the LB plates with different concentrations of lysozyme. Previous study has shown that WT of *S. coelicolor* is mildly sensitive to lysozyme even at 250 μg/ml (Keenan et al., 2019), which was also confirmed as a positive control in this study (Fig. 2.16). Surprisingly, the results showed that Δ*ssdA* mutant of *S. coelicolor* is slightly more resistant to lysozyme than the wild type (Fig. 2.17), which may partly due to the increased thickness of spore cell wall (Bennett, 2006). The wild-type sensitivity of *S. coelicolor* Δ*ssdA* to lysozyme was restored after introduction of *ssdA in trans* with either *S. venezuelae ssdA* or *S. coelicolor ssdA* (data not shown), indicating a functional conservation of SsdA in *Streptomyces* species. The result indicates that deletion of *ssdA* affects the integrity of

glycan strands of PG. Taken all stress assay results together, I conclude that SsdA plays a direct or indirect role in cell wall biosynthesis or modification.

Deletion of *ssdA* results in accumulation of spore wall muropeptide monomers

Since evidence support an altered PG layer in the absence of *ssdA*, we collaborated with Dr. Evi Stegmann's lab at University of Tübingen and characterized the spore wall PG. The purified PG sacculi of spores were isolated and digested with the muramidase mutanolysin. The generated PG fragments were separated by HPLC, and prominent peaks were assigned for MS analysis. As shown in Fig. 2.18A, the HPLC chromatograph for monomeric muropeptides showed a similar profile between WT and Δ*ssdA* mutant, the intensity of some peaks, however, are much more enriched in the mutant. A similar phenotype was observed for *S. coelicolor* Δ*ssdA* mutant (Fig. 2.18B), which might explain the thick spore wall in the mutant. The peaks with prominent intensity difference were analyzed by MS, and the preliminary PG monomeric structures were elucidated and required for further verification. In addition to the monomers, analysis of PG cross-linking is also in progress.

Deletion of *ssdA* results in compromised exploratory behavior

Streptomyces exploration is a novel developmental mode of growth and it was identified while coculturing *S. venezuelae* with yeast (Jones et al., 2017). It is only present in some *Streptomyces* species, but missing in others, such as *S. coelicolor, S. avermitilis, S. griseus, and S. lividans* (Jones et al., 2017). The explorer cells of *Streptomyces* are present as non-branching vegetative hyphae that can rapidly spread over solid surfaces (Jones et al., 2017). Physical association with yeast triggers this behavior (Jones et al., 2017), but little is known about proteins in the pathway that could affect the growth rate of explorer cells. Because my results demonstrated that *ssdA* affects vegetative growth in *S. venezuelae*, I asked whether *ssdA* affected

the growth of *Streptomyces* explorer cells. To test this, the Δ*ssdA* mutant was grown beside *Saccharomyces. cerevisiae* on standard YPD (yeast extract-peptone-dextrose) agar. As expected, wild type explorer cells grew rapidly and colonized almost half of the surface of a agar plate after 14 days of growth (Fig. 2.20A). However, the exploration rate is much slower in the Δ*ssdA* mutant, leading to a significant smaller surface area than wild type after 14 days (Fig. 2.20A and B). The results indicate that *ssdA* plays a direct or indirect role in growth of explorer cells on YPD medium when growing in close proximity with yeast.

Previous study also showed that glucose inhibits *Streptomyces* exploration and wild type can explore on glucose-free medium in the absence of yeast (Jones et al., 2017). In order to test the exploratory behavior of Δ*ssdA* mutant under glucose-free condition, I inoculated *Streptomyces* strains on YP (yeast extract-peptone) agar in the absence of yeast. After incubation, results showed that both wild-type and Δ*ssdA* mutant were able to explore on YP agar, but the colony of explorer cells were of different morphologies (Fig. 2.20C). The Δ*ssdA* mutant contained a whitish surface compared to wild type and the filaments radiating from center of the exploratory mycelium were not as striking in morphology as wild type. Surprisingly, surface area quantification did not show significant size difference for the exploratory mycelium between WT and Δ*ssdA* mutant. These assays are preliminary and have only been conducted one time. Repeating the experiment normalizing the CFU of the inoculum for different strains is needed to confirm the quantification result.

Previous study suggested that explorer cells of *S. venezuelae* respond to different nutritional conditions (Jones et al., 2017). To test the exploration behavior of the Δ*ssdA* mutant under a different carbon source, YP medium supplemented with 2% glycerol was first used. I noticed that the explorer cells on this medium grows in a similar pattern no matter in the

presence or absence of yeast stimulation. Fig. 2.20E showed the *Streptomyces* cells grew alone. As observed from the figure, wild-type mycelium grew with a similar morphology as growing with yeast on YPD agar, but the spreading is more robust than on YPD agar. The mycelium almost colonized the entire surface of an agar plate after 11 days growth. However, for the Δ*ssdA* mutant, the morphology was similar with what was observed for exploratory mycelium on YP medium plate: whitish colony surface and little or no radiated filaments. By quantification, the surface area of Δ*ssdA* mutant was shown to be significantly smaller than wild type on YP-glycerol (Fig. 2.19F). The genetic complementation strain (Δ*ssdA/ssdA*$^{+}$) was able to restore all of the wild-type phenotypes observed on YPD, YP, and YP with glycerol agar.

S. coelicolor is one of the *Streptomyces* species that does not exhibit exploratory growth (Jones et al., 2017). Another genetic complementation strain Δ$ssdA_{sve}/ssdA_{sco}^{+}$ was also used to test the exploration spreading on three tested conditions, and results showed that the exploration was restored to the wild-type level (data not shown), further confirming the functional conservation for *ssdA* in two different *Streptomyces* species. To investigate if deletion of *ssdA* for *S. coelicolor* changed this behavior, *S. coelicolor* Δ*ssdA* mutant was cultured with *S. cerevisiae*, and the results showed no difference to *S. coelicolor* wild type. No obvious exploration occurred in the *S. coelicolor* Δ*ssdA* mutant (data not shown), confirming that *S. coelicolor* did not exhibit exploratory growth under the tested conditions.

Preliminary results showed that volatile signals produced by wild-type *S. venezuelae* induce exploration of physically separated Δ*ssdA* mutant

Jones et. al. (2017) showed that *S. venezuelae* explorer cells produced volatile organic compounds (VOCs) as signals to induce the exploration behavior of a wild-type *Streptomyces* strain at a distance (Jones et al., 2017). It is possible that defect in Δ*ssdA* mutant could be unable

to produce VOC but still able to respond the signals. To determine if VOCs emission by the wild type strain could overcome the exploration defect of Δ*ssdA* mutant, I designed a two-compartment assay. First, I inoculated one compartment with wild type coculture with *S. cerevisiae* on YPD agar as the exploring strain, and inoculated the adjacent compartment with Δ*ssdA* mutant alone on YPD medium to receive VOCs emitted wild type. As shown in Fig. 2.21A, Δ*ssdA* mutant mycelium appeared to be a larger size than the negative control shown on Fig. 2.21D. The mycelium spread was not as extensive as wild type (positive control) located in the same, separate two-compartment system (Fig. 2.21A). In parallel, similar assay was also conducted on YP (Fig. 2.21B) and YP with 2% glycerol (YPG) agar (Fig. 2.21C), where wild-type *S. venezuelae* growing on YP and YPG served as the VOC producer. Under both conditions, the exploration behaviors were induced for both wild type and Δ*ssdA* mutant growing on YPD medium, as demonstrated by the larger mycelium size compared to negative control on Fig. 2.21D. However, the mycelium of the VOC-induced explorer cells on YPD agar were all morphologically different from the ones induced by physical interaction with yeast, but the reason is not yet known. In future experiments, *ssdA* mutant could be used as the donor explorer cells to determine if VOCs produced by Δ*ssdA* mutant can induce exploratory behavior of wild type growing on YPD agar.

DISCUSSION

After completion of sporulation septation, *S. coelicolor* spore maturation involves the formation of a thick, lysozyme-resistant spore wall, which is accomplished concomitantly with the rounding of the cylindrical pre-spores into an ovoid shape. The mechanism of the process of changing shape, however, is largely unknown. In this chapter, I confirmed that a deletion of a novel gene *ssdA* had a spore shape defect in *S. coelicolor* as the insertion mutant. *ssdA* was first identified by a transposon-based insertion mutagenesis (Bennett, 2006). Then, I characterized the function of *ssdA* in *S. venezuelae* and revealed that it is crucial for spore germination and vegetative growth, sporulation, and spore maturation in *S. venezuelae*.

I first showed that the Δ*ssdA* mutant was delayed for morphological differentiation on solid medium and in liquid medium (Fig. 2.4 and 2.6). Further microscopic examination revealed that spore germination and the germ tube extension rate were affected by the absence of *ssdA* (Fig. 2.7). DivIVA is a landmark protein at the tip of vegetative hyphae, however, neither the localization pattern nor the fluorescent intensity of DiviVA-mCherry was affected in the Δ*ssdA* mutant, indicating that SsdA has an effect on cell wall metabolism directly or indirectly to affect vegetative growth. Also, sporulation was also affected in the Δ*ssdA* mutant, and heterogeneously-sized spores were produced (Fig. 2.9). The sporulation defect in *ssdA*-deficient strain due to the compromised FtsZ-Ypet localization (Fig. 2.10), the earliest protein that arrives at future cell division site and is crucial for sporulation-specific cell division in *Streptomyces* (McCormick et al., 1994). TEM analysis result showed that some spore chains of *ssdA* mutant have thickened cell wall and cell separation issues. The spore size and spore separation defects in the mutant are more striking during differentiation in liquid medium, where prespore compartments are larger and have difficulty in separation from the chain, even after prolonged

growth (Fig. 2.19). In addition to affect the traditional development, *ssdA* also affects the exploratory behavior in *S. venezuelae* (Fig. 2.20).

SsdA-EGFP localization was observed and results showed that it localizes in vegetative hyphae, sporulation septa, and the periphery of spores, consistent with its roles in cell wall development. The *ssdA-egfp* fusion expressed from its own promoter was able to restore the mutant phenotype (Fig. 2.11), but the signal was barely detectable, perhaps indicating that a very low amount of the protein accumulates in the cells. Therefore, SsdA-EGFP localization was observed under the control of a constitutive promoter *ermE**. I have constructed another genetic complementation strain containing the full untruncated leader transcript of *ssdA* and *ssdA-egfp* fusion that was controlled under *ermE** promoter. The result showed that this particular construct was not able to restore the mutant phenotype on agar plate, and no protein localization signal could be observed. These indicate the likely presence of a post-transcriptional control for *ssdA* expression that leads to a low protein output.

The presented results also showed that deletion of *ssdA* resulted in a defective PG layer, and this was supported by increased sensitivity of Δ*ssdA* mutant to moderate heat, osmotic stress, and cell-wall targeting antibiotics (Fig. 2.14 and 2.15). Preliminary HPLC-MS result further demonstrated that the concentration for some intermediates of spore sacculus was higher in the *ssdA* mutant than wild-type (Fig. 2.18), consisting with a thicker cell wall for the mutant. How *ssdA* deletion contributes to difference needs further investigation. I propose that SsdA functions as membrane tether to recruit or stabilize the enzymes involved in cell wall synthesis, degradation or modification. *ssdA* mutant is more sensitive to salt stress than wild type, even at 2% of NaCl concentration. SigB is a master regulator that affects osmotic and oxidative response as well as morphological differentiation in *S. coelicolor,* and deletion of *sigB* in *S. coelicolor* leads

to an extremely salt-sensitive phenotype (Kol et al., 2010; Lee et al., 2005), indicating that future experiments should be investigated if *ssdA* transcription is initiated by SigB.

A *whiD* mutant in *S. coelicolor* also displays a spore size and shape defect as well as a spore wall thickening defect that are more drastic than what we observed for *S. coelicolor ssdA* mutant (Molle et al., 2000). This might be caused by the fact that *whiD* encodes a transcription factor that can affect the phenotypic defects though controlling expression of an array of genes. Of which, *ssdA* might be one target of WhiD.

SsdA is a predicted integral membrane protein with transmembrane segments at both N-terminal and C-terminal domains, and between which is a large soluble domain in cytoplasm (Fig. 2.3). The interaction of the central soluble cytoplasmic domain was investigated in a bacterial two-hybrid assay, and result showed that the loop can interact with itself (Fig. 2.13B). In an effort to identify other potentially interacting partners, I used the cytoplasmic domain of *S. venezuelae* SsdA as a bait to screen a *S. coelicolor* bacterial two-hybrid library, and this method was successful in identifying an interacting partner for partitioning protein ParH (Hasipek, 2016). However, there were no functional hits identified under my attempts, possibly due to the incomplete gene coverage for the two-hybrid library. Then, I tested for interactions with sporulation-specific divisome proteins, including SsgA, SsgB, SepF1, SepF2, SepF3, SepH, DynA, and DynB (Ramos-León et al., 2021; Schlimpert et al., 2017), and the results showed an interaction between the SsdA cytoplasmic domain and DynB (Fig. 2.13B), a dynamin protein that stabilizes the Z ring via interaction with several other components in the divisome (Schlimpert et al., 2017). I also showed that the N-terminal region of the large soluble domain is important for interactions with itself and with DynB, and deletion of amino acids from 406 to 469 was sufficient to abolish the interactions (Fig. 2.13B). Furthermore, missing the amino acids

between 406 and 469 failed to complement the morphological differentiation on solid medium (Fig. 2.5). No obvious domain or motif was reported for the approximate 60 amino acids, and why this region is important for protein interactions and functions is unknown yet. This helps explain at least the septal localization pattern of SsdA-EGFP, and suggests that SsdA might play role in sporulation septation by stabilization of the divisome, which thus affect sporulation septa assembly and spore maturation. In the future, a Δ*ssdA* Δ*dynB* double mutant needs to be isolated and stability of the Z ring will be examined by time-lapse microscopy. The localization of SsdA-EGFP in a *dynB* mutant would also be examined to determine if its septal localization is disrupted.

SCO7007 is a small protein (299 amino acids) in *S. coelicolor* that is similar to SsdA located elsewhere on the chromosome. The 22-299 amino acids is similar to the C-terminal LPG synthase TM domain of SsdA (amino acids 645-925 of $SsdA_{sco}$). Although a *ssdA* ortholog is present in almost all sequenced *Streptomyces* species, a *sco7007* ortholog is missing in some of *Streptomyces* species, such as *S. venezuelae*. Of interest, the well-studied *Streptomyces* species that contain *sco7007* ortholog, including *S. coelicolor*, *S. avermi*tilis, and *S. lividans*, are incapable of exploration (Jones et al., 2017), indicating a potentially negative effect on exploration for *sco7007* homolog. I have made a genetic complementation vector that contains *sco7007* as the only ORF and its promoter region, and used this vector to complement *S. venezuelae* Δ*ssdA* mutant (data not shown). However, the morphogenesis of the genetic complementation strain was not restored to the wild-type level. The exploration was not examined for this construct yet. In future, a *sco7007* mutant would be isolated in *S. coelicolor* to see if it contributes to spore shape and exploration in *S. coelicolor*.

In conclusion, SsdA is a novel protein that plays a pleiotropic role during *Streptomyces* development. I provide evidences that deletion of *ssdA* affects spore germination, vegetative growth, sporulation, spore maturation, and exploration. I also showed there is an increased concentration of the spore wall intermediates in the *ssdA* mutant, indicating SsdA plays a role related with cell wall. This assumption was also corroborated with the SsdA-EGFP localization pattern, where it localizes at the places where cell wall is actively synthesized and degraded for growth, septum formation, and spore wall maturation. The particular function that SsdA plays is still not clear yet. It would be important to screen the genomic library to identify additional interacting partners and reveal the function and mechanism.

Table 2.1 *E. coli* strains used in this study

Strain	Genotype	Reference/Source
TG1	*supE thi-1* Δ(*lac-proAB*) Δ(*mcrB-hsdSM*)*5* (r_k^- m_k^-),)/F′ *traD36 proAB lacI*^{q}*Z*Δ*M15*	Sambrook et al. (1989)
TOP10	F$^-$ *mcrA* Δ(*mrr-hsdRMS-mcrBC*) Φ*80lacZ*Δ*M15*Δ*lacX74 deoR recA1 araD139* Δ(*araA-leu*)*697 galU galK*	Invitrogen
BW25113	F$^-$ Δ(*araD-araB*)*567* Δ*lacZ4787*(::*rrnB-3*) λ$^-$ *rph-1* Δ(*rhaD-rhaB*)*568 hsdR514*	Datsenko and Wanner (2000)
ET12567	F$^-$ *dam-13*::Tn*9 dcm-6 hsdM hsdR recF143 zjj-201*::Tn*10 galK2 galT22 ara-14 lacY1 xyl-5 leuB6 thi-1 tonA31 rpsL136 hisG4 tsx-78 mtl-1 glnV44*	MacNeil et al. (1992)
BT340	F$^-$ Δ*(argF-lac)169* Φ*80*Δ*lacZ58(M15) glnV44(AS)* λ$^-$ *rfbC1 gyrA96 recA1 endA1 spoT1 thiE1 hsdR17/* pCP20	Cherepanov and Wackernagel (1995)
BTH101	F$^-$ *cya-99 araD139 galE15 galK16 rpsL1 hsdR2 mcrA1 mcrB1*	Euromedex
JM109	*endA1 recA1 gyrA96 thi hsdR17* (r_k^- m_k^+), *relA1 supE44* Δ*(lac-proAB)/*F′ *traD36 proAB lacI*^{q}*Z*Δ*M15*	Yanisch-Perron et al. (1985)

Table 2.2 *Streptomyces* strains used in this study

Strain	Genotype	Reference/Source
WT[1]	*S. venezuelae* NRRL B-65442	Gomez-Escribano et al. (2021)
NS6[2]	Δ*ssdA*::*aac(3)IV*	This study
NS7[2]	Δ*ssdA*::*frt*	This study
NS11	Δ*ssdA*::*aac(3)IV attB*$_{\Phi BT1}$::pMS82	This study
NS12	Δ*ssdA*::*aac(3)IV attB*$_{\Phi BT1}$::pNS40 (*P*$_{ssdA}$-*ssdA*)	This study
NS13	Δ*ssdA*::*frt attB*$_{\Phi BT1}$::pMS82	This study
NS14	Δ*ssdA*::*frt attB*$_{\Phi BT1}$::pNS40 (*P*$_{ssdA}$-*ssdA*)	This study
NS18	WT *ssdA-egfp-aac(3)IV*	This study
NS20	Δ*ssdA attB*$_{\Phi BT1}$::pSS204 (*P*$_{divIVA}$-*divIVA-mcherry*)	This study
NS21	WT *attB*$_{\Phi BT1}$::pSS204 (*P*$_{divIVA}$-*divIVA-mcherry*)	This study
NS22	Δ*ssdA attB*$_{\Phi BT1}$::pKF351 (*P*$_{ftsZ}$-*ftsZ-ypet*)	This study
NS23	WT *attB*$_{\Phi BT1}$::pKF351 (*P*$_{ftsZ}$-*ftsZ-ypet*)	This study
NS24	Δ*ssdA attB*$_{\Phi BT1}$::pNS46 (*P*$_{ssdA}$-*ssdA-egfp*)	This study
NS25	WT *attB*$_{\Phi BT1}$::pNS46 (*P*$_{ssdA}$-*ssdA-egfp*)	This study
NS27	Δ*ssdA attB*$_{\Phi BT1}$::pNS42 (*P*$_{ssdA}$-*ssdA*$_{1-230}$)	This study
NS28	Δ*ssdA attB*$_{\Phi BT1}$::pNS44 (*P*$_{ssdA}$-*ssdA*$_{1-581}$)	This study
NS32	Δ*ssdA attB*$_{\Phi BT1}$::pNS62 (*P*$_{ssdA}$-*ssdA*$_{\Delta 41-179}$)	This study

Strain	Genotype	Reference/Source
NS35	Δ*ssdA attB*$_{\Phi BT1}$::pNS73(*P*$_{ssdAsco}$-*ssdA*$_{sco}$)	This study
NS39	Δ*ssdA attB*$_{\Phi BT1}$::pNS79 (*P*$_{ssdA}$-*ssdA*$_{\Delta 406-469}$)	This study
NS40	WT *attB*$_{\Phi BT1}$::pIJ10257	This study
NS41	Δ*ssdA attB*$_{\Phi BT1}$::pIJ10257	This study
NS44	WT *attB*$_{\Phi BT1}$::pNS88 (*P*$_{ermE*}$-*ssdA-egfp*)	This study
NS45	Δ*ssdA attB*$_{\Phi BT1}$::pNS88 (*P*$_{ermE*}$-*ssdA-egfp*)	This study
WT[1]	*S. coelicolor* A3(2) MT1110 (prototrophic SCP1$^-$ and SCP2$^-$ derivative of the wild-type strain, 1147)	Hindle and Smith (1994); (Hopwood, 1985)
NS30[2]	Δ*ssdA*$_{sco}$::*aac(3)IV*	This study
NS33	Δ*ssdA*$_{sco}$::*aac(3)IV attB*$_{\Phi BT1}$::pMS82	This study
NS34	Δ*ssdA*$_{sco}$::*aac(3)IV*::pNS40 (*P*$_{ssdA}$-*ssdA*)	This study
NS37	Δ*ssdA*$_{sco}$::*aac(3)IV*::pNS73 (*P*$_{ssdA}$-*ssdA*$_{sco}$)	This study

1. Two wild-type *Streptomyces* species (*S. venezuelae* and *S. coelicolor*) were used in this study.

2. The *ssdA* mutant isolated from *S. venezuelae* was denoted as Δ*ssdA*, and isolated from *S. coelicolor* was denoted as Δ*ssdA*$_{sco}$.

Table 2.3 Cosmids and plasmids used in this study

Cosmid/Plasmid	Description	Reference/Source
pIJ773	Source of the *aac(3)IV-oriT* cassette used for PCR-targeted mutagenesis	Gust et al. (2003a)
pIJ790	Expression of λ RED recombination plasmid	Gust et al. (2003a)
pIJ799	Source of the apramycin resistance gene *aac(3)IV* and *oriT* used to target *bla*, marker replacement of *bla* to *aac(3)IV*	Gust et al. (2003b)
pUZ8002	Non-transmissible helper plasmid for mobilization of *oriT*-containing cosmids and plasmids	Paget et al. (1999)
pMS82	Plasmid cloning vector for integration at the *ΦBT1* attachment site. Marker *hyg*	Gregory et al. (2003)
pCR2.1-TOPO	TOPO TA cloning vector	Invitrogen
pCR4-TOPO	TOPO TA cloning vector	Invitrogen
pUT18[1]	Bacterial two-hybrid (BACTH) vector used to create a fusion to the N-terminus of the CyaA T18 polypeptide	(Karimova et al., 1998)
pUT18C[1]	Bacterial two-hybrid (BACTH) vector used to create a fusion to the C-terminus of the CyaA T18 polypeptide	(Karimova et al., 1998)
pKT25[1]	Bacterial two-hybrid (BACTH) vector used to create a fusion to the C-terminus of the CyaA T25 polypeptide	(Karimova et al., 1998)
pKNT25[1]	Bacterial two-hybrid (BACTH) vector used to	(Karimova et al.,

Cosmid/Plasmid	Description	Reference/Source
	create a fusion to the C-terminus of the CyaA T25 polypeptide	1998)
H24 *parB-egfp*	Source of *egfp-aac(3)IV* cassette	(Jakimowicz et al., 2005)
Sv-6-E07	Cosmid that contains *ssdA*	John Innes Centre
pNS22	Sv-6-E07 Δ*ssdA*::*aac(3)IV*	This study
pNS23	Sv-6-E07 Δ*ssdA*::*frt*	This study
pNS24	Sv-6-E07 Δ*ssdA*::*frt bla*::*oriT-aac(3)IV*	This study
pNS25	Sv-6-E07 *ssdA-egfp-aac(3)IV*	This study
pNS40	pMS82 carrying P_{ssdA}-*ssdA*. Complementation plasmid containing *ssdA* and its own promoter region was amplified and inserted into *Eco*RV/*Spe*I-digested pMS82	This study
pNS42	pMS82 carrying P_{ssdA}-$ssdA_{1-230}$. Expression the N-terminal 4 TM segments of SsdA from its native promoter. Amplified and inserted into *Eco*RV/*Spe*I-digested pMS82	This study
pNS44	pMS82 carrying P_{ssdA}-$ssdA_{1-581}$. Expression the N-terminal 4 TM segments and central cytoplasmic region of SsdA from its native promoter. Amplified and inserted into *Eco*RV/*Spe*I-digested pMS82	This study

Cosmid/Plasmid	Description	Reference/Source
pNS62	pMS82 carrying P_{ssdA}-$ssdA_{\Delta 41\text{-}179}$. pNS40 was recombineered and aa 41-179 (part of N-terminal 4 TM segments) was replaced with a *Xho*I restriction site	This study
pNS46	pMS82 carrying P_{ssdA}-*ssdA-egfp.* Expressing *ssdA-egfp* from its native promoter. Amplified and inserted into *Eco*RV/*Spe*I-digested pMS82	This study
pNS48[1]	BACTH plasmid. Central cytoplasmic region of *ssdA* (encoding aa 226-581) into *Xba*I/*Kpn*I-digested pUT18	This study
pNS49[1]	BACTH plasmid. Central cytoplasmic region of *ssdA* (encoding aa 226-581) into *Xba*I/*Kpn*I-digested pUT18C	This study
pNS50[1]	BACTH plasmid. Central cytoplasmic region of *ssdA* (encoding aa 226-581) into *Xba*I/*Kpn*I-digested pKT25	This study
pNS51[1]	BACTH plasmid. Central cytoplasmic region of *ssdA* (encoding aa 226-581) into *Xba*I/*Kpn*I-digested pKNT25	This study
pSS204	*divIVA-mcherry* expressed from its native promoter in pMS82. Integrates at the ΦBT1 attachment site.	Gift from Susan Schlimpert
pKF351	*ftsZ-ypet* expressed from its native promoter. Integrates at the ΦC31 attachment site. Marker *aac(3)IV*	(Donczew et al., 2016)
pGWS793	*sepG-blaM* expressed from *ftsZ* promoter of *S.*	(Zhang et al., 2016)

Cosmid/Plasmid	Description	Reference/Source
	coelicolor and used in *E. coli*	
pWGS796	*blaM* including its signal peptide expressed from *ftsZ* promoter of *S. coelicolor* and used in *E. coli*	(Zhang et al., 2016)
pNS69	Expressing $SsdA_{1\text{-}77}$ (the first TM-segment) fused to BlaM. Amplified and inserted into *Stu*I/*Bam*HI-digested pGWS793 to construct $ssdA_{1\text{-}77}$-*blaM* fusion	This study
pNS70	Expressing $SsdA_{1\text{-}161}$ (the first and second TM-segments) fused to BlaM. Amplified and inserted into *Stu*I/*Bam*HI sites-digested pGWS793 to construct $ssdA_{1\text{-}161}$-*blaM* fusion	This study
pNS79	pMS82 carrying $ssdA_{\Delta 406\text{-}469}$ expressed from its native promoter. Created by recombineering pNS40 and replacing aa 406-469 with *Xho*I	This study
pIJ10257	Cloning vector containing the *ermE** constitutive promoter and ribosome binding site. Integrates at the ΦBT1 attachment site. Marker *hyg*	(Hong et al., 2005)
pNS87	*ssdA-egfp* in pCR4-TOPO. The fragment was amplified with oligos 104 and 108 using pNS25 as a template	This study
pNS88	*ssdA-egfp* in pIJ10257. *ssdA-egfp* was liberated from pNS87 by *Nde*I/*Hin*dIII digestion and inserted into *Nde*I/*Hin*dIII-digested pIJ10257	This study
pNS93	*ssdA* transcript leader (5' UTR)-*ssdA-egfp* in pCR4-TOPO. The fragment was amplified with	This study

Cosmid/Plasmid	Description	Reference/Source
	oligos 106 and 108 using pNS25 as a template	
pNS94	*ssdA* transcript leader (5' UTR)-*ssdA-egfp* in pIJ10257. *ssdA-egfp* including its untranslated leader was liberated from pNS93 by *Nde*I/*Hin*dIII digestion and inserted into *Nde*I/*Hin*dIII-digested pIJ10257	This study
pSS105[1]	DynB in pKT25	(Schlimpert et al., 2017)
pNS96	$SsdA_{226-488}$ in pCR4-TOPO. The fragment was amplified with oligos 60 and 102	This study
pNS110[1]	BACTH plasmid. $SsdA_{226-488}$ into *Xba*I/*Kpn*I-digested pUT18	This study
pNS111[1]	BACTH plasmid. $SsdA_{226-488}$ into *Xba*I/*Kpn*I-digested pUT18C	This study
pNS112[1]	BACTH plasmid. $SsdA_{226-488}$ into *Xba*I/*Kpn*I-digested pKT25	This study
pNS113[1]	BACTH plasmid. $SsdA_{226-488}$ into *Xba*I/*Kpn*I-digested pKNT25	This study
pNS97	$SsdA_{473-581}$ in pCR4-TOPO. The fragment was amplified with oligos 109 and 61	This study
pNS102[1]	BACTH plasmid. $SsdA_{473-581}$ into XbaI/KpnI-digested pUT18	This study
pNS103[1]	BACTH plasmid. $SsdA_{473-581}$ into *Xba*I/*Kpn*I-	This study

Cosmid/Plasmid	Description	Reference/Source
	digested pUT18C	
pNS104[1]	BACTH plasmid. $SsdA_{473-581}$ into *Xba*I/*Kpn*I-digested pKT25	This study
pNS105[1]	BACTH plasmid. $SsdA_{473-581}$ into *Xba*I/*Kpn*I-digested pKNT25	This study
pNS98	$SsdA_{\Delta 406-469}$ in pCR4-TOPO. The fragment was amplified with oligos 60 and 61 and template pNS79	This study
pNS106[1]	BACTH plasmid. $SsdA_{\Delta 406-469}$ into *Xba*I/*Kpn*I-digested pUT18	This study
pNS107[1]	BACTH plasmid. $SsdA_{\Delta 406-469}$ into *Xba*I/*Kpn*I-digested pUT18C	This study
pNS108[1]	BACTH plasmid. $SsdA_{\Delta 406-469}$ into *Xba*I/*Kpn*I-digested pKT25	This study
pNS1091	BACTH plasmid. $SsdA_{\Delta 406-469}$ into *Xba*I/*Kpn*I-digested pKNT25	This study
Cosmids or plasmids are used for *S. coelicolor* [2]		
3B6	*S. coelicolor* cosmid that contains *ssdA*	John Innes Centre
pGK1	3B6 $ssdA_{sco}$::*aac(3)IV*	This study
pNS72	P_{ssdA}-$ssdA_{sco}$ in pCR4-TOPO. The fragment of $ssdA_{sco}$ together with its promoter was amplified with oligos 78 and 79	This study

Cosmid/Plasmid	Description	Reference/Source
pNS73	P_{ssdA}-$ssdA_{sco}$ in pMS82. $ssdA_{sco}$ including its promoter region was liberated from pNS72 by digestion with *Eco*RV and *Spe*I, and ligated into *Eco*RV/*Spe*I-digested pMS82	This study

1. Bacterial two-hybrid plasmids used in this study

2. Plasmids and cosmids are constructed from two *Streptomyces* species (*S. venezuelae* and *S. coelicolor*). *S. coelicolor*-derivatives are labeled with sco for differentiation.

Table 2.4 Oligonucleotides used in this study

NO.	Oligonucleotide	Sequence	Application
45	Sv *ssdA* KO F	CGAACGAGAACGACACGACACG CATGCAGAGACGGACATGATTCC GGGGATCCGTCGACC	Construction of *ssdA* deletion with oligo 46
46	Sv *ssdA* KO R	CCGGCAGGACCGGCACCCACAG GGTCAGCAGGCGGTAGAGTGTA GGCTGGAGCTGCTTC	Construction of *ssdA* deletion with oligo 45
47	Sv *ssdA* KO chk*Eco*RV F	GATACGATATCTCGGGCAGTTCT CCGGTCTCC	(1). Verification of *ssdA* deletion (2). Amplification of *ssdA* promoter, coding region, and short 5' non-coding region
48	Sv *ssdA* KO chk*Spe*I R	GATCACTAGTGGGCGGCGGAGAT CGGCATAG	
57	*ssdA* 3' homology F	CTGGCTCTGCTTCAACTGGCTGA CGAAGCGCGAAGCGCTGCTGCCG GGCCCGGAGCTG	Construction of *ssdA-egfp* expression strain with 58
58	Post *ssdA* homology R	GCCACGGCGTTTCGCGCCGCGGC GGCCCCGGCGCCCGCTACATATG TAGGCTGGAGCTGCTTC	Construction of *ssdA-egfp* expression strain with 57
59	*ssdA-egfp* check F	GCTCACCGCCACCTTCGTGTTC	Verification of *ssdA-egfp* fusion with primer JS3 (Sallmen II, 2019)
60	*ssdA* CPD *Xba*I	TCTAGAGATGTCGCCCAACGTCC GCCCCAC	Amplification of $ssdA_{226\text{-}581}$ with oligo 61
61	*ssdA* CPD *Kpn*I	GGTACCCGGGTCCGCGGCTTGAT CCGC	Amplification of $ssdA_{226\text{-}581}$ with oligo 60
62	Sv *ssdA* first	ACTAGTCTAGCGGACGTTGGGCG	Amplification of $ssdA_{1\text{-}}$

NO.	Oligonucleotide	Sequence	Application
	4TM *Spe*I R	AGCCGACC	$_{230}$ and its promoter with primer 47
63	Sv *ssdA* loop *SpeI* R	ACTAGTCTAGGTCCGCGGCTTGATCCGCTCC	Amplification of $ssdA_{1\text{-}581}$ and its promoter with primer 47
69	*ssdA* N-TM KO F	GCTCGCCGCCCGGGTCCACCGGCCCTCCGACCTGATGCGGCTCGAGATTCCGGGGATCCGTCGACC	Construction an in-frame deletion of aa 41-179 of *ssdA* with oligo 70
70	*ssdA* N-TM KO R	ACGCGTCGAGCAGCAGGACCACCCAGAGCGACACCCGCCACTCGAGTGTAGGCTGGAGCTGCTTC	Construction an in-frame deletion of aa 41-179 of *ssdA* with oligo 69
75	*ssdA Stu*I Fwd	AAGGCCTATGGTGATGGCCCCGGACACCC	Amplification of $ssdA_{1\text{-}77}$ with oligo 76
76	*ssdA* post TM1 BamHI Rev	ATAGGATCCGGGGCGCCGACGGCACCCTTG	Amplification of $ssdA_{1\text{-}77}$ with oligo 75
77	*ssdA* post TM2 *Bam*HI Rev	GCTGGATCCTAGTTGTGCACCGGGTCGGTC	Amplification of $ssdA_{1\text{-}161}$ with oligo 75
78	*ssdAsco* KO chk*Eco*RV F	GCTGGATCCTAGTTGTGCACCGGGTCGGTC	(1). Verification of $ssdA_{sco}$ deletion (2). Amplification of $ssdA_{sco}$ promoter, coding region, and short 5' non-coding region
79	*ssdAsco* KO chk*Spe*I R	TCACTAGTAGCCGGGAGGGATTCGGCATG	
88	*ssdA*406-469 F	CCGCCGGCTCACCGGGGACGCGATCCTGGTGGATCGTTCCCTCGAGATTCCGGGGATCCGTCGACC	Construction an in-frame deletion of aa 406-469 of *ssdA* with oligo 89
89	*ssdA*406-469 R	GGGCCAGTCTCCGCAGCGTCGCGCGCGTGGAGCGGCTCAGCTCGAGTGTAGGCTGGAGCTGCTTC	Construction an in-frame deletion of aa 406-469 of *ssdA* with oligo 88

NO.	Oligonucleotide	Sequence	Application
90	*ftsZsco* Seq F	CCGTCCCAATCGGCATCAGTCG	Sequencing primer for *ssdA* truncations-*blaM* fusion
91	*blaM* Seq R	CGAAAACTCTCAAGGATCTTAC	Sequencing primer for *ssdA* truncations-*blaM* fusion
102	CPD261_*Kpn*I_R	GGTACCCGCGAGCGCTCCCGGGCCAGTC	Amplification of $ssdA_{226\text{-}488}$ with oligo 60
109	*ssdA*_coil_*Xba*I_F2	ATGCTCTAGAGATGTCCACGCGCGCGACGCTGCG	Amplification of $ssdA_{473\text{-}581}$ with oligo 61
104	*ssdA_Nde*I_FWD	CATATGGTGATGGCCCCGGACACC	Amplification of *ssdA-egfp* with oligo 108
108	*egfp_Hin*dIII_REV	AAGCTTACTTGTACAGCTCGTCCATG	Amplification of *ssdA-egfp* with oligo 104

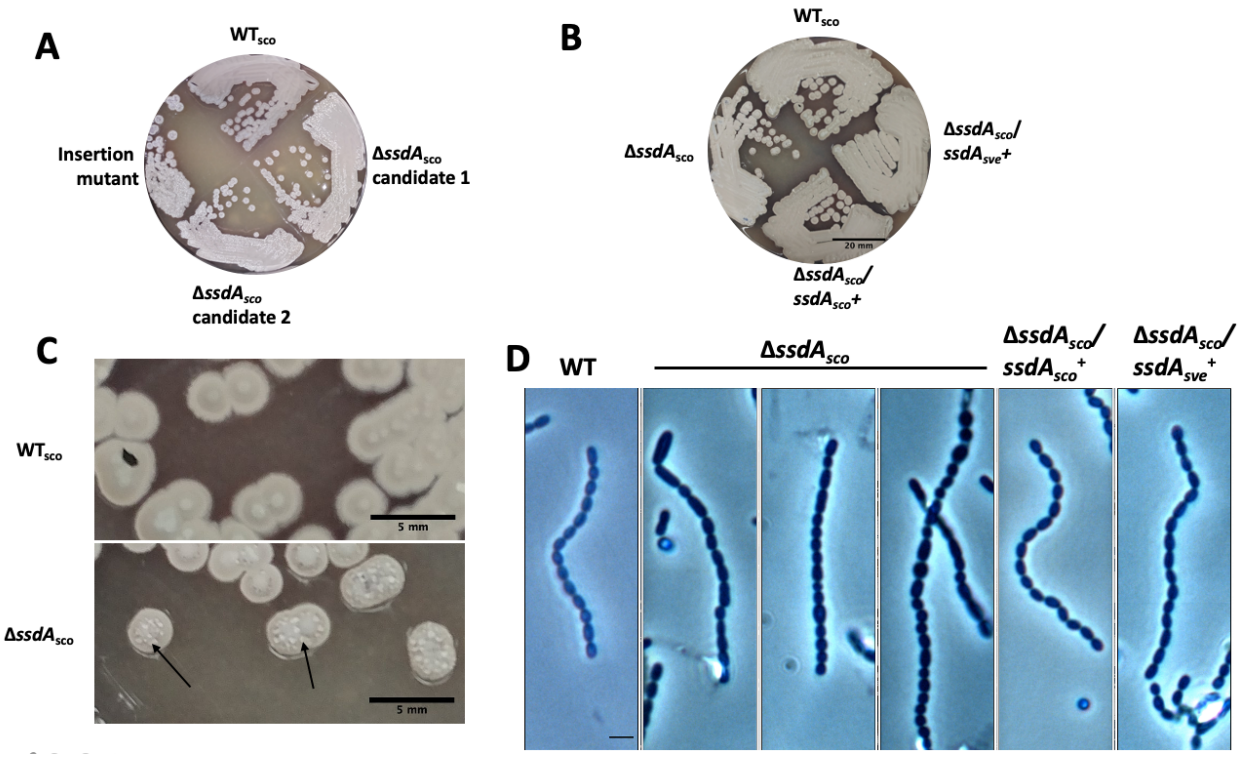

Figure 2.1 Phenotype comparison for *S. coelicolor* wild type and *ssdA* null mutant stains. (A) Compared to the normal grey mycelium of wild type, *S. coelicolor ssdA* mutant strains (Δ*ssdA*$_{sco}$) have a white aerial mycelium colony phenotype (2 null mutants created by recombineering and a Tn5-based insertion mutant). (B) Macroscopic phenotype of *S. coelicolor* Δ*ssdA*$_{sco}$ mutant candidate 1 (NS30) was complemented *in trans* with either *S. coelicolor ssdA* (Δ*ssdA*/*ssdA*$_{sco}^{+}$, NS37) or *S. venezuelae ssdA* (Δ*ssdA*/*ssdA*$_{sve}^{+}$, NS34). (C) Magnified views of *S. coelicolor* WT (WT$_{sco}$) and Δ*ssdA*$_{sco}$ mutant (NS30) from the image B to show that the aerial mycelium is very hydrophobic as demonstrated by the droplets of water that accumulated on the growth surface of a Δ*ssdA* mutant. (A-C) Strains were streaked on SFM agar and images were taken after 7 days incubation at 30°C. (D) Deletion of *S. coelicolor ssdA* results in heterogeneous spore sizes and shapes. Phase-contrast micrographs of coverslip impressions with aerial hyphae and spore chains for WT, Δ*ssdA*$_{sco}$, and complemented strains (Δ*ssdA*/*ssdA*$_{sco}^{+}$ and Δ*ssdA*/*ssdA*$_{sve}^{+}$) are shown. Strains were grown on SFM solid medium for 8 days at 30°C. Genetic complementation of a deletion mutant with either *S. coelicolor* or *S. venezuelae ssdA*$^{+}$ was able to restore the uniform spore shape phenotype observed for the wild-type strain. Scale bar 2 μm.

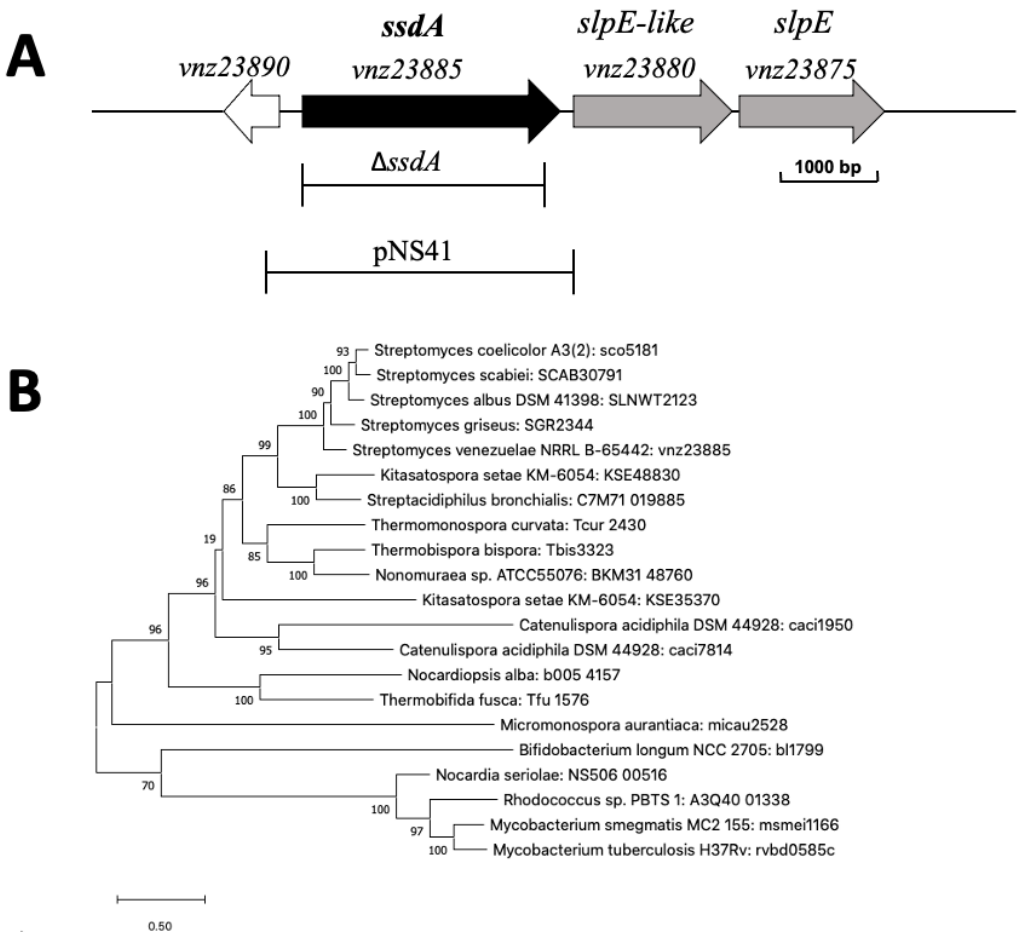

Figure 2.2 SsdA is widespread in Actinomycetes. (A) A physical map of the *S. venezuelae* chromosome that contains *ssdA* and its adjacent genes. The mutant of the unmarked in-frame deletion for the isolated S. *venezuelae ssdA* mutant is indicated as Δ*ssdA*. pNS41 is a site-specific integration plasmid that contains the entire *ssdA* and its promoter region and was used for constructing a genetic complementation strain. (B) Phylogenetic analysis of SsdA in *Actinobacteria*. A phylogenetic tree was constructed using MEGA (version X) using amino acid sequences of SsdA homologs from 5 *Streptomyces* species and 14 Actinomycete genus. Some species have two homologs of SsdA. Scale bar corresponds to 0.5 substitutions per site. Numbers on the branches indicate branch support values obtaining from 100 bootstrap replicates and are reported as percentages.

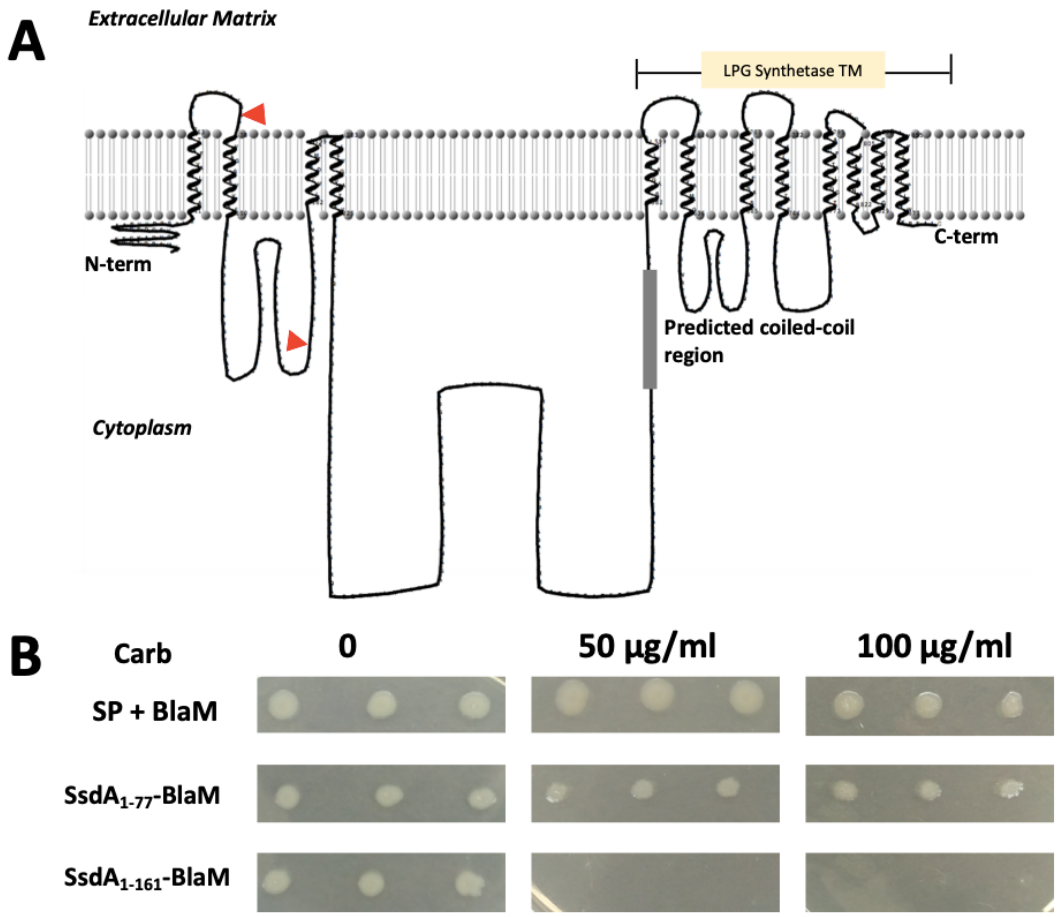

Figure 2.3 Predicted membrane topology of SsdA. (A) Shown is a model for a SsdA topology. Putative transmembrane segments were identified using program TMHMM, and a topological model was generated using program TMRPres2D. Red arrow heads indicate the positions of two BlaM fusions constructed and used for orientation of the N-terminus. The position of a weakly predicted coiled-coil region is shown (grey box). The C-terminus of SsdA is similar to a conserved lysophosphatidylglycerol (LPG) synthase transmembrane (TM) domain. (B) BlaM is functional in the periplasmic space. SsdA'-BlaM fusions were expressed in *E. coli* and cells were plated on LB medium containing different concentrations of carbenicillin (Carb). SP + BlaM is the construct containing the original wild-type BlaM signal peptide (SP). $SsdA_{1-77}$-BlaM and $SsdA_{1-161}$-BlaM are the two constructs expressing protein variants with BlaM fused to the first predicted TM and first two predicted TM segments, respectively.

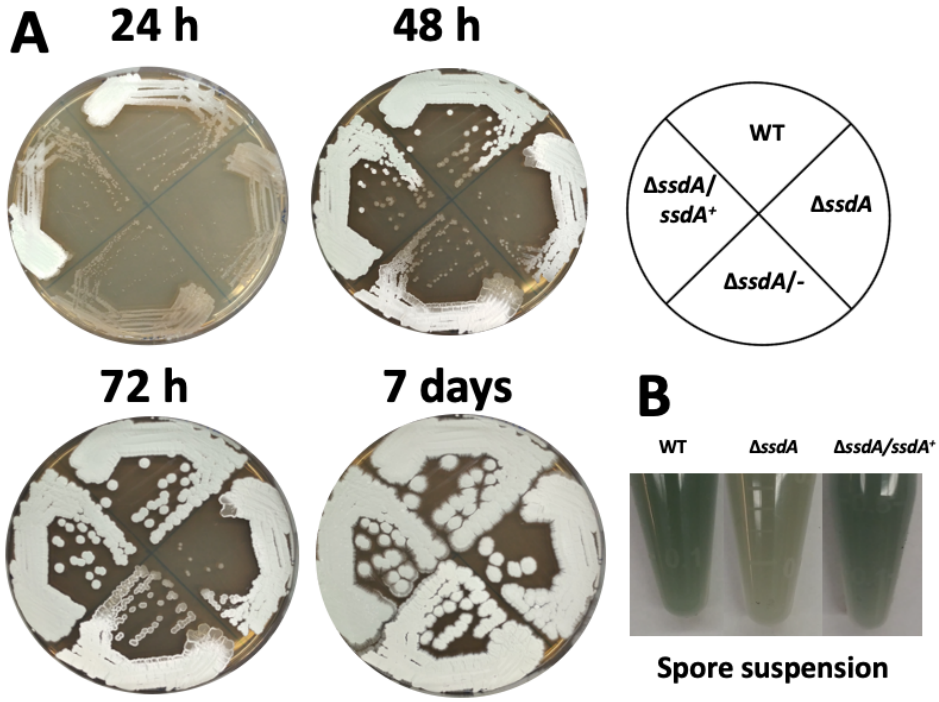

Figure 2.4 *ssdA* is required for normal morphological differentiation of *S. venezuelae* on solid medium.

(A) Strains were grown on MYM solid medium at 30°C, and photographed at the indicated time points. WT is wild-type strain. Δ*ssdA*/*ssdA*$^{+}$ (NS14) strain shows the genetically complemented strain created by integrating pNS40 *in trans* at the ΦBT1attachment site. The mutant strain containing the integration vector (pMS82) alone (Δ*ssdA*/-, NS13) was used as a negative control. A delayed development (aerial mycelium formation) was observed for the *ssdA* null mutant (NS7). (B) Spore suspensions of WT, Δ*ssdA* mutant (NS7), and complemented strain Δ*ssdA*/*ssdA*$^{+}$ (NS14) were made by harvesting the aerial mycelia after growth on MYM solid medium for 4 days. Isolated pores were resuspended and suspensions were photographed. A less green color (spore-associated pigment) was seen in the Δ*ssdA* strain.

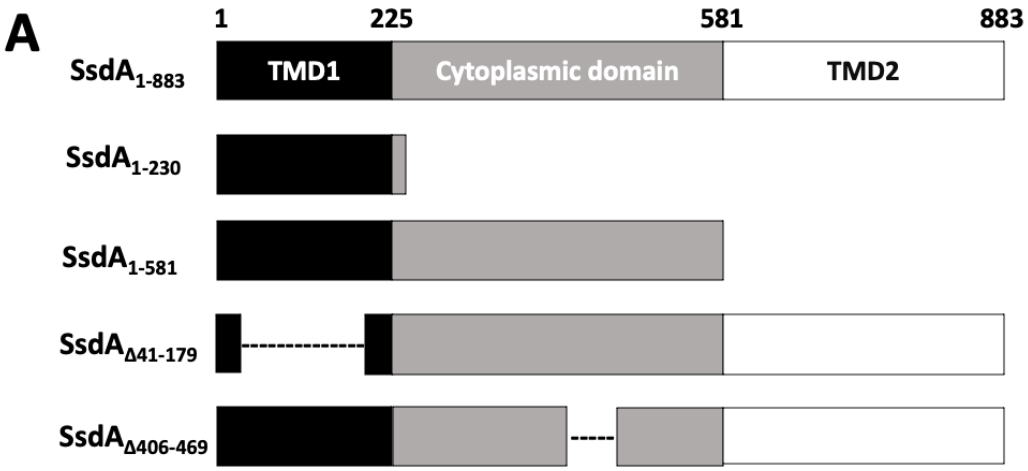

B

Strain	$SsdA_{1-883}$	$SsdA_{1-230}$	$SsdA_{1-581}$	$SsdA_{\Delta41-179}$	$SsdA_{\Delta406-469}$
Complemented? (Y/N)	Y	N	N	N	N

Figure 2.5 Genetic complementation of *ssdA* mutant with truncations of *ssdA*. (A) Schematic diagrams of constructs expressing SsdA ($SsdA_{1-883}$), 2 C-terminal truncations ($SsdA_{1-230}$ and $SsdA_{1-581}$), and 2 internal deletions ($SsdA_{\Delta41-179}$ and $SsdA_{\Delta406-469}$) are shown. Transmembrane domains at the N-terminus and C-terminus are represented by TMD1 and TMD2, respectively. Dashed lines (---) indicate deleted regions. Numbers above the diagrams are SsdA amino acid numbers. (B) Only full-length SsdA ($SsdA_{1-883}$) complemented Δ*ssdA* mutant macroscopically on MYM medium. Y represents yes and N represents no complementation.

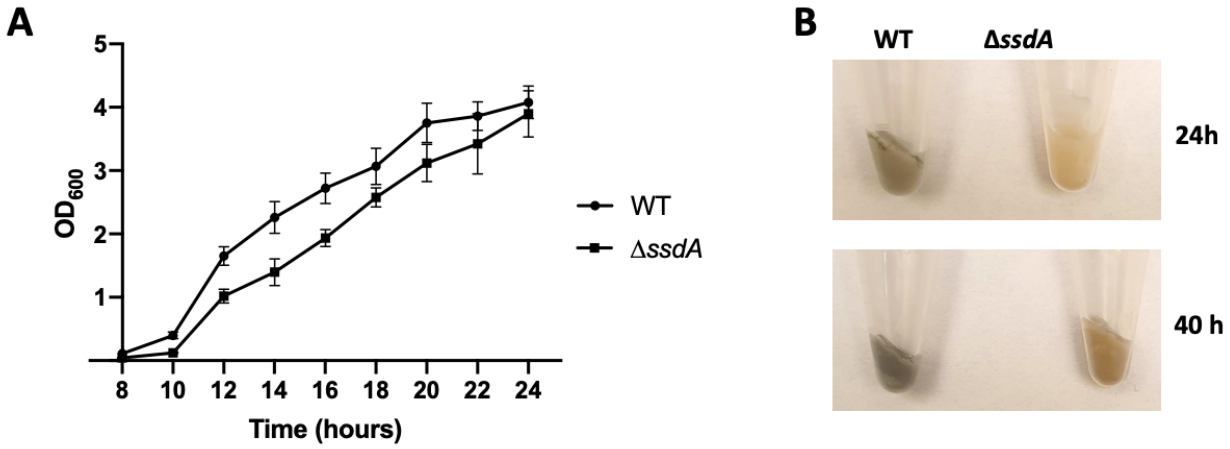

Figure 2.6 *ssdA* is required for normal growth and development of *S. venezuelae* in liquid medium. (A) Growth curves in MYM liquid medium at 30°C for the WT (•) and Δ*ssdA* mutant (NS7) were measured at OD_{600}. Apparent absorbance differences were observed between WT and Δ*ssdA* mutant. Results are the average of three independent growth experiments. Error bars represent the SD. (B) *S. venezuelae* sporulates in liquid culture producing pigmented spores. MYM cultures of WT and Δ*ssdA* mutant, were centrifuged and pellet (mixture of mycelial fragments and spores) was photographed at the indicated times. For (A) and (B), strains were started with the same number of spores.

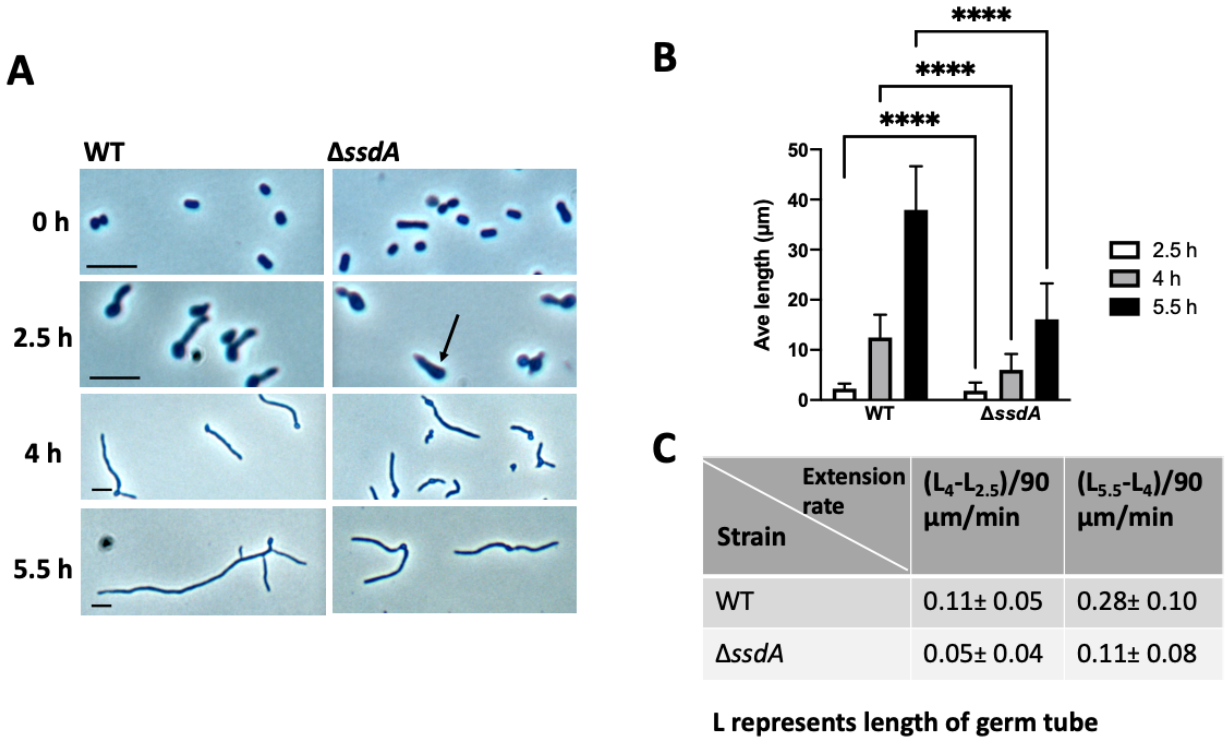

C

Strain \ Extension rate	$(L_4-L_{2.5})/90$ µm/min	$(L_{5.5}-L_4)/90$ µm/min
WT	0.11± 0.05	0.28± 0.10
Δ*ssdA*	0.05± 0.04	0.11± 0.08

L represents length of germ tube

Figure 2.7 A *ssdA* mutant has germination and growth defects. (A) Wild type and Δ*ssdA* mutant (NS7) strains were germinated and grown in MYM liquid. Freshly made spore suspensions containing around 10^7 spores were inoculated into 5 mL of MYM liquid medium, incubated at 30°C and 200 rpm. Samples, taken at the indicated time points, were mounted onto a 2% agarose pad and observed with a phase-contrast microscope. The arrow indicates the irregularly swollen spore with germ tube. Hyphal branches are evident for the wild type strain at 5.5 h. Scale bar 2 µm. (B) The average germ tube length from the longest hyphae tip to the germinated spore was measured manually using ImageJ software. Statistics was conducted by two-way ANOVA, **** P<0.0001. N is between 150 and 200 for each. (C) Germ tube extension rate were estimated between 2.5 hour to 4 hour (L_4-$L_{2.5}$) and 4 hour to 5.5 hour ($L_{5.5}$-L_4) in µm/min. Data are presented as mean ± SD. The extension rates were calculated from the data in panel B.

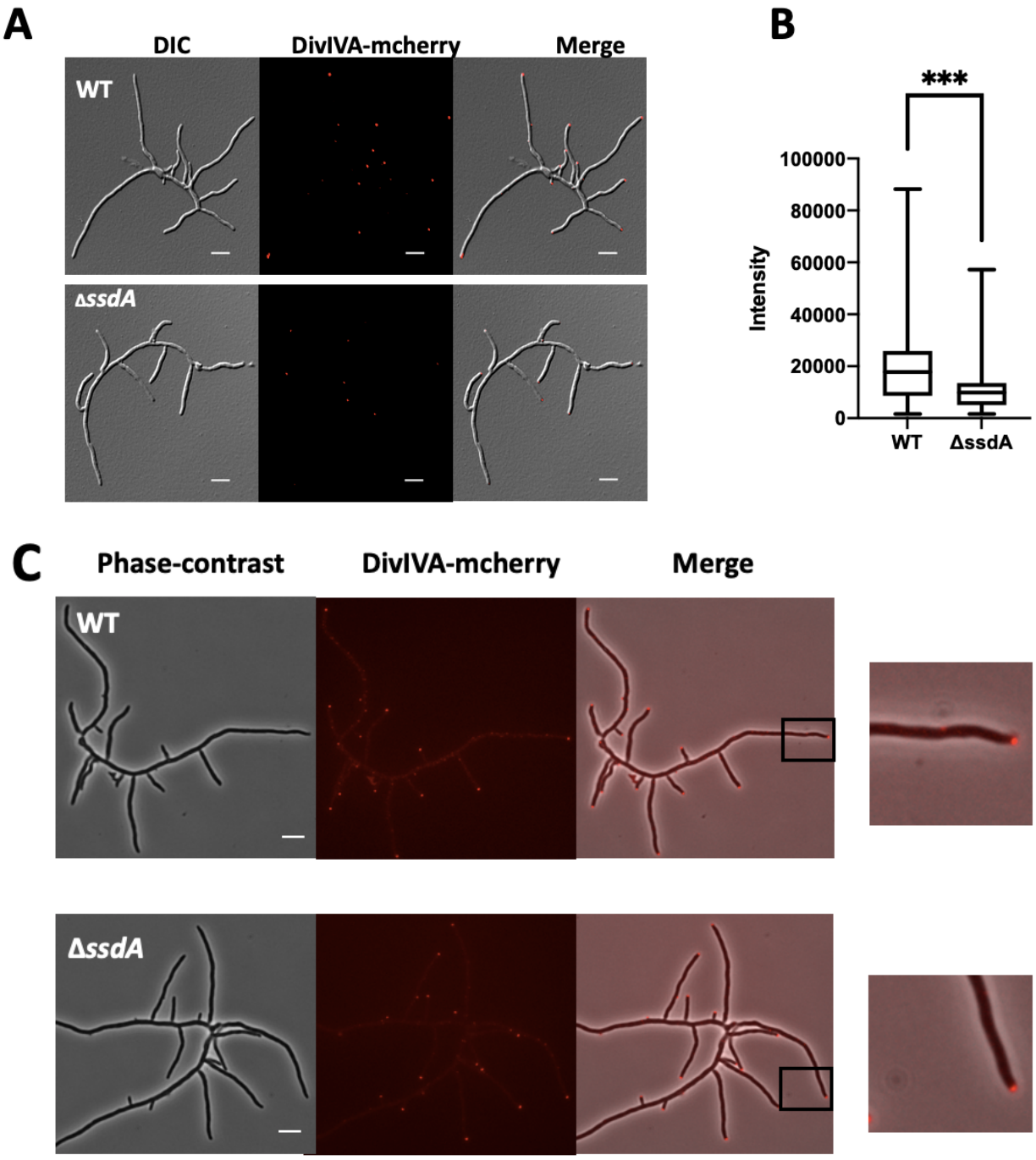
A
DIC
DivIVA-mcherry
Merge
WT
ΔssdA
B
***
100000
80000
60000
40000
20000
0
Intensity
WT
ΔssdA
C
Phase-contrast
DivIVA-mcherry
Merge
WT
ΔssdA

Figure 2.8 DivIVA-mCherry localization in WT and Δ*ssdA* mutant. (A) Subcellular localization of fluorescent protein DivIVA-mCherry is shown for a WT and Δ*ssdA* mutant strains. Strains were grown in MYM liquid medium for 6.5 hours (in WT background) and 8 hours (in the Δ*ssdA* mutant background), respectively. Scale bar 5 μm. (B) Box-whisker plot showing the fluorescence intensity distribution of DivIVA-mCherry foci for WT and Δ*ssdA* mutant strains. Box denotes the 25th percentile, median, and 75th percentile, respectively, and whiskers denote the min and max. Statistics was conducted using unpaired t test, *** $P<0.001$. (C) Subcellular localization of fluorescent protein DivIVA-mCherry is shown for a WT and Δ*ssdA* mutant strains in exponentially growing hyphae. The enlarged potions highlight in the boxes are shown. Scale bar 5 μm. Figures are conducted by Dr. Klas Flärdh at Lund University. Experiments will be repeated to solve the discrepancy of two independent results.

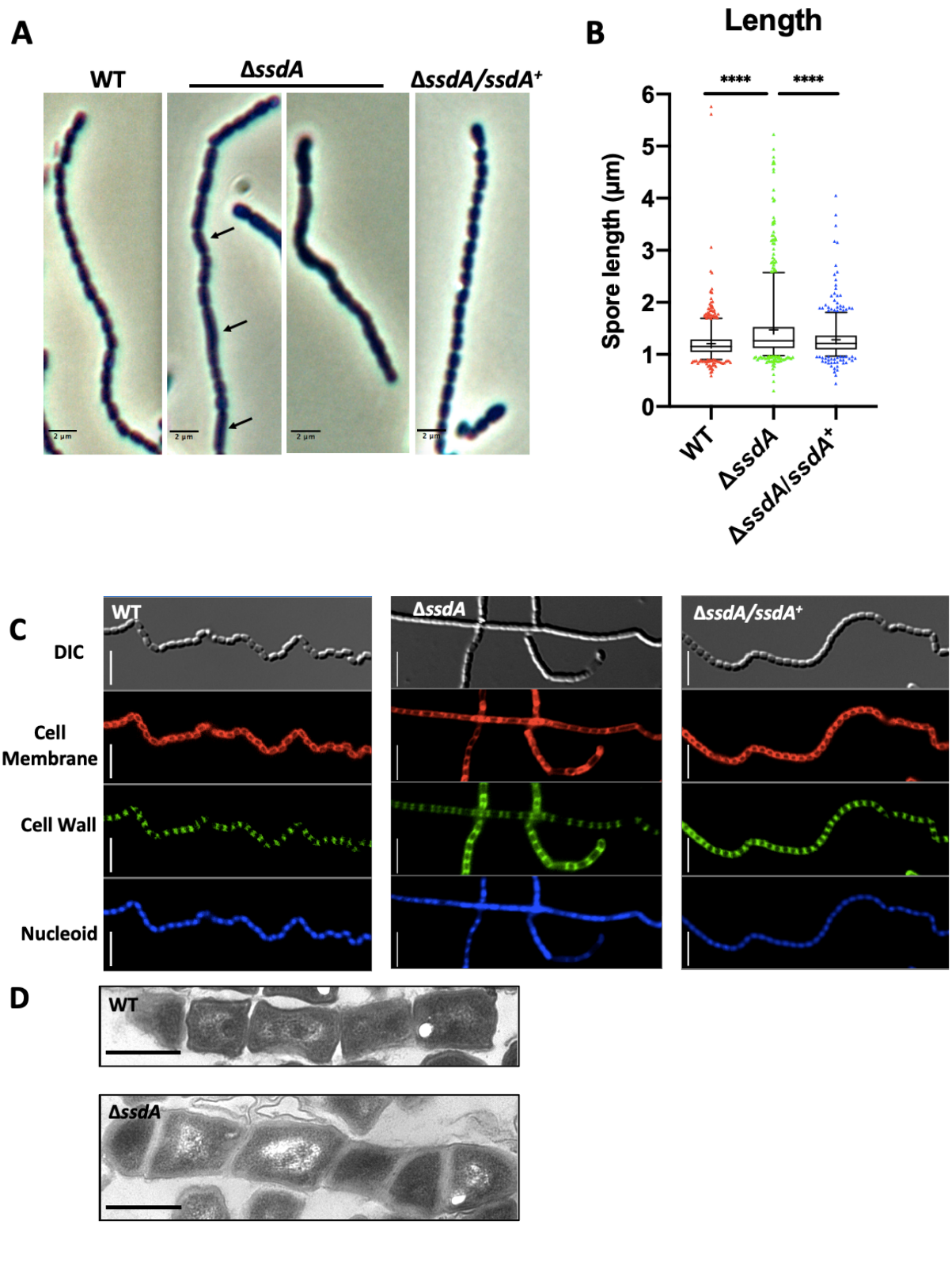
A
WT
ΔssdA
ΔssdA/ssdA+
B
Length
****
****
Spore length (μm)
0
1
2
3
4
5
6
WT
ΔssdA
ΔssdA/ssdA+
C
DIC
Cell Membrane
Cell Wall
Nucleoid
WT
ΔssdA
ΔssdA/ssdA+
D
WT
ΔssdA

Figure 2. 9 Effect of the deletion of *ssdA* on spore size and shape. (A) Phase-contrast micrographs of representative mature spore chains are shown. Strains were grown on MYM solid medium for 5 days at 30°C, and coverslip impressions were observed using a phase-contrast microscope. Arrows point to the larger spores of the Δ*ssdA* mutant. (B) Measurements of spore length were generated using an auto measurement tool of Nikon NIS-Elements software from phase-contrast images of spore suspensions harvested after strains were grown at the same condition as (A). Box-whisker plot showing the spore length distributions of wild type (WT N=908), Δ*ssdA* mutant (NS7, N=1027), and complemented strain Δ*ssdA*/*ssdA*$^{+}$ (NS14, N=675) are graphed. Boxes denote the 25th percentile, median, and 75th percentile, respectively, and whiskers denote the 5th and 95th percentile. Data not included in the box-whisker are shown as dots. The + represents the mean value of WT (1.20±0.32 μm), Δ*ssdA* mutant (1.47±0.81 μm), and Δ*ssdA*/*ssdA*$^{+}$ (1.28±0.33 μm), respectively. Statistics were conducted using one-way ANOVA, **** P<0.0001) (C) Epi-fluorescence micrographs of spore chains (after 5 days of incubation on MYM agar at 30°C) stained for cell wall with fluorescein-conjugated WGA (green), cell membrane with FM4-64 (red), and DNA with DAPI (blue). White arrows indicate the positions of septa. Scale Bar 5 μm (D) TEM micrograph of spore chains after 4 days of growth on MYM agar at 30°C. Mutant spore walls appear thicker and strain with less intensity than wild type. Scale Bar 1 μm.

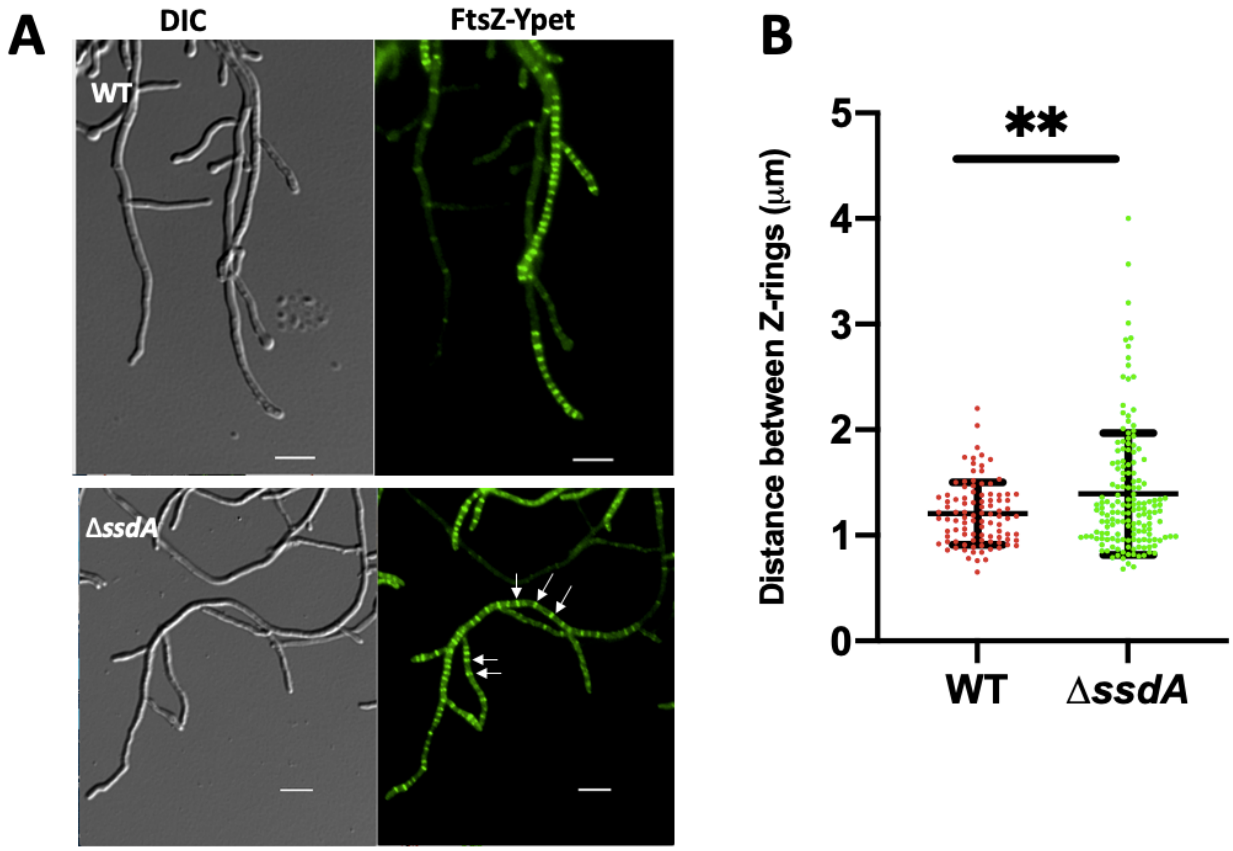

Figure 2.10 FtsZ-Ypet localization is compromised in the absence of *ssdA*. (A) Subcellular localization of fluorescent protein Ypet fused to FtsZ (FtsZ-Ypet) for WT and Δ*ssdA* mutant strains. Arrows indicate irregularly spaced Z rings. Strains were grown in MYM liquid medium for 20 hours (in WT background) and 22 hours (in the Δ*ssdA* mutant background), respectively. Scale bar 5 μm. (B) Distance of Z rings in sporulating hyphae for WT and Δ*ssdA* mutant strains. The mean distance between adjacent Z rings (mean ± SD) from at least 5 sporulating hyphae for each strain is shown. All values are plotted as red dots and green dots for WT and Δ*ssdA* mutant, respectively. Statistics was conducted using unpaired t test, ** P<0.01.

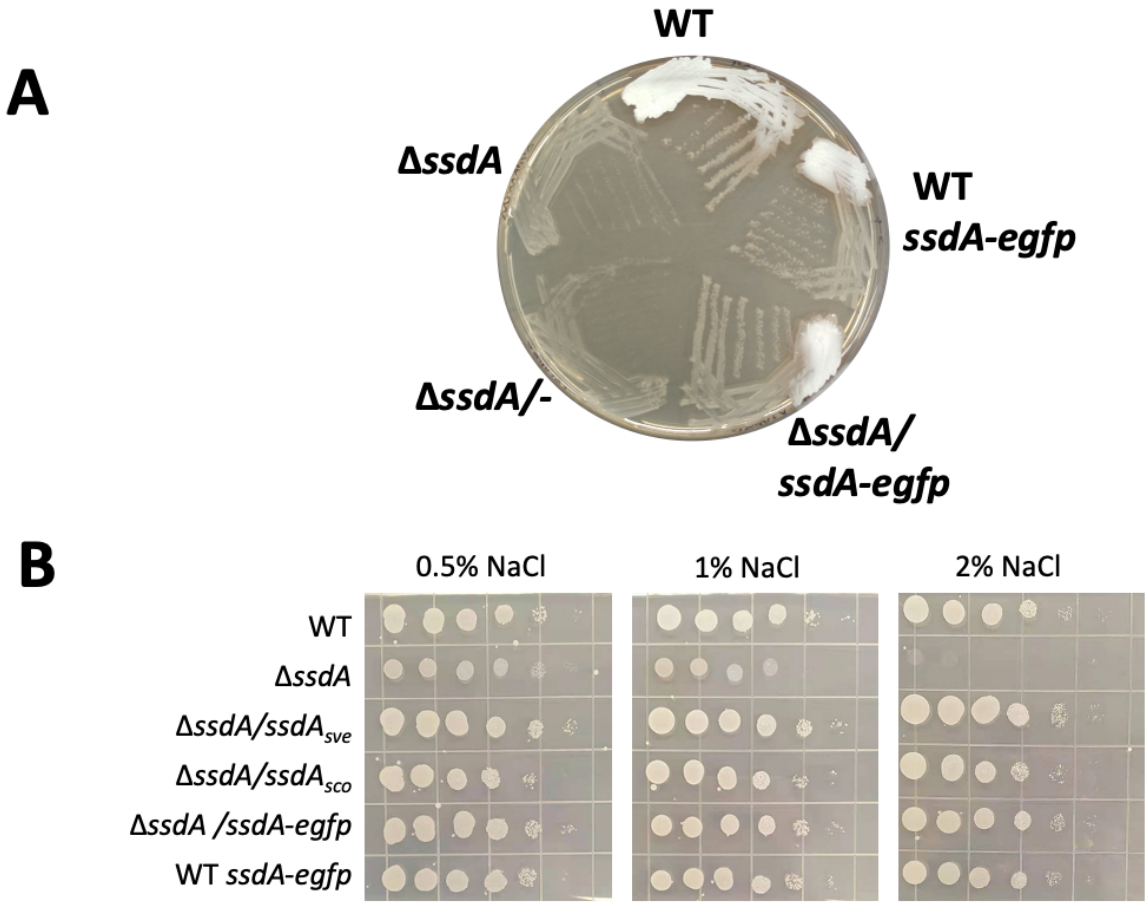

Figure 2.11 SsdA-EGFP fusion is functional. (A) Strains were streaked on MYM solid medium, and photographed after 1 day incubation at 30°C. Shown are *S. venezuelae* strains of wild-type (WT), Δ*ssdA* mutant (NS7), a *ssdA-egfp* fusion integrated as the only copy of *ssdA* at the native site of the chromosome via homologous recombination (WT *ssdA-egfp*, NS18), and Δ*ssdA* mutant complemented in trans using a *ssdA-egfp* fusion construct (Δ*ssdA*/*ssdA-egfp*, NS24). The mutant strain containing the integration vector alone (Δ*ssdA*/-, NS13) was used as a negative control. (B) 10-fold serial dilutions of spores were spotted on standard LB agar containing different concentrations of NaCl. Photographs were taken after 1 day incubation at 30°C. The *S. venezuelae* Δ*ssdA* mutant was complemented in trans with S. venezuelae *ssdA* (Δ*ssdA*/$ssdA_{sve}$, NS14), *S. coelicolor ssdA* gene (Δ*ssdA*/$ssdA_{sco}$, NS35), and *S. venezuelae ssdA-egfp* (Δ*ssdA*/*ssdA-egfp*, NS24). *ssdA-egfp* fused at the native site of the chromosome as the only copy of *ssdA* (WT *ssdA-egfp*, NS18).

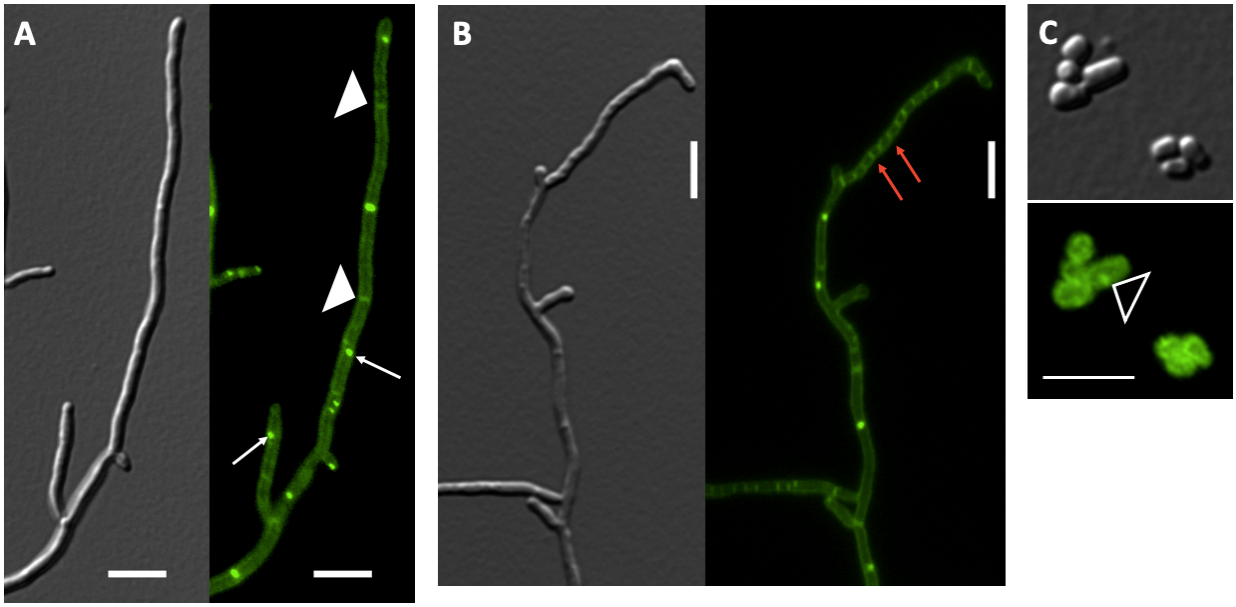

Figure 2.12 SsdA-EGFP localizes in vegetative hyphae, at sporulation septa, and periphery of mature spores. (A) SsdA-EGFP localizes in vegetative hyphae. Filled arrow heads indicate probable sites of the vegetative cross-wall. White arrows point to the foci representing the future branching sites. (B) SsdA-EGFP localizes at sporulation septa (red arrows). (C) SsdA-EGFP localizes to the periphery of the mature spores (open arrow head). *ssdA-egfp* was expressed from a constitutive *ermE** promoter and integrated in trans to the ΦBT1 site of WT. Background was set at the level of autofluorescence in a wild-type strain lacking a fluorescent protein fusion. Scale bar 5 μm.

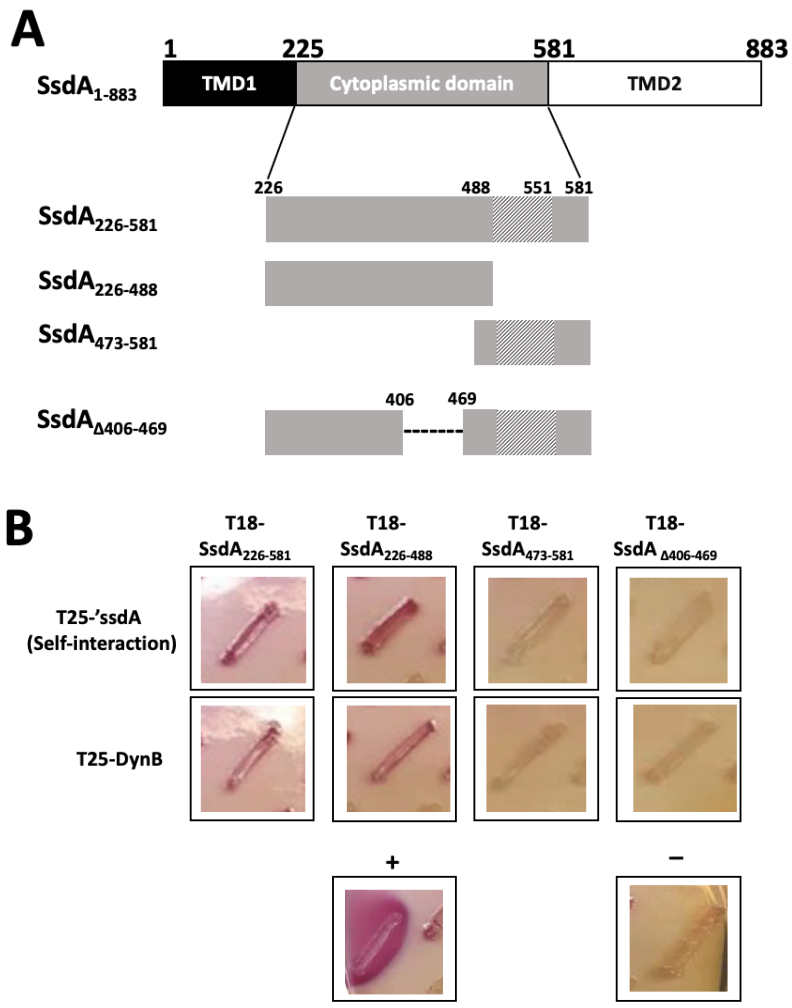
A
1
225
581
883
SsdA1-883
TMD1
Cytoplasmic domain
TMD2
226
488
551
581
SsdA226-581
SsdA226-488
SsdA473-581
406
469
SsdAΔ406-469
B
T18-SsdA226-581
T18-SsdA226-488
T18-SsdA473-581
T18-SsdA Δ406-469
T25-'ssdA (Self-interaction)
T25-DynB
+
–

Figure 2.13 SsdA interactions for constructs were tested in a Bacterial two-hybrid assay. (A) Only the large central cytoplasmic loop region of SsdA was tested in a Bacterial two-hybrid assay. Schematic diagrams of variants of the central cytoplasmic domain of SsdA are shown. Box with stripes indicate the location of a weakly predicted coiled-coil region. $SsdA_{226\text{-}581}$ represents the full length of the central cytoplasmic domain. $SsdA_{\Delta 406\text{-}469}$ represents the codon for amino acids from 406 to 469 were deleted (shown as dashed lines). Numbers above the diagrams are SsdA amino acid numbers. (B) Bacterial two-hybrid analysis of self-interactions among SsdA variants and interactions between SsdA variants and DynB. Fresh transformants carrying plasmids with protein fusion to the T18 and the T25 domain were patched onto MacConkey maltose agar supplemented with 0.5 mM IPTG, ampicillin, and kanamycin, and incubated overnight at 30°C. One representative growth patch of each tested interaction is shown. Positive and negative controls are shown at the bottom. The red/pink color indicates a positive protein-protein interaction and clear color indicates no interaction. No interaction has been observed between $SsdA_{226\text{-}581}$ and SepF1, SepF2, SepF3, SepH, DynA, SsgA or SsgB (data not shown).

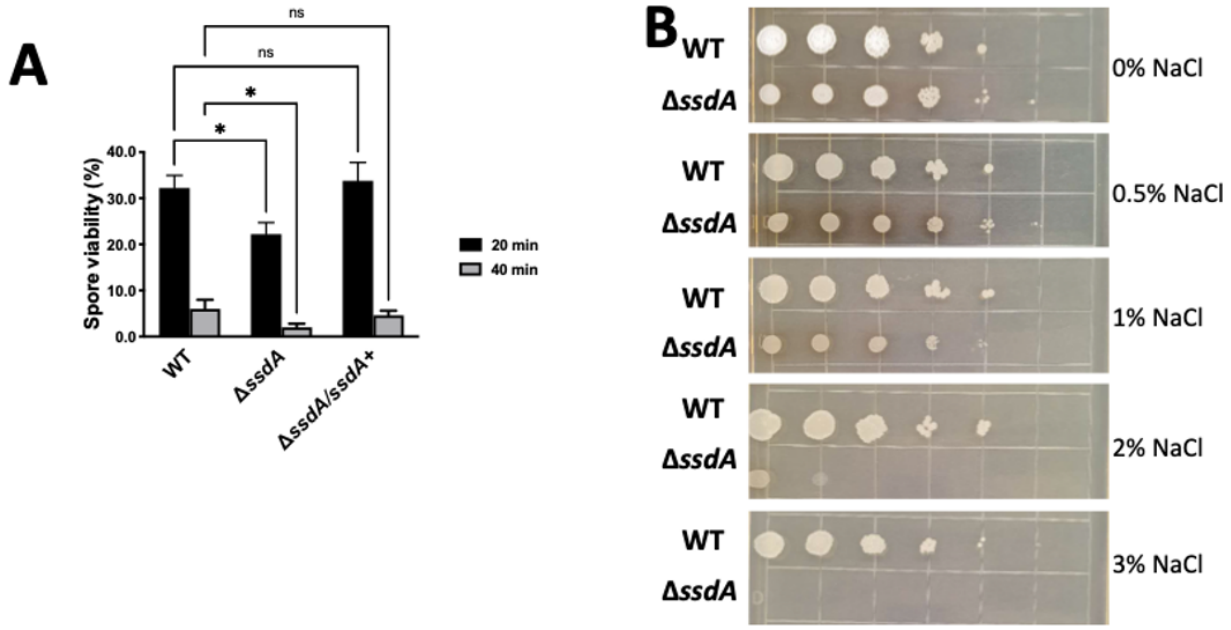

Figure 2.14 A *ssdA* mutant is more sensitive to heat and osmotic stress. (A) Shown are the results of a heat stress assay. Heat treatment of freshly isolated spores was carried out at 55°C for the indicated incubation times. Results are the average of three independent replicates and error bars represent SD. Asterisks indicate the significance for Δ*ssdA* mutant (NS7) when compared to WT. An asterisk (*) indicates a P value of <0.05. Genetic complementation strain Δ*ssdA*/*ssdA*$^{+}$ (NS14) restores heat sensitivity to the wild-type level. (B) Shown are the results of an osmotic stress assay. Serial dilutions of spores were spotted on standard LB agar plates containing different concentrations of NaCl. Photographs were taken after 2 days of incubation at 30°C. The size of the spots were noticeably smaller for the Δ*ssdA* strain than that for WT strain under all tested conditions, which is consistent with the germination and growth defect measured for the Δ*ssdA* mutant (Fig. 2.6). Genetic complementation strain Δ*ssdA*/*ssdA-egfp*$^{+}$ (NS24) restores osmotic sensitivity to the wild-type level (Fig. 2.13B).

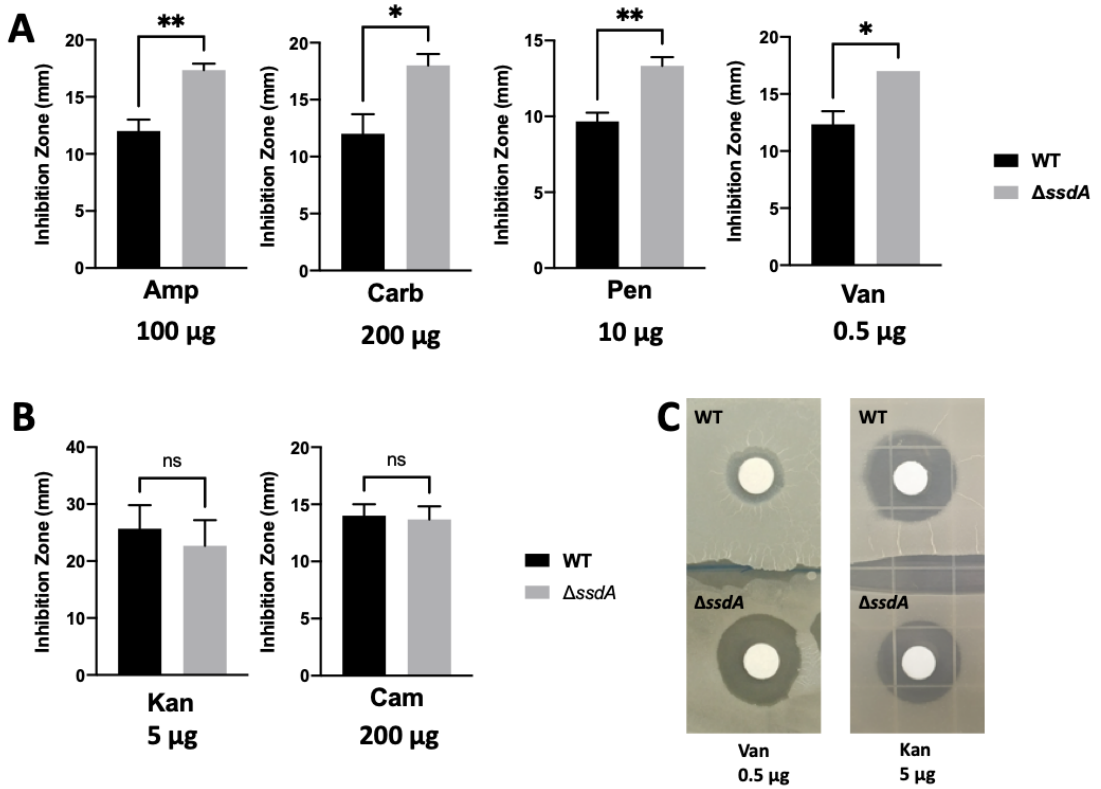

Figure 2.15 A ***ssdA*** **mutant is more sensitive to cell-wall targeting antibiotics**. (A) The resistance to cell wall-targeting antibiotics ampicillin (Amp), carbenicillin (Carb), penicillin (Pen), and vancomycin (Van) were tested by applying filter disks containing the indicated amount of antibiotics. Freshly inoculated LB plates containing 0.5% NaCl were spread with equal amounts of normalized viable spore suspensions for WT and the Δ*ssdA* mutant (NS7). (B) Two antibiotics [kanamycin (Kan) and chloramphenicol (Cam)] that target the ribosome were tested as a negative control. For A and B, the size of growth inhibition zone was measured after 1 day of incubation at 30°C. Diameters of the inhibition zones were measured in (mm). Results are the average from three independent spore stocks, and error bars are SD. An asterisk (*) indicates a P value of <0.05, ** indicates P<0.01, and ns indicates date are not significant. (C) Representative pictures of inhibition zones are shown. Van (cell wall-targeted) and Kan (ribosome-targeted) are shown as an example.

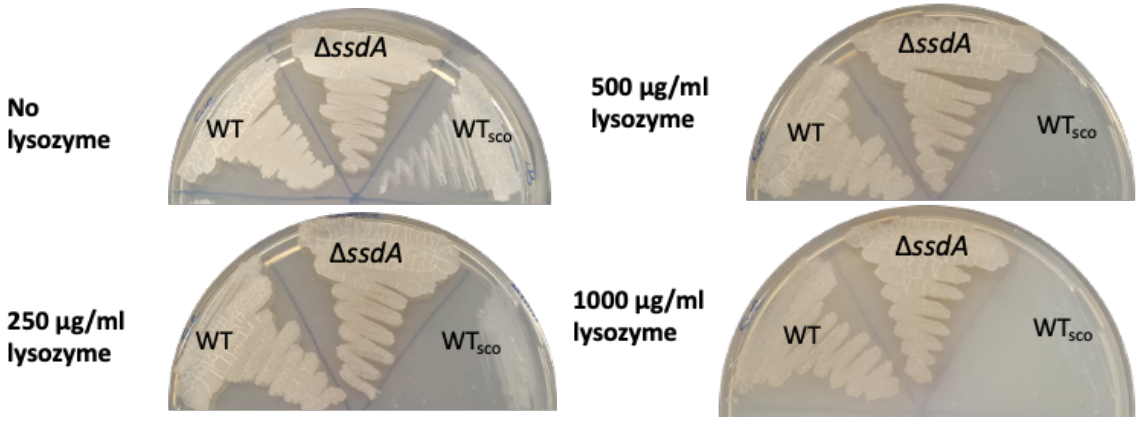

Figure 2.16 *S. venezuelae* wild type and *ssdA* mutant are highly resistant to lysozyme treatment. *S. venezuelae* spores for the wild type and Δ*ssdA* mutant (NS7) stains were streaked on standard LB agar plates (0.5% NaCl) containing different concentrations of lysozyme (label to left of each petri plate). Wild-type *S. coelicolor* (WT_{sco}) was used as a positive control to demonstrate that lysozyme treatment was effective. Photographs were taken after 1day incubation at 30°C.

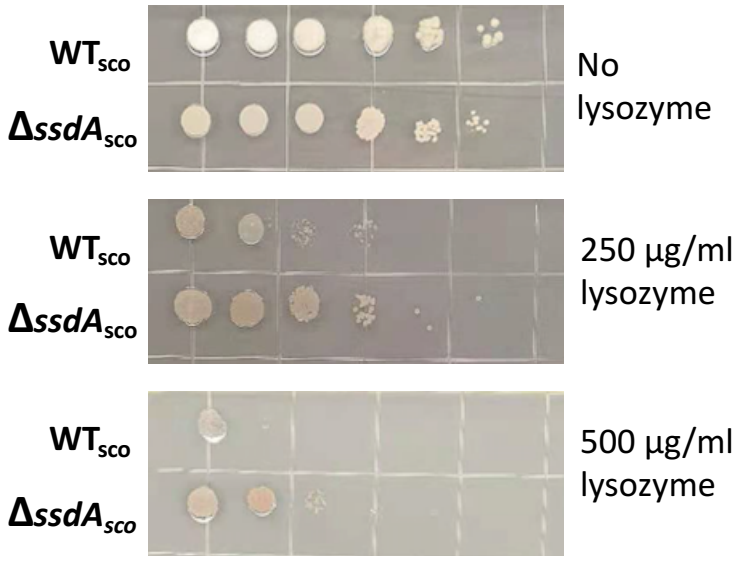

Figure 2.17 A ***S. coelicolor ssdA*** **mutant is more resistant to lysozyme than the wild-type strain.** Ten-fold serial dilutions of *S. coelicolor* spores were spotted on standard LB agar (0.5% NaCl) containing different concentrations of lysozyme (label to right of each petri plate). Shown is the lysozyme sensitivity for *S. coelicolor* wild type (WT_{sco}) and *ssdA* mutant ($\Delta ssdA_{sco}$, NS30), respectively. Photographs were taken after 3 days incubation at 30°C. Pictures are a representative from an analysis of 3 independent spore suspensions.

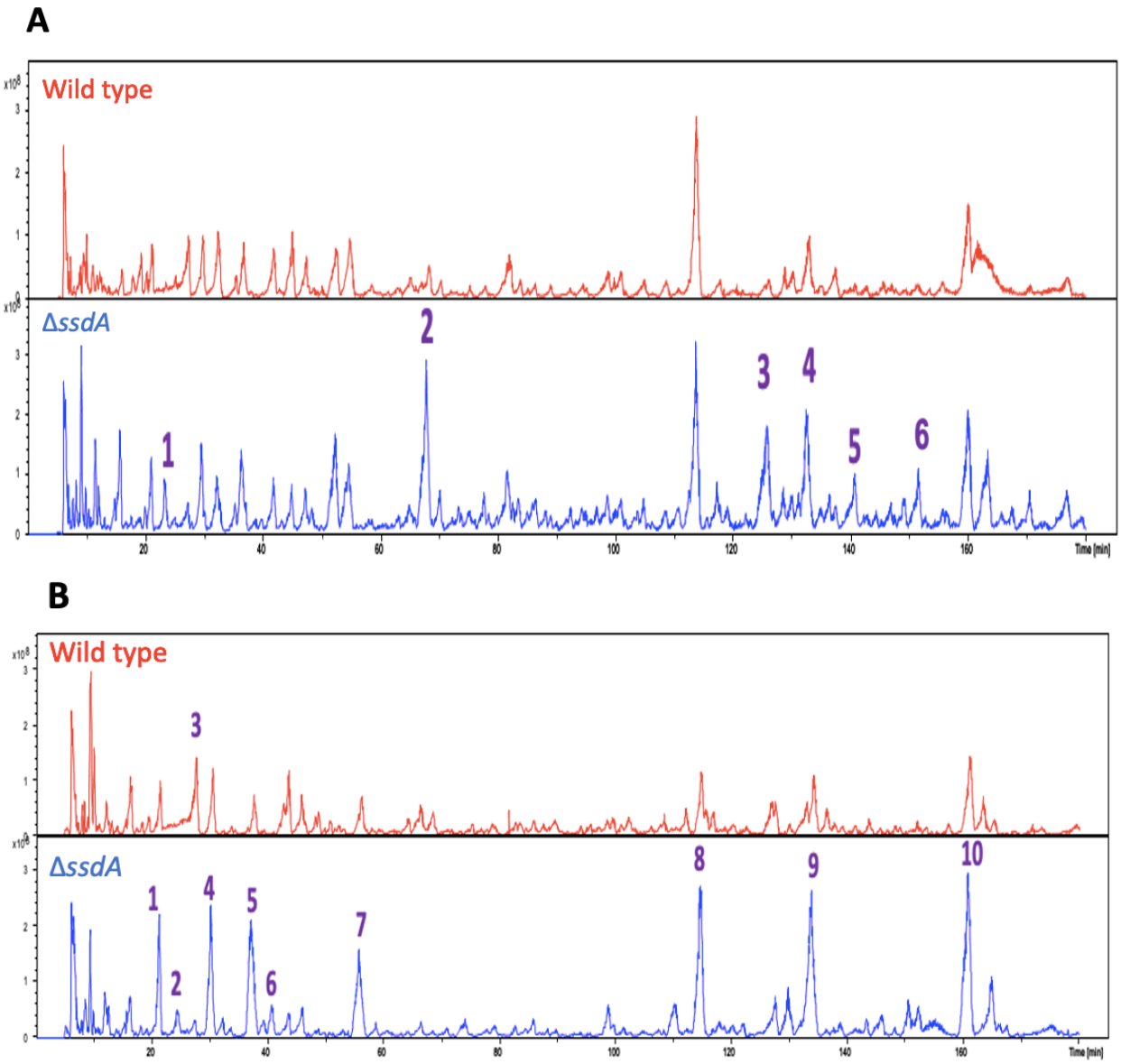

Figure 2.18 A *ssdA* mutant enriches monomeric muropeptides of spore wall. HPLC chromatographs are shown for both *S. venezuelae* (A) and *S. coelicolor* (B). For each panel, wild-type graph is shown as red at top, and Δ*ssdA* mutant is shown as blue at bottom. PG was separated from the isolated spore cell sacculus, and then digested by mutanolysin. The resulting fragments were subjected to the HPLC analysis. Numbers indicate the peaks that have different intensity between WT and Δ*ssdA* mutant. *S. venezuelae* spores were harvested after growth at 30°C on MYM agar after 5 days of incubation, while *S. coelicolor* spores were harvested after growth at 30°C on SFM agar after 7 days of incubation.

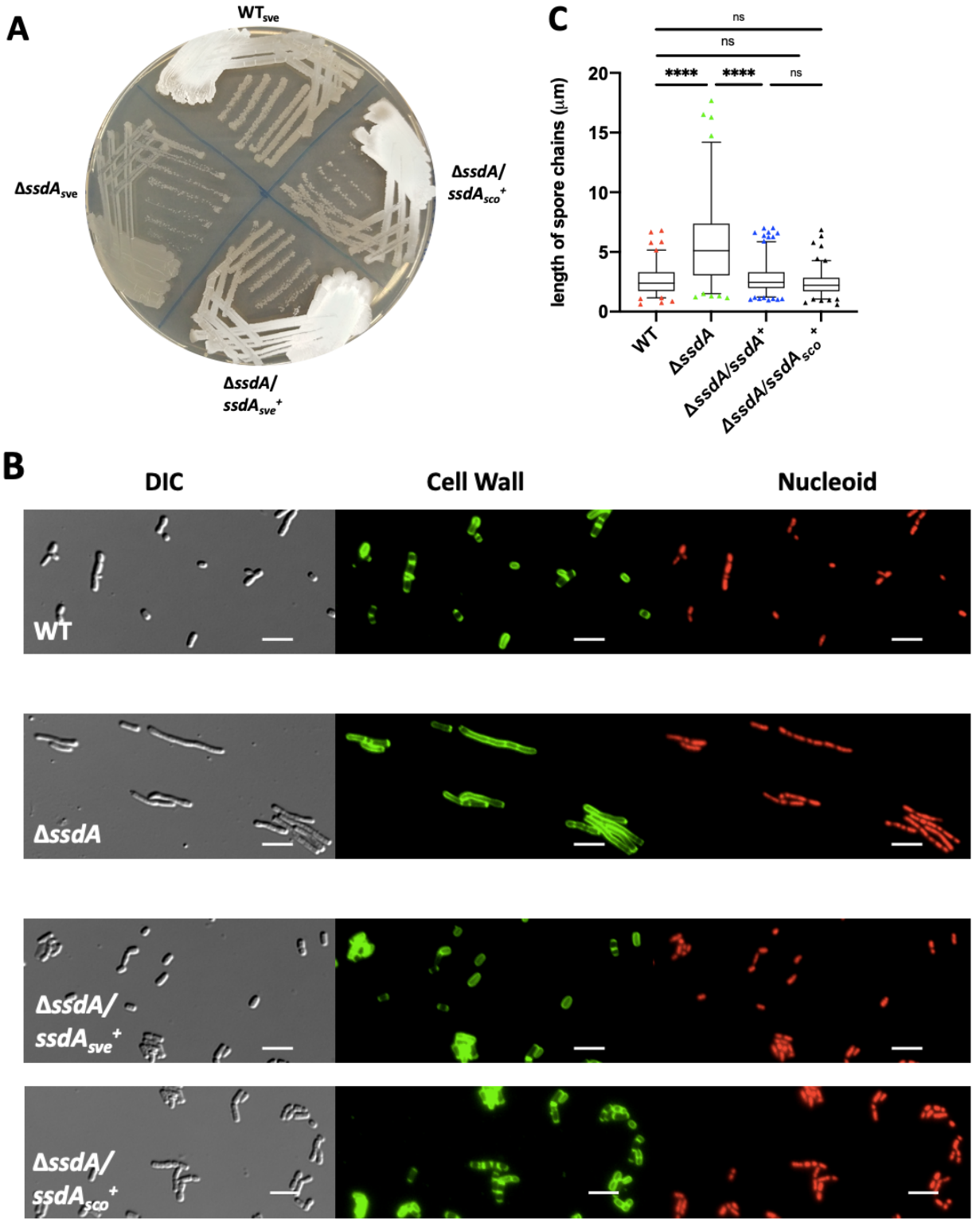
A
WTsve
ΔssdAsve
ΔssdA/ssdAsco+
ΔssdA/ssdAsve+
C
ns
ns
****
****
ns
length of spore chains (μm)
20
15
10
5
0
WT
ΔssdA
ΔssdA/ssdA+
ΔssdA/ssdAsco
B
DIC
Cell Wall
Nucleoid
WT
ΔssdA
ΔssdA/ssdAsve+
ΔssdA/ssdAsco+

Figure 2.19 SsdA function is conserved in *Streptomyces*. *ssdA* of *S. coelicolor* was able to complement the phenotypes caused by deletion of *ssdA* in S. *venezuelae* (Δ*ssdA*/*ssdA*$_{sco}^{+}$). (A) Strains were streaked on MYM agar and images were acquired after 1 day incubation at 30°C. (B) Epi-fluorescence micrographs of spore chains (41 hours in MYM liquid) after staining the cell wall with fluorescein-conjugated WGA (green), and DNA with PI (red). Scale bar 5 um. (C) Box-whisker plot showing the length distribution of spore chain or spores for WT (N=101), Δ*ssdA* mutant (N=113), and complemented strains Δ*ssdA*/*ssdA*$^{+}$ (N=196) and Δ*ssdA*/*ssdA*$_{sco}^{+}$ (N=98). Box denotes the 25th percentile, median, and 75th percentile, respectively, and whiskers denote the 5th and 95th percentile. Data not included in the box-whisker are shown as dots. Statistics was conducted using one-way ANOVA, **** P<0.0001. This figure together with Fig. 2.1 indicates SsdA function is conserved in *Streptomyces*.

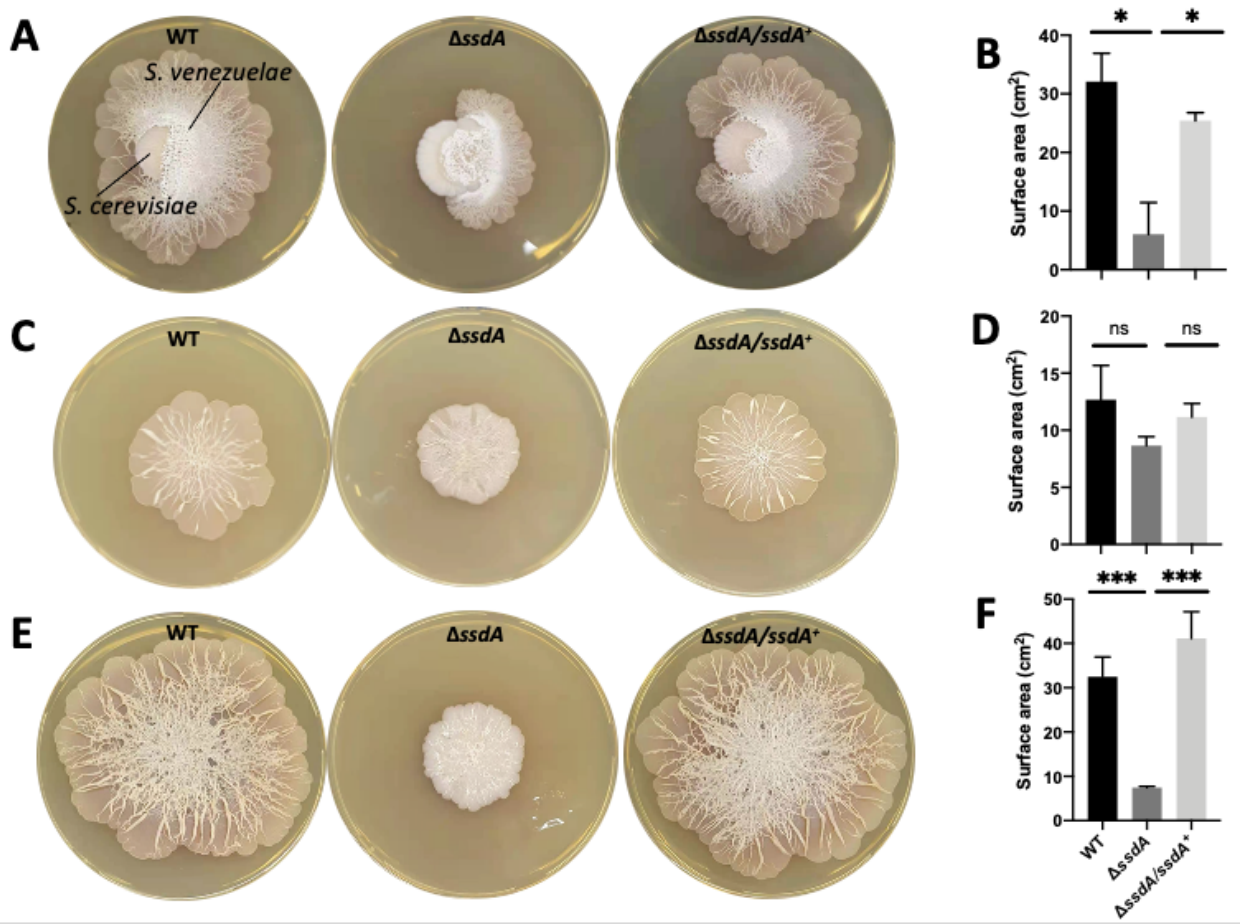

Figure 2.20 A ***ssdA* mutant compromises vegetative exploration growth.** Representative images of *Streptomyces* explorer cell growth with the corresponding quantification data for surface area when grown on YPD medium cocultured with *Saccharomyces cerevisiae* (A and B). *S. venezuelae strains* were grown alone on YP medium (C and D), and YP with 2% glycerol medium (E and F). Strains include wild-type *S. venezuelae* (WT), Δ*ssdA* mutant (NS7), and the complemented strain (Δ*ssdA/ssdA*$^{+}$, NS14). (A) *S. venezuelae* was grown beside *S. cerevisiae* at 30°C for 14 days. (C and E) *S. venezuelae* was grown alone at 30°C for 10 days. (B, D and F) Results are the average from three independent experiments, and error bars are SD. Statistics were conducted using one-way ANOVA. An asterisk (*) indicates a P value of <0.05, *** indicates P<0.001, and ns indicates date are not significant.

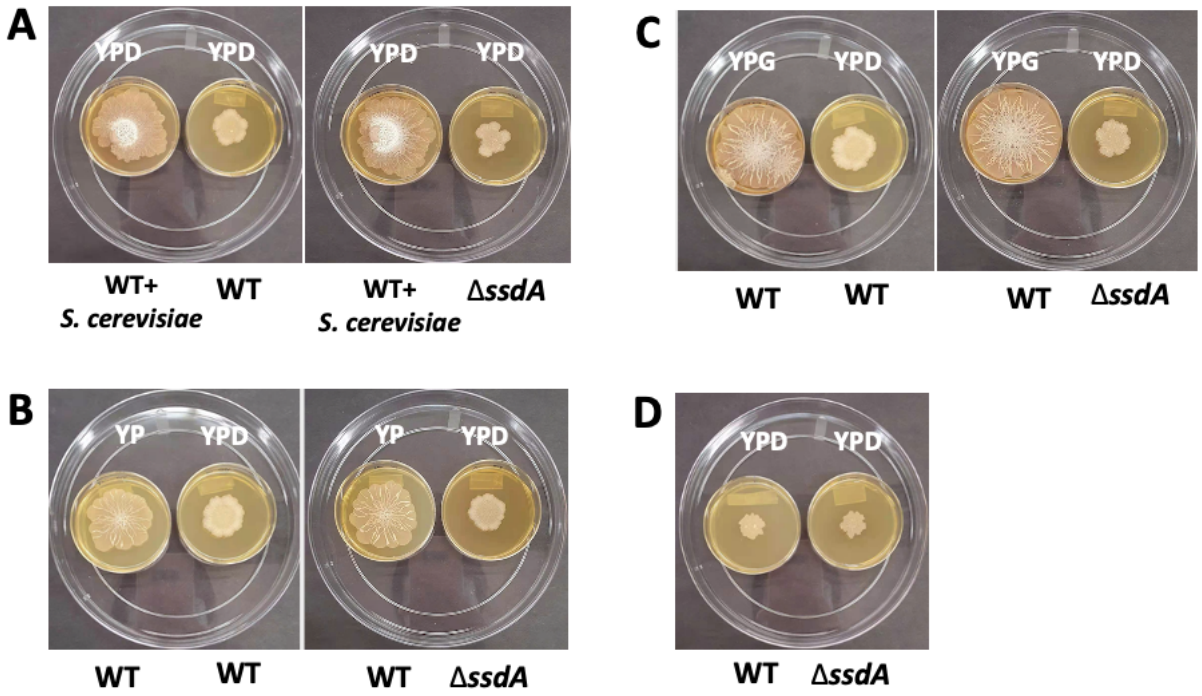

Figure 2.21 Volatile organic compounds released by wild-type *S. venezuelae* induce exploration of a physically separated *ssdA* mutant strain. (A-C) For each image, the small petri dish on the left side of the big petri dish is wild-type *S. venezuelae* growing with yeast on standard YPD dextrose agar (A), growing alone on YP agar without additional carbon source (B) and YP with 2% glycerol (YPG) agar (C). In each big compartment, wild type is used as volatile signals producer to induce the exploration of wild type (left compartment, positive control) and Δ*ssdA* mutant (right compartment). (D) Shown is a negative control that both WT and Δ*ssdA* mutant growing alone did not explore on YPD medium. Images were taken after incubation at 30°C for 10 days.

REFERENCES

Allan, E.J., and Prosser, J.I. (1983). Mycelial growth and branching of *Streptomyces coelicolor* A3 (2) on solid medium. Microbiology *129*, 2029-2036.

Bagchi, S., Tomenius, H., Belova, L.M., and Ausmees, N. (2008). Intermediate filament-like proteins in bacteria and a cytoskeletal function in *Streptomyces*. Mol Microbiol *70*, 1037-1050.

Baker Brachmann, C., Davies, A., Cost, G.J., Caputo, E., Li, J., Hieter, P., and Boeke, J.D. (1998). Designer deletion strains derived from *Saccharomyces cerevisiae* S288C: a useful set of strains and plasmids for PCR‐mediated gene disruption and other applications. Yeast *14*, 115-132.

Bennett, J. (2006). Molecular genetic analysis of division and development in *Streptomyces coelicolor*. (Ph. D. dissertation. Duquesne University, Pittsburgh, PA).

Binnie, C., Butler, M.J., Aphale, J.S., Bourgault, R., DiZonno, M.A., Krygsman, P., Liao, L., Walczyk, E., and Malek, L.T. (1995). Isolation and characterization of two genes encoding proteases associated with the mycelium of *Streptomyces lividans* 66. J Bacteriol *177*, 6033-6040.

Broome-Smith, J.K., Tadayyon, M., and Zhang, Y. (1990). Beta-lactamase as a probe of membrane protein assembly and protein export. Mol Microbiol *4*, 1637-1644.

Bush, M.J., Tschowri, N., Schlimpert, S., Flardh, K., and Buttner, M.J. (2015). c-di-GMP signalling and the regulation of developmental transitions in streptomycetes. Nat Rev Microbiol *13*, 749-760.

Caccamo, P.D., and Brun, Y.V. (2018). The Molecular Basis of Noncanonical Bacterial Morphology. Trends Microbiol *26*, 191-208.

Cherepanov, P.P., and Wackernagel, W. (1995). Gene disruption in *Escherichia coli*: TcR and KmR cassettes with the option of Flp-catalyzed excision of the antibiotic-resistance determinant. Gene *158*, 9-14.

Datsenko, K.A., and Wanner, B.L. (2000). One-step inactivation of chromosomal genes in *Escherichia coli* K-12 using PCR products. Proc Natl Acad Sci USA *97*, 6640-6645.

Ditkowski, B., Holmes, N., Rydzak, J., Donczew, M., Bezulska, M., Ginda, K., Kedzierski, P., Zakrzewska-Czerwinska, J., Kelemen, G.H., and Jakimowicz, D. (2013). Dynamic interplay of

ParA with the polarity protein, Scy, coordinates the growth with chromosome segregation in *Streptomyces coelicolor*. Open Biol *3*, 130006.

Donczew, M., Mackiewicz, P., Wrobel, A., Flardh, K., Zakrzewska-Czerwinska, J., and Jakimowicz, D. (2016). ParA and ParB coordinate chromosome segregation with cell elongation and division during *Streptomyces* sporulation. Open Biol *6*, 150263.

Egan, A.J.F., Errington, J., and Vollmer, W. (2020). Regulation of peptidoglycan synthesis and remodelling. Nat Rev Microbiol *18*, 446-460.

Flärdh, K. (2003). Essential role of DivIVA in polar growth and morphogenesis in *Streptomyces coelicolor* A3(2). Mol Microbiol *49*, 1523-1536.

Flärdh, K., and Buttner, M.J. (2009). *Streptomyces* morphogenetics: dissecting differentiation in a filamentous bacterium. Nat Rev Microbiol *7*, 36-49.

Flärdh, K., Richards, D.M., Hempel, A.M., Howard, M., and Buttner, M.J. (2012). Regulation of apical growth and hyphal branching in *Streptomyces*. Curr Opin Microbiol *15*, 737-743.

Fröjd, M.J., and Flärdh, K. (2019). Apical assemblies of intermediate filament-like protein FilP are highly dynamic and affect polar growth determinant DivIVA in *Streptomyces venezuelae*. Mol Microbiol *112*, 47-61.

Fuchino, K., Bagchi, S., Cantlay, S., Sandblad, L., Wu, D., Bergman, J., Kamali-Moghaddam, M., Flardh, K., and Ausmees, N. (2013). Dynamic gradients of an intermediate filament-like cytoskeleton are recruited by a polarity landmark during apical growth. Proc Natl Acad Sci USA *110*, E1889-1897.

Gomez-Escribano, J.P., Holmes, N.A., Schlimpert, S., Bibb, M.J., Chandra, G., Wilkinson, B., Buttner, M.J., and Bibb, M.J. (2021). *Streptomyces venezuelae* NRRL B-65442: genome sequence of a model strain used to study morphological differentiation in filamentous actinobacteria. J Ind Microbiol and Biotechnol.

Grantcharova, N., Lustig, U., and Flardh, K. (2005). Dynamics of FtsZ assembly during sporulation in *Streptomyces coelicolor* A3(2). J Bacteriol *187*, 3227-3237.

Gregory, M.A., Till, R., and Smith, M.C. (2003). Integration site for *Streptomyces* phage phiBT1 and development of site-specific integrating vectors. J Bacteriol *185*, 5320-5323.

Gust, B., Challis, G.L., Fowler, K., Kieser, T., and Chater, K.F. (2003a). PCR-targeted *Streptomyces* gene replacement identifies a protein domain needed for biosynthesis of the sesquiterpene soil odor geosmin. Proc Natl Acad Sci USA *100*, 1541-1546.

Gust, B., Chandra, G., Jakimowicz, D., Yuqing, T., Bruton, C.J., and Chater, K.F. (2004). Lambda red-mediated genetic manipulation of antibiotic-producing *Streptomyces*. Adv Appl Microbiol *54*, 107-128.

Gust, B., O'Rourke, S., Bird, N., Kieser, T., and Chater, K. (2003b). Recombineering in *Streptomyces coelicolor*. Norwich: The John Innes Foundation.

Hasipek, M. (2016). Characterization of *Streptomyces coelicolor* ParH in development-associated chromosome segregation. In Biological Science (Duquesne University, Pittsburgh, PA, USA).

Heichlinger, A., Ammelburg, M., Kleinschnitz, E.M., Latus, A., Maldener, I., Flardh, K., Wohlleben, W., and Muth, G. (2011). The MreB-like protein Mbl of *Streptomyces coelicolor* A3(2) depends on MreB for proper localization and contributes to spore wall synthesis. J Bacteriol *193*, 1533-1542.

Hempel, A.M., Wang, S.B., Letek, M., Gil, J.A., and Flardh, K. (2008). Assemblies of DivIVA mark sites for hyphal branching and can establish new zones of cell wall growth in *Streptomyces coelicolor*. J Bacteriol *190*, 7579-7583.

Hindle, Z., and Smith, C.P. (1994). Substrate induction and catabolite repression of the *Streptomyces coelicoior* glycerol operon are mediated through the GyIR protein. Mol Microbiol *12*, 737-745.

Holmes, N.A., Walshaw, J., Leggett, R.M., Thibessard, A., Dalton, K.A., Gillespie, M.D., Hemmings, A.M., Gust, B., and Kelemen, G.H. (2013). Coiled-coil protein Scy is a key component of a multiprotein assembly controlling polarized growth in *Streptomyces*. Proc Natl Acad Sci USA *110*, E397-406.

Hong, H.J., Hutchings, M.I., Hill, L.M., and Buttner, M.J. (2005). The role of the novel Fem protein VanK in vancomycin resistance in *Streptomyces coelicolor*. J Biol Chem *280*, 13055-13061.

Hopwood, D.A. (1985). Genetic manipulation of Streptomyces. a laboratory manual.

Jakimowicz, D., Gust, B., Zakrzewska-Czerwinska, J., and Chater, K.F. (2005). Developmental-stage-specific assembly of ParB complexes in *Streptomyces coelicolor* hyphae. J Bacteriol *187*, 3572-3580.

Jeong, Y., Kim, J.N., Kim, M.W., Bucca, G., Cho, S., Yoon, Y.J., Kim, B.G., Roe, J.H., Kim, S.C., Smith, C.P.*, et al.* (2016). The dynamic transcriptional and translational landscape of the model antibiotic producer *Streptomyces coelicolor* A3(2). Nat Commun *7*, 11605.

Jones, S.E., Ho, L., Rees, C.A., Hill, J.E., Nodwell, J.R., and Elliot, M.A. (2017). *Streptomyces* exploration is triggered by fungal interactions and volatile signals. Elife *6*.

Karimova, G., Pidoux, J., Ullmann, A., and Ladant, D. (1998). A bacterial two-hybrid system based on a reconstituted signal transduction pathway. Proc Natl Acad Sci USA *95*, 5752-5756.

Keenan, T., Dowle, A., Bates, R., and Smith, M.C.M. (2019). Characterization of the *Streptomyces coelicolor* Glycoproteome Reveals Glycoproteins Important for Cell Wall Biogenesis. mBio *10*.

Kieser, T., Bibb, M.J., Buttner, M.J., Chater, K.F., and Hopwood, D.A. (2000). Practical *Streptomyces* genetics, Vol 291 (John Innes Foundation Norwich).

Kleinschnitz, E.M., Heichlinger, A., Schirner, K., Winkler, J., Latus, A., Maldener, I., Wohlleben, W., and Muth, G. (2011). Proteins encoded by the mre gene cluster in *Streptomyces coelicolor* A3(2) cooperate in spore wall synthesis. Mol Microbiol *79*, 1367-1379.

Kol, S., Merlo, M.E., Scheltema, R.A., de Vries, M., Vonk, R.J., Kikkert, N.A., Dijkhuizen, L., Breitling, R., and Takano, E. (2010). Metabolomic characterization of the salt stress response in *Streptomyces coelicolor*. Appl Environ Microbiol

76, 2574-2581.

Krogh, A., Larsson, B., von Heijne, G., and Sonnhammer, E.L. (2001). Predicting transmembrane protein topology with a hidden Markov model: application to complete genomes. J Mol Biol 3*05,* 567-580.

Kumar, S., Stecher, G., Li, M., Knyaz, C., and Tamura, K. (2018). MEGA X: Molecular Evolutionary Genetics Analysis across Computing Platforms. Mol Biol Evol 3*5,* 1547-1549.

Lee, E.J., Karoonuthaisiri, N., Kim, H.S., Park, J.H., Cha, C.J., Kao, C.M., and Roe, J.H. (2005). A master regulator σB governs osmotic and oxidative response as well as differentiation via a network of sigma factors in St*reptomyces coelicolor.* Mol Microbiol 5*7,* 1252-1264.

MacNeil, D.J., Occi, J.L., Gewain, K.M., MacNeil, T., Gibbons, P.H., Ruby, C.L., and Danis, S.J. (1992). Complex organization of the St*reptomyces avermitilis g*enes encoding the avermectin polyketide synthase. Gene 1*15,* 119-125.

Mazza, P., Noens, E.E., Schirner, K., Grantcharova, N., Mommaas, A.M., Koerten, H.K., Muth, G., Flardh, K., van Wezel, G.P., and Wohlleben, W. (2006). MreB of St*reptomyces coelicolor is* not essential for vegetative growth but is required for the integrity of aerial hyphae and spores. Mol Microbiol 6*0,* 838-852.

McCormick, J.R. (2009). Cell division is dispensable but not irrelevant in St*reptomyces.* Curr Opin Microbiol 1*2,* 689-698.

McCormick, J.R., and Flärdh, K. (2012). Signals and regulators that govern St*reptomyces de*velopment. FEMS Microbiol Rev 3*6,* 206-231.

McCormick, J.R., Su, E.P., Driks, A., and Losick, R. (1994). Growth and viability of St*reptomyces coelicolor m*utant for the cell division gene ft*sZ.* Mol Microbiol 1*4,* 243-254.

Molle, V., Palframan, W.J., Findlay, K.C., and Buttner, M.J. (2000). WhiD and WhiB, homologous proteins required for different stages of sporulation in St*reptomyces coelicolor A3*(2). J Bacteriol 1*82,* 1286-1295.

Munita, J.M., and Arias, C.A. (2016). Mechanisms of Antibiotic Resistance. Microbiol Spectr 4.

Paget, M.S., Chamberlin, L., Atrih, A., Foster, S.J., and Buttner, M.J. (1999). Evidence that the extracytoplasmic function sigma factor ςE is required for normal cell wall structure in St*reptomyces coelicolor A*3 (2). J Bacteriol 1*81,* 204-211.

Ramos-León, F., Bush, M.J., Sallmen, J.W., Chandra, G., Richardson, J., Findlay, K.C., McCormick, J.R., and Schlimpert, S. (2021). A conserved cell division protein directly regulates FtsZ dynamics in filamentous and unicellular actinobacteria. Elife 1*0,* e63387.

Sallmen II, J.W. (2019). Genetic and Biochemical Analysis of a Conserved, Multi-Gene System Regulating Spore-Associated Proteins in St*reptomyces coelicolor.* (Duquesne University).

Sambrook, J., Fritsch, E.F., and Maniatis, T. (1989). Molecular cloning: a laboratory manual (Cold spring harbor laboratory press).

Sarkar, P., Yarlagadda, V., Ghosh, C., and Haldar, J. (2017). A review on cell wall synthesis inhibitors with an emphasis on glycopeptide antibiotics. Medchemcomm 8*,* 516-533.

Schlimpert, S., Flardh, K., and Buttner, M. (2016). Fluorescence time-lapse imaging of the complete S. *venezuelae l*ife cycle using a microfluidic device. J Vis Exp 1*08,* 53863.

Schlimpert, S., Wasserstrom, S., Chandra, G., Bibb, M.J., Findlay, K.C., Flardh, K., and Buttner, M.J. (2017). Two dynamin-like proteins stabilize FtsZ rings during St*reptomyces s*porulation. Proc Natl Acad Sci USA 1*14,* E6176-E6183.

Schwedock, J., McCormick, J.R., Angert, E.R., Nodwell, J.R., and Losick, R. (1997). Assembly of the cell division protein FtsZ into ladder-like structures in the aerial hyphae of St*reptomyces coelicolor.* Mol Microbiol 2*5,* 847-858.

Sigle, S., Ladwig, N., Wohlleben, W., and Muth, G. (2015). Synthesis of the spore envelope in the developmental life cycle of St*reptomyces coelicolor.* Int. J. of Med. Microbiol. 3*05,* 183-189.

Stecher, G., Tamura, K., and Kumar, S. (2020). Molecular Evolutionary Genetics Analysis (MEGA) for macOS. Mol Biol Evol 3*7,* 1237-1239.

Stuttard, C. (1982). Temperate phages of St*reptomyces venezuelae:* lysogeny and host specificity shown by phages SV1 and SV2. Microbiology 1*28,* 115-121.

Vollmer, B., Steblau, N., Ladwig, N., Mayer, C., Macek, B., Mitousis, L., Sigle, S., Walter, A., Wohlleben, W., and Muth, G. (2019). Role of the Streptomyces spore wall synthesizing complex SSSC in differentiation of St*reptomyces coelicolor A3*(2). Int J Med Microbiol 3*09,* 151327.

Vollmer, W., Blanot, D., and de Pedro, M.A. (2008a). Peptidoglycan structure and architecture. FEMS Microbiol Rev 3*2,* 149-167.

Vollmer, W., Joris, B., Charlier, P., and Foster, S. (2008b). Bacterial peptidoglycan (murein) hydrolases. FEMS Microbiol Rev 3*2,* 259-286.

Woldemeskel, S.A., and Goley, E.D. (2017). Shapeshifting to Survive: Shape Determination and Regulation in Ca*ulobacter crescentus.* Trends Microbiol 2*5,* 673-687.

Yanisch-Perron, C., Vieira, J., and Messing, J. (1985). Improved M13 phage cloning vectors and host strains: nucleotide sequences of the M13mpl8 and pUC19 vectors. Gene 3*3,* 103-119.

Young, K.D. (2010). Bacterial shape: two-dimensional questions and possibilities. Annu Rev Microbiol 6*4,* 223-240.

Zhang, L., Willemse, J., Claessen, D., and van Wezel, G.P. (2016). SepG coordinates sporulation-specific cell division and nucleoid organization in St*reptomyces coelicolor.* Open Biol 6*,* 150164.

CHAPTER 3: CHARACTERIZATION OF *WHID* REQUIREMENT FOR SPORULATION AND SPORE MATURATION IN *STREPTOMYCES VENEZUELAE*

INTRODUCTION

Streptomyces are sporulating, filamentous soil bacteria particularly important for the soil environment, biotechnology and the medical field. They possess a complex developmental life cycle with the alternation of vegetative mycelium, aerial mycelium, and spores. There are two classes of developmental regulators that govern the life cycle: Bld (Bald) and Whi (White), which are required for the formation of fluffy aerial mycelium and pigmented mature spores, respectively. The earliest genetic screening in *S. coelicolor* identified eight separate *whi l*oci: *whiA*, *whiB*, *whiD*, *whiE*, *whiG*, *whiH*, *whiI*, and *whiJ*, and further microscopic analysis revealed that the aerial hyphae structure of the mutants was mainly divided into six types, ranging from the complete absence of any stage of sporulation to the presence of normal spores (Chater, 1972). Of these, WhiB and WhiD are two important members of the WhiB-like (Wbl) family, which are specifically present in *Actinomycetes*, such as *Streptomyces*, *Mycobacterium*, and *Corynebacterium* (Davis and Chater, 1992). Wbl proteins are unusually small (81-139 residues) and carry four conserved cysteines that form an oxygen- and nitric oxide-sensitive [4Fe-4S] iron-sulfur cluster (Jakimowicz et al., 2005; Singh et al., 2007; Smith et al., 2010; Stewart et al., 2020). *Actinobacteria* typically contain multiple Wbl paralogues with diverse functions, such as regulation of virulence, antibiotic resistance, and cell division (Bush, 2018).

The *S. coelicolor* encodes 14 Wbl proteins with 11 encoded on the chromosome and 3 encoded on the large, linear plasmid SCP1 (Bush, 2018). Three proteins WhiB, WhiD, and WblA have been shown to have an effect on development (Davis and Chater, 1992; Fowler-

Goldsworthy et al., 2011; Molle et al., 2000). WblA is involved in the early stage of aerial hyphae formation. Deletion of *S. coelicolor wblA* results in a developmental defect, with some aerial hyphae appearing thinner than wild-type and failing to sporulate (Fowler-Goldsworthy et al., 2011). Although the direct binding targets of WblA have not yet been identified, microarray analysis indicated that WblA regulates a set of genes involved in antibiotic production, morphological differentiation and oxidative stress (Kang et al., 2007; Kim et al., 2012; Yu et al., 2014). WhiB initiates with sporulation septation and thus a *whiB* mutant produces long, tightly coiled aerial hyphae without visible speta, which resembles the phenotype of *whiA* mutants. The identical phenotype arises due to the fact that WhiB and WhiA are transcription factors that function cooperatively to co-regulate a large regulon of sporulation-related genes (Bush et al., 2016).

In contrast with the non-sporulating phenotype for a *whiB* mutant, *whiD* mutants of *S. coelicolor* showed reduced levels of sporulation and those spores that are formed are heat sensitive, lyse extensively, and are highly irregular in size, arising in part from irregularity in sporulation septum placement, or perhaps from spore swelling and lysis (Molle et al., 2000). In addition to spore size heterogeneity, these variable-sized spores are frequently further partitioned into irregular, smaller units through the deposition of additional septa, which are often laid down in several planes very close to the spore poles. These mini-compartments appeared to be devoid of chromosomal DNA. Another striking feature is that the *whiD* null mutants also show extremely variable deposition of spore wall; most spores are thin-walled (20- to 30- nm), but some spores are observed with irregularly thickened cell wall (up to 170 nm) at the junctions between spores (Molle et al., 2000). All of the phenotypes suggest that WhiD is involved in sporulation septation and maturation during the life cycle, however the underlying molecular

mechanism about how WhiD functions remains unclear. Recent study revealed that *S. venezuelae* WhiD exists in a monomer-dimer equilibrium with a C-terminal extension being crucial for protein dimerization (Stewart et al., 2020). *In vitro*, *S. venezuelae* WhiD forms a tight, specific complex with domain 4 of the *Streptomyces* principal sigma factor HrdB, and this interaction greatly reduces the sensitivity of 4Fe-4S cluster to reaction with O_2 and NO (Stewart et al., 2020). However, how WhiD functions in *S. venezuelae* has not been reported yet. In this chapter, I report the isolation of a *whiD* mutant for *S. venezuelae*, and demonstrate that the *whiD* mutant has a white colony phenotype and produces heterogeneous spore sizes and shapes. The results also show that the *whiD* mutant is drastically sensitive to heat stress and slightly sensitive to salt stress.

MATERIALS AND METHODS

Bacterial strains, media, and growth conditions

E. coli strains used in this study are listed in Table 3.1. The *E. coli* strain TG1 was used for basic cloning and maintenance of plasmid, and was grown at 37°C using LB (Lennox) medium, which contains 0.5 % NaCl and 0.1% glucose (Sambrook et al., 1989). LB was supplemented with antibiotics, when appropriate, at the following final concentrations: ampicillin (100 μg/ml), carbenicillin (100 μg/ml), kanamycin (50 μg/ml), apramycin (50 μg/ml), chloramphenicol (25 μg/ml), or hygromycin (50 μg/ml). When hygromycin was used, LB medium without salt (NaCl) was used as the growth medium for selection. When growing *E. coli* strains for competent cell production, SOB medium (Stuttard, 1982) were used as the growth medium.

Streptomyces strains used in this study are listed in Table 3.2. *S. venezuelae* strains were grown at 30°C using MYM (maltose-yeast extract-malt extract) (Kieser et al., 2000) liquid and solid media made with 50% deionized water and 50% tap water and supplemented at 1:500 with R2 trace element solution (Kieser et al., 2000). When appropriate, the final concentrations of the following antibiotics were added: apramycin (50 μg/ml), nalidixic acid (20 μg/ml), or hygromycin (50 μg/ml).

Plasmids and general DNA techniques

Cosmids and plasmids used in this study are listed in Table 3.3. Plasmid DNA was extracted using the ZR Plasmid Miniprep Kit (Zymo, D4016). Cosmid DNA was extracted by phenol/chloroform extraction and ethanol precipitation (Sambrook et. al, 1989). A salting out procedure was used to isolate genomic DNA from *Streptomyces* (Gust et al., 2003b). Extracted DNA samples were resuspended in sterile TE or nanopure water supplemented with RNaseA.

DNA restriction enzymes (New England Biolabs), *Taq* and Phusion Polymerase (New England Biolabs) were used following the manufacturers' instructions.

Isolation of a *whiD*-null mutant for *S. venezuelae*

A *whiD*-null was isolated using a recombineering (recombination-mediated genetic engineering) method to replace the entire *whiD* gene with an apramycin-resistance gene *aac*(*3)IV* (Gust et al., 2003a; Gust et al., 2003b). Specifically, oligonucleotides 53 and 54 were used to amplify and add *whiD* homology to the *aac(3)IV* cassette isolated from *Eco*RI/*Hin*dIII-digested plasmid pIJ773. The generated PCR product was electroporated into the *E. coli* strain BW25113/pIJ790 containing cosmid Sv-6-G03 to create cosmid pNS31. pNS31 was then introduced into the chromosome of *S. venezuelae* strain via homologous recombination after conjugation. The candidates that were apramycin-resistant and kanamycin-sensitive were selected and verified by PCR using primers 55 and 56. The successfully verified strain was named NS10 (Δ*whiD*::*aac(3)IV*).

Construction of a complementation strain for *whiD*-null mutant

A complementation strain was constructed by integrating a vector *in trans* at the ΦBT1 attachment site that contains the *whiD* coding region and its promoter region. Specifically, oligonucleotides 55 and 56 were used to amplify *whiD* together with its promoter region using Phusion high fidelity polymerase. The amplified fragment was ligated into pCR2.1-TOPO vector (Invitrogen) according to manufacturer's instructions to create pNS39. pNS39 was digested with *Eco*RV and *Spe*I, and the generated fragment was inserted into the *Eco*RV/*Spe*I-digested pMS82 to create pNS54. pNS54 was introduced into the chromosome of *whiD* mutant strain of *S. venezuelae* by integration at the ΦBT1 attachment site to produce NS17 (*ΔwhiD*::*aac(3)IV*

attB$_{\Phi BT1}$::*P*$_{whiD}$-*whiD*). As a control, pMS82 was introduced into the chromosome of *whiD* mutant strain of *S. venezuelae* by integration at the ΦBT1 attachment site to produce NS16.

Phase-contrast microscopy

For imaging of spore chains, a coverslip was placed on the surface of colonies. The coverslip impression was then lifted and mounted using 20% glycerol. Samples were analyzed using a Nikon phase-contrast microscope (Eclipse E400) with 100x Oil objective (NA=1.25), and images were captured using a MicroPublisher 5.0 digital camera (QImaging) and the associated QCapture software. Micrographs were processed using ImageJ software (Stecher et al., 2020).

Spore size measurement

Spore chains were imaged using the phase-contrast microscopy. The spore sizes were measured in chains automatically using the measurement tool of the Nikon NIS-Elements software BR (Version 5.02.00). Generally, a binary layer was created to highlight spore chains by setting the threshold. Automatic separation was applied in the spore chains to separate the spores. The size of the separated spores was generated automatically. For those spores that were not well separated using the automatic separation tool, manual separation tool was used to separate the spores prior to measurement.

Spore stress assays

For a heat stress assay, spores were harvested after 4 day growth on MYM agar. The generated spore suspension was passed through a sterile cotton to remove mycelia and other debris. Diluted spores in nano-pure water were treated at 55°C for designated times and plated on LB. After 1-day incubation at 30°C, the colony-forming units (CFU) were counted and spore

viability was calculated by using the equation of CFU with treatment divided by CFU without treatment.

For a salt stress assay, a 10-fold serial of dilution of spores was spotted on LB agar containing different concentrations of NaCl. Photographs were taken after 1 day and 3 days of incubation at 30°C.

RESULTS

Transcription of *S. venezuelae whiD* is developmentally regulated

Triphosphate-end capture RNA-sequencing result was obtained from StrepDB, and result showed that transcription of *whiD* in *S. venezuelae* initiates at a pre-sporulation stage and culminates at mid/late sporulation stage; and it was not detected during vegetative growth (Fig. 3.1A), consistent that *whiD* is developmentally regulated and plays a potential role in sporulation and spore maturation. The triphosphate-end capture identified two transcription start sites (TSS) with closely spaced two promoters *whiDp1* and *whiDp2*, both of which were first detected at presporulation stage (14 hours) (Fig. 3.1B). The nucleotide sequence of identified *whiD* promoter region for *S. venezuelae* is similar with the one identified for *S. coelicolor* using an S1 nuclease mapping method (Molle et al., 2000), indicating a conserved regulatory mechanism for *whiD* expression.

Δ*whiD* mutant forms heterogeneous spores in *S. venezuelae*

In order to investigate the role of WhiD in *S. venezuelae* development, a *whiD* null mutant (Δ*whiD*::*acc(3)IV*) was generated by replacing the entire coding region of *whiD* with an apramycin-resistance cassette using a PCR-targeting recombineering method (Fig. 3.2A). Consistent with the phenotype in *S. coelicolor* (Chater, 1972), the aerial mycelium of colonies for *S. venezuelae* Δ*whiD* mutant also appeared white (Fig. 3.2B), indicating a defect in synthesis of the polyketide spore pigment. To confirm the observed phenotype was due to the absence of *whiD*, a genetic complementation strain (Δ*whiD*/*whiD*$^{+}$) was constructed by integration of pNS54 at the ΦBT1 *attB* locus of the chromosome that pNS54 contains *whiD* as the only open reading frame and its promoter region (Fig. 3.2A). As shown in Fig. 3.2B, the pigment on the

colony surface of Δ*whiD* mutant was restored, although the color seems lighter than for the WT. It is not clear why the spore pigment was not fully restored in the complemented strain.

In order to examine the microscopic phenotype, coverslip impression slides of spores produced from an MYM solid medium were observed using a phase-contrast microscopy. The length of mature spores of the Δ*whiD* mutant was more heterogeneous, ranging from the normally sized ones to long filaments without obvious constriction at regular intervals, normally associated with spore formation (Fig. 2.7A and B). Statistical analysis of spore length revealed a significant difference for spores produced by the Δ*whiD* mutant than in WT, with mean length 1.24 ± 0.54 μm for WT and 1.59 ± 0.94 μm for the Δ*whiD* mutant. The genetic complementation strain (*whiD*/*whiD*$^{+}$) rescued the spore length size to the WT level, at 1.33 ± 0.21 μm, indicating that the defective spore length of Δ*whiD* was caused by deletion of *whiD*. In addition to the spore length defect in the Δ*whiD* mutant, the spore shape was also affected. As shown by arrows in Fig. 3.3A, the spores were more inclined to be more box-shaped compared to WT. The more drastic spore shape defect for Δ*whiD* mutant than for Δ*ssdA* mutant suggests that *ssdA* might be a target regulated by WhiD. Collectively, deletion of *whiD* resulted in a macroscopically white phenotype and microscopically heterogeneous spores, suggesting a sporulation defect for the Δ*whiD* mutant.

***S. venezuelae* Δ*whiD* mutant is sensitive to heat stress**

Previous studies have demonstrated that *whiD* mutant of *S. coelicolor* fails to develop the thick spore wall characteristic of the wild-type spores, and deletion of *whiD* in *S. coelicolor* results in a dramatic sensitivity to heat stress (McVittie, 1974; Molle et al., 2000). To investigate if *S. venezuelae* Δ*whiD* mutant has a similar phenotype, diluted spores of WT and Δ*whiD* mutant were incubated in water at 55°C for different times. The result showed that after a heat treatment

for just 2 minutes (mins), the viability of Δ*whiD* had dropped to around 30% of WT, and spores barely survived after 4 mins of incubation at the elevated temperature, indicating an impaired cell envelope in the Δ*whiD* mutant (Fig. 3.4). The dramatic heat sensitivity in the absence of *whiD* was rescued when reintroducing *whiD* into chromosome *in trans*. The heat sensitivity profile of Δ*whiD* is quite different from what was observed for the Δ*ssdA* mutant, where very mild sensitivity was observed even after incubating for 20 mins and 40 mins (Fig. 2.8B), suggesting that *ssdA* is not the only target of WhiD that affect spore cell wall.

***S. venezuelae* Δ*whiD* mutant is slightly sensitive to salt stress**

The sensitivity of Δ*whiD* mutant to salt was also tested by supplementing LB medium with different concentrations of NaCl, following the same protocol as was conducted for analysis of Δ*ssdA* mutant. The results showed that a Δ*whiD* mutant exhibited the similar growth robustness as WT on LB with 3% NaCl (Fig. 3.5). When increasing the salt concentration to 6%, Δ*whiD* mutant has a sight sensitivity when compared to WT, which was restored to WT level in the complemented strain. By contrast, the sensitivity of Δ*ssdA* mutant is much more dramatic with reduced growth at 1% concentration and no growth at 3% concentration (Fig. 2.8B). The different sensitivities to salt between Δ*whiD* mutant and Δ*ssdA* mutant suggested that *ssdA* may be not under the control of WhiD.

DISCUSSION

Over the past decades, some progresses have been made in deciphering how Bld and Whi proteins regulate the morphological and physiological differentiation in *Streptomyces*. However, our understanding of how WhiD regulates development is not very well known**.** In this study, I isolated a Δ*whiD* mutant in *S. venezuelae*, and result showed a white colony surface in the Δ*whiD* mutant, consistent with previously reported phenotype for *S. coelicolor* Δ*whiD* mutant (Chater, 1972). Furthermore, deletion of *whiD* resulted in spores with highly irregular and larger spore sizes, indicating a sporulation defect for the Δ*whiD* mutant (Fig. 3.3). Frequent mini-spore compartments or lysed spores were not observed from the phase-contrast micrographs. This is different from what was reported for *S. coelicolor* Δ*whiD* mutant, where spores were lysed extensively and additional septa were often laid down in several planes, as shown by TEM microscopy, leading to the mini-compartmental ghost spores (Molle et al., 2000). The reasons that the mutant phenotype difference in two different *Streptomyces* species are not clear yet. It is noteworthy to mention that *S. venezuelae* WhiD has a C-terminal extension of 18 amino acids that is missing in *S. coelicolor* WhiD, although it is present in a range of other WhiD homologues (Stewart et al., 2020). This C-terminal extension has served as the place of WhiD self-interaction, contributing to a WhiD monomer-dimer equilibrium state. It is not clear why the C-terminal extension exists in some WhiD while absent in others, and how the dimerization affects its function needs further investigation. High-resolution SEM and TEM could be used to observe the detailed spore morphology of Δ*whiD* mutant for *S. venezuela*e. To better visualize the sporulation septa of Δ*whiD* mutant, wheat germ agglutinin could be used to stain the cell wall of the sporulation septa and imaged by fluorescence microscopy. In addition, FtsZ localization

might be observed in the Δ*whiD* mutant background to determine if there is disruption of FtsZ localization, which is required for normal spore length.

Similar to a *S. coelicolor* Δ*whiD* mutant, the *S. venezuelae* Δ*whiD* mutant is extremely sensitive to heat stress (Fig. 3.4), possibly arising from the abnormal spores produced by deletion of *whiD*. In addition, Δ*whiD* has a mild sensitivity to salt stress. These results indicated an impaired spore envelope in the absence of *whiD* in *S. venezuelae*. The phenotypes of sensitivity to heat and salt stresses for Δ*whiD* are quite different from a *S. venezuelae* Δ*ssdA* mutant, suggesting that *ssdA* and *whiD* affect the cell wall structure/composition in a different way. To characterize the cell wall defect, the spore sacculus of the Δ*whiD* mutant could be isolated and analyzed by HPLC-MS to determine potential perturbations of cell wall structure.

Two transcription start points (TSS) for *S. venezuelae whiD* were determined by Dr. Mark Buttner's laboratory in John Innes Centre using a triphosphate end capture RNA-seq method (Fig. 3.1), and the two TSSs are consistent with those identified for *S. coelicolor whiD* using a high-resolution S1 mapping, indicating a similar regulatory mechanism on *whiD* expression in these two different *Streptomyces* species. Genome-wide ChIP-seq results in *S. venezuelae* showed that *whiD* is not the target of WhiAB regulators (Bush et al., 2013; Bush et al., 2016). ChIP-chip analysis in *S. coelicolor* showed that BldD bonded at the intergenic region between *whiD* and the divergently transcribed gene *bldM*, but the binding site is within *bldM* promoter region rather than *whiD* (den Hengst et al., 2010), indicating that *whiD* is not the direct target of BldD as well. The identified promoters of *whiD* were both developmentally regulated and were first detected at pre-sporulation stage with similar transcription levels. The transcription level was then increased at later stages. It is not known how the two promoters coordinate and contribute to the control of development.

The Wbl protein WhiB functions as a transcription factor by directly interacting with an unrelated DNA-binding protein WhiA in *Streptomyces* and *Corynebacteria* (Bush et al., 2016; Lee et al., 2018). It is reasonable to hypothesize that all Wbl proteins, including WhiD, might function by interacting with a helix-turn-helix motif-containing protein. A screening of a bacterial two-hybrid library might be necessary to find out WhiD-interacting partners containing a DNA-binding motif. A genome-wide chromatin immunoprecipitation sequencing analysis (ChIP–seq) could be carried out in parallel to identify the WhiD regulon. Recently it has been reported that *S. venezuelae* WhiD forms a tight heterodimer with the house-keeping sigma factor HrdB *in vitro* (Stewart et al., 2020), and the interactions between Wbl proteins and the principal sigma factor have been widely reported in *Mycobacterium tuberculosis* (Burian et al., 2013; Wan et al., 2021). It is not known if additional DNA-binding protein is required for *Streptomyces* developmental control, and how WhiD works in concert with sigma factor HrdB *in vivo* needs further investigation.

Table 3.1 *E. coli* strains used in this study

Strain	Genotype	Reference/Source
TG1	*supE thi-1* Δ(*lac-proAB*) Δ(*mcrB-hsdSM*)*5* ($r_K^- m_K^-$)/ F′ *traD36 proAB lacI*^{q}*ZΔM15*	(Sambrook et al., 1989)
TOP10	F$^-$ *mcrA* Δ(*mrr-hsdRMS-mcrBC*) Φ*80lacZΔM15ΔlacX74 deoR recA1 araD139* Δ(*araA-leu*)*697 galU galK*	Invitrogen
BW25113	F$^-$Δ(*araD-araB*)*567* Δ*lacZ4787* (::*rrnB-3*) λ$^-$ *rph-1* Δ(*rhaD-rhaB*)*568 hsdR514*	(Datsenko and Wanner, 2000)
ET12567	F$^-$ *dam-13*::Tn*9 dcm-6 hsdM hsdR recF143 zjj-201*::Tn*10 galK2 galT22 ara-14 lacY1 xyl-5 leuB6 thi-1 tonA31 rpsL136 hisG4 tsx-78 mtl-1 glnV44*	(MacNeil et al., 1992)

Table 3.2 *Streptomyces* strains used in this study

Strain	Genotype	Reference/Source
WT	*S. venezuelae* NRRL B-65442	Gomez-Escribano et al. (2021)
NS10	Δ*whiD*::*aac(3)IV*	This study
NS16	Δ*whiD*::*aac(3)IV attB*$_{\Phi BT1}$::pMS82.	This study
NS17	Δ*whiD*::*aac(3)IV attB*$_{\Phi BT1}$::pNS54 (*P*$_{whiD}$-*whiD*).	This study

Table 3.3 Cosmids and plasmids used in this study

Cosmid/Plasmid	Description	Reference/Source
pIJ773	Source of the *aac(3)IV-oriT* cassette used for PCR-targeting based mutagenesis	Gust et al. (2003a)
pIJ790	Modified λ RED recombination plasmid	Gust et al. (2003a)
pUZ8002	Non-transmissible *oriT* helper plasmid for mobilization of *oriT*-containing cosmids and plasmids	Paget et al. (1999)
pMS82	Plasmid cloning vector for integration at the *Streptomyces* ΦBT1 attachment site	Gregory et al. (2003)
pCR2.1-TOPO	TOPO TA cloning vector	Invitrogen
Sv-6-G03	Cosmid that contains *S. venezuelae whiD*	John Innes Centre
pNS31	Sv-6-G03 Δ*whiD*::*aac(3)IV*	This study
pNS39	P_{whiD}-*whiD* fragment amplified with oligos 55 and 56, and cloned into pCR2.1-TOPO	This study
pNS54	P_{whiD}-*whiD* was liberated from pNS39 by digestion with *Eco*RV and *Spe*I, and ligated into *Eco*RV/*Spe*I-digested pMS82	This study

Table 3.4 Oligonucleotide used in this study

No.	Oligonucleotide	Sequence	Application
53	Sv_whiD_KO_ F	CCTATCCGTTCGACACGGTTTCAAGGGGACAAGCGCAATGATTCCGGGGATCCGTCGACC	Construction of *whiD* deletion by a PCR-targeting strategy
54	Sv_whiD_KO_ R	CTCGCCTATCTCCGGAAGTGTCTGAGGAAACGTTCCTTCATGTAGGCTGGAGCTGCTTC	
55	Sv_whiD_KO_ check_F	GTCGTTCATCGAAAGCTATGCCC	(1). Verification of *whiD* deletion (2). Amplification of *whiD* promoter and coding region
56	Sv_whiD_KO_c heck_R	GAGATCGTGGCCCTGACGCTG	

A

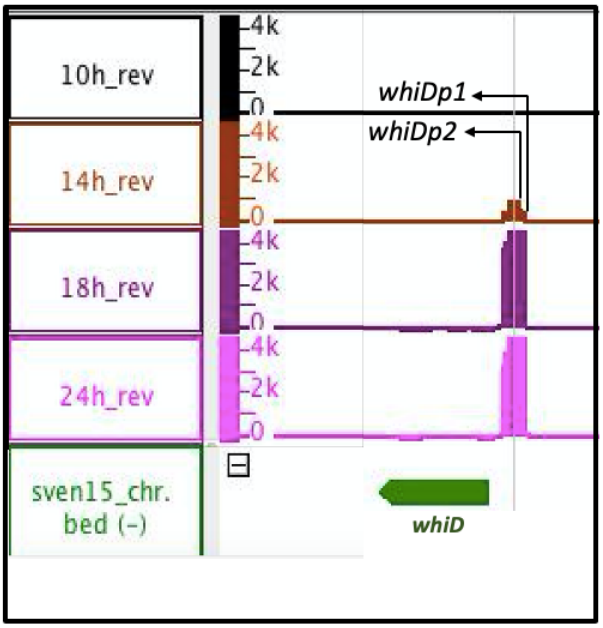

B

GTCGTTCATCGAAAGCTATGCCCCATTTAGCGGGTTTTCTTCCCTTTTCGCGGTGTCTGTG

whiDp1 whiDp2

GCTAGATTCGCAATGAGTCATATTTACATCTACTTAGACAGTAGGTGTACCGACCCGGAC

CGGCGGGGCCCCGAGGAGCCCGGCCATCAGCCATCCACCCGCCCACCTATCCGTTCGACAC

GGTTTC**AAGGGG**ACAAGCGCAATGGCAGATTTCTCCCGCCTTCCCGGACCCA

SD sequence

Figure 3.1 *whiD* has two transcription start sites. (A) The profile for *whiD* transcription start site (TSS) generated from strand-specific triphosphate-end capture RNA-seq data. Two closely-spaced TSSs are indicated. The data *was* deposited on StrepDB by Dr. Mark Buttner's laboratory at John Innes Centre (http://streptomyces.org.uk/vnz_tss.html) and was analyzed using Integrated Genome browser. The time points represent the transition throughout development in liquid culture: Vegetative (10h), pre-sporulation (14h), onset of sporulation (18h) and mid/late sporulation (24h). The scale indicates the number of reads abundance of transcription end detected. (B) Nucleotide sequence of the *whiD* promoter region. Two TSSs are shadowed in yellow and named *whiDp1* and *whiDp2*. The putative Shine-Dalgarno (SD) *sequence* is bolded, and the 5' end of the whiD coding sequence is in blue. The two TSSs and RBS of *whiD* in *S. venezuelae* are similar to that of for *S. coelicolor* (Molle et al., 2000*)*.

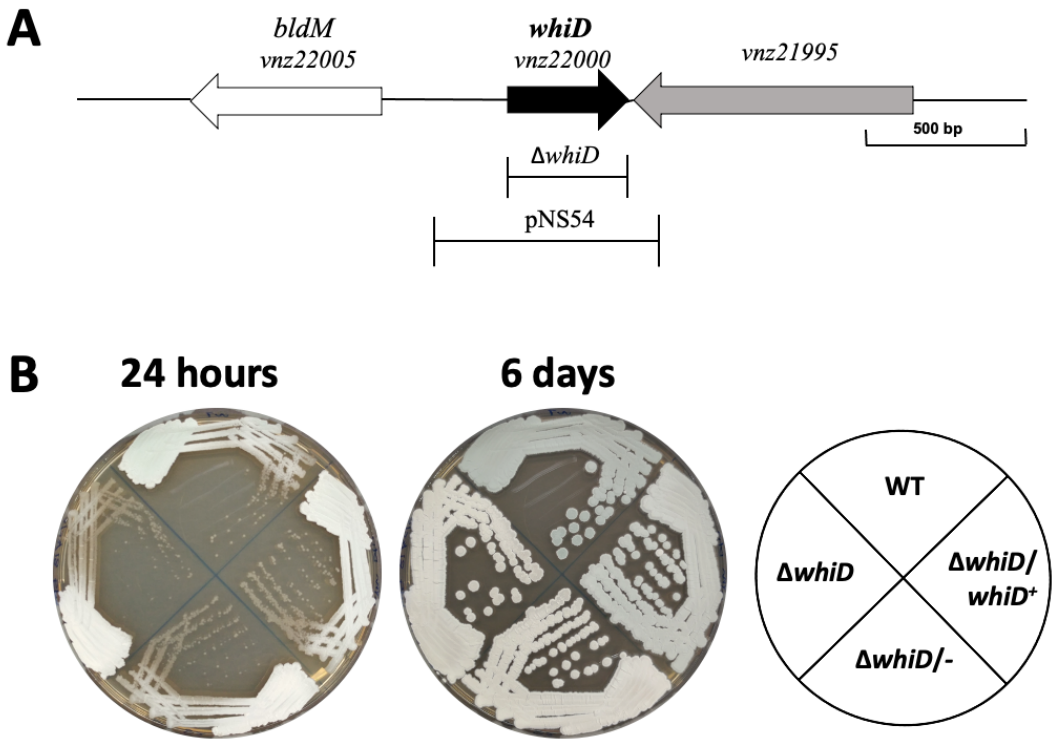

Figure 3.2 Deletion of *whiD* results in a white colony phenotype. (A) A physical map of the *S. venezuelae* chromosome that contains *whiD* and its adjacent genes. The *whiD* null mutation marked by an apramycin resistance gene is shown as Δ*whiD*. pNS54 is a site-specific integration plasmid that contains the entire *whiD* and its promoter region and was used for constructing a genetic complementation strain. (B) Strains were grown on MYM solid medium at 30°C, and photographed at indicated time points. Strains include wild-type *S. venezuelae* (WT), the *ΔwhiD* mutant (NS10), the complemented strain Δ*whiD*/*whiD*$^{+}$ (NS17). NS17 was made by integrating pNS54 *in trans* at the ΦBT1attachment site, and the mutant strain containing the integration vector alone, Δ*whiD*/- (NS16), was used as a negative control.

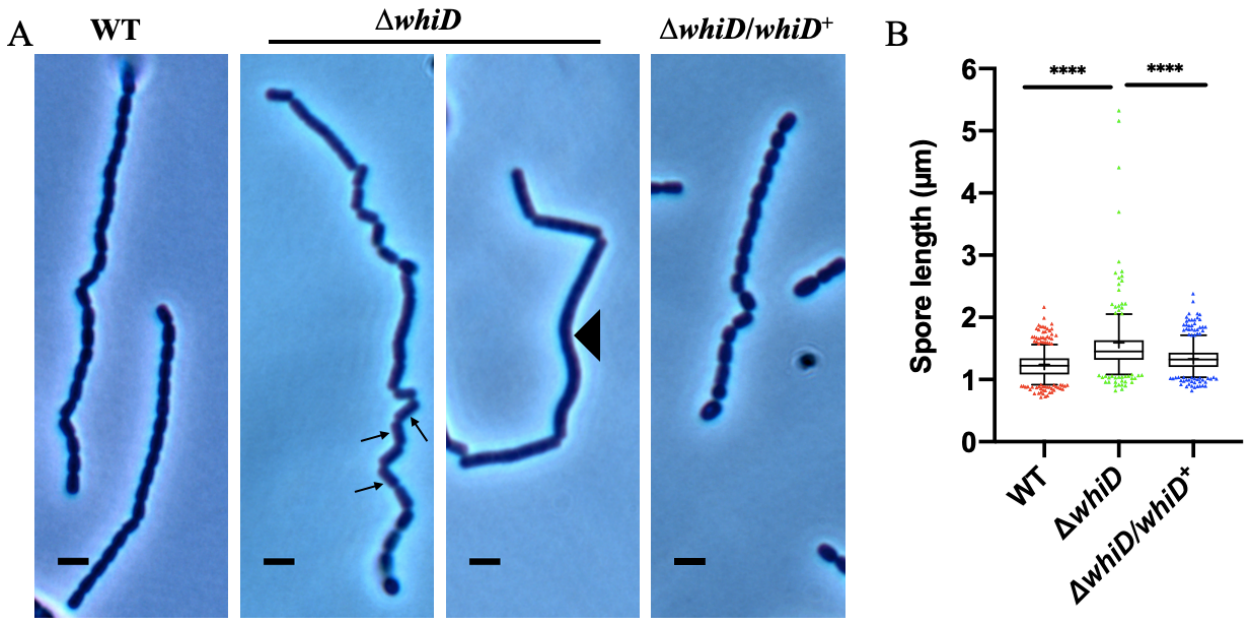

Figure 3.3 Deletion of *whiD* results in a spore size and shape defects. (A) Phase-contrast micrographs of mature spore chains of wild-type *S. venezuelae* (WT), the *ΔwhiD* mutant (NS10), the complemented strain Δ*whiD*/*whiD*$^{+}$ (NS17) are shown. Strains were grown on MYM solid medium for 4 days at 30°C, and coverslip impressions were observed using phase-contrast microscopy. Scale bar 2 µm. Arrows indicate more box-shaped spores and arrow head indicates the long filament. (B) Box-whisker plot showing the measured spore length distributions of WT (N=733), Δ*whiD* mutant (N=549), and complemented strain Δ*whiD*/*whiD*$^{+}$ (N=653). Box denotes the 25th percentile, median, and 75th percentile, respectively, and whiskers denote the 5th and 95th percentile. Data not included in the box-whisker are shown as dots. The + represents the mean value with WT being 1.24±0.54 µm, Δ*whiD* mutant being 1.59±0.94 µm, and Δ*whiD*/*whiD*$^{+}$ being 1.33±0.21 µm, respectively. Statistics was conducted using one-way ANOVA, **** P<0.0001.

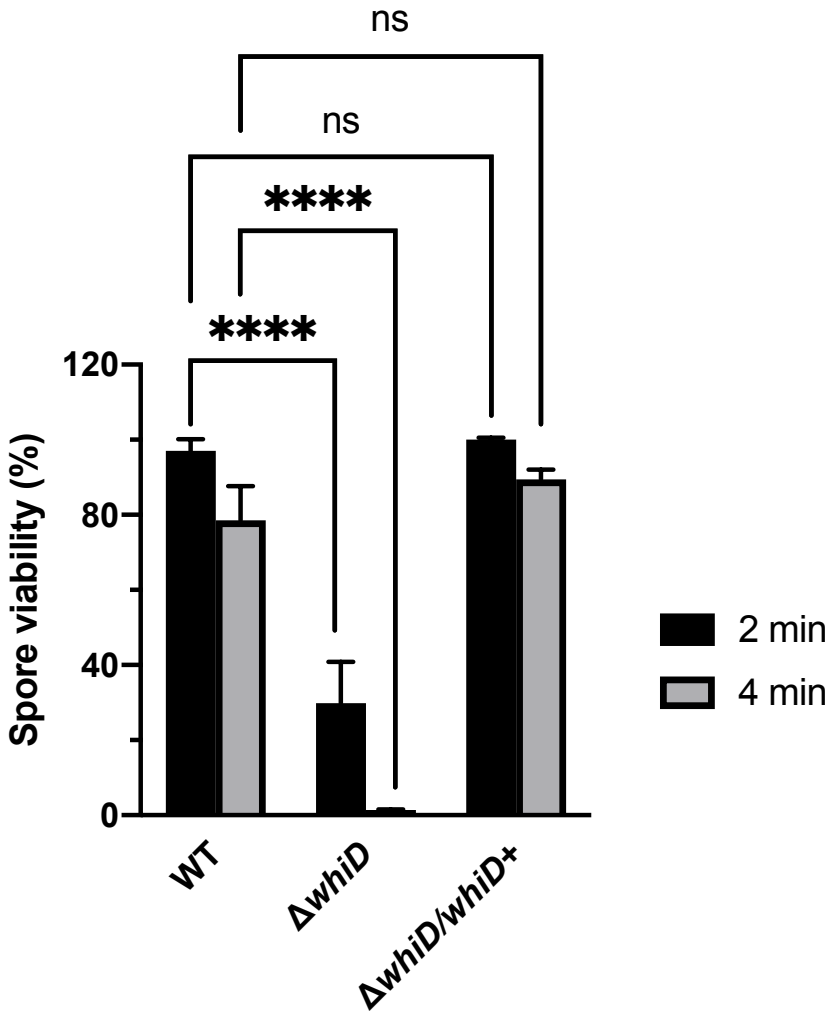

Figure 3.4 Deletion of *whiD* results in increased heat sensitivity. Freshly isolated spores were treated at 55°C for the indicated incubation times. Results are the average of three independent replicates and error bars represent SD. Asterisks indicate the difference for Δ*whiD* mutant when compared to WT. Statistics was conducted using two-way ANOVA, **** P<0.0001.

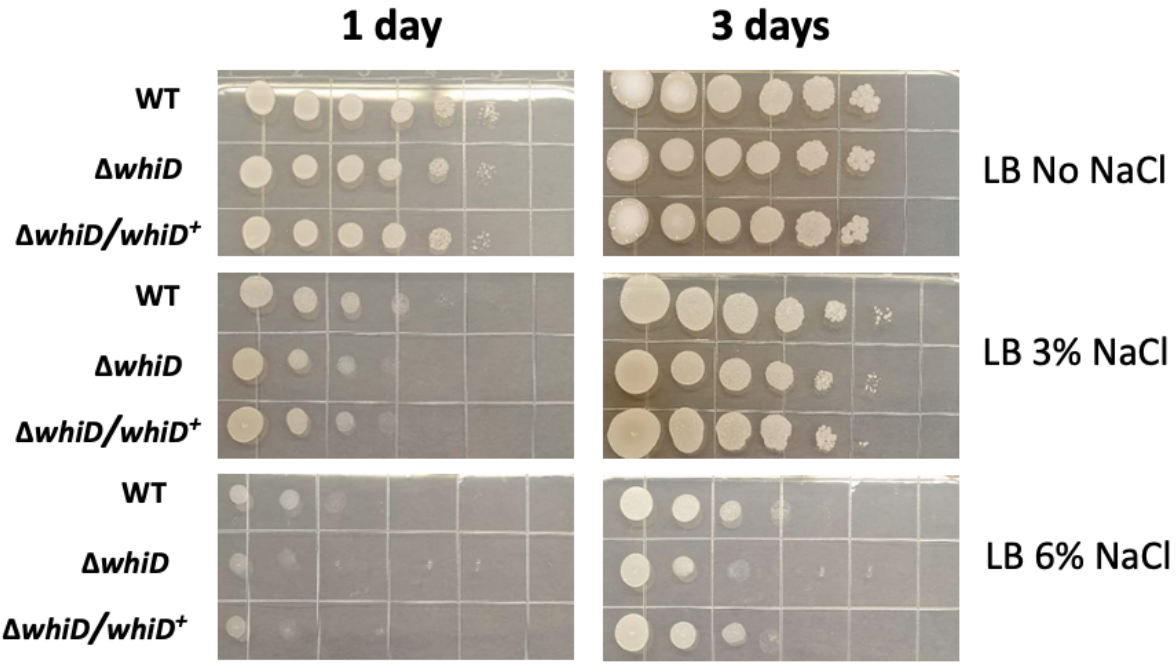

Figure 3.5 Deletion of *whiD* results in a slightly increased sensitivity to osmotic stress. Serial spore dilutions were spotted on standard LB agar plates containing different concentrations of NaCl. Photographs were taken after 1 day and 3 days incubation at 30°C.

REFERENCES

Burian, J., Yim, G., Hsing, M., Axerio-Cilies, P., Cherkasov, A., Spiegelman, G.B., and Thompson, C.J. (2013). The mycobacterial antibiotic resistance determinant WhiB7 acts as a transcriptional activator by binding the primary sigma factor SigA (RpoV). Nucleic Acids Res *41*, 10062-10076.

Bush, M.J. (2018). The actinobacterial WhiB-like (Wbl) family of transcription factors. Mol Microbiol *110*, 663-676.

Bush, M.J., Bibb, M.J., Chandra, G., Findlay, K.C., and Buttner, M.J. (2013). Genes required for aerial growth, cell division, and chromosome segregation are targets of WhiA before sporulation in *Streptomyces venezuelae*. mBio *4*, e00684-00613.

Bush, M.J., Chandra, G., Bibb, M.J., Findlay, K.C., and Buttner, M.J. (2016). Genome-wide chromatin immunoprecipitation sequencing analysis shows that WhiB is a transcription factor that cocontrols its regulon with WhiA To initiate developmental cell division in *Streptomyces*. mBio *7*, e00523-00516.

Chater, K. (1972). A morphological and genetic mapping study of white colony mutants of *Streptomyces coelicolor*. Microbiology *72*, 9-28.

Datsenko, K.A., and Wanner, B.L. (2000). One-step inactivation of chromosomal genes in *Escherichia coli* K-12 using PCR products. Proc Natl Acad Sci USA *97*, 6640-6645.

Davis, N.K., and Chater, K.F. (1992). The *Streptomyces coelicolor whiB* gene encodes a small transcription factor-like protein dispensable for growth but essential for sporulation. Mol Gen Genet *232*, 351-358.

den Hengst, C.D., Tran, N.T., Bibb, M.J., Chandra, G., Leskiw, B.K., and Buttner, M.J. (2010). Genes essential for morphological development and antibiotic production in *Streptomyces coelicolor* are targets of BldD during vegetative growth. Mol Microbiol *78*, 361-379.

Fowler-Goldsworthy, K., Gust, B., Mouz, S., Chandra, G., Findlay, K.C., and Chater, K.F. (2011). The actinobacteria-specific gene wblA controls major developmental transitions in *Streptomyces coelicolor* A3(2). Microbiology *157*, 1312-1328.

Gomez-Escribano, J.P., Holmes, N.A., Schlimpert, S., Bibb, M.J., Chandra, G., Wilkinson, B., Buttner, M.J., and Bibb, M.J. (2021). *Streptomyces venezuelae* NRRL B-65442: genome

sequence of a model strain used to study morphological differentiation in filamentous actinobacteria. J Ind Microbiol and Biotechnol.

Gregory, M.A., Till, R., and Smith, M.C. (2003). Integration site for *Streptomyces* phage phiBT1 and development of site-specific integrating vectors. J Bacteriol *185*, 5320-5323.

Gust, B., Challis, G.L., Fowler, K., Kieser, T., and Chater, K.F. (2003a). PCR-targeted *Streptomyces* gene replacement identifies a protein domain needed for biosynthesis of the sesquiterpene soil odor geosmin. Proc Natl Acad Sci USA *100*, 1541-1546.

Gust, B., O'Rourke, S., Bird, N., Kieser, T., and Chater, K. (2003b). Recombineering in *Streptomyces coelicolor*. Norwich: The John Innes Foundation.

Jakimowicz, P., Cheesman, M.R., Bishai, W.R., Chater, K.F., Thomson, A.J., and Buttner, M.J. (2005). Evidence that the *Streptomyces* developmental protein WhiD, a member of the WhiB family, binds a [4Fe-4S] cluster. J Biol Chem *280*, 8309-8315.

Kang, S.H., Huang, J., Lee, H.N., Hur, Y.A., Cohen, S.N., and Kim, E.S. (2007). Interspecies DNA microarray analysis identifies WblA as a pleiotropic down-regulator of antibiotic biosynthesis in *Streptomyces*. J Bacteriol *189*, 4315-4319.

Kieser, T., Bibb, M.J., Buttner, M.J., Chater, K.F., and Hopwood, D.A. (2000). Practical *Streptomyces* genetics, Vol 291 (John Innes Foundation Norwich).

Kim, J.S., Lee, H.N., Kim, P., Lee, H.S., and Kim, E.S. (2012). Negative role of *wblA* in response to oxidative stress in *Streptomyces coelicolor*. J Microbiol Biotechnol *22*, 736-741.

Lee, D.-S., Kim, P., Kim, E.-S., Kim, Y., and Lee, H.-S. (2018). *Corynebacterium glutamicum* WhcD interacts with WhiA to exert a regulatory effect on cell division genes. Antonie Van Leeuwenhoek *111*, 641-648.

MacNeil, D.J., Occi, J.L., Gewain, K.M., MacNeil, T., Gibbons, P.H., Ruby, C.L., and Danis, S.J. (1992). Complex organization of the *Streptomyces avermitilis* genes encoding the avermectin polyketide synthase. Gene *115*, 119-125.

McVittie, A. (1974). Ultrastructural studies on sporulation in wild-type and white colony mutants of *Streptomyces coelicolor*. J Gen Microbiol *81*, 291-302.

Molle, V., Palframan, W.J., Findlay, K.C., and Buttner, M.J. (2000). WhiD and WhiB, homologous proteins required for different stages of sporulation in *Streptomyces coelicolor* A3(2). J Bacteriol *182*, 1286-1295.

Paget, M.S., Chamberlin, L., Atrih, A., Foster, S.J., and Buttner, M.J. (1999). Evidence that the extracytoplasmic function sigma factor ςE is required for normal cell wall structure in *Streptomyces coelicolor* A3 (2). J Bacteriol *181*, 204-211.

Sambrook, J., Fritsch, E.F., and Maniatis, T. (1989). Molecular cloning: a laboratory manual (Cold spring harbor laboratory press).

Singh, A., Guidry, L., Narasimhulu, K.V., Mai, D., Trombley, J., Redding, K.E., Giles, G.I., Lancaster, J.R., Jr., and Steyn, A.J. (2007). *Mycobacterium tuberculosis* WhiB3 responds to O2 and nitric oxide via its [4Fe-4S] cluster and is essential for nutrient starvation survival. Proc Natl Acad Sci USA *104*, 11562-11567.

Smith, L.J., Stapleton, M.R., Fullstone, G.J., Crack, J.C., Thomson, A.J., Le Brun, N.E., Hunt, D.M., Harvey, E., Adinolfi, S., and Buxton, R.S. (2010). *Mycobacterium tuberculosis* WhiB1 is an essential DNA-binding protein with a nitric oxide-sensitive iron–sulfur cluster. Biochem. J *432*, 417-427.

Stecher, G., Tamura, K., and Kumar, S. (2020). Molecular Evolutionary Genetics Analysis (MEGA) for macOS. Mol Biol Evol *37*, 1237-1239.

Stewart, M.Y.Y., Bush, M.J., Crack, J.C., Buttner, M.J., and Le Brun, N.E. (2020). Interaction of the *Streptomyces* Wbl protein WhiD with the principal sigma factor sigma(HrdB) depends on the WhiD [4Fe-4S] cluster. J Biol Chem *295*, 9752-9765.

Stuttard, C. (1982). Temperate phages of *Streptomyces venezuelae*: lysogeny and host specificity shown by phages SV1 and SV2. Microbiology *128*, 115-121.

Wan, T., Horová, M., Beltran, D.G., Li, S., Wong, H.-X., and Zhang, L.-M. (2021). Structural insights into the functional divergence of WhiB-like proteins in *Mycobacterium tuberculosis*. Mol Cell *81*, 2887-2900. e2885.

Yu, P., Liu, S.P., Bu, Q.T., Zhou, Z.X., Zhu, Z.H., Huang, F.L., and Li, Y.Q. (2014). WblAch, a pivotal activator of natamycin biosynthesis and morphological differentiation in *Streptomyces chattanoogensis* L10, is positively regulated by AdpAch. Appl Environ Microbiol *80*, 6879-6887.

CHAPTER 4: SUMMARY AND FUTURE DIRECTIONS

Characterization of SsdA, a novel spore shape determination protein in *Streptomyces*

S. coelicolor spore maturation is a complex process that involves spore wall thickening, spore shape metamorphosis from cylindrical pre-spores into ellipsoid spores, and deposition of a grey polyketide pigment on the spore surface that turns the aerial mycelium from white to grey (Bush et al., 2015). Very limited knowledge is known about the details of the spore maturation process. In an effort to identify more proteins that take part in this process, a whole genome-wide transposon-mediated mutagenesis was conducted in *S. coelicolor* and a potential candidate was identified that might play a role in spore shape determination, and thus its name SsdA (Bennett, 2006). To independently confirm the observations, a *ssdA*-null mutant was isolated in *S. coelicolor*, and results showed that a *S. coelicolor ssdA* null mutant had a similar phenotype to the insertion mutant. Hydrophobic aerial hyphae with heterogeneous spore compartments in size and shape were produced (Fig. 2.1), confirming the potential role of *ssdA* in spore shape determination.

To better characterize the function of this gene, I switched from working with *S. coelicolor* to *S. venezuelae* due to its advantages, such as rapid growth and ability to sporulate in submerged culture (Bush et al., 2015). Deletion of *ssdA* for *S. venezuelae* resulted in a delayed morphological differentiation both on solid medium and in liquid medium, which can be at least partially explained by the spore germination defect and reduced initial germ tube extension rate in the absence of *ssdA*. In addition, sporulation was also affected in the Δ*ssdA* mutant. A *S. venezuelae* Δ*ssdA* mutant generated heterogeneously-sized spores (Fig. 2.9). The sporulation defect is more striking in liquid medium, where prespore compartments were larger and have difficulty in cell-cell separation, even after a prolonged incubation time (Fig. 2.19). The observed

phenotype was supported by observation of SsdA-EGFP localization, which was shown to localize in vegetative hyphae, at sporulation septa, and the periphery of spores, consistent with its roles in development as supported by the null mutant.

Of interest, despite a high amino acid sequence identity for SsdA among different *Streptomyces* species, SsdA affects morphological differentiation in a slightly different way for *S. coelicolor* compared to *S. venezuelae*. First, there is no obvious delayed morphological differentiation observed in the *S. coelicolor* Δ*ssdA* mutant under tested conditions. SsdA might affect development in a medium-dependent way, so it might be necessary to test growth of Δ*ssdA* mutant of *S. coelicolor* on other media. Second, the effect of *ssdA* on spore shape in more striking for *S. coelicolor* than in *S. venezuelae*. In the *S. venezuelae* Δ*ssdA* mutant, the spores tend to more box-shaped or elongated when compared to WT, however, frequently round and/or swollen spores observed in addition to the long spores in *S. coelicolor* Δ*ssdA* mutant. This might be caused by the difference of spore characteristics between two species: *S. venezuelae* mature spores are more rectangular while *S. coelicolor* are more ellipsoid (Bush et al., 2015). An increase in aerial hyphae hydrophobicity shown by the accumulation of water droplets was not observed in *S. venezuelae* Δ*ssdA* mutant as well. Of note, despite of the difference in phenotypes, *S. coelicolor* Δ*ssdA* mutant can be complemented by *S. venezuelae ssdA*, and vice versa, indicating that SsdA is conserved in *Streptomyces* species, and the differences observed were due species differences.

Furthermore, we revealed that deletion of *ssdA* in *S. venezuelae* resulted in spore sensitivity to heat, osmotic stress, and cell-wall targeting antibiotics, including ampicillin, carbenicillin, penicillin and vancomycin. In collaboration with Dr. Evi Stegmann's lab at University of Tübingen (Germany), the spore sacculus of the Δ*ssdA* mutant was isolated and

analyzed by HPLC-MS. Preliminary result revealed accumulations of spore wall precursors after deletion of *ssdA*. This is likely an indirect effect of *ssdA* deletion.

SsdA is a predicted integral membrane protein with a transmembrane domain at N-terminus and C-terminus, and between is a predicted cytoplasmic domain (Fig 2.3). Genetic deletion results showed that all three domains are important for proper function of SsdA (Fig. 2.5). The central cytoplasmic domain was tested in a bacterial two-hybrid assay, and results showed that it can interact with itself. Further screening of the sporulation-related proteins showed that it can interact with DynB. No interaction was observed in other tested proteins: SepF1-SepF3, SepH, DynA, SsgA and SsgB. The interaction between SsdA and DynB needs further confirmation using an independent method like a pull-down assay. If it is shown to be an effective interaction, a Δ*ssdA*Δ*dynB* double mutant would be isolated, and sporulation septation and FtsZ ring stability could be examined.

I hypothesize that SsdA functions as a structural protein to affect morphological differentiation of the life cycle. The interaction with DynB provides an insight into how SsdA contributes to the sporulation-specific cell division. In future, the interactions would be tested between SsdA and proteins of TIPOC (Bush et al., 2015) , and between SsdA and proteins of SSSC complex (Vollmer et al., 2019), to reveal how SsdA affect the hyphal growth and spore maturation, respectively (Fig. 4.1). Due to the low accumulation of SsdA protein in the cell, it is also likely that SsdA functions as a signal effector protein in a cascade pathway that regulates cell wall biosynthesis, degradation, and modification.

Transcriptomic analysis showed that *ssdA* is a development-regulated gene (Jeong et al., 2016), so determining how it is regulated would also be noteworthy to investigate. To do this, a direct screening for factors binding to the *ssdA* regulatory region could be conducted using a

DNA-affinity capture assay coupled with LC-MS/MS analysis (Bekiesch et al., 2016; Park et al., 2009).

Characterization of WhiD for sporulation and spore maturation in *S. venezuelae*

Early genetic studies in *S. coelicolor* identified two different kinds of regulatory proteins Bld and Whi, which are required for the formation of aerial hyphae and the sporulation of aerial hyphae, respectively. After decades of endeavors, important progress has been made towards understanding how these fascinating regulators control the cellular processes that underlie growth and development, but additional regulators are still waiting for further investigation. WhiD is a crucial regulator belonging to a large family with unknown functions in *Streptomyces* species. In this study, I found that deletion of *whiD* resulted in a white colony surface. Microscopic examination revealed that spores of Δ*whiD* are in irregular shapes and larger size, suggesting a sporulation defect in Δ*whiD*. The spore shape defect for the Δ*whiD* mutant also indicated that WhiD might be a potential candidate for control of *ssdA* expression. The Δ*whiD* spores showed highly sensitivity to heat stress and mild sensitivity to osmotic stress, which is different from what were observed in the Δ*ssdA* mutant, suggesting that *ssdA* is not the only target of WhiD in controlling spore cell wall. In the future, the spore sacculus of the Δ*whiD* mutant could be isolated and analyzed by HPLC-MS to determine potential perturbations of cell wall structure and composition.

Different from *S. coelicolor* WhiD, *S. venezuelae* WhiD ortholog has a C-terminal extension of 18 amino acids, which is important for WhiD self-interaction (Stewart et al., 2020). To further characterize the protein WhiD, C-terminal truncation could be constructed and analyzed using genetic and biochemical methods. WhiD is a transcription factor with unknown targets identified so far, a genome-wide chromatin immunoprecipitation sequencing analysis

(ChIP–seq) could be used to identify the WhiD regulon in *S. venezeulae*. Wbl proteins in general lack a distinct DNA-binding motif. WhiD paralog WhiB functions as a transcription factor by directly interacting with a DNA-binding protein WhiA in *Streptomyces* and *Corynebacteria* (Bush et al., 2016; Lee et al., 2018). The interaction between WhiB and DNA-binding protein WhiA raises the possibility that other Wbl proteins, including WhiD, might also function via direct interactions with a protein containing a helix-turn-helix motif. Therefore, a screening of a genomic library might be necessary to find out a WhiD-interacting partner containing a DNA-binding motif.

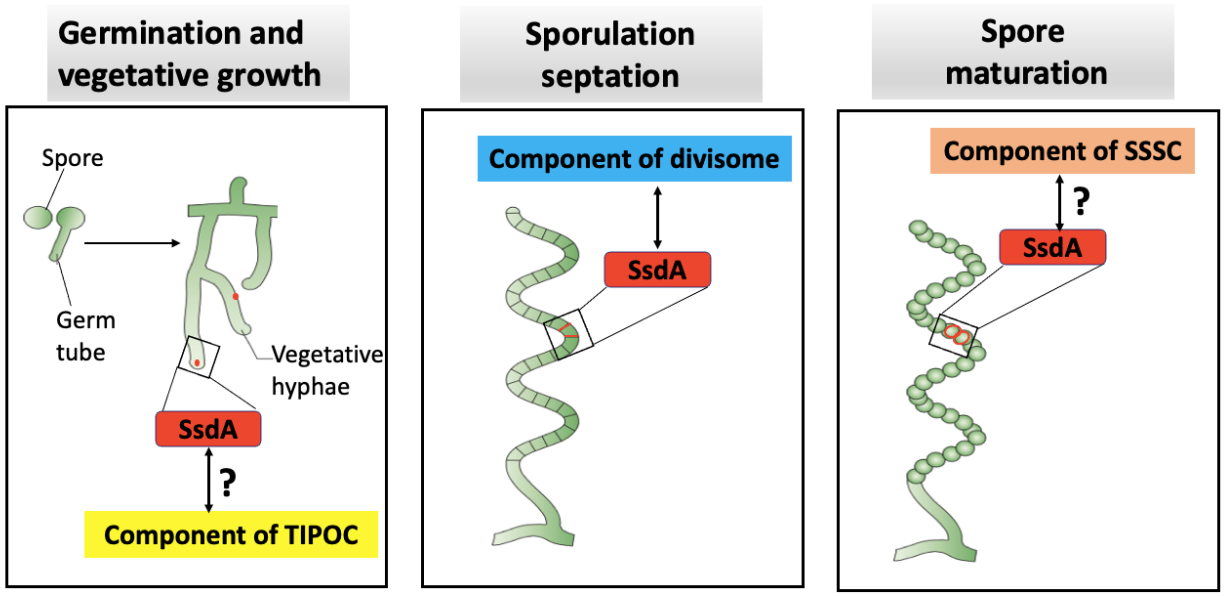

Figure 4.1 Model for SsdA function at various sites during *Streptomyces* life cycle. Representative SsdA localizations are depicted in red and highlighted in black box. (Left) SsdA affects spore germination and vegetative growth by localizing at the hyphal tip and future branching sites. Potential interactions would be tested with proteins located at the tip organizing center (TIPOC). (Middle) SsdA affects sporulation septation by localizing at the sporulation septa and interacting with one of the divisome proteins DynB. (Right) SsdA affects spore maturation by localizing at the periphery of mature spores. Potential interactions would be tested with proteins of *Streptomyces* spore wall synthesizing complex (SSSC). Figures were adapted from Flärdh and Buttner (2009).

REFERENCES

Bekiesch, P., Franz-Wachtel, M., Kulik, A., Brocker, M., Forchhammer, K., Gust, B., and Apel, A.K. (2016). DNA affinity capturing identifies new regulators of the heterologously expressed novobiocin gene cluster in *Streptomyces coelicolor* M512. Appl Microbiol Biotechnol *100*, 4495-4509.

Bennett, J. (2006). Molecular genetic analysis of division and development in *Streptomyces coelicolor*. (Ph. D. dissertation. Duquesne University, Pittsburgh, PA).

Bush, M.J., Chandra, G., Bibb, M.J., Findlay, K.C., and Buttner, M.J. (2016). Genome-wide chromatin immunoprecipitation sequencing analysis shows that WhiB is a transcription factor that cocontrols its regulon with WhiA To initiate developmental cell division in *Streptomyces*. mBio *7*, e00523-00516.

Bush, M.J., Tschowri, N., Schlimpert, S., Flärdh, K., and Buttner, M.J. (2015). c-di-GMP signalling and the regulation of developmental transitions in streptomycetes. Nat Rev Microbiol *13*, 749-760.

Flärdh, K., and Buttner, M.J. (2009). *Streptomyces* morphogenetics: dissecting differentiation in a filamentous bacterium. Nat Rev Microbiol *7*, 36-49.

Jeong, Y., Kim, J.N., Kim, M.W., Bucca, G., Cho, S., Yoon, Y.J., Kim, B.G., Roe, J.H., Kim, S.C., Smith, C.P.*, et al.* (2016). The dynamic transcriptional and translational landscape of the model antibiotic producer *Streptomyces coelicolor* A3(2). Nat Commun *7*, 11605.

Lee, D.-S., Kim, P., Kim, E.-S., Kim, Y., and Lee, H.-S. (2018). *Corynebacterium glutamicum* WhcD interacts with WhiA to exert a regulatory effect on cell division genes. Antonie Van Leeuwenhoek *111*, 641-648.

Park, S.S., Yang, Y.H., Song, E., Kim, E.J., Kim, W.S., Sohng, J.K., Lee, H.C., Liou, K.K., and Kim, B.G. (2009). Mass spectrometric screening of transcriptional regulators involved in antibiotic biosynthesis in *Streptomyces coelicolor* A3(2). J Ind Microbiol Biotechnol *36*, 1073-1083.

Stewart, M.Y.Y., Bush, M.J., Crack, J.C., Buttner, M.J., and Le Brun, N.E. (2020). Interaction of the *Streptomyces* Wbl protein WhiD with the principal sigma factor sigma(HrdB) depends on the WhiD [4Fe-4S] cluster. J Biol Chem *295*, 9752-9765.

Vollmer, B., Steblau, N., Ladwig, N., Mayer, C., Macek, B., Mitousis, L., Sigle, S., Walter, A., Wohlleben, W., and Muth, G. (2019). Role of the Streptomyces spore wall synthesizing complex SSSC in differentiation of *Streptomyces coelicolor* A3(2). Int J Med Microbiol *309*, 151327.